COORDINATE FRAMES IN INERTIAL NAVIGATION

by

MYRON KAYTON

B.M.E., The Cooper Union, 1955

S.M., Harvard University, 1956

MASS. INST. OF TECHNOLOGY
SEP 21 1960
LIBRARY

SUBMITTED IN PARTIAL FULFILLMENT

OF THE REQUIREMENTS FOR THE DEGREE OF

DOCTOR OF PHILOSOPHY

at the

MASSACHUSETTS INSTITUTE OF TECHNOLOGY

August, 1960

Signature of Author Myron Kayton

Department of Aeronautics and Astronautics
August 16, 1960

Certified by Signature redacted (Prof. W. Wrigley)
Thesis Supervisor

Signature redacted (Prof. R. L. Halfman)
Thesis Supervisor

Signature redacted (Mr. J. Hovorka)
Thesis Supervisor

Accepted by Signature redacted (Prof. L. Trilling)
Chairman, Departmental Committee on
Graduate Students

MRL

Aero
Thesis
1960

COORDINATE FRAMES IN INERTIAL NAVIGATION

by

Myron Kayton

Submitted to the Department of Aeronautics and Astronautics on August 16, 1960 in partial fulfillment of the requirements for the degree of

Doctor of Philosophy

ABSTRACT

A vehicle is assumed to be navigating in the vicinity of a planet such as the Earth. The vehicle carries an accelerometer platform which, in general, is isolated from angular motions of the vehicle and is caused to rotate independently in inertial space by means of angular inertial sensors ("inersors") such as gyroscopes.

A navigation coordinate frame, z^i, can be defined which is fixed with respect to the planet. General navigation equations can be derived which express the gyro drive signals and the position coordinates, z^i, in terms of the accelerometer outputs, subject only to the condition that the input axes of the accelerometers follow the unit vectors of the navigation coordinate frame. To solve these equations in any particular coordinate frame, five classes of parameters are needed:

1. The transformation equations from the Earth-centered, Earth-fixed Cartesian y_i frame to the arbitrary z^i are needed. The transformation equations enter the navigation equations as elements of the metric tensor of the z^i space and as certain partial derivatives of the form $\partial y_i / \partial z^j$.

2. $\bar{G}$ or $\bar{g}$ must be known as a function of the z^i in order to interpret the accelerometer outputs in terms of acceleration.

3. The inertial angular velocity of the accelerometer platform, $\bar{\omega}_{IA}$, is needed. This is measured with gyroscopes or with more exotic inersors.

4. Twelve initial conditions are required:
   a. Vehicle position, z^i_0.
   b. Vehicle velocity, $\dot{z}^i_0$.
   c. Platform orientation.
   d. Platform angular velocity.

These must be inserted initially and may be updated en route.

5. Time and the inertial angular velocity of the planet are needed. The spin rate of the Earth measures time to one part in 10^7.

Several z^i coordinate frames are examined and applied to suitable missions. In particular, the definitions of coordinate frames to mechanize various "vertical" directions in vehicles above the Earth are discussed. A novel integral mechanization of the longitude channel is derived for use in any symmetric coordinate frame. Some examples are analysed in detail.

The limitations on the navigation process imposed by astronomic and geodetic limitations are considered at length. It is shown that the conventional Earth-centered, "inertially-non-rotating" coordinate frame, x_i, actually rotates at 10^{-6} deg./hr. in inertial space. Furthermore, the angular velocity of the Earth relative to the x_i frame does not lie entirely along the geographic polar axis but has a component of 5×10^{-5} deg./hr. perpendicular to it. Other limitations of this nature are discussed including some which cause errors as large as one mile if uncorrected. Figures 5-14 and 5-15 summarize these limitations.

Mathematical models of the gravity field are proposed for use in various coordinate frames, to navigational accuracy. The horizontal components of $\overline{g}$ and $\overline{G}$ in several coordinate frames are considered in detail as functions of altitude. The effect on the system of an imperfect knowledge of $\overline{g}$ is examined.

Unusual problems connected with inertial navigation on other planets of the solar system are considered briefly. The entire thesis is written to allow immediate application to navigation on these planets.

Thesis Supervisors: Dr. Walter Wrigley, Professor of Instrumentation and Astronautics.
Robert Louis Halfman, Associate Professor of Aeronautics and Astronautics.
John Hovorka, Lecturer, Department of Aeronautics and Astronautics.

ACKNOWLEDGMENT

The author wishes to thank the members of the staff of the Massachusetts Institute of Technology, particularly his thesis supervisors, Professor Walter Wrigley, Professor Robert L. Halfman and Mr. John Hovorka, for their suggestions and for their encouragement of this thesis. The author also wishes to express his appreciation to:

Dr. Bruce C. Murray of the United States Air Force Cambridge Research Center for his valuable criticism of the material on geodesy and gravimetry.

Mrs. I. Fischer, Mrs. Davis and Lt. Col. A.M. Ahmajan of the United States Army Map Service for their criticism of Section 3.K.

fellow students R.G. Stern, Capt. P.V. Osburn (USAF), Lcdr. H.W. Smith (RCN) and T.C. Blaschke and former students, Professor J.L. Stockard and Lcdr. R.C. Duncan (USN) for their many suggestions.

The author is especially indebted to the National Science Foundation without whose support, from 1958 to 1960 at M.I.T. and 1955 to 1956 at Harvard, neither this thesis nor my graduate education would have been possible.

Above all, the author thanks his wife, Paula, for her assistance in preparing the manuscript and for her forbearance while this thesis was being written.

CONTENTS

CONTENTS

CONTENTS

CONTENTS

CONTENTS

INDEX OF FIGURES

CHAPTER 2.

CHAPTER 3.

FIGURES

FIGURES

Chapter One

INERTIAL SPACE AND TIME

> ". . . . . the great success of Newtonian physics led to the paradoxical situation of the adherence to the concepts of absolute time and absolute space, on the one hand, and their absence from practical physics, on the other."
>
> Max Jammer
> Reference 180, p. 138.

1.A. INTRODUCTION.

The concepts of time and inertial space are fundamental in mechanics and hence in its application to inertial navigation. Time is regarded as the independent variable in the formulation of the laws of mechanics. Inertial space is a coordinate frame in which these laws can be written in a particularly simple manner. The aim of this chapter is to consider briefly the meaning and the measurement of these concepts.

1.B. INERTIAL SPACE.

The laws of mechanics owe their present form to the concept of force developed during Newton's time. Force is not essential to mechanics; it is "but an invention to satisfy our desires for explanation" (Ref. 180, p. 209). Several formulations of the laws of motion have been based on energy, momentum, the Lagrangian, the Hamiltonian and similar force-free concepts.

In the Newtonian formulation, objects are considered to exert forces on each other which are dependent on their relative positions and velocities. The present configuration of the bodies allows the forces to be calculated; the forces determine the change in configuration. As Jammer observes in CONCEPTS OF FORCE (ibid.), force is merely an artificial intermediary between the present and future configurations of a group of material bodies.

Macroscopic forces are conventionally divided into contact, gravitational and electromagnetic forces. Atomic and nuclear interactions are of no direct interest to the navigation system engineer.

Newton's formulation of mechanics implicitly defines inertial space as any coordinate frame in which the acceleration of a particle is proportional to the net force acting on it. In order to operationally specify such an inertial frame, a hypothetical experiment is necessary. Two small test particles could be selected and all other masses in the universe removed to a large distance. Then all contact forces

on the two particles could be removed. Since all other masses are at a large distance, the net force on each particle is presumably zero and the particles move in straight lines at constant velocity in inertial space. The origin of a coordinate frame could be located on either test particle and the coordinate frame oriented so both particles appear to move in straight lines. Such a coordinate frame is inertial by virtue of Newton's Law. Furthermore, any other coordinate frame which does not rotate relative to this one and whose origin moves at constant velocity relative to it is also inertial.

This hypothetical experiment is unsatisfactory because it has never been performed and cannot be performed. The effect of a large mass at a large distance is unknown; the experiment is not operational. Still, the definition implies that if space is homogeneous so that the results of the hypothetical experiment do not vary from place to place, all inertial coordinate frames are relatively non-rotating and differ at most by a constant relative linear velocity.

Einstein's theory of gravitation is another formulation of the laws of mechanics, provided that only gravitational forces are included; electromagnetic and atomic (contact) forces must be omitted. In Einstein's view, particles always follow geodesic paths in a warped four dimensional space. The curvature of the space depends only on the mass density distribution throughout the space. The Newtonian observer, seeing the particles follow curved paths (geodesics in the warped space), conceives that forces act on the particles. The Einsteinian observer substitutes the geometrical picture of a curved

space for the concepts of force and inertial space. The Newtonian equations are true only in the privileged inertial frame; the relativistic equations are true in any coordinate frame whatsoever since the curvature tensor transforms in the same manner as the energy-momentum tensor. At velocities much less than that of light, both formulations yield identical results but through different mechanical models. At high velocities, the results differ. Limited experimental evidence to date indicates that the Einsteinian formulation is more nearly correct than the Newtonian (see refs. 161, 166, 172, 181 and 186, for example).

If the Einsteinian observer selects a coordinate frame at random, the particles appear to travel in non-geodesic paths; "forces" act on them. It is only when the observer selects the proper coordinate frame that the particles appear to move on a geodesic path. This preferred coordinate frame is calculable from the mass density distribution in space. Professor J. A. Wheeler, in a lecture at M. I. T. on October 22, 1959, suggested the following analogy. Suppose the path of an aircraft, flying from New York to London, is observed on a Mercator map. The airplane appears to move in an arc since it is following a geodesic path on the surface of the Earth. The observer can attribute the curved path to the existence of a force attracting the aircraft toward the north pole or he can realize that a coordinate transformation onto a sphere will remove the polar force. The "force" has been transformed away by a suitable choice of coordinates.

The geometric interpretation has been successful in practice only for a limited number of special cases, the equations being too difficult to solve in the presence of many particles. Furthermore, electromagnetic and atomic forces have not been incorporated into the theory. Persons such as J. A. Wheeler in the United States and V. Fock in the U. S. S. R. are presently attempting to include electromagnetic forces in a "unified field theory." In such a theory, particles might follow geodesic paths in a four, five or six dimensional space where the local curvature of the space would be determined by the mass and charge distributions and by the relative velocities of the particles. Atomic and nuclear interactions are far from being self-consistent much less being included in a unified field theory.

Newtonian mechanics substitutes the concepts of force and inertial space for Einstein's geometric concept of geodesic paths in a space warped by the presence of mass. However, the inertial space concept is still a useful approximation at low velocities. To assess its accuracy and applicability three questions must be answered:

1. Where may the origin of an inertial frame be placed?
2. How must the inertial fram be oriented?
3. How accurately do the Newtonian laws hold in this inertial frame?

1.C. THE ORIGIN OF AN INERTIAL COORDINATE FRAME.

The existence of inertial coordinate frames in Newtonian mechanics is a postulate. Thus it must be assumed that at least one inertial frame exists. This distasteful assumption essentially postulates the existence of an absolute space and is responsible for Einstein's alternative formulation of mechanics without a preferred inertial frame.

The classical reasoning proceeds as follows. Assume that the inertial frame, S_1, exists. Suppose that the masses m_1 and m_2 exert a mutual gravitational attraction, $\overline{F}_{G_0}$, and that the remaining masses in the universe exert the gravitational and electromagnetic forces, $\overline{F}_{G_1}$ and $\overline{F}_{E_1}$ on m_1 and $\overline{F}_{G_2}$ and $\overline{F}_{E_2}$ on m_2. Suppose a coordinate frame, S_2, non-rotating relative to S_1, is placed on m_1. Let $\overline{R}_1$ locate m_1 in S_1 and $\overline{R}_2$ locate m_2 in S_2. Then:

$$m_1 \ddot{\overline{R}}_1 = -\overline{F}_{G_0} + \overline{F}_{G_1} + \overline{F}_{G_2}$$

$$m_2(\ddot{\overline{R}}_1 + \ddot{\overline{R}}_2) = \overline{F}_{G_0} + \overline{F}_{G_2} + \overline{F}_{E_2}$$

so:

$$\ddot{\overline{R}}_2 = \left(\frac{\overline{F}_{G_2}}{m_2} - \frac{\overline{F}_{G_1}}{m_1}\right) + \left(\frac{\overline{F}_{E_2}}{m_2} - \frac{\overline{F}_{E_1}}{m_1}\right) + \frac{m_1 + m_2}{m_1 m_2}\overline{F}_{G_0} \qquad (1\text{-}1)$$

Hence if S_1 is inertial, S_2 is also inertial to the extent that differences of the gravitational and electromagnetic accelerations are negligible within S_2. In S_2, the apparent gravitational force on m_2 must be increased from $\frac{\gamma m_1 m_2}{r^2}$ to $\frac{\gamma(m_1+m_2)m_2}{r^2}$ as in the usual two-body problem (Ref. 219, p. 80).

If an inertial coordinate frame is centered on a body which is massive compared to nearby bodies of interest, $m_1 + m_2 \approx m_1$ and the gravitational force which appears to act on the smaller body is much greater than the gradient forces. Thus, operational inertial coordinate frames on large planets and satellites are useful because the planet's gravitational attraction is far greater than the gradient forces exerted by nearby bodies. But, if an operational inertial frame is placed at the mass center of a small artificial or natural satellite, the gradient force of the primary may be comparable to, or larger than the attraction of the satellite. For such a coordinate frame to be useful, the gradient forces must be explicitly included as an apparent additional gravitational force.

For example, suppose m_1 is the Sun. A heliocentric coordinate frame, centered at the mass center of the Sun and non-rotating relative to the distant galaxies (see Section 1. D), is a convenient inertial coordinate frame for computing the orbits of planets and solar system probes. The closest large mass to the Sun is the triple star system Alpha Centauri. This star system causes a gravitational difference across the diameter of the Earth's orbit:

$$\Delta G = \frac{\partial G}{\partial r}\Delta r = \frac{\gamma m_s}{r_s^3}\, 2\Delta r \qquad (1\text{-}2)$$

$$\frac{\Delta G}{g_0} = \frac{m_s}{m_E}\left(\frac{r_E}{r_s}\right)^2 \frac{4r_b}{r_s} \approx 3\times 10^{-19}\ \text{gee}$$

where:

γ is the universal gravitational constant.

m_s is the mass of these stars ≈ two Sun masses (Ref. 168).

r_s is the distance of these stars from the solar system ≈ 4.3 light years.

r_b is the radius of the Earth's orbit around the Sun ≈ 1.6×10^{-5} light year.

m_E is the mass of the Earth.

r_E is a radius of the Earth = 4000 miles.

g_o is any value of the Earth's surface gravity.

This difference of 3×10^{-19} gee would take 14.5 years to produce a one foot displacement on a test body in the heliocentric inertial frame. Thus, the center of the Sun is suitable as an origin for a highly accurate inertial frame, if the mass of the Sun is increased by the mass of the planet when computing the orbit of that planet.

The effects of very distant stars and galaxies may be important in determining the inertia of bodies within the solar system, as discussed in Section 1.D.

The mass center of the Earth is also a convenient origin for an inertial frame which is useful in the study of orbits of the Earth and of lunar satellites and for the investigation of phenomena near the surface of the Earth. An Earth-centered frame, non-rotating relative to the distant galaxies, is an accurate inertial frame for most purposes but, when necessary, the gravity gradients of the other objects in the solar system can be included. The largest gradient is that caused by the Moon, because of its proximity. The difference in gravity on both sides of the Earth, caused by the gradient of the Moon's gravitational field, is:

$$\frac{\Delta G}{g_0} = 2\,\frac{m_M}{m_E}\left(\frac{r_E}{r_M}\right)^3 \approx 10^{-7}\ \text{gee}$$

where r_M is the distance between the mass centers of the Earth and Moon. 10^{-7} gee can be neglected for applications to small devices on the Earth but must be included, for example, when studying long-term effects on the orbits of Earth satellites.

The mass center of an artificial satellite of the Earth is also a suitable location for an inertial coordinate frame, if the axes are properly oriented so as to be non-rotating relative to the distant galaxies. Because the gravitational attraction of an artificial satellite on a nearby body is small compared to the gradients of the gravitational fields of the Earth and Moon, a satellite-centered, inertial frame must explicitly include gradients.

1. D. MACH'S PRINCIPLE.

Suppose an experiment is performed in which a pail of water is given different angular velocities relative to the Earth while observing the surface of water in the pail. Except at the equator, it will be found that a particular angular velocity of the pail relative to the Earth, namely that in which the pail is non-rotating relative to the distant galaxies, causes the water surface to be flat.

Newton maintained that absolute rotation could be detected by observing the plane of oscillation of a free pendulum or the surface of the

water in the pail. The modern observer might make the same claim for a rate gyro. The absolute coordinate frame thus defined appears not to rotate relative to the distant galaxies. Clemence (Ref. 162) believes that the "kinematic" inertial space defined by the distant galaxies does not rotate faster than 0.1 second of arc per century (3.2×10^{-11} deg./hr.) relative to the "dynamic" inertial space defined by Newton's laws. Nevertheless, the concept of an absolute space is repugnant in an operational sense since only relative motions are detectable and all experimental efforts to find an absolute inertial space (the ether, for example) have failed.

The key to the paradox, that absolute space was theoretically necessary but unmeasurable in practice, is the realization that if the surface of the water in the pail is curved when the pail rotates relative to the fixed stars, that an interaction must exist between the water and the stars. "(Newton's) simple assumption that the surface of the water in the pail would be as curved even if it were rotating in free space, as when rotating in space filled with starry matter, is not susceptible of physical verification" (Ref. 180, p. 106). It is only the relative angular velocity between the pail of water, the pendulum or the rate gyro and the stars that is relevant or observable. Hence a proper formulation of mechanics should not involve an absolute inertial space but should contain only the relative motion between the observer and the fixed stars. Kinematically, only the relative motion is observable so dynamically, nothing else should be necessary. But Newton's formulation gives preferred status to the inertial frame; only in that coordinate

frame is torque equal to the time rate of change of angular momentum. Additional terms are required in arbitrarily rotating frames. Clearly there must be a physical interaction between the fixed stars and local matter which results in a Coriolis and centripetal force when there is relative angular motion. This is the generalized form of Mach's principle.

The plane of a swinging pendulum rotates relative to the Earth because the distant stars, rotating around the Earth, apply Coriolis and centripetal forces to the pendulum. Thus, the assumption of an absolute inertial space has been replaced by the assumption of a long-range interaction between local matter and the distant stars. The latter assumption is to many persons the less objectionable, especially if direct experimental evidence of the long-range interaction should be found.

Sciama, at the University of Cambridge, has been studying long-range interactions which might yield the Coriolis and centripetal forces (Refs. 201, 202 and 203). His "gravmagnetic" $\frac{1}{r}$ interaction, suggested by analogy to the electromagnetic forces, has also been suggested by Wheeler and other unified field theorists on other grounds. Clearly, a covariant formulation of mechanics which does not presuppose an absolute inertial space but uses $\frac{1}{r}$ and $\frac{1}{r^2}$ interactions between mass particles may soon be a reality.

These same long-range interactions may also account for the inertia of all bodies. When a body accelerates relative to the distant

stars, a $\frac{1}{r}$ interaction results which is proportional to acceleration and which local observers may interpret as the inertial reaction. This classical form of Mach's principle is vital in modern cosmology since it offers the exciting possibility that the structure of the distant universe might be discerned by means of purely local measurements.

1. E. THE ORIENTATION OF AN INERTIAL COORDINATE FRAME.

Mach's principle asserts that inertia and inertial space are related to interactions between local matter and the distant stars. The local orientation of an inertial coordinate frame and the inertia of a local body then depends on a large number of statistical interactions. A measure of the angular stability of the inertial reference frame is the change in spacing between the heavenly bodies. Many heavenly bodies appear to have "proper motions" caused by:

1. relative motions between galaxies, motions of stars within the Milky Way galaxy and orbital motions within multiple star groups. The Milky Way galaxy rotates as a whole with an average period of 200×10^6 years (Ref. 207) or at 2×10^{-10} deg./hr. but since the Sun participates in this rotation, only the radial gradient of tangential velocity is observable as "star-streaming." This results in an apparent parallax caused by the Sun's motion in the Milky Way.

2. apparent parallax caused by the Earth's annual motion around the sun.

The largest measured proper motion is 10.3 seconds of arc per year for Barnard's star. Typical maximum proper motions are one second of arc per year (Ref. 156, p. 509). The measurement of proper motion from photographic plates is complicated by the unknown motion of those stars used as references. Galactic proper motions have not yet been detected but are presently being sought (Ref. 163, pp. 2-64). Thus, star motions are less than 0.1 second of arc per year = 3×10^{-9} deg./hr. and, as noted in Section 1.D., galactic motions do not exceed 3×10^{-11} deg./hr. Thus, 10^{-9} deg./hr. is an upper bound on the inherent error in the angular orientation of inertial space, manifested by motion among the fixed stars.

It has thus far been implied that all inertial frames are relatively non-rotating since each does not rotate relative to the same bulk of fixed stars and galaxies. However, the theory of relativity appears to inject a small qualification.

Measurements which are made between relatively accelerating orbital bodies do not agree, though each presumably qualifies as an origin for an operational inertial frame. In particular, the results of such measurements can be "explained" by postulating that an observer in each frame sees the other's inertial axes rotating relative to the fixed stars at a rate:

$$\frac{d\theta}{dt} = \frac{\gamma_o - 1}{V_o^2} \left| \bar{V}_o \times \bar{f}_T \right|$$

where:

$$\gamma_o^2 = \frac{1}{1 - V_o^2/c^2}$$

V_o is the velocity of one body in an inertial frame centered at the other.

f_T is the acceleration of one body, in an inertial frame centered at the other.

For a circular orbit:

$$\frac{d\theta}{dt} = \frac{\gamma_o - 1}{V_o^2} V_o f_T \approx \frac{V_o f_T}{2c^2} = \frac{V_o^3}{2rc^2}$$

This result was originally derived by Thomas (Ref. 237, pp. 162-3) to explain the radiation from an electron accelerating around a nucleus.

As an illustration, consider observers on the Earth and Sun. Each can establish a coordinate frame which he regards as non-rotating relative to the fixed stars. But if the solar observer makes measurements in the Earth coordinate frame or the Earth observer in the solar frame, each believes the other's "inertial" frame to be rotating relative to the fixed stars at a rate $\frac{V_o^3}{2rc^2}$, for a circular orbit.

Each observer maintains that his own coordinate frame is indeed inertial but that the other's is not. This situation, so typical in relativity, results because of the necessity of using light signals to communicate between frames.

For example, measurements of the precession of the apsides of the Moon's orbit relative to the fixed stars will differ by this amount, as observed by heliocentric and Earth-centered observers.

The angular velocity of a terrestrial inertial coordinate frame relative to the fixed stars, as observed in solar coordinates, or vice-versa, is evaluated as:

$$\frac{d\theta}{dt} = \frac{(62000)^3}{2(93\times10^8)(186300\times3600)^2} = 1.6\times10^{-10} \text{ deg./hr.}$$

whereas between the Earth and an orbiting satellite:

$$\frac{d\theta}{dt} = \frac{(25000)^3}{2(2.2\times10^7)(186200\times5280)^2} = 6\times10^{-8} \text{ deg./hr.}$$

These magnitudes are considerably less than can be observed using non-astronomic instrumentation. Indeed, when considering such low angular rates, the definition of a meaningful experiment to measure the relative angular velocity of such non-coincident coordinate frames is not immediately obvious because the two observers cannot communicate simultaneously.

10^{-7} deg./hr. represents a lower limit to the accuracy of inertial velocity measurements made between Earth satellites and the Earth.

Another limitation on the definition of angular velocity may result from the quantization of angular momentum implied by wave mechanics. On an atomic scale, angular momentum can occur only in integral multiples of $\hbar$. Even if this quantization also exists on a macroscopic scale, it would not be readily detectable since the increments of $n\hbar$ are so small, they appear continuous. For example, consider a gyroscope whose inner gimbal has a moment of inertia of three gm. $-cm.^2$ about its output axis (one tenth that of a HIG-4 gyroscope). The angular velocity of this gimbal can change in increments no smaller than:

$$\Delta\omega = \frac{\Delta H}{I} = \frac{\hbar}{I} = 7\times10^{-23} \text{ deg./hr.}$$

The servo loop on the output axis cannot null the angular velocity of the gimbal to better than a multiple of 10^{-22} deg./hr., a dozen and a half orders of magnitude from present performance levels. Section 1.J. summarizes this section.

1. F. TIME SCALES.

The universe might be described, at any time, by giving the energy states of all atoms and the positions and velocities of all particles in the manner of Laplace's omniscient mathematician. Time is then a measure of the changes in these states; when the universe passes from one condition to another it has aged. A totally new state, never experienced before, is called the future. The probability of the universe repeating a long sequence of states is so miniscule that we say time never repeats itself.

To define time by means of a sequence of repetitive events is a tautology. Repetition implies a prior definition of time since different classes of repetitive events proceed at different rates and can be used equally well to define different time scales. Some common time scales measured by repetitive events are discussed below.

For civil affairs, a suitable time scale must be readily measured and generally accepted. The rotation rate of the Earth commonly measures the civil day and the passage of the seasons, the civil year. Mean solar time is discussed in Section 1. G.

For astronomic purposes, these are not necessarily adequate. The primary use of time astronomically is to predict the relative positions of the heavenly bodies. The equations which define these positions are the Newtonian equations of dynamics, modified by relativistic corrections as needed for a solar system observer. Except at enormously high velocities within the solar system, time "decouples" from the

three space dimensions in the same manner for all observers. Thus, the independent variable in these equations is "gravitational" or "ephemeris" time. Hence, if it is believed that the equations of motion of a heavenly body, say the Earth, can be written quite completely, then the position of that body in the heavens will measure Ephemeris Time, by inverting the equations of motion. Indeed, the Ephemeris Time scale was formally introduced into the American Ephemeris and Nautical Almanac in 1960. Ephemeris Time is measurable to between one part in 10^8 and one part in 10^{10}, depending on the length of the interval to be measured (Ref. 162, p. 8).

Atomic physics has introduced an important frequency scale. When atoms are excited they absorb energy and later reradiate it, at discrete frequencies. These frequencies can be reproduced to one part in 10^{10} or better thus defining a time interval scale but not a time-epoch scale.

The comparison between the ephemeris and atomic time scales over periods of many years is now a major problem in physics. Since Milne's cosmology (Ref. 192) makes use of two different fundamental time scales, which are presently changing relative to each other at the rate of one part in 10^9 per year (Ref. 164, p. 571), there is some speculation that their physical counterparts are the atomic and Ephemeris Time scales (for example, Ref. 166). If the comparison shows that the two time scales proceed at different rates, interest will surely be intensified into the possibility that the gravitational constant, the velocity of light and the ratio of inertial to gravitational mass may be functions of epoch.

1.G. ASTRONOMIC TIME SCALES.

If the Earth were a point mass circling a spherical Sun, in the absence of other planets and satellites, the orbit would be a plane ellipse, non-rotating in inertial space, as described in Appendix C. The presence of the Moon and the other planets and the finite size of the Earth (the ellipticity of the Sun is so small it has never been measured) cause the orbit elements to change measurably. For example, the ephemeris (Ref. 156, pp. 490-91) gives the present rates of change or some orbit elements as:

$$\frac{di}{dt} = 47 \text{ sec. arc/century}$$

$$\frac{d\Omega}{dt} = 54.77 \text{ sec. arc/century}$$

$$\frac{d\Upsilon}{dt} = 0.01 \text{ sec. time/century}$$

$$\frac{d\epsilon}{dt} = -0.0000418 \text{ century}^{-1}$$

The projection onto the celestial sphere of the Sun's apparent path relative to the stars, as viewed from the Earth, is called the ecliptic. A mean ecliptic is defined which precesses at a uniform rate relative to the fixed stars. The Sun's apparent perturbations are always within one half second of arc of the mean ecliptic (Ref. 163).

The spin axis of the Earth does not maintain a fixed inertial direction. A slow change in direction of the Earth's axis results from the "gravitational gradient" torques exerted on the Earth by the Sun, the Moon and the planets (Ref. 55). The motion of the spin axis has three major components:

1. a gross non-uniform motion in a cone of half-angle 23° 27' whose axis is approximately perpendicular to the ecliptic. The period is 25, 800 years.

2. an oscillation whose double-amplitude is eighteen seconds of arc about the cone. The period is 18.6 years.

3. an irregular "planetary precession" at 0.1 second of arc per year.

This complicated motion of the spin axis is regarded as being made up of two parts. One is a uniform conical precession. The other is a small irregular nutation about the mean precessing spin axis. The terminology follows that used for the classical spinning top (Ref. 219, p. 159 ff.). As the spin axis changes its orientation in space, the Earth's mantle itself wobbles relative to the spin axis, as discussed in Appendix A. This "migration of the pole" is independent of the inertial orientation of the spin axis.

The precession and nutation of the Earth's spin axis in space causes the celestial equator to precess and nutate. A mean celestial equator is defined perpendicular to the mean precessing pole. The equinox is defined as the intersection of the ecliptic and the celestial equator. The direction along which the Sun crosses from the southern to the northern celestial hemisphere is called the vernal equinox:

1. the "true equinox" or "equinox of data" is the intersection of the instantaneous ecliptic with the instantaneous celestial equator.

2. the "mean equinox" is the intersection of the mean ecliptic

and the mean equator.

3. a "fixed equinox" is the position of the mean equinox at some specified date, say midnight January 1, 1950 or 1960.

The various equinoxes have been used historically as origins for the measurement of right ascension. The celestial equators have been used as references for the measurement of declination.

A fixed equinox is truly an inertially non-rotating line. The mean equinox is not; it precesses uniformly along the mean equator at a rate of about fifty seconds of arc per year (1.6×10^{-6} deg./hr.). The difference in orientation between the mean and true equinox is the "nutation of the equinoxes," resolved into a nutation in right ascension and a nutation in declination. The former measures the difference between mean and true sidereal time.

The true and mean sidereal days are defined as the intervals between successive transits of the true and mean vernal equinox over the astronomic meridian. The true and mean sidereal days never differ in length by more than 0.01 second of time (Ref. 188, p. 226). Sidereal time is the fundamental time observation which the astronomer makes.

Mean solar time is theoretically defined in terms of the mathematically uniform motion of a fictitious mean Sun along the mean ecliptic. Simplified tables are included in the national ephemerides to allow mean solar time to be calculated from sidereal time.

Ephemeris Time is defined in terms of the motion of the Earth

around the Sun. Ephemeris Time differs from mean solar time by virtue of the changes in the spin rate of the Earth and discrepancies between the periods of the mean Sun and the actual Sun. Since the Moon moves across the heavens ten times faster than the Sun, Ephemeris Time is actually measured using the motion of the Moon, as discussed in Section 1.H.

Mean solar time, as measured at Greenwich, is now known as Universal Time. It was formerly known as Greenwich Mean Time in England and as Greenwich Civil Time in the United States.

1.H. THE MEASUREMENT OF TIME.

Ephemeris Time is defined using the motion of the Earth in the solar system and is measured using the position of the Moon, for convenience. Brown's "Tables of the Motion of the Moon" (Ref. 160) predict the Moon's position versus Ephemeris Time. The Markowitz Dual-Rate Moon Camera can photograph the Moon against a star background to measure its position accurately. Brown's tables are entered with this observed position to find the tabulated Ephemeris Time of observation. In the words of the 1960 ephemeris, "...the measure of time is determined by the inverse relation expressing the time as a function of the position, and this relation is the practical means of determining its numerical value." (Ref. 156, p. 482.).

Mean sidereal time is defined by successive meridian transits of

the mean vernal equinox. Sidereal time is the fundamental time of observation for astronomers. Mean solar time is found from sidereal time using the equation of the mean Sun in the ecliptic. The raw Universal Time (mean solar time at Greenwich) is designated UT_o. When corrected for migration of the poles and for the seasonal variation in spin rate of the Earth, it is designated UT_2 and rarely differs from UT_o by more than 0.1 second (Ref. 188). UT_2 cannot be calculated exactly until some months after observation but an approximate UT_2 is broadcast on radio and corrected by means of later published tables. UT_2 is broadcast by NSS, operated by the United States Naval Observatory, and by WWV, operated by the National Bureau of Standards. The American Practical Navigator (Ref. 4, p. 491) claims that NSS broadcasts UT_2 to an accuracy of 0.01 second but that WWV is reliable only for frequency.

By comparing UT_2 with Ephemeris Time, the non-seasonal component of the fluctuation in spin rate of the Earth is detectable, statistically. This fluctuation is generally not larger than one part in 10^7 per day and one part in 10^8 over longer periods of time, as discussed in Appendix A.

Between astronomic observations, time is kept by pendulum clocks, quartz crystal clocks, atomic clocks or combinations thereof. The Shortt Pendulum Clock was universally in use before World War II. Its pendulum oscillates in a vacuum and receives impulses every thirty seconds as it passes through the vertical position. The Shortt Clock is discussed in detail by Bomford (Ref. 87, pp. 232-233). It can maintain

an accuracy of 0.01 to 0.02 second for several days, according to that reference.

Quartz clocks were introduced about 1944. They are thermostatically controlled quartz-crystal oscillators, discussed in detail by Smith (Ref. 205). He gives their accuracy as one part in 10^8 per year when oscillating at 1000, 000 cps, but notes that the crystal deteriorates with age in several years. Observatories commonly use many (five to twelve) such clocks whose crystals are differently aged and plot the error curves for each clock from sidereal measurements.

Atomic clocks produce a constant frequency output equal to the frequency of one of the spectral lines reradiated after absorption of energy by Cesium, Rubidium or Ammonia molecules. Microwave energy is supplied to a tube of this material and the frequency servoed to that of maximum absorption for one spectral line. The resonant frequency is then used to control the frequency of a quartz clock. The bandwidth at resonance is narrowed by reducing the density and temperature of the confined gas. Lyons (Ref. 227) discusses atomic clocks in detail. The Cesium clock is reputed to have an accuracy of one part in 10^{10} indefinitely at present (Ref. 170). The absence of long term drift makes the atomic clock ideal for relativity experiments, time-keeping, navigation velocity measurements (Doppler shifts), etc.

1.J. SUMMARY.

Included among the information required by the inertial navigator are time and the inertial angular velocities of his instruments and of the Earth.

Time interval, not time epoch, is implicit in the navigation process since it is the independent variable of integration in the computer. Time interval or frequency is also necessary in the power supply of a device such as a gyro wheel. The ultimate accuracy of Ephemeris Time is at least one part in 10^{10} as measured in astronomic observatories. However, for accuracies greater than a part in 10^{9}, it may be necessary to distinguish between atomic and Ephemeris Times. Since solid-state properties of materials regulate the computer processes, the computer operates on an atomic time scale. The inertial sensors must function on a hybrid time base whose exact definition awaits the unification of mechanics and atomic physics. The inertial behavior of the sensors introduces Ephemeris Time but material properties such as viscosity, which balance the inertia forces, are derived atomically. For accuracies greater than one part in 10^{8}, relativistic navigation equations are required at orbital speeds.

For accuracies poorer than one part in 10^{7}, mean solar or mean sidereal time can be substituted for Ephemeris Time and the spin rate of the Earth assumed uniform. For accuracies less than one part in 10^{6}, the distinction between true sidereal and mean sidereal time is not discernible.

The measurement of the inertial angular velocity of the instrument package is presently limited by imperfections in the sensors (gyro drift) not by limitations on the nature of inertial space. However, it appears that if inertial sensors improve to an accuracy of 10^{-7} deg./hr., relativistic effects may require a redefinition of the term "inertial angular velocity." At 10^{-9} deg./hr. the measurement of inertial space by means of the fixed stars becomes suspect and at 10^{-11} deg./hr., it becomes useless.

Knowledge of the inertial angular velocity of the Earth is necessary in order to transform inertial measurements into an Earth-bound coordinate frame. The spin rate of the Earth is conventionally given as the mean sidereal period, 86, 164.09 ephemeris seconds. Clearly this is not the correct inertial period since sidereal days are measured between transits of the precessing mean equinox. The time between transits of a fixed star, the inertial day, is 86, 164.10 ephemeris seconds, a difference of one part in 10^7 compared to the mean sidereal day. The spin rate of the Earth can be considered constant to one part in 10^7.

The adjective "sidereal" is used in two different senses by astronomers. Sometimes, as in "sidereal year," it refers to rotation in inertial space. Otherwise, as in "sidereal day," it refers to rotation relative to the equinox. This writer suggests that "sidereal" be replaced by "inertial" or "equinoctial" when referring to inertial space or the equinoxes, respectively.

The inertial precession of the Earth's spin axis and its migration

relative to the geographic polar axis cause the Earth-centered "inertially-non-rotating" coordinate frame, x_i, to have an inertial angular velocity perpendicular to the spin axis of about $360^{\circ} \times \sin 23\frac{1}{2}^{\circ}$ per 25,800 years or 6.4×10^{-7} degree per hour. Hence, if the nutation is included, the component of inertial angular velocity normal to the instantaneous spin axis probably does not exceed 10^{-6} deg./hr. Migration of the instantaneous pole relative to the geographic pole causes the Earth to have an angular velocity of 5×10^{-5} deg./hr. relative to x_i, perpendicular to the polar axis.

Figure 5-14 shows a tabular summary of this chapter.

Chapter Two

THE SHAPE, ANGULAR VELOCITY AND GRAVITY FIELD OF A PLANET

2.A. INTRODUCTION.

A planet such as the Earth, is of interest to navigators as a base on which to locate points of interest and as the source of gravity and magnetic fields. Besides locating origins, destinations and check-points, the navigator uses the planet's surface as a reference for the measurement of velocity and direction.

The direction of the gravity field around the planet is of interest since most instruments must be oriented in some known way relative to the planet and the gravity field provides a convenient direction. In particular, the inertial navigator must know the components of gravity in his navigational coordinate frame so he can subtract them from the accelerometer outputs (see Chapter Four). But in order to relate the

accelerometer outputs to the accelerometer's position relative to the planet, the navigator must know the angular velocities of inertial space and of the planet with respect to the accelerometer platform.

Consequently, this chapter considers the size, shape, angular velocity and gravity field of a planet in general. The Moon, Mars and Venus are considered because they are likely to be the earliest explored. Jupiter is discussed as a typical major planet. All are referred to as the "navigable planets" for convenience. Chapter Three is concerned entirely with geodesy, the science of locating points on the surface of the Earth, and Chapters Four and Five apply this information to navigation.

2.B. GRAVITY POTENTIAL AND GRAVITATIONAL POTENTIAL OF A ROTATING MASS.

The Newtonian gravitational potential at the point (x, y, z) of a collection of N masses, m_i, located at the points (x_i, y_i, z_i) is:

$$V = \sum_{i=1}^{i=N} \frac{\gamma m_i}{\left[(x-x_i)^2 + (y-y_i)^2 + (z-z_i)^2\right]^{1/2}} \qquad (2\text{-}1)$$

where γ is the Newtonian constant of gravitation=6.668×10^{-8} dyne-cm.^{2}/gm.^{2} (Ref. 154, pg. 282). V is a scalar function of position and de-

fines a scalar field at each point in space. The gravitational force acting on a point test mass, dm_T, is:

$$\overline{dF_T} = dm_T \overline{\nabla} V$$

where $\overline{\nabla}$ is the vector gradient operator defined in Appendix D for those coordinate frames of interest in this thesis. The gravitational force per unit mass defines the vector gravitational field at each point in space, in magnitude and direction.

Suppose a test mass is constrained not to move relative to a coordinate frame whose origin is located at the center of mass of the N particles and which is non-rotating in inertial space. Then if the only forces which act on the test particle are the gravitational force, $dm_T \overline{G}$, and the constraint force, $\overline{dF_c}$, the specific constraint force, $\overline{f_c} = \frac{\overline{dF_c}}{dm_T}$, clearly is the negative of the gravitational force:

$$\overline{dF_c} + dm_T \overline{G} = 0$$

$$\frac{\overline{dF_c}}{dm_T} = \overline{f_c} = -\overline{G} \qquad (2\text{-}2)$$

Hence the constraint force measures the gravitational field.

Suppose the collection of N masses rotates rigidly at a constant angular velocity, $\overline{\omega}_{IP}$. Then a constraint force, $\overline{f_c}$, is needed to hold the test mass fixed in this rotating coordinate frame:

$$\overline{f_c} = -\overline{G} + \overline{\omega}_{IP} \times (\overline{\omega}_{IP} \times \overline{r})$$

$$= -\overline{\nabla} V + \overline{\omega}_{IP} \times (\overline{\omega}_{IP} \times \overline{r}) \qquad (2\text{-}3)$$

where $\overline{r}$ is the instantaneous position vector locating the test mass.

Figure 2-1

THE SPHERICAL AND CYLINDRICAL COORDINATES OF THE POINT, P.

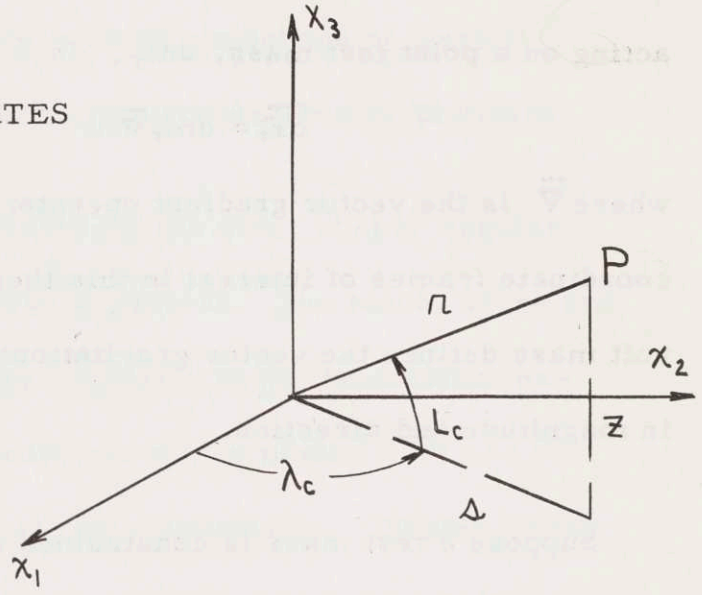

Figure 2-2

THE GEOID AND COGEOID OF A PLANET

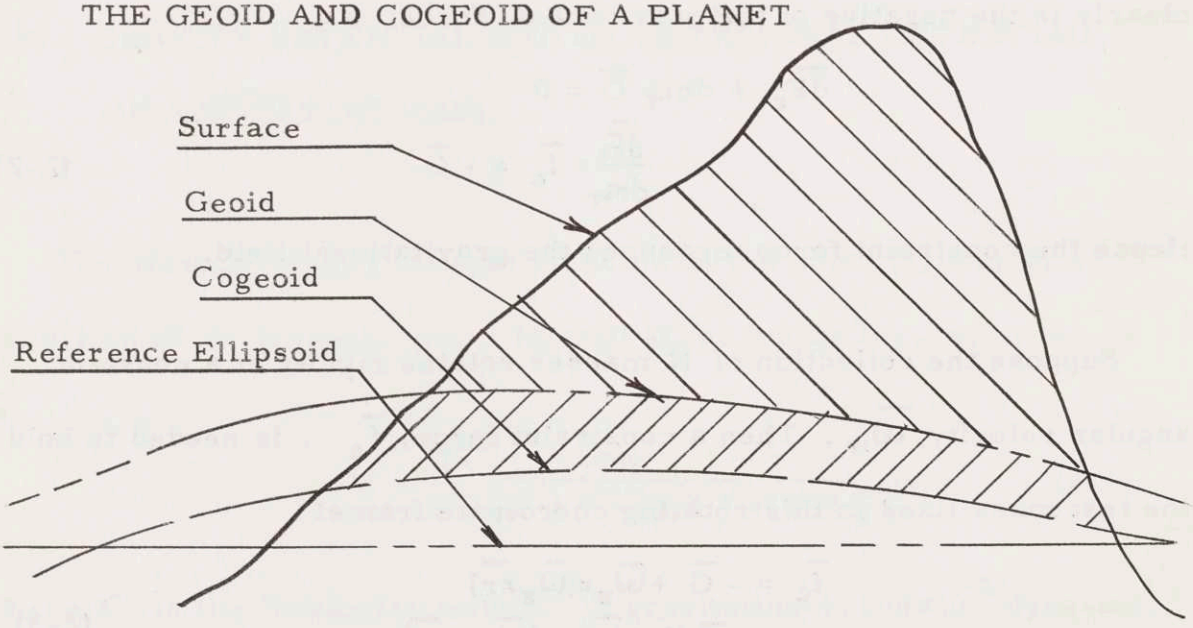

Since the curl of $\overline{\omega}_{IP} \times (\overline{\omega}_{IP} \times \overline{r})$ is zero, $\overline{f}_c$ can be expressed as the gradient of a scalar potential, U:

$$\overline{g} = \overline{\nabla} U$$
$$U = V + V' \tag{2-4}$$

where V is the gravitational potential of Equation (2-1) and the rotation potential, V', is:

$$V' = \frac{\omega_{IP}^2 s^2}{2} \tag{2-5}$$

in cylindrical coordinates. s is the distance from the axis of rotation to the test mass. V' in spherical coordinates is:

$$V' = \frac{\omega_{IP}^2 r^2}{2} \cos^2 L_c \tag{2-6}$$

where L_c is the geocentric latitude, Figure 2-1, and in confocal, ellipsoidal coordinates:

$$V' = \frac{\omega_{IP}^2 c^2}{2} \cosh^2 \xi \cos^2 \eta \tag{2-7}$$

where c is the focal distance of the ellipsoid representing the geoid of the planet. ξ and η are the elliptic and hyperbolic coordinates, respectively, as defined in Appendix C.

Using the results of Appendix D. 5., the rotation potential in geographic coordinates is:

$$V' = \frac{\omega_{IP}^2}{2} (\rho_p + h_g) \cos^2 L_g \tag{2-8}$$

where:

L_g is the geographic latitude of the test mass,

h_g is its height above the reference ellipsoid

ρ_P is the prime radius of curvature of the ellipsoid at a point geographically below the test mass.

Thus, in a uniformly rotating coordinate frame, a position-dependent potential, U, can be defined whose gradient at any point, P, is the specific force necessary to hold a test mass fixed at P in the rotating coordinate frame. Following Wrigley (Ref. 82, pg. 6) U is designated the "gravity potential." If the test mass is moving relative to the rotating coordinate frame, the constraint force cannot, in general, be derived from a position-dependent potential and Coriolis' Law must be used in its entirety.

Clearly, the constraint force can be regarded as the sum of two components. One is equal and opposite to the gravitational attraction between the collection of N particles and the test mass. The other component provides sufficient centripetal acceleration to constrain the test mass to a circular path in inertial space.

2.C. THE SHAPE OF A ROTATING FLUID.

The study of the shape and gravity field of the planets logically begins with an examination of the possible shapes that can be assumed by a fluid rotating rigidly at constant speed relative to inertial space, in hydrostatic equilibrium and held together by its own gravitation. This problem was considered at the turn of the century by Poincaré (Ref. 138) and later by Lamb (Ref. 226). The condition which such a fluid must satisfy is that three surfaces; the interface between the fluid and the surrounding medium, a surface of constant pressure and an equipotential surface of gravitation and rotation (constant U), must all coincide (Ibid., pg. 698).

The interface must be a surface of constant pressure since a fluid in equilibrium cannot sustain shear. No matter what the shape of the surface or the internal density distribution, the center of volume of the interface must coincide with the mass center of the rotating mass since it is a bounding equipotential and contains all of the rotating mass (Ref. 87, pg. 334).

Lamb shows that any mass of fluid which is non-rotating in inertial space must assume the equilibrium form of a sphere, independent of its internal density distribution (Ref. 226, pg. 699). As its inertial angular velocity increases from zero, the sphere elongates along its equator

Figure 2-3

THE MACLAURIN ELLIPSOIDS

ω_{ip} is the angular velocity of the rigidly rotating fluid

ρ is the density of the homogeneous fluid

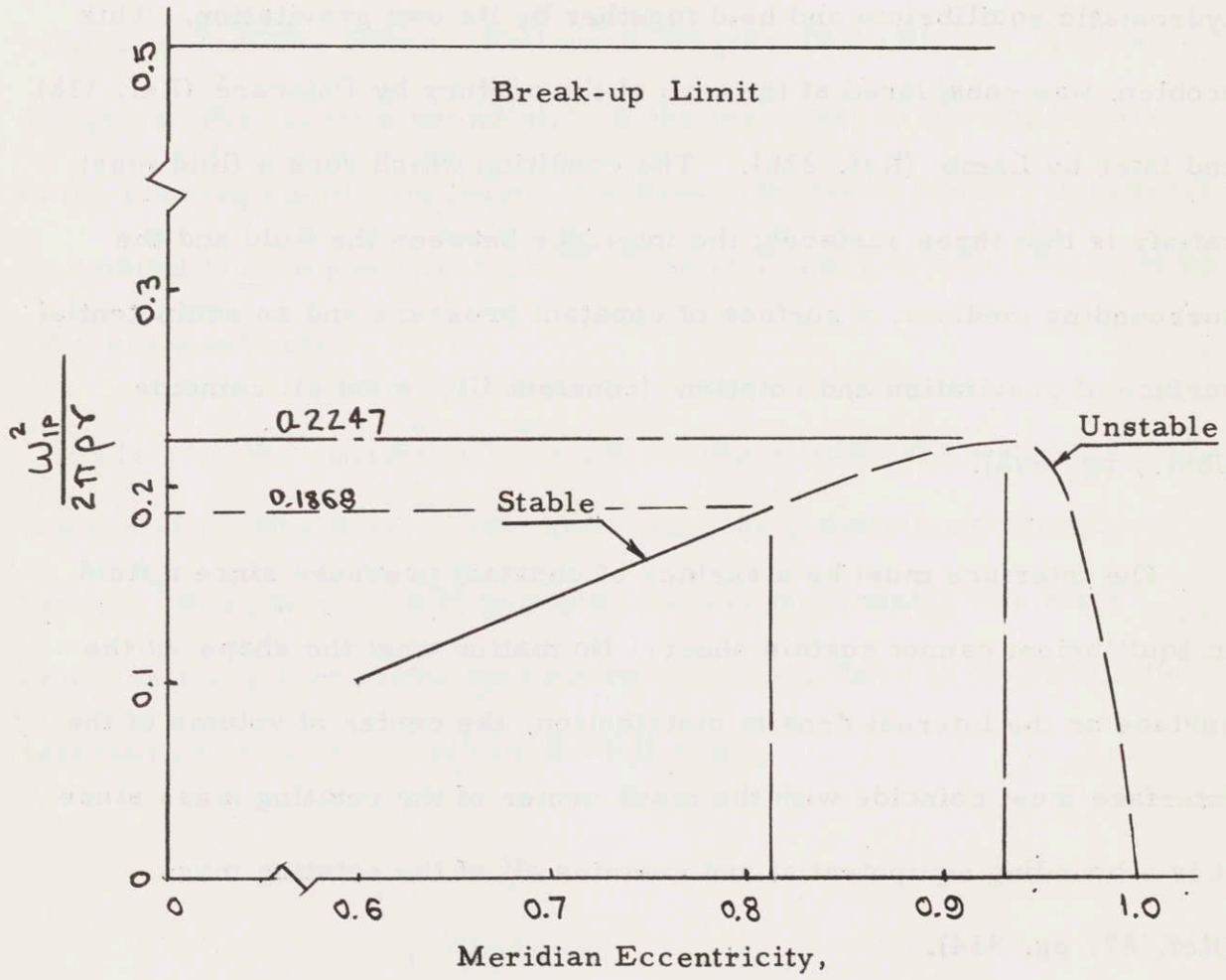

Calculated from data in Reference 226, pg. 702.

since the mass attraction is inadequate to supply the centripetal acceleration required to hold a spherical form.

The elongated shape assumed by the fluid is not uniquely determined by the inertial angular velocity. For a homogeneous fluid which is rotating at a constant inertial angular velocity in hydrostatic equilibrium, two families of possible shapes are of interest. One is a family of ellipsoids of rotation called MacLaurin ellipsoids which are symmetrical about the axis of rotation. The meridian eccentricity, ϵ, which results from any angular velocity, $\bar{\omega}_{ip}$, is shown in Figure 2-3 in non-dimensional form. Appendix C derives the relation between $\frac{\omega_{ip}^2}{2\pi\rho\gamma}$ and ϵ but the graph is calculated from data in Reference 226, pg. 702. For any angular velocity, two ellipsoidal surfaces are possible but only one is stable (solid line). Clearly, for speeds above $\frac{\omega_{ip}^2}{2\pi\rho\gamma} = 0.1868$, the MacLaurin family is not stable and the fluid assumes an elongated, non-ellipsoidal shape. For any lower speeds:

$$0 < \frac{\omega_{ip}^2}{2\pi\rho\gamma} < 0.1868$$

the fluid can assume an oblate ellipsoidal shape whose meridian eccentricity decreases to zero as the angular velocity of the fluid tends to zero.

A second family of shapes that can be assumed by a homogeneous rotating fluid are the triaxial ellipsoids of Jacobi. Figure 2-4 shows

Figure 2-4

POSSIBLE ELLIPSOIDAL SHAPES

OF A HOMOGENEOUS ROTATING FLUID

a_1 and a_2 are the equatorial semi-diameters

b is the semi-diameter along the axis of rotation

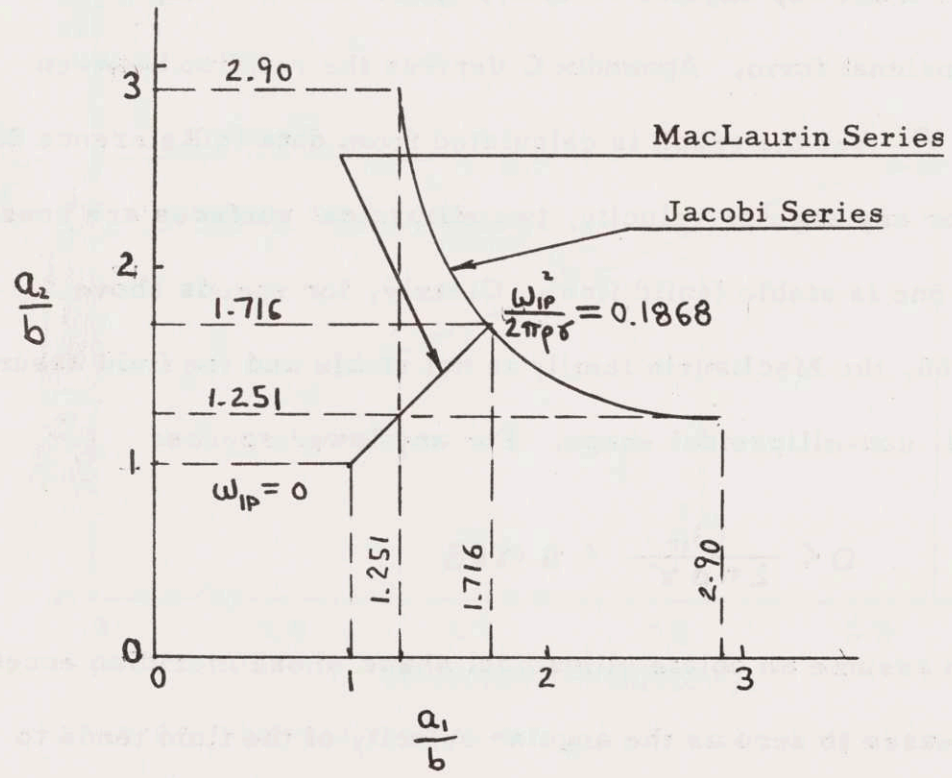

Figure adapted from References 138, pg. 163 and 226, pg. 705.

the ratios of the two equatorial principal axes of these ellipsoids to the length of the polar axis, with ω_{ip} as a parameter (Refs. 138, pg. 163 and 226 pg. 705). The 45° straight line locus from $\omega_{ip} = 0$ to $\frac{\omega_{ip}^2}{2\pi\rho\gamma} = 0.1868$ represents the MacLaurin family. The hyperbola-like locus is the Jacobi family. As the angular velocity of the fluid increases from zero, the shape of the fluid progresses from that of a sphere through either the family of MacLaurin ellipsoids or the Jacobi ellipsoids and then to elongated but non-ellipsoidal forms which finally break up when $\frac{\omega_{ip}^2}{2\pi\rho\gamma} = \frac{1}{2}$

Figure 2-5 shows the ratio $\frac{\omega_{ip}^2}{2\pi\rho\gamma}$ for the navigable planets. Since each is < 0.1868, any of these planets can assume the shape of a stable MacLaurin ellipsoid based on the accepted value of its average density. The shapes of planets, as distinguished from those of ideal fluids, are discussed in Section 2.E.

2.D. THE GEOID AND COGEOID.

The shape of the Earth has been extensively studied. Simple observation indicates that the surface of the Earth is not ellipsoidal. The surface features vary 50,000 feet from mountain top to ocean depth and are a very complex surface for mapping or navigation.

Figure 2-5

ANGULAR VELOCITY CHARACTERISTICS

OF THE NAVIGABLE PLANETS

Planet	$\omega_{IP} \times 10^5$ rad./sec.	ρ_{AV} gm./cm^3	$\frac{\omega_{IP}^2}{2\pi\rho\gamma}$	Break-up	
				$\omega_b \times 10^5$ rad./sec.	$\uparrow_b$ hrs.
Venus	?	4.9	?	102	1.7
Earth	7.2921	5.52	0.00232	108	1.62
Mars	7.0882	3.85	0.00310	89.7	1.94
Jupiter	17.7	1.33	0.0561	52.6	3.31
Moon	0.266	3.33	5.1×10^{-6}	83.6	2.09

Data from References 156, pg. 502; 200, Table 4; 121, pg. 139.

The surfaces of constant gravity potential, U, of the Earth, including Newtonian gravitation and rotation, are called geops. These are much smoother than the actual surface, undulating only about 200 meters (Ref. 122, pg. 151). The smoothness of the geops compared to the surface leads to the conclusion that large mass excesses on the surface of the Earth, which should cause a larger rise in the geops than is noted, are compensated by mass deficiencies below the surface. This is the theory of isostasy (Ref. 121, pg. 172 ff.) which postulates that about 30 to 100 kilometers below the surface, the pressure of the overlying rock is uniform, averaged over areas of several square miles and that the material above floats hydrostatically.

Over the oceans, the geops are generally parallel to the mean water surface, undulating slightly near such ocean features as trenches, islands and continental shelves. They rise slightly under mountains (but only about 100 meters under a 20,000 foot mountain) whereas in valleys, the valley floor dips below them. The geops are affected somewhat by the passage of the Sun and Moon overhead since these heavenly bodies change the gravitational potential slightly.

Figure 2-6 shows a point, P, fixed to the surface of the Earth. Suppose P and the mass centers of the Earth and Moon are in line, as shown. Then the magnitude of the downward force on P is approxi-

Figure 2-6

THE EFFECT OF THE MOON OR SUN

ON THE HEIGHT OF THE GEOID

$\overline{EP} = r_E$

$\overline{EM} = r_M$

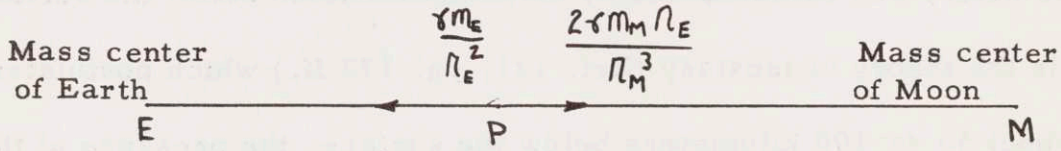

Figure 2-7

LIBRATIONS OF THE MOON

Gravitational gradient torque exerted by the Earth on the Moon.

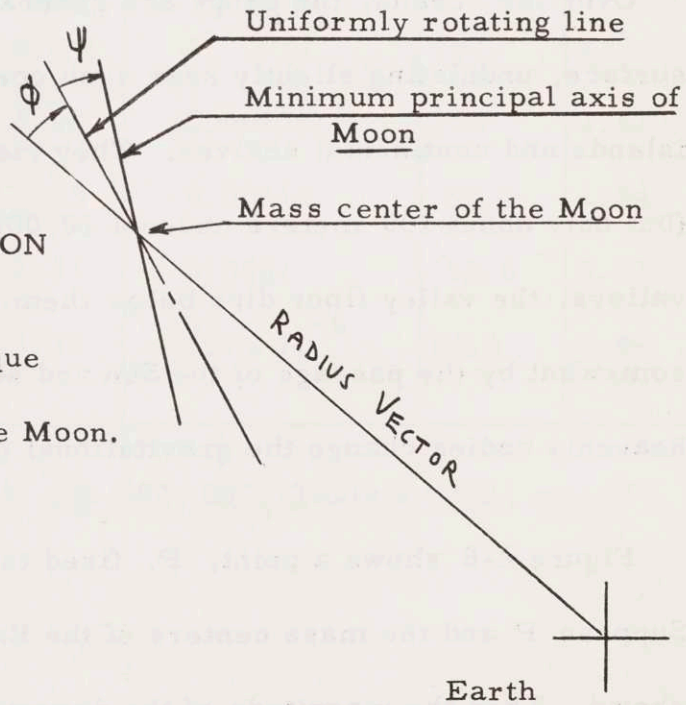

mately:

$$G = \frac{\gamma m_E}{r_E^2} - \frac{\gamma m_M}{(r_M - r_E)^2} + \frac{\gamma m_M}{r_M^2}$$

$$\simeq \frac{\gamma m_E}{r_E^2} + \frac{2\gamma m_M r_E}{r_M^3}$$

m_E and m_M are the masses of the Earth and Moon. r_M is the distance of the Moon from the Earth and r_E is the radius of the Earth.

An observer in Earth-centered coordinates can derive this gravitational field from a scalar potential, V_p :

$$V_p = -\frac{\gamma m_E}{r_E} + \frac{\gamma m_M r_E^2}{r_M^3}$$

When the Moon moves from the +x to the -x axis, V_p changes by:

$$\Delta V_p = \frac{\partial V_p}{\partial r_M} 2 r_E$$

$$= -6 \frac{\gamma m_M}{r_M^4} r_E^3$$

In order to restore the potential to its constant value, the point, P, must move an amount Δr_E relative to the Earth:

$$\Delta r_E = \frac{\Delta V_p}{\partial V_p / \partial r_E}$$

$$\simeq \frac{-6 \frac{m_M}{m_E} \left(\frac{r_E}{r_M}\right)^4 r_E}{1 + 2 \frac{m_M}{m_E} \left(\frac{r_E}{r_M}\right)^3} \qquad (2\text{-}9)$$

The change in height of the geop caused by the Sun is:

$$m_S = 3.3 \times 10^{-6}\ m_E$$

$$r_E = 4000 \text{ miles}$$

$$r_S = 10^{8} \text{ miles}$$

$$\Delta r_E = 10^{-4} \text{ foot}$$

The change in height of the geop caused by the Moon is:

$$m_M = m_E / 82$$

$$r_M = 240,000 \text{ miles}$$

$$\Delta r_E = 0.23 \text{ foot}$$

Hence the maximum displacement of any geop near the Earth's surface caused by the motions of the heavenly bodies is a three inch diurnal rise and fall. This is negligible compared to the one meter present accuracy in the measurement of the geoid. It sets a lower bound on the accuracy of a levelling survey (Section 3.D.).

Similarly, a change in the Earth's spin rate of one part in 10^7 will cause a change in the elevation of the geops at the equator of $\Delta\Omega_E'$ where:

$$g = G - \omega_{IE}^2 \Omega_E$$

$$\Delta g = \frac{\partial g}{\partial \omega_{IE}} \Delta\omega_{IE} = \frac{\partial g}{\partial \Omega_E} \Delta\Omega_E'$$

$$\Delta\Omega_E' = \frac{\omega_{IE} \Omega_E^2 \Delta\omega_{IE}}{G + \frac{\omega_{IE}^2 \Omega_E}{2}} \simeq 0.007 \text{ ft.} \qquad (2\text{-}10)$$

which is insignificant. Even at twice the radius of the Earth, the change in the gravity field that results from small changes in the Earth's spin rate is insignificant.

The geop coinciding with mean sea level is singled out as the "geoid." The relation between the actual sea level at various points on the Earth and the geoid is exceedingly difficult to measure. A purely stagnant ocean should coincide with the geoid. However, wave action, the tides propelled around the Earth each day by the Sun and Moon and the presence of winds and currents all cause the sea level to depart from the geoid. Stommel (Ref. 144) estimates the variation caused by winds and Coriolis-driven currents to be ± 4 feet and geodetic surveys have confirmed this (Section 3.D.).

The geops lie beneath the surface of the Earth in places and thus are not bounding equipotentials of the mass of the Earth. Hence the centers of volume of those geops which are not entirely external to the surface need not coincide with the mass center of the Earth (Ref. 87, pg. 334). Bomford (Ibid., pg. 336) estimates a discrepancy of only one meter between the center of volume of the geoid and the mass center of the Earth. Since navigation beneath the surface of the Earth is of little present interest (the case of a submarine which travels outside the rocky surface of the Earth but beneath substantial amounts of water is considered separately), only those geops external to the Earth are considered. $\bar{g} = \bar{\nabla} U$ is normal to the geops by definition.

It is clear that the knowledge of the direction of gravity determines a lower limit of accuracy for navigation. Section 2.F. shows that it is convenient to define the direction of the actual gravity vector, $\bar{g}$, at a point by specifying the direction of a reference gravity field, $\bar{g}'$, at that point and the "deflection of the vertical," $\bar{\delta}_v$, which is the vector angle from $\bar{g}'$ to $\bar{g}$. The selection of a reference direction at any point is discussed in Section 2.F. Thus, a complete knowledge of $\bar{g}$ requires the definition of a reference vector gravity field and the measurement of the vector deflection of the vertical throughout space. Clearly this is impractical but a compromise between measuring the actual field fully and relying exclusively on the reference field can be effected. The compromise involves the definition of the cogeops, each of which is a bounding equipotential of a fictitious Earth and is obtained by removing the mass outside the geoid according to a prearranged scheme.

Consider a geop, say the geoid. Figure 2-2 shows the surface of the Earth, the geoid and an ellipsoid of rotation used as a reference surface (Section 3.G.). The cross-hatched area protrudes from the geoid. To obtain the cogeoid, this external material is removed and the new equipotential is computed. The removal of mass depresses the equipotential slightly, exposing more mass outside the new equipotential. This too is removed. This removal is repeated until the equipotential approaches a limiting surface called the "cogeoid" which contains all the remaining mass of the Earth (Ref. 87, pg. 339).

The mass of the atmosphere is ignored since near the surface of the Earth, the atmosphere reduces gravity by only one part in 10^6 (Ref. 104, pg. 60).

This same process process can be repeated with each geop to get a corresponding cogeop at the same potential. Clearly, in removing mass outside the geoid, the mass of the Earth has been reduced slightly. This is unimportant for navigation since it merely changes the magnitude of gravity but not its direction. However, if the mass center of the total mass removed is not at the mass center of the Earth, the new mass center of the fictitious Earth will be displaced as much as 600 meters (Ref. 87, pg. 335) from that of the actual Earth. Thus, the compensation schemes for determining the mass removal must insure that the mass center of the Earth is not displaced and must assume some density distribution in the removed material to enable the separation of the geoid to the cogeoid to be computed. Many compensation schemes exist such as the Bowie, Airy, Hayford and Pratt compensations (Refs. 87, pgs. 338-363; 104, pgs. 148-183). The cogeops are clearly not unique but depend on the compensation scheme used. Those geops which lie entirely outside the surface of the Earth coincide with the cogeops at the same potential.

The cogeops and cogeoid are important because they are bounding equipotentials of the contained mass. Thus, their centers of volume

lie at the mass center of the Earth, if they are correctly compensated. Because of this, the theorems of Stokes and Vening-Meinesz can be used to find their shapes relative to an assumed reference surface, purely from gravity measurements. Such a procedure is called a "gravimetric survey" and is discussed in Section 3. J. 2. From these same gravity measurements, the absolute deflection of the vertical can be calculated relative to some assumed reference surface, whose origin is at the mass center of the Earth. Such deflections of the vertical are especially valuable since they cannot be found by astro-geodetic methods.

The shape of the geoid of another planet cannot be evaluated until extensive gravimetric and astrogeodetic surveys have been initiated. Hence, for the use of early visitors to the planets, such niceties as the difference between the geoid, cogeoid and reference surface must be ignored and all reference be made to a combined reference surface and provisional geoid established by indirect methods as in Section 2. E. Accurate values of surface gravity, size and shape must await a landing followed by gravimetric and astrogeodetic surveys. The early vehicles are advised to be self-adaptive to small changes in gravity and the reference coordinate frame.

2.E. THE SHAPES AND ANGULAR VELOCITIES OF THE PLANETS.

The first visits to other planets, whether by manned or automatic vehicles, will be conducted in appalling ignorance of the size, shape and gravity fields of the planets, as noted in Section 2.D. Hence, early astronauts must have advance estimates available of the gravity field and of the size and shape of the planet before arrival. This section will discuss suitable reference surfaces for the navigable planets and the inertial angular velocities which these reference surfaces must have.

Figure 2-5 shows the ratio $\frac{\omega_{1P}^2}{2\pi\rho\gamma}$ for the navigable planets. Since each is <0.1868, any of these planets can assume the shape of a Mac-Laurin ellipsoid based on the accepted value of its average density, as discussed in Section 2.C. The assumptions that lead to an ellipsoidal form are:

1. The body is homogeneous.
2. The body cannot sustain inertial shear (it is in internal equilibrium) or tension.
3. The body rotates rigidly.
4. The rigidly rotating body turns at constant angular velocity in inertial space.

These assumptions are considered one at a time insofar as they pertain to a planet.

1. The planets cannot be homogeneous since the weight of the overlying material must cause enormous internal pressures which would result in the segregation of material by density and in an increase in density because of compression and change of crystal phase. At least three density discontinuities are known within the Earth (Ref. 104, pgs. 6-13) including the now famous Mohorovičic discontinuity through which the "Mohole" is to be drilled (Ref. 85).

Density inhomogenieties can be especially prominent in planets such as Jupiter and Saturn which have gaseous and liquid outer layers of unknown depth. Jeffreys, Message and others (Refs. 119; 120; 128) at the University of Cambridge in England are deducing the density distributions within the planets on the basis of observations of the planet's satellites. This interesting geophysical study is possible since, as shown in Appendix F, the orbit of a satellite precesses at a rate determined by constants in the spherical harmonic expansion of the gravitational potential. In turn, these constants are functions of the density distribution within the planet (Ibid. also Refs. 121, pgs. 145-162 and 133 ff.). Hence, by observing the motion of a planet's satellites, the density distribution within the planet may be inferred. Jeffreys (Ref. 121, pgs. 157 ff.) states that Venus, the Earth and Mars have cores whereas the Moon does not.

2. The assumption of fluid equilibrium is resonable for the planets

since they probably originated as hot, fluid masses which later cooled to their present temperatures (Ref. 121, pgs. 283-284). However, even if the planets condensed from cold dust (Ibid. and Ref. 200, pg. 133), they have been rotating about their present spin axes long enough to be in hydrostatic equilibrium unless large internal stresses can be sustained without flow.

Recent studies by O'Keefe (Ref. 135) of artificial Earth satellite orbits show that the equipotential surfaces of the Earth are not symmetric about the equatorial plane but in fact are slightly pear-shaped (that is, the potential contains odd spherical harmonics of third order and higher, Section 2.F.5.). This result is of enormous interest to geophysicists since it indicates the existence of stresses within the Earth. Though Brenner et al. (Ref. 90) have disputed the existence of odd harmonics, O'Keefe's results apprear substantially correct.

3. Rigid rotation is an excellent mathematical model for the rocky planets such as the Moon, Venus, Mars and the Earth but is less precise for Jupiter and the other major planets. In the former group of planets, the mantle rotates slowly relative to the core (0.22°/yr. in the case of the Earth, according to Reference 104, pg. 28). Furthermore, the core itself is probably not rigid. In the case of Jupiter, which has fluid outer shells, the angular velocity is a function of radius and latitude. The 1960 Nautical Almanac (Ref. 156, pg. 422) gives the

period in the equatorial belt as $9^h 50^m 30^s.003$ (System I) and in temperate latitudes as $9^h 55^m 40^s.632$ (System II), a difference of 0.8%.

It might also be expected that the amplitude of the polar migration for a highly spherical planet such as Venus may be considerably larger than for the Earth.

3. Though the angular velocity of Mars (and perhaps of Jupiter) appears to be known almost as accurately as that of the Earth, the author knows of no data concerning spin rate fluctuations or polar migration of any planets other than the Earth.

However, in spite of the fact that the assumptions of page 47 are not fully justified, an oblate ellipsoid of rotation should be suitable as an analytic surface on which any of these planets can be mapped. In particular, the Earth is conventionally mapped onto such an ellipsoid whose dimensions are discussed in Section 3.G. There is some evidence that those equipotential surfaces of gravitation and rotation (the surfaces of constant U) which lie near the surface of the Earth resemble the triaxial ellipsoids of Jacobi more than the symmetric ellipsoids of MacLaurin. The principal diameters of such a triaxial ellipsoid appear to lie in the equatorial plane and differ by 150 meters (Ref. 200, pg. 120), 200 meters (Ref. 87, pg. 386) or 212 meters (Ref. 104, pg. 80) depending on whose inconclusive evidence is used. The fact that the

surfaces of constant U may resemble slightly triaxial ellipsoids or slighly pear-shaped figures is of little concern to navigators in the selection of a reference surface. It is evident that if pear-shapedness and triaxiality are small, an ellipsoid of rotation will be a more convenient surface than either a triaxial ellipsoid or pear-shaped figure, even if the latter are more nearly correct representations of the outer equipotential surfaces.

The size and shape of a reference surface to represent the Earth is obtained from careful gravimetric and astrogeodetic survey data (Chapter Three) but for a planet, this is presently impossible. Only a limited number of indirect methods is available:

1. The distance to the Moon is known to 0.1 km. (one part in 10^5) from radar measurements (Ref. 208, pg. 70) while the distances to the other navigable planets are known to one part in 10^6 A.U. (Ref. 156, tables of each planet). However, since the A.U. is known only to one part in 10^3 or 10^4 (Ref. 197, pg. 696), the distance in terms of accelerometer or Doppler radar calibrations in a navigation system is only known to one part in 10^3 or 10^4.

Hence by measuring the size of the planet's disc on a photographic plate, the linear diameter of the planet is found to an accuracy of 0.3% for Mars and 1% for Jupiter. (Ref. 197, pg. 709), Figure 2-8. The

Figure 2-8

KINEMATIC PROPERTIES OF THE PLANETS

		Reference Ellipsoid			
		Semi-Major Axis, a. Km.	Reciprocal Flattening, 1/f		
			Dynamic	Telescopic	Ref. Sfce.
Moon	$27.^{d}321661$	1741	-	800	800
Venus	23 hrs. to 224.7 days	0.973 a_E = 6210 km. ± 1%	-	-	∞
Earth	$23.^{h}934472$ (inertial) $23.^{h}934470$ (sidereal)	6,378.4	297.3 to 300	297.0	297.0
Mars	$24.^{h}66964$	0.532 a_E = 3390 km. ± 0.3%	192	190	191 ± 0.5%
Jupiter	$9^{h}50^{m}30.^{s}003$ (System I) $9^{h}55^{m}40.^{s}632$ (System II)	10.97 a_E = 70,000 km. ±1%	15.4	15.4	15.4 ± 2%

Data from References 87, pg. 200; 121, pgs. 252-253; 156, pgs. 485, 497, 499, 502, 521; 169, pg. 8-10; 191, pg. 249; 197, pgs. 709, 710, 696; 198, pg. 21; 208, pg. 111.

sizes of Mercury and the outermost planets are known much less accurately but are of no interest here. Figure 2-8 shows the geometric eccentricities of the planets observed by measuring the image of the planet in a telescope.

2. As discussed in Appendix F, observations of a planet's satellites determine the constants in the spherical harmonic expansion of the gravitational potential. MacCullagh's Theorem (Section 2.F.5.) shows that J_2, the coefficient of the second harmonic, is:

$$J_2 = \frac{I_T - I_S}{m_P a^2} \qquad (2\text{-}11)$$

where: I_S and I_T are the polar and equatorial moments of the planet.

m_P is the mass of the planet.

a is its semi-major axis.

The flattening or eccentricity can be calculated from J_2 if a density distribution is assumed. The eccentricity calculated this way is called the "dynamic eccentricity," Figure 2-8.

Based on presently available information, the size and eccentricity of ellipsoids of rotation which are suitable as reference surfaces for the planets are shown in Figure 2-8. The selection of a reference surface for the Earth is discussed in detail in Section 3.G.

The Earth, Mars and Jupiter spin far more rapidly than they revolve around the Sun. However, the Moon, and probably Venus, rotate in inertial space at their orbital rates, probably because of tides which acted on them before they solidified (Ref. 121, Chap. 8). These tides cause the primary's and secondary's spin rates to decrease and cause the orbit rate to accelerate until first the secondary rotates at orbit rate and finally the primary does too. Presently, though these planets are relatively solid, the body tides are strong enough to maintain equality between the orbit and spin rates of the secondary.

The spin rates of Mars and Jupiter probably fluctuate no more than that of the Earth. The most rapid secular fluctuation would occur for Venus, if its spin rate were not yet equal to its orbit rate (Ref. 195, pg. 262). Though Venus would then slow down twice as rapidly as does the Earth (Ibid.), its day would lengthen only 0.003 second/century. Figure 2-8 shows the author's compilation of information concerning the spin rates of the navigable planets. Sidereal rates refer to rotation relative to the planet's mean vernal equinox (which precesses in inertial space) whereas inertial rates are relative to inertial space.

The Moon and probably Venus have had their spin rates slowed to their orbit rates. Venus period is something between 23 hours (Ref. 169, pgs. 8-10) and its orbital period, 224.7 mean solar days (Ref. 208, pg. 111).

The inertial spin rate of the Moon remains very nearly constant except for gravitational gradient effects. Figure 2-7 shows the Moon orbiting the Earth in an exaggerated plane elliptic orbit. The $6\frac{1}{2}°$ angle between the axis of rotation of the Moon and the normal to the Moon's orbit is assumed to be zero. $(\phi+\Psi)$ is the angle between the radius vector connecting the centers of the Earth and Moon and the smallest principal axis of inertia of the Moon. Because of the gradient of the Earth's gravitational field at the Moon, the Earth exerts a torque on the Moon of magnitude (Refs. 55 and 121, pg. 252):

$$T = \frac{\partial G_M}{\partial r_M} \frac{\sin 2(\phi+\Psi)}{2} (I_2 - I_3)$$

where:

$$G_M = \frac{\gamma m_M}{r_M^2}$$

I_1 is the Moon's principal moment of inertia about the spin axis (maximum moment of inertia)

I_3 is the Moon's moment of inertia about the principal axis pointed toward the Earth (minimum I).

I_2 is the intermediate principal moment of inertia of the Moon.

r_M is the distance between the mass centers of the Earth and Moon.

This small torque causes small variations in the inertial angular velocity of the Moon. If Ψ is the angle between the Moon and a uniformly rotating reference grid, in the plane of the orbit:

$$I_1 \ddot{\psi} = \frac{\partial G_M}{\partial r_M}(I_2 - I_3)(\phi + \psi)$$

$$\ddot{\psi} - \frac{\partial G_M}{\partial r_M}\frac{I_2 - I_3}{I_1}\psi = \frac{\partial G_M}{\partial r_M}\frac{I_2 - I_3}{I_1}\phi$$

which is a second order "gravitational pendulum" oscillation whose natural frequency, ω_N, is:

$$\omega_N^2 = -\frac{\partial G_M}{\partial r_M}\left(\frac{I_2 - I_3}{I_1}\right) = 2\frac{I_2 - I_3}{I_1}\omega_{ORBIT}^2 \qquad (2\text{-}12)$$

Observations show that (Ref. 121, pg. 252):

$$\frac{I_2 - I_3}{I_1} = 0.0002$$

so the natural period is fifty months. Thus the Moon's inertial spin rate has a superimposed fluctuation whose period is fifty months and whose amplitude is not observable but is variously estimated as $\pm 2 \times 10^{-9}$ radian (Ibid.) and ± 1 foot at the surface of the Moon (Ref. 200, pg. 169) $= \pm 1.74 \times 10^{-7}$ radian. On this basis, the extreme instantaneous Moon rate fluctuates 4×10^{-9} orbit rate. Hence even including random fluctuations in rate such as occur on the Earth, the Moon's angular velocity is likely to be constant within one part in 10^7 or better.

The librations of the Moon are not caused by variations in the Moon's inertial spin rate. These librations are an apparent oscillation of the Moon with respect to a line of sight from the Earth's surface. They result because:

1. The changing angle, ϕ, in Figure 2-7 allows the Earth observ-

er to see more than half the Moon.

2. The $6\frac{1}{2}$ ° angle between the Moon's spin axis and orbit axis allows the Earth observer to see "over the north pole" and "under the south pole."

3. The varying inclination of the Moon's orbit to the ecliptic allows the Earth observer to see more than half the Moon.

4. The diurnal parallax, which causes an Earth observer to move 8000 miles per day perpendicularly to the line of sight to the Moon, permits the Earth observer to see around both sides of the Moon.

These librations permit the Earth observer to see 59% of the Moon's surface (Ref. 158, pg. 134).

As noted in Appendix A, the writer knows of no published information relating to the migration of the pole of the other planets. Figure 2-8 summarizes the selection of reference surfaces for the planets and of the inertial angular velocities which these surfaces must have. The specification of the gravity and gravitational field of a planet, in particular, the Earth, is discussed in Section 2. F.

2.F. THE GRAVITY AND GRAVITATIONAL FIELD OF THE EARTH.

2.F.1. INTRODUCTION.

The gravitational field around a planet is always of interest to a navigator but is of special interest to the inertial navigator since the accuracy with which he can determine position depends directly on how well he can subtract gravitation from his accelerometer outputs. However, the actual gravitational field around a planet is not thoroughly predictable because of density inhomogenieties within the planet. Hence it is proposed that the navigator establish a reference gravity or gravitational field which is a simple function of position outside the planet and which closely approximates the actual field. The navigator normally uses the reference field in place of the unpredictable actual field, accepting any difference between them as an irremovable error. If large local discrepancies exist and are predictable, they can be included in the gravity calculation.

This section considers the establishment of reference gravity and gravitational fields, in a variety of coordinate frames, in the space surrounding a planet.

Near the Earth, the reference field is defined in such a manner as to correspond closely to the usual definition of gravity, $\bar{g} = \bar{\nabla} U$.

Density irregularities in the Earth cause the actual surfaces of constant U to be "bumpy" but the reference U surfaces must be smoothed for convenience of computation.

At larger distances, when $\bar{g}$ can no longer be taken normal to the reference ellipsoid, the gravitational field, $\bar{G} = \bar{\nabla} V$, is more useful. This is especially clear in Figure 2-9 which shows contours of constant U and V. At large distances from the planet, the constraint force, $-\bar{g}$, acting on a test mass which is fixed with respect to the planet, is nearly perpendicular to the axis of rotation, in a direction bearing little relation to the navigation problem.

The rotation potential, V', is discussed in Section 2.B. and expressed in several coordinate frames of interest. Thus, only the Newtonian gravitational potential of a mass having the shape and density distribution which the planet assumes under rotation need be investigated in more detail.

At very large distances from the planet, its potential becomes measurably disturbed by the presence of other heavenly bodies. Hence if $\bar{G}$ or $\bar{g}$ is to be predicted, an ephemeris of these heavenly bodies is required. Section 2.F.2. discusses this problem in more detail.

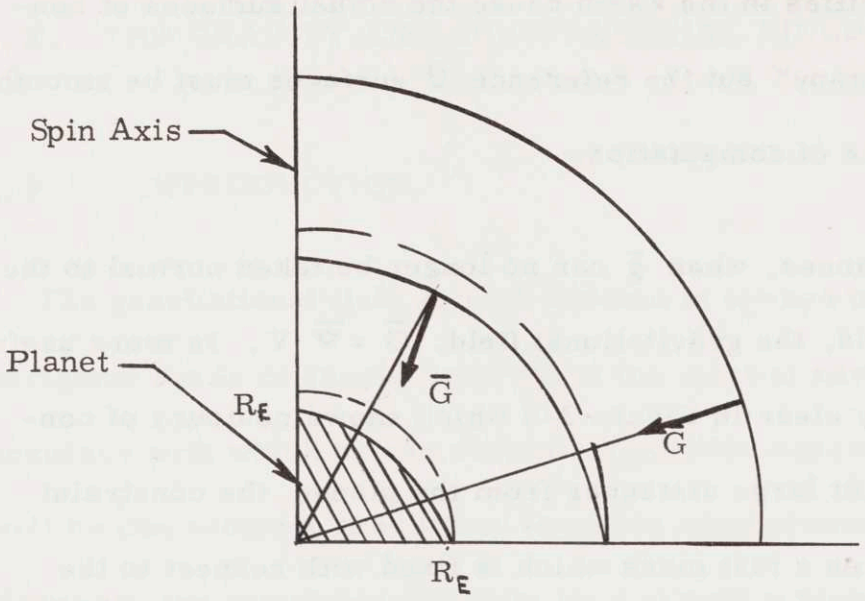

Constant V

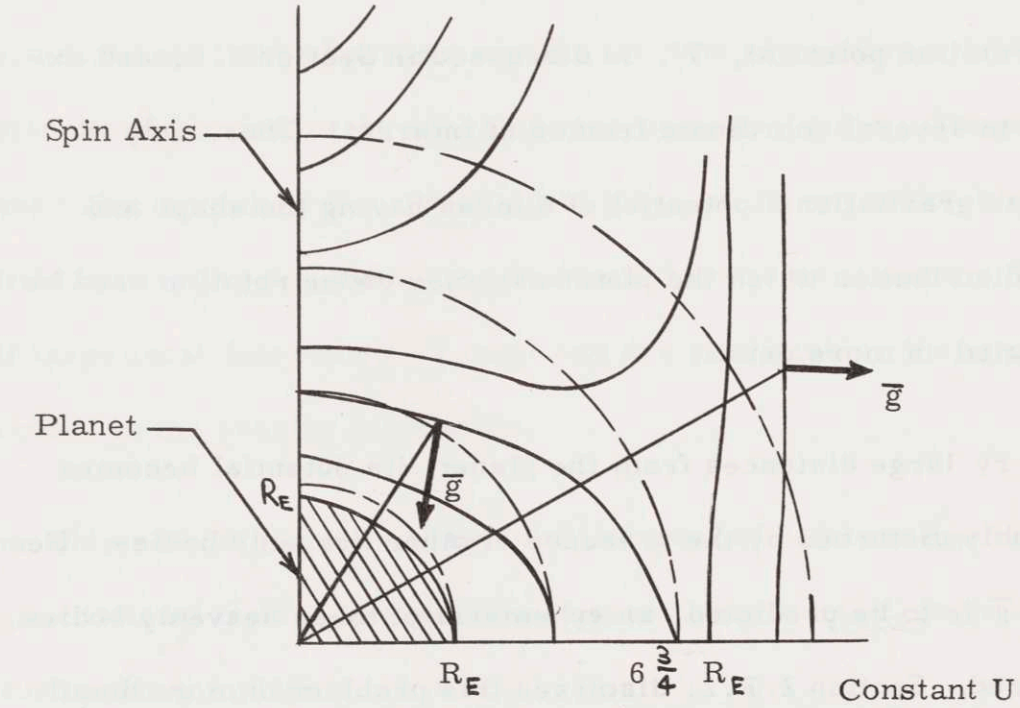

Constant U

Figure 2-9

CONTOURS OF CONSTANT V AND U

AROUND AN ISOLATED ROTATING PLANET

2.F.2. PERTURBATION OF A PLANET'S GRAVITATIONAL FIELD BY HEAVENLY BODIES.

The gravitational potential, V, at any point, P, is the sum of the potentials of all the masses in the universe. But a planet is not an isolated mass in empty space; the Sun, other planets and satellites come near it and affect its gravitational field. Section 2.E. shows that the maximum variation in the vertical component of gravitation near the surface of the Earth caused by motions of the heavenly bodies is two parts in 10^7 in magnitude and 0.026 seconds of arc in angle (Ref. 104, pgs. 119-120). The change in gravitation caused by removal of the Earth's atmosphere would be one part in 10^6 (Ibid., pg. 60).

If a vehicle navigates at a distance, r_p, from the mass center of a planet of mass, m_p, then nearby heavenly bodies perturb the geocentric horizontal component of gravitation which acts on the vehicle. If the vehicle navigates in planetocentric coordinates, an observer on the planet detects a gravitational force on the vehicle which is $\frac{\gamma m_p}{r_p^2}$ plus a force equal to the vector difference between the heavenly body's attraction on the mass centers of the planet and vehicle. The horizontal component of this perturbing acceleration does not reach 10^{-6} gee for a vehicle near the Earth, unless it is more than half way to the Moon.

Hence, within about one part in 10^6 and 0.05 seconds of arc, the

gravity or gravitational field near the surface of the Earth is a vector function of position only and does not depend on time, as it would at large distances where an ephemeris of the heavenly bodies would be needed to find the local gravitational potential. Also to this accuracy, the mass of the atmosphere is negligible and $\nabla^2 V = 0$ everywhere outside the Earth's surface. Thus, the derivations of Section 2.B. concerning the potential function of an isolated mass are applicable near the surface of the Earth and analagously, near the surfaces of the other planets.

2.F.3. THE GEODETIC MEASUREMENT OF GRAVITY.

A gravity survey at a sequence of fixed points on a planet measures $\overline{g} = \overline{\nabla} U$. Gravity surveys have been made on the surface of the Earth by the government geologic and geodetic surveys, the oil companies and by university and military groups. Since the gravity force is the negative of the constraint force needed to hold a test mass fixed relative to the rotating planet, it can be measured directly only where such a constraint force is readily applied; namely on the solid surface of the planet.

The conventional unit of measuring gravity is the gal = one cm./sec.^{2} At a fixed station on the Earth, the absolute value of $\overline{g}$

can be found to about one milligal (Ref. 92) after several hours of timing a pendulum. Gravity differences between stations are usually measured to 0.1 milligal (Ref. 104, pg. 156) but can be measured to one microgal (10^{-9} gee) using Earth tide meters (Ibid., pg. 120). When measurements are made to 0.1 milligal or less, the effect of the passage of the Moon overhead must be included.

The classical definition of the deflection of the vertical is the angle between $\bar{g}$ and the normal to the reference ellipsoid at the observing point. At fixed points on the Earth, the deflection of the vertical can be measured to better than 0.3 second of arc astrogeodetically and to three seconds of arc or worse gravimetrically (Chapter Three).

In a vehicle moving with respect to the Earth, gravity must be inferred from the reading of a vertical accelerometer or its equivalent. An observer on the vehicle measures the "vertical" component (assuming he can both define and locate a suitable vertical) of the vehicle's inertial acceleration minus gravitation. This accelerometer measures a sum of gravity, acceleration relative to the Earth and Coriolis corrections caused by the rotation of the Earth. The Vening-Meinesz submarine gravimeter can read gravity to five milligals (Ref. 104, pgs. 117-118), after a half-hour reading interval. Very recently, successful airborne measurements of gravity have been made to a claimed accuracy of ten milligals, averaged over thirty to sixty mile

distances (Refs. 131 and 148). Such results are not sufficiently accurate for geophysical prospecting but may be suitable for gravimetric surveys. Section 5.F.3. discusses the measurement of gravity from a moving vehicle in more detail.

Deflections of the vertical are not directly measurable from a moving vehicle. The required astrogeodetic angles cannot be measured accurately enough or rapidly enough from a moving vehicle nor can geodetic position on the reference ellipsoid be found sufficiently accurately. However, if detailed measurements of gravity are available over the entire Earth, the deflections of the vertical may be calculated everywhere (Section 3.J.2.).

The measurement of gravitation outside the atmosphere can be made to some extent by observing the orbits of Earth satellites. As explained in Appendix F, observations of the perturbations of the orbit permit the observer to determine the relative weight of each harmonic in the potential expansion. The scale of the potential must be determined by means of ground measurements.

The older method of computing gravitation above the Earth is discussed by Jeffreys (Ref. 121, pgs. 135-138) and outlined in Section 2.F.5. In this method, V is inferred from measurements of gravity on the Earth.

2. F. 4. ANOMALIES AND THE DEFLECTION OF THE VERTICAL.

A map of the actual $\overline{G}$ or $\overline{g}$ field is technologically not feasible. Instead, reference $\overline{g}$ and $\overline{G}$ fieldsare defined in the space around the planets which are as nearly identical as possible to the actual fields, yet are simply expressed. Hence, four fields can be defined at each point in space:

Actual and reference gravitation, $\overline{G}$ and $\overline{G}'$, respectively.

Actual and reference gravity, $\overline{g}$ and $\overline{g}'$, respectively.

The following definitions will be adopted.

The gravitational anomaly at any point is:

$$\delta G = |\overline{G}| - |\overline{G}'| \tag{2-13}$$

and the gravity anomaly is:

$$\delta g = |\overline{g}| - |\overline{g}'| \tag{2-14}$$

The gravitational deflection of the vertical is the vector angle from $\overline{G}'$ to $\overline{G}$:

$$\overline{\delta}_v = \hat{G}' \times \hat{G} \tag{2-15}$$

and the gravity deflection of the vertical is:

$$\overline{\delta}_v = \hat{g}' \times \hat{g} \tag{2-16}$$

In conventional geodesy, the reference direction of the vertical used to define the gravity deflection of the vertical is the normal to the local reference ellipsoid but for navigation purposes, the reference direction must sometimes be a function of altitude. The gravity deflection of the

vertical is commonly resloved into two components. The magnitude of the north component, called the 'prime deflection of the vertical," measures the west deflection of $\bar{g}$ from the meridian plane. The magnitude of the east component, called the "meridian deflection of the vertical," measures the north deflection of $\bar{g}$ from the normal to the reference ellipsoid.

If the actual fields were well-enough known, the reference fields could be defined in such a way as to minimize the mean square anomaly, mean square deflection or some other error parameter, subject to suitable constraints on the reference field to make it smoother than the actual field. The definition of a reference field in this manner is currently a major problem in geodesy (Refs. 98, 104 and 123 for example). Insufficient information is currently available to carry out this procedure so the reference fields are established on theoretical grounds subject to general confirmation by measurement.

Clearly, the anomalies and deflections of the vertical are dependent as much on the definition of the reference field as on the measurement of the actual field.

The behavior of the deflection of the vertical with respect to some reference field at appreciable heights above the reference ellipsoid has not been measured. However a crude estimate can be made as

follows:

If an anomalous mass were embedded near the surface of the Earth, its gravitational field would fall with the square of the distance from it but the deflection of the vertical would fall as the cube of the distance. However, if the anomalous mass consists of a mass deficiency "floating" vertically above a mass excess, the gravitational field would fall as the cube of altitude above the dipole and δ_v would fall roughly as the fourth power of altitude at large distances. Near the anomalous dipole mass, the deflection increases from zero at the dipole to a maximum at some altitude and then falls with the fourth power of altitude.

If the anomalous mass or dipole is eighty kilometers below the surface of the Earth (Ref. 87, pg. 308), then at an altitude of forty kilometers, the deflection of the vertical is reduced between:

$$\left(\frac{80}{120}\right)^3 = 0.30$$

and

$$\left(\frac{80}{120}\right)^4 = 0.20$$

of its value at the surface. Hence the deflection of the vertical might be expected to fall to $\frac{1}{4}$ of its surface value at an altitude of 25 miles. Because of the small angles involved, this is true of either the gravity or gravitational anomaly when compared to any reference direction which is approximately radial.

This writer knows of no information concerning precise estimates of the geographic horizontal component of gravity at altitudes of tens of miles above the Earth.

These data concerning anomalies and deflections of the vertical are used in Chapter Five. Typical deflections of the vertical and magnitude anomalies are shown in Figure 2-10.

Figure 2-10

TYPICAL GRAVITY ANOMALIES

AND DEFLECTIONS OF THE VERTICAL

	Anomaly Milligals	Deflection of the Vertical Seconds of Arc
Commonly less than	10 to 20	10
Rarely greater than	50	30
Never greater than	400	90

2.F.5. ANALYTIC EXPRESSIONS FOR GRAVITATION.

At very large distances from a distributed mass such as a planet, the gravitational potential is independent of the shape and density distribution within the planet since it appears to be a point mass. Hence the simplest approximation is:

$$V = \frac{\gamma m_p}{r} \tag{2-17}$$

where r is the distance of the test mass from the mass center of the planet.

For closer distances or higher accuracies, a second order approximation is used called "MacCullagh's Theorem," which expresses the potential at a distance point, P, in terms of certain moments of inertia of the planet(Ref. 236, pgs. 340 ff.):

$$V = \frac{\gamma m_p}{r}\left[1 + \frac{I_1 + I_2 + I_3 - 3I_{OP}}{2m_p r^2}\right] \tag{2-18}$$

where:

I_1, I_2 and I_3 are moments of inertia of the planet about any three orthogonal axes through its mass center, O.

I_{OP} is the moment of inertia of the planet about the line, $\overline{OP}$.

If the planet is symmetric about an axis of figure but has otherwise

arbitrary density distribution and shape:

$$I_{OP} = I_S \sin^2 L_c + I_T \cos^2 L_c$$

where:

I_S is the moment of inertia about the principal axis of symmetry = I_3

I_T is the transverse principal moments of inertia = $I_1 = I_2$

Then:

$$V = \frac{\gamma m_p}{r} \left[1 + \frac{I_T - I_S}{m_p r^2} P_2 (\sin L_c) \right] \qquad (2\text{-}19)$$

$P_2(x)$ is the Legendre polynomial of second degree.

For still higher accuracy or closer distance, the MacCullagh formula is not adequate to approximate the actual field near the planet. The potential of the purely radial field is disturbed both by the grossly non-spherical distribution of the planet's mass and by the local surface irregularities. The actual field around the planet has the general character of the MacCullagh approximation with local superimposed perturbations.

Appendix B develops a convenient tool for describing the actual gravitational field quantitatively. Omitting the small effect of the mass of the atmosphere, $\nabla^2 V = 0$ everywhere outside the planet. Hence V can be expressed as an infinite sum of spherical harmonics in the spherical coordinates λ, L_c and r :

$$V = \frac{\gamma m_p}{r} \sum_{n=0}^{\infty} \sum_{m=0}^{\infty} (b_{nm} \cos m\lambda + c_{nm} \sin m\lambda)\left(\frac{a}{r}\right)^n P_{nm}(\sin L_c) \qquad (2\text{-}20)$$

Here, $\cos m\lambda\, P_{nm}(\sin L_c)$ is a typical tesseral harmonic of order m and degree n, defined uniquely at each point of the unit sphere. The tesseral harmonics of order zero, $P_{no}(\sin L_c)$, are the Legendre polynomials of the first kind, $P_n(\sin L_c)$. The higher order tesseral harmonics vary both with latitude and longitude.

Equation (2-20) can theoretically match the actual measured field to arbitrary accuracy by using enough terms, b_{nm} and c_{nm}, but no more accurately than one part in 10^6 if $\bar{G}$ is to be a function of position alone). In general, the equation is embarrassingly rich in arbitrary constants considering the meager gravitational data available, although Zhongolovich and Kaula, for example, have attempted to fit observed gravitational data into this form (Refs. 104, pg. 270 and 124).

As a result, the actual potential field is usually assumed to arise from a mathematical model of the planet consisting of an inhomogeneous ellipsoid of rotation whose potential is in the form:

$$V = \frac{\gamma m_p}{r} \sum_{n=0}^{\infty} J_n \left(\frac{a}{r}\right)^n P_n(\sin L_c) \qquad (2\text{-}21)$$

and which is covered by a thin skin whose density varies with latitude and longitude to produce the observed perturbations compared to Equation (2-20). Equation (2-20) is the most general form for the pot-

ential distribution around a symmetric planet in spherical coordinates. If the origin of coordinates is at the mass center of the planet, $J_1 = 0$ (Ref. 187, pg. 334). The MacCullagh approximation is merely a truncation of the remaining series at the second term. Section 2.C. shows that if a planet were in fluid equilibrium and unable to sustain internal tension and shear, it must be symmetric about a plane through the mass center and perpendicular to the axis of rotation. Hence all odd J_n must vanish in such a case.

Several methods exist for estimating the J_n coefficients of a planet. Perhaps the simplest is to assume that the planet is a homogeneous ellipsoid of rotation whose meridian eccentricity is that observed by means of geodetic or telescopic shape measurements. Then MacCullagh's Theorem gives the potential to second order as:

$$I_1 = I_2 = \frac{m\rho}{5}(a^2 + b^2)$$

$$I_3 = \frac{2}{5} m a^2$$

$$V = \frac{\gamma m_\rho}{r}\left[1 - \frac{1}{5}\left(\frac{c}{a}\right)^2 \left(\frac{a}{r}\right)^2 P_2 (\sin L_c) \right] \qquad (2\text{-}22)$$

The higher order J_n are obtained from the closed form expression for the potential of a homogeneous ellipsoid of rotation given in cylindrical coordinates in Appendix E. The potential is transformed from cylindrical coordinates to spherical coordinates in Appendix E to give:

$$V = \frac{\gamma m_\rho}{r}\left[1 - \frac{1}{5}\left(\frac{c}{a}\right)^2\left(\frac{a}{r}\right)^2 P_2(\sin L_c) + \frac{3}{35}\left(\frac{c}{a}\right)^4\left(\frac{a}{r}\right)^4 P_4(\sin L_c) - \cdots\right] \qquad (2\text{-}23)$$

For a homogeneous International reference ellipsoid:

$$J_2 = -\frac{\epsilon^2}{5} = -0.0013445$$

$$J_3 = 0$$

$$J_4 = \frac{3}{35}\epsilon^4 = 3.87 \times 10^{-6}$$

Figure 2-11 clearly shows that these are not good approximations to the measured J_n for the Earth.

A more refined estimate is to retain the ellipsoidal shape of the planet but assume an unknown radial density distribution. Then by requiring that $U = V + V'$ be constant (independent of L_c) when the equation for the reference ellipsoid:

$$\frac{r^2 \cos^2 L_c}{a^2} + \frac{r^2 \sin^2 L_c}{b^2} = 1$$

is substituted, Jeffreys (Ref. 121, pgs. 136-137) shows that:

$$J_2 = -\frac{2}{3}\left[f - \frac{n}{2} + f\left(\frac{n}{7} - \frac{f}{2}\right)\right]$$

$$J_3 = 0$$

$$J_4 = \frac{4}{35} f\,(7f - 5n) \qquad (2\text{-}24)$$

where:

$$n = \frac{\omega_{1P}^2 a^3 (1-f)}{\gamma m_p}$$

$$f = \frac{a-b}{a}$$

n is not directly measurable on the Earth but it can be calculated indirectly with sufficient accuracy to find J_2 to one part in 10^5.

Gravity on the reference ellipsoid is the gradient of U, whose

Figure 2-11

GRAVITATIONAL POTENTIAL OF THE EARTH

FROM OBSERVATIONS OF ARTIFICIAL SATELLITES

Calculated from Reference 134, pg. 903 and Appendix E. The potential is assumed to be symmetric about the geographic polar axis and to have the form:

$$V = \frac{\gamma m_E}{r}\left[1 + \sum_{n=2}^{\infty} J_n \left(\frac{a}{r}\right)^n P_n(\sin L_c)\right]$$

Harmonic / Author	J_2	J_3	J_4
Jacchia (1959)	-0.0010827 ±0.05%	0	2.42×10^{-6} ± 20%
King-Hele (1959)	-0.0010831 ±0.015%	0	1.36×10^{-6} ± 12%
Kozai (1959)	-0.0010832	2.20×10^{-6} ± 4%	2.12×10^{-6}
O'Keefe - NASA (1959)	-0.0010826 ± 0.05%	2.42×10^{-6} ± 10%	1.70×10^{-6} ± 3%
Theoretical, assuming an inhomogeneous ellipsoid of the same eccentricity and spin rate as the Earth.	-0.0010713	0	2.96×10^{-6}
Theoretical, assuming a homogeneous ellipsoid of the same eccentricity as the Earth.	-0.0013445	0	3.87×10^{-6}

magnitude Jeffreys calculates as (Ibid., pgs. 129-131):

$$g_{h=0} = \frac{\partial U}{\partial r} \quad \text{on the ellipsoid}$$

$$= g_{eq}\left[1 + B_2 \sin^2 L_g + B_4 \sin^2 2L_g\right] \qquad (2\text{-}25)$$

where:

g_{eq} is the equatorial value of gravity on the surface of the reference ellipsoid

$$B_2 = \frac{5}{2}n - f + \frac{15}{4}n^2 - \frac{17}{14}fn$$

$$B_4 = \frac{f}{8}(f - 5n)$$

A gravity measurement made at some known latitude together with geodetic information about L_g, a and f of the reference ellipsoid allows the calculation of n, B_2 and B_4, and therefore of J_2 and J_4.

A third and more direct method of measuring the actual J_n is to observe the perturbations in the orbits of satellites around the Earth. By observing the artificial satellite, 1958β2, O'Keefe and others were able to estimate the first few J_n for the Earth very exactly (Refs. 134 and 135). Their results are summarized in figure 2-11 from which it is evident that the odd J_3 term may not be zero. Though other authors have questioned O'Keefe's calculations (Ref. 90), rebuttals by O'Keefe (Ref. 133 and a letter in the July, 1960 SCIENTIFIC AMERICAN) strongly indicate that the existence of an odd J_3 term is incontrovertible. The odd Legendre polynomials are not symmetric about the equator so the existence of odd harmonics would mean that the gravitational field and hence the geoid are not symmetric about the equator.

If the odd J_n were not zero, the Earth would be said to be slightly pear-shaped.

Even the two-dimensional series, Equation (2-21), is too complicated for navigation. Instead, only the most significant terms are retained to describe the reference field and the remaining terms omitted as an irremovable error. Except possibly on the highly elliptic Jovian planets, the series for the reference potential can always be truncated after several harmonics. Since the spherical harmonics are orthogonal, the coefficients of the lower order terms do not depend on the presence or absence of higher order terms. Hence J_2, J_3 and J_4 are independent of the term at which the series is truncated.

By including more J_n terms in the mathematical model of V, the gravitational field can be predicted more exactly. However, the navigation system designer prefers a simple computation to a small increment in predictability. The difference between the actual components of gravitation and those predicted by the mathematical model is regarded as anomalous. An enormous number of tesseral harmonics would be needed to analytically represent local deflections of the vertical with any degree of fineness.

Section 2.F.6. shows that the uncertain J_3 term affects the horizontal component of $\overline{G}$ about as much as does the J_4 term, on the reference

ellipsoid. Hence if J_4 is included in the mathematical model, the unknown J_3 should also be included. But even if J_3 were certain, Equation (2-28) shows that it appears in an awkward manner in the gravitational expressions. Furthermore, when calculating the horizontal components of $\bar{G}$, as in Sections 2.F.6. to 2.F.8., it is found that the effect of the J_4 term extends only to order 10^{-6} gee or less, which is negligible for this discussion since navigation accuracies often require only 5×10^{-5} gee and since deflections of the vertical alone may exceed 5×10^{-5} gee. In view of these complications, the mathematical model is regarded as reliable only to the second harmonic but is calculated with the fourth harmonic included, in order to assess its effect. Hence:

$$V = \frac{\gamma m_p}{r}\left[1 + J_2\left(\frac{a}{r}\right)^2 P_2(\sin L_c) + J_4\left(\frac{a}{r}\right)^4 P_4(\sin L_c)\right] \quad (2\text{-}26)$$

The next few subsections calculate the horizontal components of gravity and gravitation in ellipsoidal, geographic and spherical coordinates, using Equation (2-26) with appropriate values of J_n.

2.F.6. HORIZONTAL GRAVITATION AND GRAVITY IN SPHERICAL COORDINATES.

Spherical coordinates are recommended for navigation at large distances from the Earth where $\overline{G}$ is of more interest than $\overline{g}$. In spherical coordinates, the horizontal direction is perpendicular to the radius vector from the center of the Earth. The horizontal component of reference gravitation, G_{L_c}, is assumed to be composed of two parts; one, G'_{L_c}, derived from the rational potential of Equation (2-26) and one, δG_{L_c}, caused by surface irregularities within the Earth. $\frac{\delta G_{L_c}}{g_r}$ is the local "deflection of the vertical" with respect to the field of the inhomogeneous ellipsoidal model Earth.

The rational portion of the geocentric horizontal component of gravitation, G'_{L_c}, is:

$$G'_{L_c} = \frac{1}{r}\frac{\partial V}{\partial L_c}$$

$$= \frac{\gamma m_e}{r^2}\left(\frac{a}{r}\right)^2 \sin 2L_c \left[\frac{3}{2}J_2 + \frac{3}{4}J_3\left(\frac{a}{r}\right)\left(5\sin L_c - \frac{1}{\sin L_c}\right) + \right.$$

$$\left. + \frac{5}{4}J_4\left(\frac{a}{r}\right)^2\left(7\sin^2 L_c - 3\right)\right] \qquad (2\text{-}27)$$

where $G_{L_c} = G'_{L_c} + \delta G_{L_c}$ and a is the equatorial semi-diameter of the reference ellipsoid. For the Earth, the only planet whose J_n larger than n = 2 have been measured, the J_n are taken from Figure 2-11. If G_{L_c} is to be calculated to an accuracy of 10^{-5} gee, then to

sufficient accuracy on the International reference ellipsoid:

$$J_2 = -0.001083$$
$$J_3 = +2.3 \times 10^{-6}$$
$$J_4 = +2.0 \times 10^{-6}$$

and numerically:

$$G'_{L_c} = -1.591 \left(\frac{a}{r}\right)^4 \sin 2L_c \left[1 - 0.00106\left(\frac{a}{r}\right)\left(5 \sin L_c - \frac{1}{\sin L_c}\right) - 0.00154\left(\frac{a}{r}\right)^2\left(7 \sin^2 L_c - 3\right)\right] \quad \text{cm./sec.}^2 \qquad (2\text{-}28)$$

Clearly for $\frac{a}{r} \simeq 1$, the J_3 and J_4 terms are equally large. Furthermore the effect of J_3 is exceedingly complicated because $\sin 2L_c$ does not readily factor out. Hence the J_3 term is hereafter omitted and included in δG_{L_c} and the potential taken as:

$$V = \frac{\gamma m_p}{r}\left[1 + J_2\left(\frac{a}{r}\right)^2 P_2(\sin L_c) + J_4\left(\frac{a}{r}\right)^4 P_4(\sin L_c)\right] \qquad (2\text{-}26)$$

as discussed earlier in Section 2.F.5. The J_4 term is carried in order to estimate its effect but is omitted in establishing a mathematical model of $\overline{G}$. The mathematical model is thus taken in the form:

$$G'_{L_c} = -1.591 \left(\frac{a}{r}\right)^4 \sin 2L_c \left[1 - 0.00154\left(\frac{a}{r}\right)^2 (7 \sin^2 L_c - 3)\right] \quad \text{cm./sec.}^2 \qquad (2\text{-}29)$$

Further studies might investigate the systematic effect on a navigation system of non-zero J_3 and J_5 terms.

G'_{L_c} is never larger than 1.6×10^{-3} gee in the space surrounding the

Earth. Thus, if J_3 and J_4 are neglected, G'_{L_c} can still be calculated to 3×10^{-6} gee which is adequate for navigation accuracy near the Earth. Hence within 5×10^{-6} gee:

$$G'_{L_c} = -1.591 \left(\frac{a}{r}\right)^4 \sin 2L_c \text{ cm./sec.}^2 \qquad (2\text{-}30)$$

The actual horizontal component of gravitation, G_{L_c}, at any point can be taken as the RMS sum of G'_{L_c} and the horizontal gravitation caused by mass anomalies. Figure 2-12 shows G_{L_c} as a function of altitude in the vicinity of 45° latitude.

G'_{L_c} is zero within 10^{-5} gee for $r > r_1$ where r_1 is:

$$10^{-5} = \frac{3}{2} J_2 \left(\frac{a}{r_1}\right)^4 \frac{\gamma m_E}{a^2}$$

$$r_1 = 3.57\, a = 14{,}100 \text{ miles} = 22{,}800 \text{ km.}$$

Thus, below 14,000 miles, the gravitational field of the Earth is not radial, within 10^{-5} gee.

Horizontal gravitation and gravity can be calculated on the surface of the reference ellipsoid, using the radius of the ellipsoid as given in Equation (c-6). Substituting into Equation (2-27) to 5×10^{-6} gee:

$$G'_{L_c}\big]_{h_g=0} = \frac{3}{2} J_2 \frac{\gamma m_p}{a^2} (1 + 2\epsilon^2 \sin^2 L_c) \sin 2L_c \qquad (2\text{-}31)$$

Evaluating this on the International ellipsoid:

$$G'_{L_c}\big]_{h_g=0} = -1.602 \sin 2L_c \text{ cm./sec.}^2 \quad \text{to } 10^{-5} \text{ gee}$$

$$G'_{L_c}\big]_{h_g=0} = -1.602 \sin 2L_c + 0.0054 \sin 4L_c \text{ cm./sec.}^2 \quad \text{to } 5 \times 10^{-6} \text{ gee}$$

Figure 2-12

MAGNITUDE OF THE HORIZONTAL COMPONENT OF GRAVITY AND GRAVITATION

VERSUS ALTITUDE

The RMS sum of δG, caused by mass anomalies, and G', caused by the non-spherical mass distribution, yields an order-of-magnitude estimate of the horizontal component of gravity or gravitation.

altitude		$\frac{g}{g_o}=\left(\frac{a}{r}\right)^2$	local defl. of vertical $\delta_v=\delta_{v_o}\left(\frac{80}{80+h}\right)^{2.5}$	anomalous horizontal G or g	Spherical $G'_{L_c}=-0.00162\left(\frac{a}{r}\right)^4$		Ellipsoidal $G'_\eta=+38.4\left(\frac{a}{r}\right)^4$		Geographic $g'_{L_g}=0.00555\left(\frac{h_g}{a}\right)$	
				δG		G_{L_c} rms sum		G_η rms sum		g_{L_g} RMS sum
miles	km.	gee	sec. of arc	gee × 10^5	gee	gee	gee	gee	gee ×10^5	gee ×10^5
0	0	1	15	7.5	-0.00162	0.0016	+0.00168	0.0017	0	7.5
2.5	4.4	1	12.4	6.2	-0.00162	0.0016	+0.00168	0.0017	0.38	6.2
12	20	0.995	6.9	3.4	-0.00161	0.0016	+0.00166	0.0017	1.7	3.8
25	40	0.985	3.6	1.8	-0.00158	0.0016	+0.00164	0.0016	3.5	3.9
63	100	0.97	0.88	0.9	-0.00153	0.0015	+0.00157	0.0016	8.8	8.8

This is the geocentric horizontal component of gravitation which is computable as a function of latitude.

A mathematical model of the systematic, geocentric horizontal component of $\bar{g}$ can be constructed in a similar manner:

$$g'_{L_c} = G'_{L_c} - \frac{\omega_{IE}^2}{2} r \sin 2L_c \qquad (2\text{-}32)$$

On the reference ellipsoid, this becomes:

$$g'_{L_c}\Big]_{h=0} = \left[\frac{3}{2} J_2 \frac{\gamma m_E}{a^2}(1+\epsilon^2) - \frac{\omega_{IE}^2 a}{2}\left(1-\frac{\epsilon^2}{4}\right)\right]\sin 2L_c +$$

$$+ \left[-\frac{3}{2} J_2 \frac{\gamma m_E}{a^2}\frac{\epsilon^2}{2} - \frac{\omega_{IE}^2 a}{8}\frac{\epsilon^2}{2}\right]\sin 4L_c - - - -$$

Substituting J_2 from Equations (2-24):

$$g'_{L_c}\Big]_{h=0} = -3.299 \sin 2L_c \quad \text{cm./sec.}^2 \qquad (2\text{-}33)$$

within 3×10^{-6} gee. Hence the approximation:

$$g'_{L_c}\Big]_{h=0} = -f \frac{\gamma m_E}{a^2} \sin 2L_c$$

is only accurate to 3×10^{-6} gee.

2.F.7. HORIZONTAL GRAVITY AND GRAVITATION IN GEOGRAPHIC COORDINATES.

Geographic coordinates are recommended for navigation within forty miles of the Earth's surface. Near the Earth, the navigation equations are probably best expressed in terms of $\bar{g}$ since g'_{L_g} is nearly zero and since geophysical data concerning deflections of the vertical are so expressed. In geographic coordinates, the horizontal direction at any point is perpendicular to the projected normal to the reference ellipsoid. The metric tensor and other geometric properties of the geographic coordinate frame are discussed in Appendix D.4.

G'_{L_g} and g'_{L_g}, the geographic horizontal components of gravitation and gravity, are found from the empirical spherical harmonic expansion, Equation (2-26), and the relations:

$$G'_{L_g} = \frac{1}{h_{L_g}} \frac{\partial V}{\partial L_g} = \frac{1}{\rho_M + h_g} \frac{\partial V}{\partial L_g} \qquad (2\text{-}34)$$

$$g'_{L_g} = \frac{1}{\rho_M + h_g} \left(\frac{\partial V}{\partial L_g} + \frac{\partial V'}{\partial L_g} \right)$$

where ρ_M is the local meridian radius of curvature of the reference ellipsoid. The transformation equations from spherical coordinates to geographic coordinates are given in Equations (D-14). The rotation potential in geographic coordinates is given in Equation (2-8) from which:

$$\frac{\partial V'}{\partial L_g} = -\frac{\omega_{IE}^2}{2} (\rho_M + h_g)(\rho_P + h_g) \sin 2L_g \qquad (2\text{-}35)$$

where ρ_P is the local prime (east-west) radius of curvature of the reference ellipsoid. G'_{L_g} and g'_{L_g} are found by expanding $\frac{\partial V}{\partial L_g}$ in terms of the geographic coordinates h_g and L_g :

$$\frac{\partial V}{\partial L_g} = -\frac{\gamma m_P}{r^2}\frac{\partial r}{\partial L_g} R + \frac{\gamma m_P a^2}{r^3} \sin L_c \frac{\partial(\sin L_c)}{\partial L_g} T \qquad (2\text{-}36)$$

where:

$$R = \left[1 + \frac{3}{2} J_2 a^2 \frac{3\sin^2 L_c - 1}{r^2} + 5 J_4 \left(\frac{a}{r}\right)^4 P_4(\sin L_c)\right]$$

$$T = \left[3 J_2 + \frac{5}{2} J_4 \left(\frac{a}{r}\right)^2 (7\sin^2 L_c - 3)\right]$$

A direct calculation from the transformation equations shows that:

$$\frac{\partial r}{\partial L_g} = -\frac{a\epsilon^2 \sin 2L_g}{(1-\epsilon^2 \sin^2 L_g)^{1/2}} \frac{\rho_M + h_g}{2r}$$

$$\frac{\partial(\sin L_c)}{\partial L_g} = S \frac{a^2(\rho_M + h_g)}{r^3} \cos L_g$$

where:

$$S = 1 + \frac{h_g}{a} \frac{2 - \epsilon^2 \sin^2 L_g}{(1-\epsilon^2 \sin^2 L_g)^{1/2}} + \left(\frac{h_g}{a}\right)^2$$

Thus:

$$g'_{L_g} = \frac{\gamma m_P}{a^2} \frac{\sin 2L_g}{2} \left[\frac{R a^3 \epsilon^2}{r^3 (1-\epsilon^2 \sin^2 L_g)^{1/2}} + \frac{(R_{BC} + h_g) a^6 S T}{r^7} - \right.$$

$$\left. - \frac{\omega_{IP}^2 a^2}{\gamma m_P} (\rho_P + h_g)\right] \qquad (2\text{-}37)$$

Equation (2-37) can be further expanded in a power series in $\frac{h_g}{a}$ and ϵ. Enough terms are carried to insure that g'_{L_g} and G'_{L_g} are accurate to 5×10^{-5} gee for $\frac{h_g}{a} < 0.01$ ($h_g < 40$ mi.). To sufficient accuracy:

$$r^2 = a^2 \left[1 - \epsilon^2 \sin^2 L_g + \epsilon^4 \sin^2 L_g \cos^2 L_g + \epsilon^6 \sin^4 L_g \cos^2 L_g + 2\frac{h_g}{a}\left(1 - \right.\right.$$

$$\left.\left. - \frac{\epsilon^4}{8} \sin^4 L_g\right) + \left(\frac{h_g}{a}\right)^2\right]$$

$$R = 1 + \frac{3}{2} J_2 \left[3 \sin^2 L_g - 1 + \epsilon^2 \sin^2 L_g \,(9 \sin^2 L_g - 7) + 2\frac{h_g}{a}(1 - \right.$$

$$\left. - 3 \sin^2 L_g)\right] + 5 J_4 P_4 (\sin L_g) \qquad (2\text{-}38)$$

$$S = 1 + \left(\frac{h_g}{a}\right)^2 + \frac{h_g}{a}\left(2 + \frac{\epsilon^4}{4}\sin^4 L_g\right)$$

$$T = 3J_2\left\{1 + \frac{5}{6}\frac{J_4}{J_2}\left[\left(7\sin^2 L_g - 3 - 17\epsilon^2\sin^2 L_g + 21\epsilon^2\sin^4 L_g\right) + 2\frac{h_g}{a}\left(3 - 7\sin^2 L_g\right)\right]\right\} \qquad (2\text{-}38)$$

Substituting Equations (2-38) into (2-37):

$$g'_{L_g} = \frac{\gamma m_p}{a^2}\frac{\sin 2L_g}{2}\left[L + M\sin^2 L_g + N\sin^4 L_g + P\frac{h_g}{a} + Q\left(\frac{h_g}{a}\right)^2\right] \qquad (2\text{-}39)$$

where:

$$L = 3J_2 + \epsilon^2 - \frac{\omega_{ip}^2 a^3}{\gamma m_p} - \frac{9}{2}J_2\epsilon^2 - \frac{27}{2}J_2\epsilon^4 - \frac{15}{2}J_4 - \frac{75}{8}J_4\epsilon^2$$

$$M = 2\epsilon^4 + \frac{35}{2}J_4 + 6J_2\epsilon^4 - \frac{225}{4}J_4\epsilon^2 - \frac{45}{2}J_2\epsilon^4 - \frac{\epsilon^2}{2}\frac{\omega_{ip}^2 a^3}{\gamma m_p}$$

$$N = 63J_2\epsilon^4 + \frac{1155}{8}J_4\epsilon^2 - \frac{3}{8}\epsilon^4\frac{\omega_{ip}^2 a^3}{\gamma m_p}$$

$$P = -3\epsilon^2 - \frac{15}{2}\epsilon^4 - \frac{\omega_{ip}^2 a^3}{\gamma m_p} + 3J_2\left(\frac{15}{2}\epsilon^2 - 4 - \frac{55}{2}\epsilon^2\sin^2 L_g\right) - 15J_4\left(7\sin^2 L_g - 3\right)$$

$$Q = 6\left(\epsilon^2 + 5J_2\right)$$

Evaluating the constants numerically:

$$L = 3.05\times10^{-5}$$

$$M = 7.05\times10^{-5}$$

$$N = -1.2\times10^{-6}$$

$$P = -0.01106 + 0.000391\sin^2 L_g$$

$$Q = 0.00786$$

Hence within 5×10^{-5} gee, $\overline{g}'$ is perpendicular to the ellipsoid on its surface since $L + M + N \approx 0$. To the same accuracy, for $\frac{h_g}{a} < 0.01$, the $\left(\frac{h_g}{a}\right)^2$ and $\frac{h_g}{a}\sin^2 L_g$ terms are negligible. Thus:

$$g'_{L_g} = -5.44\left(\frac{h_g}{a}\right)\sin 2L_g \quad \text{cm./sec.}^2 \qquad (2\text{-}40)$$

$$0 \underset{85}{<} h_g < 35 \text{ naut. mi.}$$

g'_{L_g} is entirely negligible within 10^{-5} gee when h_g is less than h_{g_1} :

$$5.44 \frac{h_{g_1}}{a} = 0.01$$
$$h_{g_1} = 7.3 \text{ mi.} = 38,000 \text{ ft.}$$

Below 38,000 feet, the geographic horizontal component of $\bar{g}$ results entirely from mass anomalies in the surface of the Earth, to this accuracy. The deflections of the vertical from this model $\bar{g}$ field must either be found empirically at each point or accepted as an irremovable error. Figure 2-12 shows that the deflection of the vertical at this altitude is probably less than thirteen to fifteen second of arc, corresponding to 7×10^{-5} gee of horizontal gravity.

The systematic, geographic horizontal component of gravity can be evaluated in geographic coordinates by setting $W_{IP} = 0$ in Equations (2-39):

$$G'_{L_g} = \frac{\gamma m_p}{a^2} \frac{\sin 2L_g}{2} \left[L_1 + M_1 \sin^2 L_g + N_1 \sin^4 L_g + P_1 \frac{h_g}{a} + Q_1 \left(\frac{h_g}{a} \right)^2 \right] \quad (2\text{-}41)$$

where:

$$L_1 = 0.00349$$
$$M_1 = 1.17 \times 10^{-4}$$
$$N_1 = -1.14 \times 10^{-6}$$
$$P_1 = -0.00760 + 0.000391 \sin^2 L_g$$
$$Q_1 = 0.00786$$

These terms are larger than the corresponding terms in the gravity expression, Equation (2-39). The simplest approximation below forty miles altitude is:

$$G'_{L_g} = 490 \sin 2L_g \left[0.00349 + 1.17\times10^{-4} \sin^2 L_g - 0.00760 \frac{h_g}{a}\right]$$

$$\text{cm./sec.}^2 \qquad 0 < h_g < 40 \text{ mi.} \qquad (2\text{-}42)$$

within 10^{-5} gee. The $\frac{h_g}{a}$ term can be neglected below 58,000 ft. to 10^{-5} gee:

$$G'_{L_g} = 1.71 \sin 2L_g \left[1 + 0.0335 \sin^2 L_g\right] \quad \text{cm./sec.}^2 \qquad (2\text{-}43)$$

Below 58,000 feet, the primary contribution to the horizontal component of gravitation in geographic coordinates is the large L_1 term.

2.F.8. HORIZONTAL GRAVITATION IN ELLIPSOIDAL COORDINATES.

Ellipsoidal coordinates are recommended for navigation over altitude ranges of several thousand miles, when the ellipsoidal shape of the Earth must be considered. For such applications, $\bar{G}$, not $\bar{g}$, is of direct interest as explained in Section 2.F.1. In ellipsoidal coordinates, the horizontal direction at any point is tangent to the ellipsoid through that point which is confocal to the reference ellipsoid. Two methods are used to evaluate G'_η, the systematic horizontal component of gravitation in ellipsoidal coordinates. One uses the theoretical closed form expression for the potential of a homogeneous ellipsoid of rotation, Equation (E-2). The other method for finding G'_η uses the spherical harmonic expansion, Equation (2-26) with empirically determined J_n.

c is the focal distance of the reference ellipsoid, ξ and η are the elliptic and hyperbolic coordinates, as discussed in Appendix C.

Appendix E derives the horizontal components of gravitation of a homogeneous ellipsoid of rotation in ellipsoidal coordinates as:

$$G_\eta' = \frac{3}{4}\frac{\gamma m_p}{c^2}\frac{\sin 2\eta}{(\cosh^2\xi - \cos^2\eta)^{1/2}}\left[-2\theta + 3(\theta\cosh^2\xi - \sinh\xi)\right] \qquad \text{(E-3)}$$

$\tan\theta = \operatorname{csch}\xi$

This can be expanded to 10^{-7} gee in a series which is valid everywhere outside the reference ellipsoid:

$$\theta\cosh^2\xi - \sinh\xi = 2\left[\frac{1}{3\sinh\xi} - \frac{1}{15\sinh^3\xi} + \frac{1}{35\sinh^5\xi} - \frac{1}{63\sinh^7\xi} - \cdots\right]$$

$$G_\eta' = \frac{\gamma m_p}{5c^2}\frac{\sin 2\eta}{\sinh^4\xi}\left[1 - \frac{12 + 7\sin^2\eta}{14\sinh^2\xi} - \frac{21\sin^4\eta + 24\sin^2\eta + 40}{56\sinh^4\xi} - \cdots\right] \qquad \text{(2-44)}$$

On the International ellipsoid where $\xi = \xi_0$ and $\cosh\xi_0 = \frac{1}{\epsilon}$:

$$\cosh^2\xi_0 = \frac{1}{\epsilon^2} = 148.8$$

$$\sinh^2\xi_0 = 147.8$$

$$\frac{\gamma m_p}{5c^2\sinh^4\xi} = 1.341 \text{ cm./sec.}^2$$

Hence, in order to calculate G_η' to 10^{-5} gee, the first two terms in Equation (2-44) are needed.

If G_η', as calculated from Equation (2-44), were correct then $\overline{g}$, as calculated from this same equation, must be perpendicular to the reference ellipsoid at its surface. This boundary condition can be checked by evaluating g_η at $\xi = \xi_0$:

$$g'_\eta = \frac{1}{c(\cosh^2\xi - \cos^2\eta)^{1/2}} \left(\frac{\partial V}{\partial \eta} + \frac{\partial V'}{\partial \eta}\right) \qquad (2\text{-}45)$$

V' is given by Equation (2-7) so:

$$\frac{\partial V'}{\partial \eta} = -\frac{\omega_{IP}^2 c^2}{2} \cosh^2\xi \sin 2\eta$$

Thus, on the International ellipsoid:

$$g'_\eta = G'_\eta + \frac{1}{c(\cosh^2\xi - \cos^2\eta)^{1/2}} \frac{\partial V'}{\partial \eta}$$

$$g'_\eta = \frac{\sin 2\eta}{c(\cosh^2\xi_o - \cos^2\eta)^{1/2}} \left[\frac{3\gamma m_p}{c\sinh^3\xi_o}\left(\frac{1}{15} - \frac{2}{35\sinh^2\xi_o} - \cdots\right) - \frac{\omega_{IP}^2 c^2}{2}\cosh^2\xi_o\right]$$

$$= 0.3750 \sin 2\eta \quad \text{cm./sec.}^2 \qquad (2\text{-}46)$$

which is not zero, within 10^{-5} gee. Clearly, Equation (2-44) is not a good approximation to G'_η since $\bar{g}$ makes an angle of 1.3 minutes of arc with the ellipsoid at 45° latitude. Thus, the potential of a homogeneous ellipsoid of rotation is <u>not</u> a satisfactory approximation to the potential of the Earth, within 10^{-5} gee.

The only form in which the actual potential distribution is more accurately given is Equation (2-26), the spherical harmonic expansion using emprical values of J_n. Thus, to obtain G'_η, Equation (2-26) must first be transformed from spherical to ellipsoidal coordinates with the substitution:

$$r^2 = c^2(\sinh^2\xi + \cos^2\eta)$$

$$\tan L_c = \tanh\xi \tan\eta$$

$$\sin^2 L_q = \frac{\sinh^2\xi \sin^2\eta}{\sinh^2\xi + \cos^2\eta}$$

and expanded in a power series in $\sinh\xi$. The author has performed this laborious calculation with the result:

$$V = \frac{\gamma m_p}{c\sinh\xi}\left[1 + \frac{A\sin^2\eta + B}{\sinh^2\xi} + \frac{C\sin^4\eta + D\sin^2\eta + E}{\sinh^4\xi}\right] \quad (2\text{-}47)$$

where:

$$A = \frac{3}{2}\left(\frac{a}{c}\right)^2 J_2 + \frac{1}{2}$$

$$B = -\frac{1}{2}\left(\frac{a}{c}\right)^2 J_2 - \frac{1}{2}$$

$$C = \frac{1}{8}\left[3 + 30\left(\frac{a}{c}\right)^2 J_2 + 35\left(\frac{a}{c}\right)^4 J_4\right]$$

$$D = -\frac{3}{4}\left[1 + 6\left(\frac{a}{c}\right)^2 J_2 + 5\left(\frac{a}{c}\right)^4 J_4\right]$$

$$E = \frac{3}{8}\left[1 + 2\left(\frac{a}{c}\right)^2 J_2 + \left(\frac{a}{c}\right)^4 J_4\right]$$

This expression for V in ellipsoidal coordinates can be verified by evaluating it for a homogeneous ellipsoid of rotation and comparing it to Equation (E-6), the series expansion of the theoretical equation. For a homogeneous ellipsoid of rotation, the J_n, given on page 73 can be substituted into Equation (2-47):

$$A = \frac{1}{5} \qquad B = -\frac{2}{5}$$

$$C = 0 \qquad D = -\frac{6}{35}$$

$$E = \frac{9}{35}$$

When these constants are inserted into Equation (2-47), the resulting expression for the potential is identical to Equation (E-6), obtained by expanding the closed form theoretical expression, Equation (E-3).

Thus, Equation (2-47) is verified.

Using the potential of Equation (2-47), G'_η is:

$$G'_\eta = A\frac{rm_p}{c^2}\frac{\sin 2\eta}{\sinh^3\xi}\frac{1}{(\cosh^2\xi-\cos^2\eta)^{1/2}}\left[1+\frac{2C\sin^2\eta+D}{A\sinh^2\xi}\right]$$

$$= A\frac{rm_p}{c^2}\frac{\sin 2\eta}{\sinh^4\xi}\left[1+\frac{(4C-A)\sin^2\eta+2D}{2A\sinh^2\xi}\right] \qquad (2\text{-}48)$$

The latter form is suitable for on-board machine computation. The boundary condition which this equation must satisfy is that on the reference ellipsoid, g_{L_g} must be zero. Using the measured J_n for the International ellipsoid:

$A = +0.2584$ $\qquad$ $B = -0.4195$

$C = -0.0355$ $\qquad$ $D = -0.1911$

and for $\xi = \xi_0$ near 45° latitude:

$$g'_\eta = G'_\eta - \frac{\omega_{IP}^2 c\cosh^2\xi_0\sin 2\eta}{2(\cosh^2\xi_0-\cos^2\eta)^{1/2}}$$

$$= 0.0132 \text{ cm./sec.}^2$$

The boundary condition for Equation (2-48) is satisfactory to 10^{-5} gee.

Thus:

to 2×10^{-5} gee:

$$G'_\eta = 37650\frac{\sin 2\eta}{\sinh^4\xi} \text{ cm./sec.}^2 \qquad (2\text{-}49)$$

from 10^{-6} gee to 2×10^{-5} gee:

$$G'_\eta = 37650\frac{\sin 2\eta}{\sinh^4\xi}\left[1-\frac{0.776\sin^2\eta+0.743}{\sinh^2\xi}\right] \text{ cm./sec.}^2 \qquad (2\text{-}50)$$

Large, known deflections of the vertical in ellipsoidal coordinates may be mechanized by the inertial navigator.

G_η' can be neglected entirely, to 10^{-5} gee, if $\xi > \xi_1$ ($r > r_1$):

$$\frac{37650}{\sinh^4 \xi_1} = 0.01$$

$$\sinh \xi_1 = 44 \approx \frac{r_1}{c}$$

$$r_1 = 23,000 \text{ km.} = 14,000 \text{ mi.}$$

Hence beyond 14,000 miles, $\overline{G}'$ is entirely vertical in ellipsoidal coordinates, to 10^{-5} gee. From the Earth's surface to 14,000 miles ($3.2 < \xi < 4.5$), the horizontal component of $\overline{G}$ is given by Equation (2-49) to 10^{-5} gee. Figure 2-12 shows typical values of G_η versus altitude, for the Earth.

2.F.9. THE MAGNITUDE OF GRAVITY ON THE EARTH.

As noted in Section 2.F.3., the magnitude of gravity can be measured direc tly only when the observer can constrain himself to be fixed relative to the Earth. Gravity measurements at a sequence of fixed points yield a map of $|\overline{g}|$. A theoretical expression for $|\overline{g}|$ as a function of position can be derived from an assumed potential. The gravity anomaly is the difference between the actual and model $\overline{g}$ fields.

Using the potential of Equation (2-26), $|\overline{g}'|$ can be found on the ellip-

soid by means of the method outlined in Section 2. F. 5. Above the ellipsoid, $|\bar{g}'|$ could be found exactly by computing $|\overline{\nabla}U|$ in geographic coordinates for $h_g > 0$. This would entail a lengthy procedure such as was used in the preceding three sections to find the horizontal components of gravity. This calculation is not performed because the navigator is not interested in the exact vertical component of gravity. On the other hand, the gravimetric geodesist is interested almost exclusively in the field on the reference ellipsoid. Equation (2-25) is conventionally used to compute the reference magnitude of gravity on the surface of the ellipsoid.

Within 500 meters above the reference ellipsoid, the gravimetric geodesist computes $g_{h=0}$ according to:

$$g_h = g_{h=0} + \frac{\partial g}{\partial h} h_g \qquad (2\text{-}51)$$

or more exactly:

$$g_h = g_{h=0} + \frac{\partial g}{\partial h} h_g + \frac{1}{2} \frac{\partial^2 g}{\partial h^2} h_g^2$$

Heiskanen (Ref. 107, pgs. 53-54) evaluates the latter on the International ellipsoid:

$$g_h = g_{h_0} - (0.30877 - 0.00044 \sin L_g)\, h_{g_{\text{meters}}} + 0.073\, h^2_{g_{\text{kmtrs.}}} \text{ milligal.} \qquad (2\text{-}52)$$

In practice, the height of the observer above the ellipsoid, h_g, is taken as the measured height of the observer above mean sea level, as determined from a levelling survey. A height error of ten feet pro-

duces a one milligal (10^{-6} gee) error in the magnitude of gravity. The actual direction of $\bar{g}$ does not coincide with the direction of the reference $\bar{g}$ because of local deflections of the vertical but since the deflection is usually less than twenty seconds of arc, the gravity magnitude error is only $\frac{\theta^2}{2} = 5 \times 10^{-9}$ gee, negligible for most purposes.

Figure 2-13 shows the parameters that have been proposed recently to describe the magnitude of gravity on various ellipsoids. The equatorial value of gravity on the reference ellipsoid, g_{eq}, is established by measuring the absolute value of gravity at some point of supposedly known geographic latitude on that ellipsoid.

By international agreement, g_{eq} is determined by the value of absolute gravity at Helmert Tower, Potsdam, East Germany when the latitude of the tower in the European grid is substituted into the standard gravity formula. Two limitations arise in establishing g_{eq}. First, the ellipsoid of the European grid does not have its center at the mass center of the Earth. Second, during the Cold War, access to Potsdam has been limited to the Scandinavian countries. Though comparisons with Potsdam have been infrequent, the Western countries have made extensive intercomparisons of gravity between major cities and observatories by flying calibrated gravimeters from point-to-point. It is generally believed that the International value, $g_{eq} = 978.0490$ cm./sec.^{2}, is too high by ten to fifteen milligals (Refs. 92, pg. 157 and 107, pg. 75).

Figure 2-13. GRAVITY FORMULAE ON REFERENCE ELLIPSOIDS

$$g_{h_o} = g_{eq}[\,1 + B_2 \sin^2 L_g + B_4 \sin^2 2L_g + D_2 \cos^2 L_g \cos 2(\lambda - \lambda_o)]$$

Author	Date	g_{eq} cm./sec.^{2}	B_2	B_4 $\times 10^6$	1/f	D_2 $\times 10^6$	λ_o Longitude of Shorter Equatorial Principal Diameter
Helmert	1901	978.030	+0.005302	-7	298.3	0	-
Heiskanen	1928	978.049	+0.005293	-7	297.3	+19	0°
International	1930	978.049	+0.0052884	-5.9	297.0	0	-
Niskanen	1945	978.0468	+0.0052978	-5.9	-	0	-4°
Jeffreys	1948	978.051	+0.005289	-5.9	297.10	0	-
Uotila	1957	978.0516	+0.0052910	-5.9	297.4	+10.6	-6°

Data from Refs. 87, pg. 306 and 107, pgs. 78 to 79.

Triaxial ellipsoids are occasionally proposed to represent the geoid (Section 2.E.). Then a triaxial gravity formula is needed to specify gravity on its surface. Such an equation is (Ref. 215, pg. 2-58):

$$g_{h=0} = g_{eq_1}[1 + B_2 \sin^2 L_g + B_4 \sin^2 2L_g + D_2 \cos^2 L_g \cos 2(\lambda - \lambda_o)]$$

where λ_o is the geographic longitude of the shorter equatorial axis. More refined estimates assume a geoid which is slightly perturbed from the shape of an ellipsoid of rotation and evaluate $g_{h=0}$ on the perturbed surface (Ref. 87, pgs. 326 - 327).

By calculating gravity as if the Earth were an ellipsoid of rotation, a systematic error is introduced whose magnitude is about $gD_2 = 2 \times 10^{-5}$ gee, from Figure 2-13. Thus if the Earth is triaxial but is assumed to be an ellipsoid of rotation for convenience of computation, the position error is only about one tenth of a mile.

The gravity field of an inhomogeneous ellipsoid of rotation is a suitable model for the reference gravity field of the Earth, for navigational accuracy

Chapter Three

GEODETIC COORDINATES

"To increase accuracy, map-makers gradually expanded the scale of their maps, first to six yards to the mile, then 100 yards.
'And then came the grandest idea of all! We actually made a map of the country on the scale of a mile to a mile!'
'Have you used it much?' I enquired.
'It has never been spread out yet,' said Mein Herr. 'The farmers objected: they said it would cover the whole country, and shut out the sunlight! So we now use the country itself as its own map and I assure you it does nearly as well.' "

Charles L. Dodgson (Lewis Carroll)
Reference 100.

3. A. INTRODUCTION.

The aim of geodesy is to assign coordinates to each fixed point on the Earth in some readily measured and commonly accepted coordinate frame which rotates with the Earth. The classical methods have inferred the coordinates of points from length and angle measurements made on the surface of the Earth.

The past decade has seen an intense revival of interest in geodesy. Electronic distance measuring devices and satellites, both active and passive, have literally added the new dimension of height to the classical tools and have increased the rapidity and accuracy of the geodetic processes. Furthermore, the requirements of the ballistic missile program have emphasized that the independent national geodetic grids do not yield sufficiently accurate navigational data for unmanned vehicles traveling between grids.

This, the most important current problem in geodesy, is of vital interest to the navigator. The problem is to give the coordinates of all points on the Earth in a single coordinate frame instead of giving them in independent local frames of limited extent. The writer has called this branch of the subject "World-Wide Geodesy" and discusses it in Section 3. K. after first presenting some necessary preliminaries.

A truly exciting prospect awaits the geodesist after the other planets have been visited. Surveys on these planets will unquestionably be necessary to guide the terrestrial visitor. Omitting the small possibility that native populations have already surveyed these planets, the geodesist will conduct surveys there, doubtless patterned after Earth-bound surveys but with the added advantage of external observation.

3. B. GEODETIC COORDINATE FRAMES.

Chapter Two discusses the shapes of the constant potential surfaces near the Earth. The surfaces of constant gravitational potential, V, and

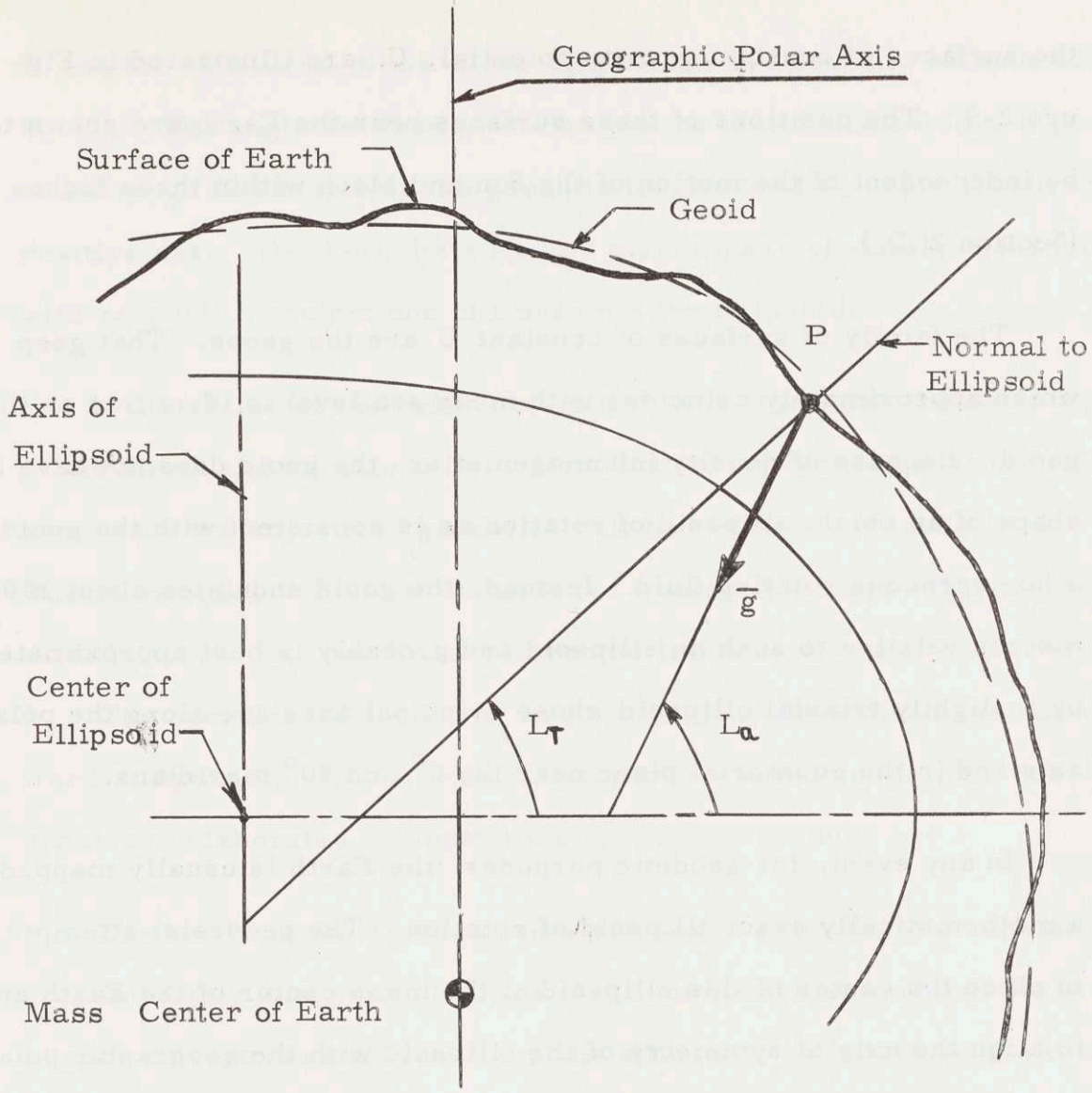

Figure 3-1

REFERENCE ELLIPSOID WHOSE CENTER
DOES NOT COINCIDE WITH
THE MASS CENTER OF THE EARTH

Note that the Axis of the Ellipsoid is Parallel to the Spin Axis of the Earth because of Laplace Azimuth Control.

the surfaces of constant gravity potential, U, are illustrated in Figure 2-9. The positions of these surfaces near the Earth are shown to be independent of the motion of the Sun and Moon within three inches (Section 2. D.).

The family of surfaces of constant U are the geops. That geop which approximately coincides with mean sea level is identified as the geoid. Because of density inhomogenieties, the geoid does not have the shape of an oblate ellipsoid of rotation as is consistent with the geoid of a homogeneous rotating fluid. Instead, the geoid undulates about ±100 meters relative to such an ellipsoid and probably is best approximated by a slightly triaxial ellipsoid whose principal axes are along the polar axis and in the equatorial plane near the 0^{o} and 90^{o} meridians.

In any event, for geodetic purposes, the Earth is usually mapped onto a mathematically exact ellipsoid of rotation. The geodesist attempts to place the center of this ellipsoid at the mass center of the Earth and to align the axis of symmetry of the ellipsoid with the geographic polar axis of the Earth (Appendix A).

Figure 3-1 shows the surface of the Earth, the geoid and an ellipsoid which has been established for mapping purposes (a "reference ellipsoid"). By definition, points above or below the ellipsoid are projected onto it along extended normals to the ellipsoid. The height of a point above the ellipsoid, measured along the normal to that ellipsoid, is called the orthometric height, h_g, of the point.

The angle between the normal to the ellipsoid which passes through

P and the equatorial plane of the ellipsoid is the geodetic latitude of P, L_T. The angle between meridian planes of the ellipsoid through P and through Greenwich is the geodetic longitude of P, λ_T, measured positive east. Geodetic distance and azimuth are similarly measured with respect to projections of lines onto the ellipsoid.

If the center of the reference ellipsoid is located at the mass center of the Earth and its axis of symmetry lies along the geographic polar axis, then the adjective "geodetic" will be replaced by "geographic." The ellipsoid is then most suitable for world-wide maps. Then geodetic latitude, L_T, becomes geographic latitude, L_g, and λ_T becomes λ_g. The coordinates L_g and λ_g are the geographic coordinates, as defined in Appendix D. The metric properties of the geographic coordinate space are elaborated in Appendix D and Chapter Four.

The height of the geoid above a reference ellipsoid at any point is conventionally designated $N(L_T, \lambda_T)$. N of course depends on the size, shape, orientation and location of the ellipsoid. A fundamental problem of geodesy is to measure N for any particular ellipsoid, as a function of L_T and λ_T.

h_g, the height above the reference ellipsoid, is necessary in the navigation equations of Chapters Four and Five. However, the height above the geoid, h_s, is of more direct interest and more easily measured. h_s, h_g and N are related according to:

$$h_g = h_s + N \tag{3-1}$$

For use in the reduction of level surveys, to be discussed in Section 3.D., the concept of potential height is defined. The geops surrounding the Earth are arbitrarily numbered and the numbers called "potential height." Two common methods of numbering exist:

1. The "geopotential number" at an altitude h_{s_1} is h_p where:

$$h_p = \int_{h_s=0}^{h_s=h_{s1}} g(h)dh \qquad (3\text{-}2)$$

It has the units of gravity × height, usually expressed in kilogal-meters and will not be used hereafter in this thesis. The potential of any geop is thus referred to the potential of the geoid.

2. Dynamic height, h_D is:

$$h_D = \frac{1}{g_o} \int_{h_s=0}^{h_s=h_{s1}} g(h)\,dh \qquad (3\text{-}3)$$

where g_o is the value of gravity at some reference point, conventionally on the reference ellipsoid at 45° latitude or where $\sin^2 L_g = \frac{1}{3}$.

Ideally, to calculate the dynamic height or geopotential number at a point, g should be measured at each height above the geoid and the integral (3-2) or (3-3) computed. These integrals are independent of the path of integration since $\overline{\nabla} \times \overline{g} = 0$ outside the Earth. In practice, such complete gravity data is neither available nor necessary. If g is given by its value on the ellipsoid, reduced by a first order free-air correction, the theoretical value can be substituted for the measured value to an accuracy of better than 0.1 per cent to relate h_D and h_g instead of h_D and h_s:

$$g_{h_g} = g_{eq}\left(1 + 0.0053\sin^2 L_g - 2\frac{h_g}{a}\right) \tag{2-51}$$

$$h_D = \frac{1}{g_{eq}\left(1 + 0.0053\sin^2 L_{g_0}\right)} \int_0^{h_g} g_{eq}\left(1 + 0.0053\sin^2 L_g - 2\frac{h_g}{a}\right) dh_g$$

$$h_D - h_g = 0.0053 h_g \left(\sin^2 L_g - \sin^2 L_{g_0}\right) \tag{3-4}$$

This equation is used in the reduction of level surveys (Section 3. D.). References 87, pp. 152 ff. and 152, p. 36 discuss dynamic height and geopotential number in detail.

Appendices C and D discuss confocal ellipsoidal coordinates, which are symmetric about the geographic polar axis. This coordinate frame is useful for navigation since it goes from geographic coordinates at the surface of the Earth (where one confocal ellipsoid coincides with the reference ellipsoid representing the geoid) to geocentric coordinates at great distances. The ellipsoidal coordinate, ξ, can be used as a non-dimensional measure of "hyperbolic height."

3. C. TYPES OF GEODETIC SURVEYS.

The classical survey techniques may be divided into three general classes:

1. vertical control surveys.
2. horizontal control surveys.
3. gravimetric surveys.

The vertical control survey seeks to find the height, h_g, of each fixed point on the Earth above the reference ellipsoid. Section 3. D.

discusses how this survey measures height above sea level and from that infers h_g and h_s.

The horizontal control survey seeks to establish two other independent coordinates needed to locate a point on the Earth. Geodetic latitude and longitude, L_T and λ_T, are by far the most commonly measured horizontal control coordinates. On continuous land masses, the astrogeodetic survey supplies the horizontal control data. Astrogeodetic surveys can be triangulations (Section 3. E.), trilaterations or traverses (Section 3. F.) in which distance and angle measurements on the Earth are combined with astronomic measurements to give the horizontal control coordinates.

Gravimetric surveys infer the shape but not the size of the geoid from measurements of the magnitude of gravity at many points on the Earth. The technique is new and potentially very valuable since it provides deflections of the vertical with respect to a reference ellipsoid which is centered at the mass center of the Earth; data not otherwise obtainable. Its chief limitation is a lack of sufficient gravity data on the Earth. Section 3. J. discusses the gravimetric survey in detail.

The use of satellites for geodetic purposes is described in Sections 2. F. 5 and 3. K. Their chief value is for geodetic measurements across oceans, which are a firm barrier to the classical survey techniques.

The over-all procedure of a geodetic survey is as follows:

1. In the field, geometric nets are laid out. Angles, lengths, heights, gravity, astronomic latitudes, longitudes and azimuths are

measured.

2. The field data are analysed to determine the most probable values of the measured quantities. The size and shape of a reference ellipsoid are selected.

3. An origin is selected for the survey. The reference ellipsoid is arbitrarily oriented and displaced at the origin.

4. Observations are reduced to the reference ellipsoid. The coordinates of the observation points on the reference ellipsoid are computed.

5. The ellipsoid is mapped onto a flat surface. This is the final result for a human navigator.

6. An optimum ellipsoid is selected. Coordinates on the arbitrary ellipsoid are mapped onto the optimum ellipsoid.

7. A single ellipsoid is selected for world-wide coverage. Coordinates on the local ellipsoid are mapped onto the world-wide ellipsoid. This is the final result for automatic navigation.

3.D. THE GEODETIC LEVEL SURVEY.

The aim of the geodetic level survey is to find the height of each point on the Earth's surface (or at least, the height of each survey station) above the reference ellipsoid. This height, designated in Section 3.B. by h_g, is exceedingly difficult to measure and of no interest outside geodesy. Hence, the level survey attempts to measure, h_s, the height of each point above the geoid. It is h_s that is shown on

Figure 3-2

TYPICAL LEVEL NET

A, B, C, D and E are Tidal Stations

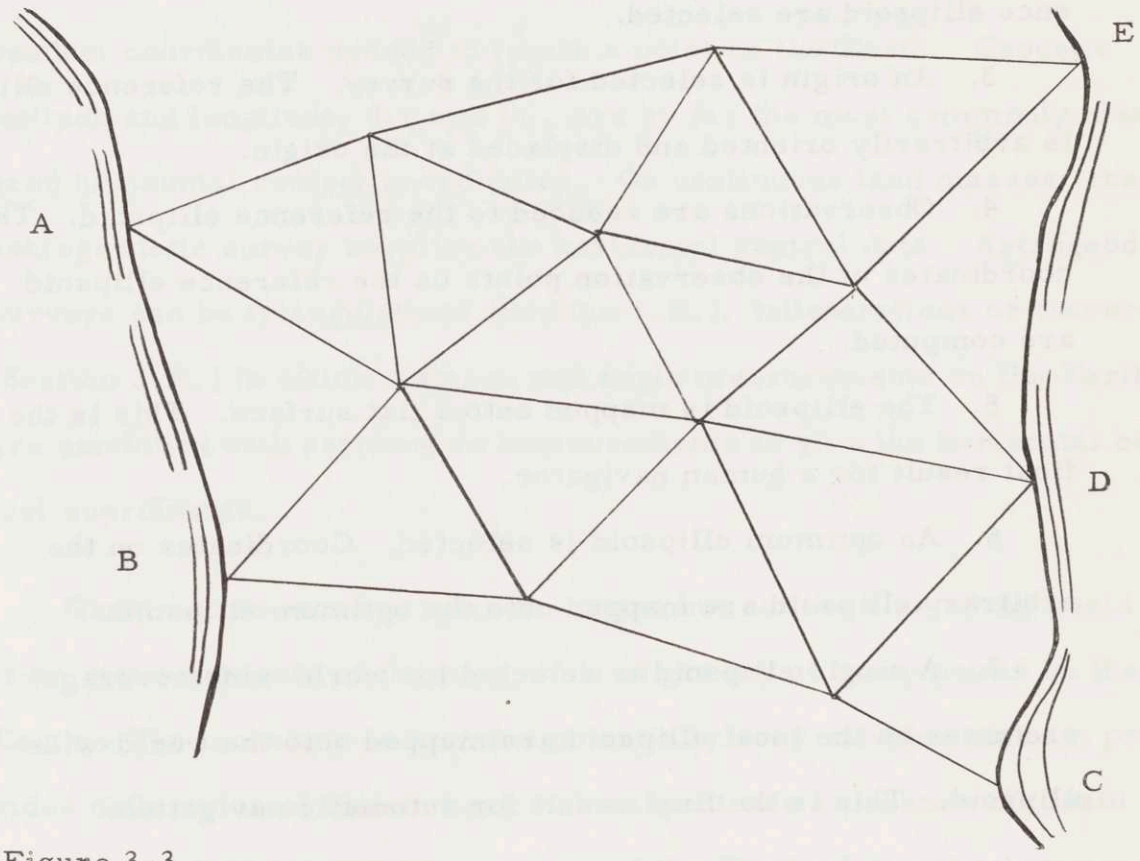

Figure 3-3

LEVELLING PROCEDURE ON A FLAT, GRAVITY-DEFLECTION- FREE EARTH.

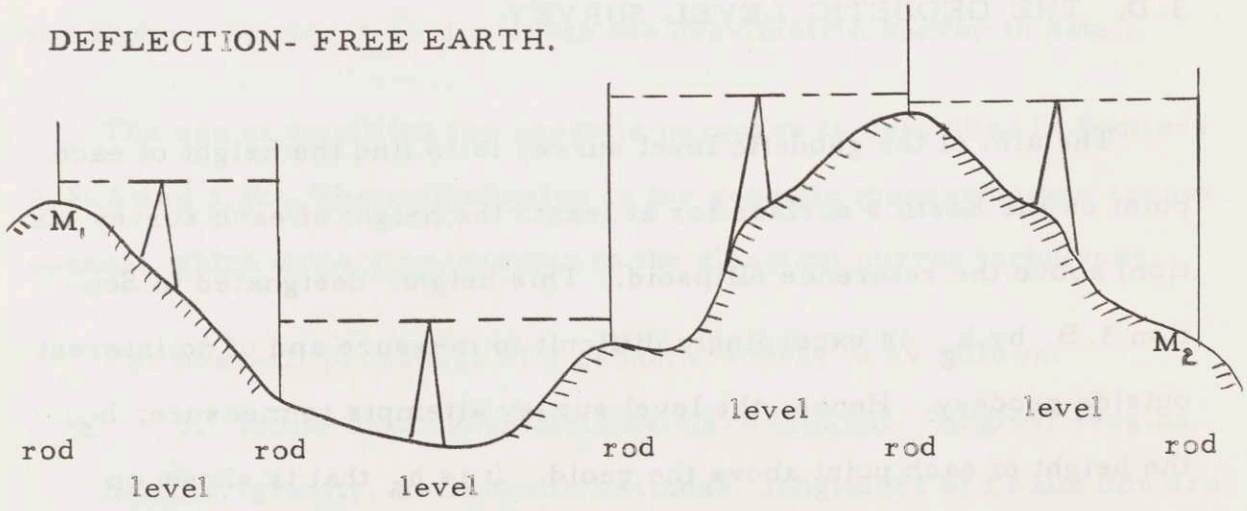

topographic maps because gravity drives things "downhill" according to h_s, not h_g.

The general procedure of a level survey is illustrated in Figure 3-2. A net of geometric figures is laid out over the area to be levelled. The lengths of the sides of the figures are about 100 to 200 miles (Ref. 87, p. 171). Wherever possible, these nets are brought to coastal points and tied to sea level as at A, B, C and D. The height differences between all vertices are measured by a process to be described below. Over small areas where the geops are roughly separated by the same distances, orthometric height is used but as the extent of the survey increases, dynamic height is used to eliminate the systematic error caused by changes in the separation between geops as a function of latitude.

A least-squares adjustment of the net, to be discussed below, gives the height of each vertex above "mean sea level," which is taken to be the geoid and in cases where N cannot be found, is also taken as the reference ellipsoid. To measure the height differences between vertices, a process called spirit leveling is used. Figure 3-3 illustrates this process on a flat, gravity-deflection-free Earth. An invar rod, calibrated in length units, is placed at the initial vertex, erected to the vertical with a spirit level and guyed in place. About 75 yards along the line to the next vertex, a geodetic level (telescope plus spirit level) is aligned perpendicular to the vertical and about 75 yards still further along, another invar rod is erected. Then by reading the calibrations

on both rods through the telescope, the height difference between the feet of the rods can be calculated. This process is repeated starting at the first vertex and proceeding across the terrain in 150 yard increments until the second vertex is reached, a distance of 100 to 200 miles. The level instruments and rods are set up on any suitable hard ground between these vertices, but every five miles or so, a permanent concrete benchmark is established for use as a local elevation reference and for possible later relevelling. References 136, 141 and 142 discuss the leveling procedure in exhaustive detail.

The rods must be close together and at roughly equal distance from the telescope to minimize refraction error (U. S. C. G. S. maximum distance is 150 meters). Rays of light from the rod to the telescope are often curved one second of arc (Ref. 87, p. 167), the refraction angle increasing with the length of sight. Hence, extremely short lines are necessary. On a statistical basis, the use of a large number of short lines does not degrade the accuracy as much as expected since the error appears to increase only with the square root of the number of sights (Ibid., p. 177).

The curvature of the Earth does not modify the results of Figure 3-3 because of the shortness of the lines. However, the presence of gravity deflections of the vertical does affect the height since the rods and level telescopes will be slightly inclined with respect to each other. However, the error varies as the cosine of the small deflection of the vertical and is conventionally omitted.

Consequently, the level survey, beginning at some benchmark, M_1 measures the orthometric height of any points on which the rods are mounted, with respect to M_1. When the line from M_1 has proceeded to the next benchmark, M_2 (about five miles from M_1), the measured orthometric height between M_1 and M_2 is corrected to dynamic height with Equation (3-3), disregarding N if it is not known. Thus, the survey is propagated over extensive areas in terms of dynamic height.

At the points A, B, C and D of Figure 3-2, where ocean ties are possible, tide gauges or "marigraphs" are located near the open sea. Sea level records are taken for at least a year, preferably more (Ref. 87, pp. 192-193), and a mean sea level established at each point. The mean sea level at each point is assumed to be the geoid and, when N is unknown, is also assumed to be the reference ellipsoid, for purposes of height computation. All mean sea levels throughout the world are thus assumed to lie on the same geop; the geoid. For example, the survey of the United States in 1929 used 26 tidal points in the Atlantic Ocean, Pacific Ocean and Gulf of Mexico, all assumed to lie on the geoid (Ref. 137, pp. 10 and 152).

The entire survey net is then reduced by means of a least-squares solution in dynamic height. The measured height at each point, h_m, is assumed to be the actual height, h_{m_a}, plus a residual, δh_m. Equations for the heights of all vertices via different paths in the net are written and a solution found for the most probable value of the δh_m. The equations are linear in δh_m with constant coefficients and are

readily programmed for digital computers so extensive areas can be reduced simultaneously. In earlier years, it was the practice to reduce several small regions independently in order to lessen the labor of computation, but such a procedure introduced arbitrary constraints (hence distortions) into the net.

Even more sophisticated reductions allow for the possibility that the surface of the ocean is acted on by forces other than Newtonian gravitation and the centripetal acceleration of rotation so that the ocean level is not a surface of constant U. The mean sea levels at the tidal stations are then also assumed to contain residual errors and are included in the reduction.

Using such a technique it was found that mean sea level at Old Point Comfort, Virginia is three feet lower, relative to the geoid, than at Prince Rupert, Canada, 2300 miles away (Ref. 152, p. 42). In the well-known case of the Panama Canal, the Atlantic and Pacific are so close that a level survey can bridge them with little error. Mean sea level in the Atlantic is 2/3 foot lower than in the Pacific (Ibid.). These results tend to confirm Stommel's calculations, mentioned in Section 2. D., that sea level can vary as much as four feet above the geoid because of currents and the Coriolis force.

The accuracy of a level survey is difficult to estimate. The U. S. C. G. S. standard for first order geodetic levelling is an error of e mm. in a length d km. where (Ref. 142, p. 2):

$$e_{mm.} = 4\sqrt{d_{km.}}$$

Over very large distances, errors appear to accumulate with length, not with the square root of length. Estimates vary from 0.0003 to 0.001 ft./mile (Ref. 87, p. 177). The International Geodetic Association in 1912 established a probable error of (Ibid.):

$$(p.e.)^2 = \eta^2 d + \sigma^2 d^2 \qquad (3\text{-}5)$$

where

$$\eta < 1 \text{ mm.}/\sqrt{\text{km.}} \quad (0.004 \text{ ft./mi.})$$

$$\sigma < 0.2 \text{ mm./km.} \quad (0.001 \text{ ft./mi.})$$

L. G. Simmons (Ref. 152, p. 4) estimates that the maximum levelling error in the center of the North American Continent is two feet. These errors are all with respect to the geoid, generally assuming that the tidal gauges are at the geoid. This assumption probably introduces an additional error of two feet.

In the course of a horizontal control survey, the height of each observation point above the reference ellipsoid is needed. Lacking information about N, the height of the geoid above the ellipsoid, it is commonly assumed that the geoid is nearly coincident with the ellipsoid. Where N is measurable (Section 3.J.) its accuracy is poorer than that of h_e so that at worst, h_g is known within fifty meters in mountainous areas.

Level surveys have identified remarkable tectonic changes in the Earth such as a 7-3/4 foot drop of the area surrounding the Hall of Records building in San Jose California from 1912 to 1954 (Ref. 137, p. 10).

For navigation, level surveys provide the vertical coordinate of points on the Earth's surface and assist in interpreting the accuracy of position data as supplied by geodetic surveys.

3. E. GEODETIC TRIANGULATION.

3. E. 1. GENERAL PROCEDURE.

The purpose of the triangulation is to establish a reference ellipsoid and to give the geodetic latitude and longitude of each observation station on the Earth's surface, on that ellipsoid. The triangulation survey is the oldest and most accurate survey technique now available.

The general procedure of the survey is to lay out a network of geometric figures, usually triangles, as in Figure 3-2 on the area to be surveyed. In general, a theodolite is erected successively at each vertex of the net and the angles between all other visible vertices observed. Occasional measurements of length are made and the remaining distances between vertices calculated from the measured lengths and angles. Astronomic measurements are made at intervals in the net in order to limit accumulated position errors. A least-squares adjustment then distributes observation errors through the net and results in the most probable values for the lengths, angles and geodetic azimuths in the net.

Having done this, the dimensions of a reference ellipsoid are selected, based on the results of past surveys. One observation station in the survey is selected as the origin of the survey and the ellipsoid is oriented and displaced as desired at the origin. It is here that an error in locating the center of the ellipsoid relative to the mass center of the Earth will occur. The observer on the Earth does not know what orientation or vertical displacement of the ellipsoid is required in order to place its center at the mass center of the Earth. Then, using equations based on the size and shape of the reference ellipsoid and knowing the length, approximate geodetic azimuth and approximate geodetic latitude of each vertex in the net, the exact geodetic latitude, longitude, and azimuth of each vertex are computed.

The usual survey ends after assigning a geodetic latitude and longitude to each observation station and by preparing maps of the survey. Strictly, the survey can finally be recomputed to second order to improve the accuracy in several respects, notably in the optimum selection of the size, shape and orientation of the reference ellipsoid. Such programs have only recently been undertaken.

3. D. 2. INSTRUMENTATION.

The geodetic survey must be conducted in the field under the most primitive conditions, and hence of necessity uses only a few types of instruments. Devices are needed to measure angle, length and astronomic latitude, longitude and azimuth (and hence time, also).

The geodetic theodolite is invariably used to measure angles. This instrument is a telescope mounted in calibrated altitude-azimuth gimbals, with provisions for spirit-leveling. References 87 and 101 discuss the geodetic theodolite in detail.

The vertices of the triangulation net are identified by permanent concrete benchmarks over which tripods or portable "Bilby towers" are erected, as high as 130 feet to view the other vertices. The theodolite incorporates an optical collimator for use in plumbing the instrument directly over the benchmark. The Bilby tower is composed of two independent structures; the center one for the instrument and the outer one for the observer (Ref. 101, pp. 26-96).

Angles are usually read to a probable error of 0.1 to 0.3 second of arc (Refs. 87, p. 67 and 113, p. 95) which accuracy can be improved by a factor of five or ten by averaging many readings (Ref. 87, p. 18).

The classical instrument for measuring length, and that most prevalent today, is the invar tape or rod. The U.S.C.G.S. uses 50 meter flat invar tapes (Ref. 152, p. 5). Each tape is calibrated by the National Bureau of Standards to an accuracy variously given as one in 10^6 (Ref. 101, p. xvii) and 2 in 10^6 (Ref. 152, p. 5) under standard conditions of support. In the field, four tapes are used to measure each base line; two have a positive coefficient of thermal expansion and two negative. The tension and method of support are carefully controlled and the temperature measured. Wind screens keep the tape hanging freely. The criteria for first order base line measurements require a probable error of one in 10^6 for each length measurement

but Simmons (Ref. 152, p. 5) suggests that the actual accuracy of measurement is only four to five parts in 10^6, a more realistic but perhaps still optimistic figure.

Two electromagnetic devices have been introduced recently to measure distance. In operation both insert an integral number of standing half-wavelengths between stations.

One of these devices, built in Sweden by Svenska AB Gasaccumulator, is the Geodimeter (Ref. 145). The Geodimeter transmits a visible light beam of constant frequency, intensity-modulated by a Kerr cell, from one station to a reflector at the other station and back. An electric signal proportional to the modulating frequency is passed through a calibrated variable delay line and compared to a signal activated by the return beam. The delay is varied until both signals null each other. Then the time of transit is given directly by the delay in the delay line. If the velocity of light in the air is known, the distance between stations, along the path taken by the beam, can be calculated. Changes in the delay time of any number of half modulating cycles are undetectable by a simple null measurement, thus leading to an ambiguity in the distances of half a wavelength of the modulating frequency. To resolve this ambiguity, a second measurement is made at a different constant modulating frequency which is not an integral multiple of the first.

The instrument's accuracy is limited chiefly by uncertainties in the velocity and path length of the light beam. The velocity of light in vacuo is probably known to somewhere between two and fifteen parts

in 10^6 (Refs. 146, p. 68 and 152, p. 5) although the manufacturers of the Tellurometer claim one part in 10^6 (Ref. 125) However, the Geodimeter operates over terrain of uncertain temperature and humidity and over an optical path of unknown length.

The "average error" for the Model 4 Geodimeter is given by the manufacturer as 0.04 foot ±5 parts in 10^6 at a range of four miles (Ref. 145), which is one part in 185,000 at 20 miles. Reference 137 however, is more enthusiastic and claims one part in 3×10^6 for bases in Thailand measured by the U. S. Army Map Service, on page 7, and one part in 500,000 compared to taped baselines, on page 8.

To reduce atmospheric variations between stations and to improve the signal-to-noise ratio, measurements are made only at night. The optimum range is one to twenty miles though operation to thirty miles is possible (Ref. 145).

The Tellurometer is a similar device, built by Tellurometer, Inc., Union of South Africa, and operating at microwave frequencies (Refs. 125 and 139). The master transmitter is mounted at one point and an active slave station (transponder) at the distant point. The device has the same problems as the Geodimeter with respect to the unknown velocity of light and path length in the atmosphere and in addition, has a wider beam width so spurious reflection from the ground and from solid objects is troublesome. It suffers from the additional disadvantage that powered active stations are necessary at both observation points but offsetting these is the advantage that observation points need not be

intervisible since microwave radiation can penetrate fog and timber (Ref. 139, p. 34). The optimum range is 10 to 25 miles, though the device can be used from 1/2 to 35 miles (Ibid.).

Though their accuracy is nominally poorer than tape, these electronic devices can measure a twenty mile long line at once without the error-accumulating procedure of measuring it in fifty meter segments over hill and dale. They will probably eventually replace tapes for the measurement of distance. Vertical angles or height differences are needed in conjunction with these devices to reduce the measured lengths to the horizontal.

3. E. 3. TRIANGULATION FIELD PROCEDURE.

A triangulation begins with a reconnaissance of the area to be surveyed (Ref. 101, p. 1 ff., p. 193). The net of triangles is designed so that in the solutions for the unknown sides, the probable errors for the computed lengths will be as low as possible. A parameter called "strength of figure" is used as a figure of merit for the shape of the net (Section 3. E. 4). The lengths of the sides of the triangles, for the usual geodetic survey, are about thirty kilometers (Ref. 113, p. 94).

The vertices of the triangles are identified by permanent concrete benchmarks, on which instruments are mounted using Bilby towers as noted in Section 3. D. 2. To measure angles, the theodolite is placed

on one station and focussed lights are placed on the other stations, aimed toward the first. All measurements are made at night to reduce refraction errors over hot ground. The observer then reads "rounds" of horizontal angles between all visible stations as many as thirty to forty times each to improve the accuracy by accumulating large angle readings. The readings are made in the form of sums of angles such as:

Reading 1: Angle 1 + angle 3 + angle 5.
Reading 2: Angle 2 + angle 3 + angle 6.
Reading 3: Angle 1 + angle 2 + angle 4.
etc.

Section 3. E. 6. discusses the reduction of this data to usable form. Vertical angles are read but cannot be used in place of the levelling survey discussed in Section 3. D. since the refraction errors over such large distances are hopelessly large for levelling purposes. Refraction of the light beams occurs in the plane of the axis of the beam and the direction of the temperature gradient. Thus, over hilly country, lateral as well as vertical refraction errors exist. It is for this reason that observations are made only at night.

Occasionally, natural landmarks such as a church steeple are selected to be vertices of the triangulation net. A theodolite cannot be located at such a point during the course of a survey; hence angles are read to it from other points. Such a point is called an "unoccupied" or "intersected" point.

References 87, 101 and 117 discuss the field procedures in detail.

The oceans are entirely unmapped, astrogeodetically, though a very few gravimetric measurements have been made using underwater and

submarine gravimeters (Ref. 107, pp. 113-117). The major obstacle is the absence of fixed points, which can be retrieved at will, on which instruments can be mounted. Recently, Ewing, Worzel and Talwani suggested a technique for establishing such fixed points in the ocean (Ref. 152, pp. 7-19). They suggest placing an array of acoustical transponders on the bottom of the sea which will define an underwater "benchmark." By interrogating the transponders with Sonar, a ship can determine its distance from the "center" of the benchmark. The authors suggested measuring distances between such benchmarks by timing the passage of underwater explosions. Though the method appears impractical because of the uncertain velocity and path of the underwater long-distance sound waves, Hiran or Transit satellite observations may provide a more accurate means of locating the underwater benchmarks. The development of ship-borne stable platforms may make astronomical measurements possible at these benchmarks.

A network of recoverable benchmarks would allow the entire surface of the Earth to be covered with a geodetic net. This would facilitate intercontinental ties and provide considerable information to the geophysicist concerning the precise shape of the geoid.

3.E.4. INSERTION OF BASE LINES.

Base lines are measured to establish a distance scale for the triangulation. A base line is about three to six kilometers long (Ref. 113, p. 2) and is usually measured by taping. Base lines are inserted into

the triangulation net wherever the probable error in computing sides of the triangles (as measured by the strength of figure parameter) increases to a preset limit. The definition of strength of figure and its application are described in Reference 101, pages 267-270. Figure 3-5 shows these preset limits for a first order survey. Typically, a base line is inserted every ten to twenty triangles (Ref. 113, p. 94). As few base lines are used as possible because of the time and cost of tape measurements.

The short base line is tied into the net of forty mile triangles by means of auxiliary triangles which have necessarily poor strength of figure, thus degrading the over-all distance accuracy still further. Electronic distance measuring devices, though of nominally poorer accuracy than tape, allow an entire side of the triangulation net to be measured as a base line.

Standard base lines exist in several countries, for checking tapes, Geodimeters and Tellurometers and for insuring that all nations use the same length standards. They are measured by means of the highly accurate Vaisala light interferometer (Ref. 115). Some existing standard base lines are shown in Figure 3-4.

3.E.5. AZIMUTH CONTROL.

The triangulation procedure calculates the size and shape of the net of triangles determined by the observation points. The orientation of the net on the Earth's surface must be established separately. This

Figure 3-4

STANDARD BASE LINES

Date	Country	Length	Accuracy
1947	Finland	864 meters	1 in 17×10^6
1953	Argentina	480 meters	1 in 9×10^6
1957	Netherlands	576 meters	1 in 11×10^6
1958	Germany	864 meters (2 sections)	1 in 20×10^6

Data from Reference 103.

requires that the azimuth of each line, reduced to the ellipsoid, be known relative to the geodetic meridian.

Astronomic azimuth, A_Q, as measured in the field, is not the same as geodetic azimuth, A_T, as defined on the mapping surface. The astronomic meridian is the plane containing the instantaneous spin axis which is parallel to $\bar{g}$. Since $\bar{g}$ and the spin axis are skew lines, the plane of the astronomic meridian of a point does not contain that point. The geodetic meridian is the plane defined by the radius vector from the center of the ellipsoid to the observation point and the geographic polar axis. Allowing for polar migration separately, the two azimuths differ if the prime deflection of the vertical is not zero.

Geodetic azimuth is not measurable but can be calculated from measured quantities. Theoretically, one calculation of geodetic azimuth should orient the entire net but in practice, errors accumulate and the error in azimuth increases, unbounded. Hence, in any net, azimuth

Figure 3-5

ACCURACY REQUIREMENTS

FOR HORIZONTAL CONTROL

First Order Triangulation	
Strength of Figure	
Desirable limit between bases.	80
Maximum limit between bases.	110
Desirable limit, single figure.	15
Maximum limit, single figure.	25
Triangle Closure	
Average not to exceed.	1 sec. of arc
Maximum not to exceed.	3 sec. of arc
Number of Observations with a One Second Direction Theodolite	16
Base Measurement	
Actual error not to exceed.	1 part in 300,000
Probable error not to exceed.	1 part in 1,000,000
Discrepancy between two measurements of a section not to exceed.	10 $\sqrt{km.}$ millimeter
Astronomic Azimuth	
Probable error.	0.3 sec. of arc
First Order Traverse	
Closing Error in Position Less Than.	1 part in 25,000
Probable Error of Main Angles.	1.5 sec. of arc
Number of Stations Between Laplace Stations	10 to 15
Astronomic Azimuth, Probable Error.	0.5 sec. of arc
References 101 and 149, pgs. 10-11	

control stations called "Laplace stations" are inserted at intervals of about ten to twenty triangles or, following recent practice, one for each base line (Ref. 113, p. 94).

At a Laplace station, astronomic measurements of latitude and longitude are made and the astronomic azimuths of some lines in the triangulation net are measured. If necessary, the astronomic measurements are corrected from the instantaneous pole to the geographic pole.

The geodetic latitude and longitude of each point in the net can be calculated as explained in 3. E. 6. in terms of the geodetic latitude and longitude at the origin, which are assumed. If the axis of the reference ellipsoid is constrained to be parallel to the geographic polar axis, it is clear that the meridian deflection of the vertical, δ_M, is:

$$\delta_M = L_a - L_T \tag{3-6}$$

and the prime deflection of the vertical is:

$$\delta_p = (\lambda_a - \lambda_T) \cos L_a \tag{3-7}$$

if $\lambda_T = \lambda_g$ at Greenwich. δ_p is also related to the astronomic and geodetic azimuths:

$$\delta_p = (A_a - A_T) \tan L_a \tag{3-8}$$

Hence, equating Equations (3-7) and (3-8):

$$A_T = A_a - (\lambda_a - \lambda_T) \tan L_a \tag{3-9}$$

Thus at any Laplace station, the geodetic azimuth can be computed from the measured astronomic azimuth, astronomic longitude and the

calculated geodetic longitude and latitude. The prime and meridian deflections of the vertical can also be calculated at the Laplace stations. Consequently, in the reduction of the horizontal control survey, azimuths are reduced to the ellipsoid within an error of about 0.3 seconds of arc (Ref. 113, p. 95 and Figure 3-5), that remains bounded because of the use of Laplace azimuth control.

The deflection of the vertical at any point can be measured by establishing a Laplace station there, measuring the astronomic latitude and longitude and comparing to the calculated geodetic latitude and longitude. However, the cost and the length of time of measurement involved in establishing a Laplace station at each point of the survey is prohibitive.

3.E.6. SURVEY REDUCTION.

The taped lengths are measured along or above the surface of the Earth, not on the ellipsoid. When these lengths are reduced to the ellipsoid, along the normals to the ellipsoid, they will be too long or too short depending on whether they are above or below the ellipsoid. If the measured line lies at an average height, h_g, above the ellipsoid then the measured length, d_M, must be reduced to:

$$\frac{\rho_A}{\rho_A + h_g} d_M$$

on the ellipsoid. ρ_A is the radius of curvature of the ellipsoid at the latitude and azimuth of the line being measured (Appendix C). In order

to maintain an accuracy of one part in 10^6 on the ellipsoid, the reduction must be applied when h_g exceeds twenty feet.

The reduced height can be written as:

$$\frac{\rho_A}{\rho_A + h_g} d_M \approx \frac{\rho_A}{\rho_A^2 + 2\rho_A(N+h_s) + (h_s N)^2} d_M = \frac{\rho_A}{\rho_A + h_s} \frac{\rho_A}{\rho_A + N} d_M \qquad (3\text{-}10)$$

In practice, h_s is known from a level survey to an accuracy of about two feet (Section 3. D.). Hence the reduction:

$$\frac{\rho_A}{\rho_A + h_s}$$

can be made accurately. However, the Molodensky correction, $\frac{\rho_A}{\rho_A + N}$ is more difficult to calculate since N is known imperfectly, if at all. N cannot be calculated until first order astrogeodetic and gravimetric surveys have been completed. Fortunately, if the reference ellipsoid is properly chosen, the Molodensky correction is appreciable only in mountainous areas where the geoid and ellipsoid are most widely separated. It has been applied only in rare cases. For example, in the traverse from Scandinavia to South Africa, the Molodensky correction accumulated to a ninety meter distance error (Ref. 98, p. 76).

The raw angle data are in the form of sums of angles between stations measured in a plane perpendicular to $\bar{g}$ at the theodolite station. These sums include repetitions of the angles in order to improve the accuracy of the readings. If n_i are the number of repetitions, the measured data are in the form:

$$\sum_{i=1}^{N} n_i \theta_i$$

A field reduction selects the most probable value of θ_i, θ_{i0} by a least squares solution, subject to the constraint that

$$\sum \theta_{i_0} = 360^\circ$$

about each observation station. Weighting factors are often inserted to account for visibility, size of the angle, etc. (Ref. 140, pp. 97-121).

Clearly, this reduction distributes errors only among those angles taken about the same point. Strictly, the errors should be distributed throughout the net but are not because of the numerical complexity which would thereby be engendered.

The angles are measured perpendicular to local gravity, not perpendicular to the ellipsoid normal. The difference varies as cos δ_v, which is so nearly unity that it is not taken into account.

The lengths and angles comprising the triangulation net on the ellipsoid are then obtained. If d_{ei} are the lengths reduced to the ellipsoid and $\theta_{oi} = \phi_i$ are the angles of the triangles, already once reduced, then relations must be satisfied of the form:

$$\sum \phi_i = 180^\circ + E_i$$

$$\frac{d_{ei}}{\sin \phi_i} = \frac{d_{ej}}{\sin \phi_j}$$

in each triangle. E_i is the spheroidal excess of the i^{th} triangle, given in Appendix C. Because of measurement errors, d_{ei} and ϕ_i will not

satisfy such relations so another least squares reduction is needed. The angles and lengths are written as sums of most probable values plus residuals:

$$d_{ei} = d_{ei_o} + \delta d_{ei}$$

$$\phi_i = \phi_{i_o} + \delta\phi_i$$

and solutions found for $\delta\phi_i$ and δd_{ei}. In this least-squares adjustment, as many triangles should be reduced simultaneously as possible in order to distribute errors over as large a net as possible without constraint. In years past, the enormous labor involved has restricted the size of the nets which could be reduced simultaneously. The advent of digital computers has made the reduction of large nets possible. For example, 1100 stations in Alaska were adjusted simultaneously, a feat requiring the simultaneous solution of 3400 linear equations for the residuals (Ref. 137, p. 6).

Rainsford discusses calculation procedures for survey reductions employing routines which identify blunders (Ref. 140, passim).

The adjustment procedure requires the knowledge of approximate latitude for computation of the spheroidal excess before the exact geodetic latitude can be calculated.

The final step in the reduction of the classical geodetic survey is to calculate the geodetic latitude and longitude of each observation station. First, the dimensions of a reference ellipsoid (of rotation) are assumed. This requires two parameters, a and ϵ or more commonly,

a and f where the flattening, f, is related to ϵ in Appendix C.

Then a Laplace station is selected as the origin of the survey. At the origin, the astronomic latitude and longitude are measured as usual and the geodetic latitude and longitude are assumed. Section 3.G. shows how the assumption of geodetic latitude and longitude at the origin fixes the orientation of the reference ellipsoid relative to the Earth. Measured astronomic azimuths are converted to geodetic azimuths using Equation (3-9).

The reduction then proceeds outward from the origin. a and f of the reference ellipsoid are known. L_T of the origin is known. Then from the length and azimuth of a line from the origin, formulae such as Reference 87, pp. 83-94 give the difference in geodetic latitude and difference in geodetic longitude between the ends of the line. In this manner, the survey is propagated outward from the origin.

Theoretically, the measured azimuth at the origin is sufficient to orient the entire net but as noted earlier, cumulative errors cause the net to "swerve" with respect to the geodetic meridian as the distance from the origin increases. Hence, Laplace control is used at intervals to correct the azimuths. A least-squares error criterion is used to distribute azimuth errors throughout the net, thus minimizing the importance of the measurement at any one azimuth station.

Thus, on the assumed reference ellipsoid, L_T and λ_T can be calculated for each point. For visual use, the ellipsoid is then mapped onto a plane surface using any of a number of transformations discussed in

Section 3. H.

The calculated L_T and λ_T of each point depends directly on the arbitrary choice of size and shape of the reference ellipsoid and on the geodetic latitude and longitude assumed for the origin. The selection of optimum ellipsoids is discussed in Sections 3. G. and 3. K.

The adjustment procedure can be summarized as follows:

a. Reduce the measured lengths to the ellipsoid using the results of the level survey and using N, where available.

b. Compute the most probable values of the measured angles from the "rounds" measured in the field, using a least-squares adjustment.

c. Establish the dimensions of a reference ellipsoid.

d. Adjust the triangulation net by least-squares. Calculate the spheroidal excess for each triangle and reduce the net to find the most probable values of the lengths and angles.

e. Assume values for L_T and λ_T at the origin.

f. Calculate L_T and λ_T of all observation stations, using formulae for that particular reference ellipsoid, working outward from the origin.

g. Optimize onto the best-fitting ellipsoid.

h. Make maps.

3. E. 7. ACCURACY.

Lengths of the base lines are nominally measured to a probable error of one part in 10^6 (Figure 3-5) but in fact are probably accurate to

only about four or five in 10^6 (Ref. 152, p. 5) especially after reduction to the ellipsoid.

Individual angle measurements are made to about 0.2 to 0.3 second of arc (Ref. 113, p. 95 and Figure 3-5) and are averaged to about 0.1 second. Astronomical angles are about equally accurate.

Calculations are carried to eight digits in length and to 0.01 second of arc, in angle. After adjustment, the triangles close within one second of arc (Ref. 149, p. 10) and lengths are accurate to about one in 100,000 (Ref. 87, p. 63). Some exceptionally accurate surveys have been made, notably the 2500 kilometer "ring" around the Baltic Sea which reportedly closed within 2.5 meters (one part in 10^6) according to Heiskanen (Ref. 103).

Meade (Ref. 152, p. 31) estimates that in the United States, the position error in a first order survey between two points d_{KM} kilometers apart is:

$$0.059\ d_{KM}^{2/3} \quad \text{meters}$$

which is one part in 200,000 at 1000 miles.

3.F. TRILATERATION AND TRAVERSE.

3.F.1. TRAVERSE.

The immediate aim of a horizontal control survey is to provide benchmarks to which local surveys can be tied. Secondarily, the

results are of invaluable geodetic importance. Thus, in large, unpopulated areas, the cost of a triangulation may not be justified. Instead, a less accurate survey procedure called a "traverse" has been used for horizontal control.

The traverse is simply a straight-line measurement of distance and azimuth, perhaps along a highway or railroad track, interspersed with many azimuth control (Laplace) stations to bound the errors.

The traverse procedure is not well-regarded by geodesists because of the lack of control on errors. Figure 3-5 shows the U. S. C. G. S. specifications for a first order traverse. Ultimately electronic distance measuring techniques combined with more frequent astronomic measurements may improve the accuracy of the traverse until it is comparable to that of a triangulation. Bomford (Ref. 87, pp. 63-65) suggests that with Laplace stations spread every two miles, the traverse accuracy should equal or exceed the triangulation accuracy.

Many areas of the western United States are still connected to the East by means of traverses.

3. F. 2. TRILATERATION.

The classical survey measures angles because the painfully slow process of measuring length with a tape is relatively inaccurate, expensive and slow. Since World War II, a plethora of electronic distance

measuring tools have become available. Among them are the Geodimeter and Tellurometer, Hiran (high-precision Shoran), Loran and Radar. These devices either measure length between two points or distance from some fixed stations.

The first three devices are widely used in attempts to achieve geodetic accuracy. Geodimeters and Tellurometers are being taken to observation stations by helicopter, Jeep or backpack and used to measure lengths between hitherto inaccessible stations. Laplace stations are interspersed for azimuth control. Then, the survey is reduced as discussed in Section 3. E. 6.

A major objection to the trilateration is that just enough information is obtained to solve the triangles whereas the triangulation contains a considerable redundancy of measured angles to check errors.

Presently, Hiran, the most accurate of the radar- or hyperbolic-type devices is said to give an accuracy as high as one part in 240, 000 (Ref. 35). The Geodimeter and Tellurometer give about one part in 10^5 or slightly better (Section 3. E. 2.). There is every reason to believe that with the increased use of trilateration, it will replace triangulation, to geodetic accuracy.

The U. S. Army Map Service, U. S. Air Force and various oil companies have made much use of trilateration. Over-all probable errors have been estimated as one part in 200, 000 for a 1000 mile Hiran survey (Ref. 50). The 10, 000 km. Hiran survey around the Caribbean Sea, closing a loop from Florida, around the Gulf of Mexico,

through Venezuela to Trinidad and returning to Florida reportedly closed within 25 meters (Ref. 98, p. 73).

3.G. SELECTION OF A REFERENCE ELLIPSOID.

An observer outside the Earth would view the selection of a reference ellipsoid as follows. First the size and shape are defined. Then the ellipsoid's center is located as close to the mass center of the Earth as possible. Finally, the ellipsoid is oriented to place its axis of symmetry parallel to the geographic polar axis of the Earth. Points on the Earth map onto the ellipsoid along the normal to the ellipsoid. The external geometric interpretation shows that seven parameters are needed to fully define a symmetric ellipsoid, nine to define a triaxial ellipsoid:

1. Size, a, and shape, f, of a symmetric ellipsoid or the three principal semi-diameters of a triaxial ellipsoid.
2. Position of the origin, three parameters.
3. Orientation of the ellipsoid, two parameters, for a symmetric ellipsoid; three for a triaxial ellipsoid.

Because the geodesist cannot view the Earth from afar, this procedure is in fact impossible. The Earth-bound observer must select an origin and define the seven parameters of a symmetric ellipsoid as follows:

1. Size, a, and shape, f, as before.
2. Geodetic latitude and longitude of the point on the ellipsoid

Figure 3-6

DIMENSIONS OF PROPOSED

REFERENCE ELLIPSOIDS

Author	Date	a meters	b meters	1/f	Notes
Everest	1830	6377,276	6356,075	300.8	
Bessel	1841	6377,397	6356,079	299.15	
Clarke	1866	6378,206	6356,584	294.98	
Clarke	1880	6378,301	6356,566	293.47	
Hayford (International)	1909	6378,388	6356,912	297.00	
Heiskanen	1928	(gravimetric)		297.3	Triaxial. $\lambda_0 = 0°$ $a_1 - a_2$ = 242 m.
Heiskanen	1929	6378,400	6357,010	298.2	Triaxial. λ_0=34°E $a_1 - a_2$ = 165 m.
Krasovsky	1938	6378,206	6356,846	298.6	
Krasovsky Triaxial	1942	6378,245	6356,863	298.3	Triaxial. λ_0= 15°E $a_1 - a_2$= 212 m.
Jeffreys	1948	6378,099	6356,631	297.10	
Hough (U.S. Army Map Service	1956	6378,270	6356,794	297.0	

Data from References 87, pg. 306; 98; 107, pgs. 80 and 230; 149. Hayford gave minor axis as 6356,909 meters which is arithmetically inconsistent with 1/f = 297.00.

which is to coincide with the origin of the survey.

3. Height of the ellipsoid above the ground surface at the origin of the survey.

4. Orientation of the ellipsoid. This requires two more parameters, implied in the Laplace control equations.

The size and shape of the reference ellipsoid are selected from the results of past surveys, Figure 3-6. The origin should be selected in an area in which the geoid is smooth. Thus, the ellipsoid can be oriented parallel to the geoid without introducing large deflections of the vertical throughout the remainder of the net.

The definition of the two orientation parameters is clear if the Earth can be viewed externally. The center of the ellipsoid is fixed and two parameters are needed to orient its axis. However, to an Earth-bound observer, the situation is more complicated. The Laplace control equations, Equations (3-6) through (3-8), are true only if the axis of the ellipsoid is parallel to the geographic polar axis; two orientation parameters of the axis of the ellipsoid relative to the geographic polar axis have been implicitly introduced and set equal to zero. One parameter is essentially an independent specification of δ_M in such a manner that δ_M, L_a and L_T satisfy Equation (3-6). The other parameter is either δ_p at the origin or A_T of a line radiating from the origin, both defined so as to satisfy Equations (3-7) and (3-8) at the origin. This procedure insures that the Laplace conditions include the constraint that the axis of the ellipsoid be parallel to the geographic polar axis of the Earth. If these constraints were not incorporated in

the Laplace equations, the axis of the reference ellipsoid would not be parallel to the geographic polar axis. However, Laplace control cannot influence the location of the center of the ellipsoid relative to the mass center of the Earth. The orientation of a triaxial ellipsoid requires the independent specification of geodetic azimuth.

The dimensions of the reference ellipsoid used by the U. S. C. G. S. are those of the Clarke Ellipsoid of 1866, Figure 3-6. The origin in the United States, and since 1913 throughout North America, is a benchmark in Kansas known as Meade's Ranch (Ref. 149, pp. 13-14). The International Ellipsoid of 1924 is used throughout most of Western Europe (Section 3. K. and Figure 3-6).

Having selected and oriented an ellipse, is this the best orientation, size and shape? To answer this question, a criterion for "best" must be defined. In years past, the "best" size and shape was that which represented the "figure of the Earth" most exactly. Today, the ellipsoids being proposed are so nearly alike that arguments as to which best represents the geoid are tautological, especially since a large error is introduced because of the separation between the center of the ellipsoid and the mass center of the Earth.

A better criterion is to select the size, shape and orientation which minimizes some parameter such as mean square N or mean square δ_v over the surveyed area. The optimization can be performed analytically using the equations shown in Reference 87, pp. 127-132 for transforming from one ellipsoid to another. Analytically, the Earth

can be mapped onto an arbitrary ellipsoid and then transformed to some ellipsoid of unknown parameters where the parameters are found by minimizing integrals of the form:

$$\oint N^2(L_T, \lambda_T)\, dS$$

or:

$$\oint (\delta_P^2 + \delta_M^2)\, dS \qquad (3\text{-}11)$$

Several recent attempts have been made to do this (Refs. 113 and 152, p. 30). A major problem is a lack of information concerning N, δ_M and δ_P relative to the first assumed ellipsoid. Section 3.J. discusses some means of measuring N, δ_M and δ_P over large areas. Meade (Ref. 152, p. 30) states that attempts are underway to reduce the entire European land mass simultaneously, allowing enough degrees of freedom to select an optimum N, δ_M and δ_P at the origin. This procedure requires the repeated solution of ten thousand simultaneous equations, using a digital computer, for various values of N, δ_M and δ_P at the origin until values are found which minimize the integrals, Equations (3-11).

The optimum ellipsoid for a restricted area on the Earth's surface will not generally have its center at the mass center of the Earth, especially if the surveyed area is small. Conversely, an ellipsoid whose center is at the mass center of the Earth will fit poorly, locally compared to an ellipsoid which has the optimum local orientation. Section 3.K. pursues this problem further.

It is noteworthy that the navigator does not require position coordinates on an optimum ellipsoid. Any ellipsoid is satisfactory for navigation provided that all points on the Earth are mapped onto the same ellipsoid and provided that the components of $\bar{g}$ and $\bar{\omega}_{IE}$ are known in the geographic coordinate frame defined by that ellipsoid.

3.H. MAPS.

The results of a geodetic survey are three coordinates, L_T, λ_T and h_g of each point in the surveyed area relative to an assumed reference ellipsoid. For visual use, these must be presented on a map which should show relative position, direction, distance, shape and area and be readily constructed (Ref. 109, p. 2).

Accurate maps must be made on flat surfaces for convenience in printing, manufacture, storing and handling. Thus, the mapping problem consists essentially of devising coordinate transformations which will map each point of the reference ellipsoid onto a flat surface with a minimum of distortion. A purely distortion-free transformation (isometric) is possible only between surfaces of the same Gaussian curvature (Ref. 221, p. 260) so a distortion-free map from an ellipsoid onto a plane is impossible.

Mapping schemes can be generally divided into two broad categories; projective and analytic. In the former, some physical process is used to project points from one surface onto the other, as in a

radial projection from a sphere onto a tangent plane. In the latter category, a complex coordinate transformation is used with no simple physical model. Maps from an ellipsoid onto a plane (as distinguished from maps onto a plane from a sphere) are usually analytic, not projective. Many books on mapping exist (Refs. 4, 89, 109, and 221) which discuss a large number of maps, each suitable to some special purpose. This section discusses the two most common maps; the Lambert conformal and transverse Mercator projections. One or the other of these has been adopted by every state of the Union for presenting the results of first order surveys. Though both are analytic maps, an approximate projective model exists to describe each transformation.

The Lambert conformal conic projection projects points from the ellipsoid onto a circular cone whose vertex is on the axis of the reference ellipsoid. The cone slices into the reference ellipsoid as in Figure 3-7, intersecting it in two standard parallels of latitude, north and south of the central region of the map. Note that distortion is independent of east-west position so the map can have an indefinite east-west extent. However, distortion changes markedly with north-south position. On the standard parallels of latitude, the north-south and east-west scales are substantially exact. Between the standard parallels the ellipsoid is above the cone and projected lengths are too small. Outside the standard parallels, the projected lengths are too large and the scale increases rapidly with distance from the standard parallels. In order that the error nowhere exceed one part in 10, 000, the maximum north-south extent of the map must be 158 miles and the

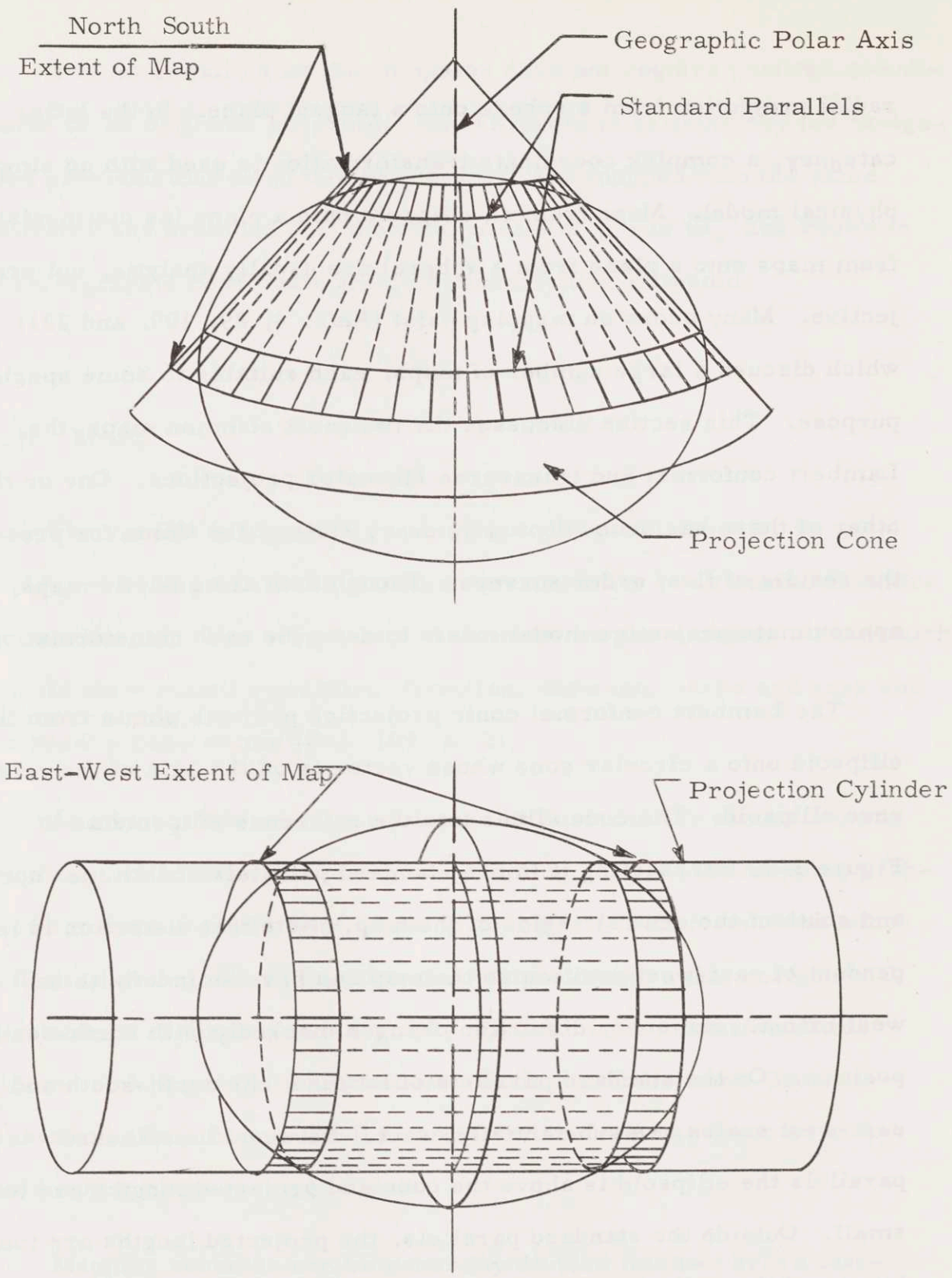

Figure 3—7

THE LAMBERT CONFORMAL PROJECTION (ABOVE)
THE TRANSVERSE MERCATOR PROJECTION (BELOW)

standard parallels placed 2/3 this distance apart (Refs. 87, pp. 132-151 or 89, pp. 310-328). Since there is no limit to the east-west extent of this map, it is used to represent areas such as the state of Massachusetts or Long Island which have predominate east-west extents. The transformation equations from L_T and λ_T to the Lambert x and y grid coordinates are found in Reference 147.

The transverse Mercator projection projects points from the ellipsoid onto an elliptic cylinder whose axis intersects the axis of the reference ellipsoid and is perpendicular to it, Figure 3-7. The size and shape of the cylinder are such that it slices into the reference ellipsoid along two plane ellipses, parallel to and equidistant from the central meridian of the map. Note that distortion is independent of north-south extent. However, distortion changes markedly with east-west position. On the two elliptic intersections between the ellipsoid and the cylinder, the north-south and east-west scales are substantially exact. Between these intersections, the ellipsoid is above the cylinder so projected lengths are too small. Outside these intersections, projected lengths are too large and the scale increases rapidly with distance from the central meridian. In order that the scale error be nowhere greater than one in 10,000, the east-west extent of the map must be limited to 158 miles and the elliptic intersections must be about 2/3 this distance apart. There is no limitation on the north-south extent of a transverse Mercator projection so it is used to represent areas such as Michigan or California which have extensive north-south dimensions. The transformation equations from L_T and λ_T to Mercator x and y grid

Figure 3-8

DEFLECTION OF THE VERTICAL AT AN AZIMUTH, A.

$\delta_A = \delta_m \cos A + \delta_p \sin A$

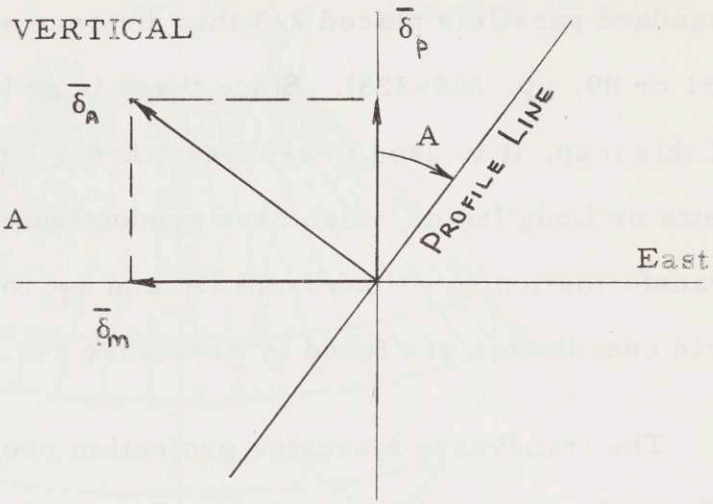

Figure 3-9

A GEOIDAL PROFILE SHOWING THE DEFLECTION OF THE VERTICAL AT AN AZIMUTH, A.

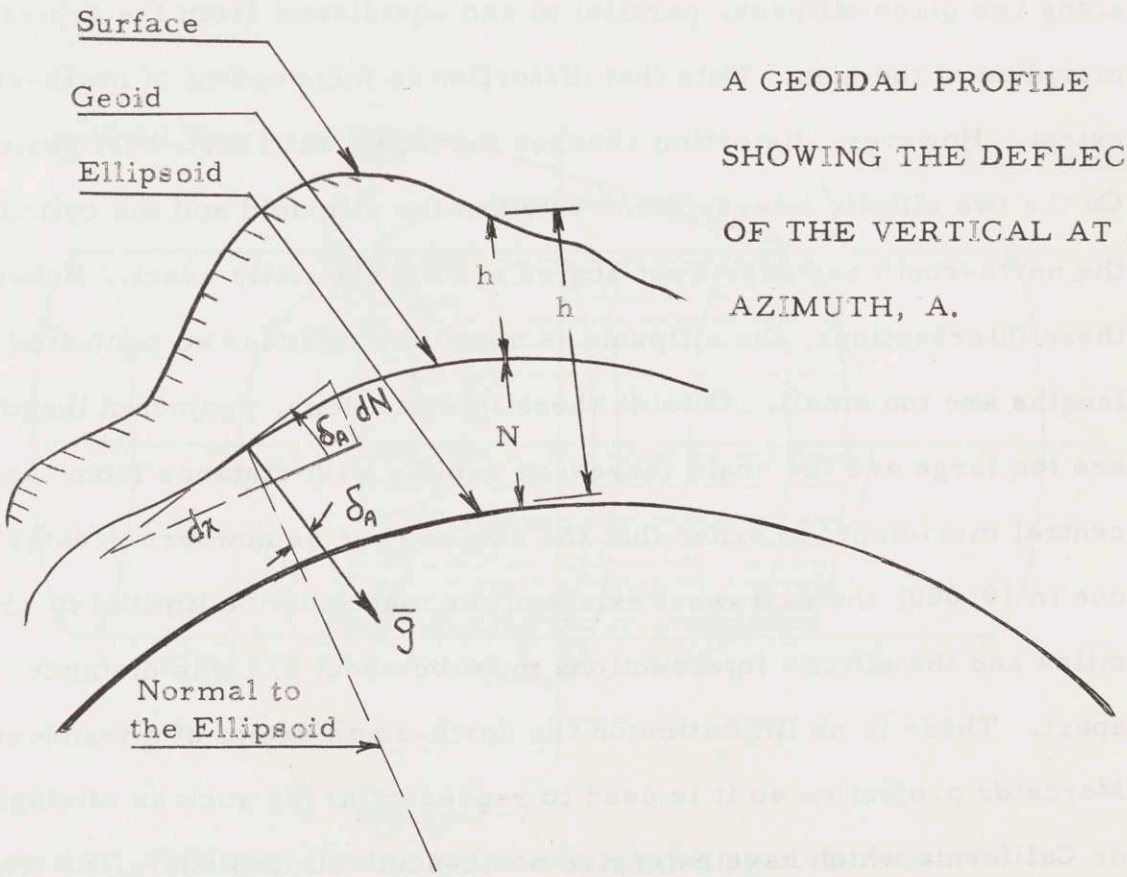

coordinates are given in Reference 147.

For local manned navigation missions, it is assumed that the pilot has a map drawn in transverse Mercator or Lambert grid coordinates and would like his navigation device to read out in these same coordinates, not in latitude and longitude. Section 5.D briefly considers the mechanization of an inertial navigator in map grid coordinates.

3.J. THE MEASUREMENT OF GEOIDAL HEIGHTS AND THE DEFLECTION OF THE VERTICAL.

3.J.1. GEOIDAL PROFILES.

The height of the geoid above a reference ellipsoid is needed in the accurate reduction of the horizontal control survey and to compute h_g, the geographic height of a point on the Earth's surface with respect to the reference ellipsoid.

In an area which has already been surveyed to first order but in which the Molodensky, or N, correction has been omitted because N is unknown, N can be calculated by the measurement of geoidal profiles. Suppose the survey has been reduced to a reference ellipsoid, omitting the Molodensky correction and that at some point, the principal deflections of the vertical are δ_M and δ_P. Then in a direction at an azimuth A, the deflection is δ_A :

$$\delta_A = \delta_M \cos A + \delta_P \sin A \qquad (3\text{-}12)$$

Figure 3-8. Figure 3-9 shows a vertical section of the Earth at an azimuth A. Since $\overline{g}$ is normal to the geoid:

$$\tan \delta_A \approx \delta_A = - \frac{dN}{dx} \tag{3-13}$$

where x is horizontal distance. The negative sign arises since conventionally, δ_M and δ_p are positive when $\overline{g}$ is southwest of the normal to the ellipsoid. Hence the difference in elevation between the geoidal heights at points P_1 and P_2 is:

$$N_{P_1} - N_{P_2} = \int_{P_1}^{P_2} \delta_A \, dx \tag{3-14}$$

Thus, if a survey is taken along a line at azimuth A, the geoidal height differences are found approximately by taking the average δ_A between P_1 and P_2:

$$N_{P_2} - N_{P_1} = \frac{\delta_{A(P_2)} + \delta_{A(P_1)}}{2} \chi_{\overline{P_1 P_2}} \tag{3-15}$$

In practice, the procedure for a geoidal profile is as follows:

a. A route is mapped over the area to be surveyed, near previously surveyed benchmarks.

b. The route is subdivided into straight-line segments at known constant azimuths. Reference 87, p. 249 gives the typical length of a segment as ten to twenty miles. The route begins at the origin of the survey where N_o has been arbitrarily defined.

c. At successive points along the profile line, astronomic latitude and longitude are measured and geodetic latitude and longitude computed. δ_M and δ_p are computed using Equations (3-6)

and (3-8), and δ_Δ using Equation (3-12). Equation (3-15) is used to calculate ΔN, and hence N, since N_o is known or assumed at the origin.

δ_V and N are referred to the ellipsoid which was arbitrarily established at the origin of the survey and whose center is not necessarily at the mass center of the Earth. Hence, geoidal heights calculated in different geodetic nets are not comparable. Bomford (Ref. 88, p. 251) estimates that with line segments fifteen miles long, N can be calculated to an accuracy of 1-1/2 to 3 feet.

3.J.2. GRAVIMETRIC SURVEYS.

The gravimetric survey attempts to calculate the geoidal height and deflection of the vertical relative to an ellipsoid which is centered at the mass center of the Earth. The method is indirect and uses as its basic data measurements of the magnitude of gravity throughout the world.

Referring to Section 2.D., the geoid is the equipotential surface of Newtonian gravitation and rotation. The cogeoid is a hypothetical boundary equipotential of the Earth. It is obtained by removing and adding mass to the Earth according to some compensation scheme until a limiting equipotential surface is obtained from which no mass protrudes. This cogeoid is a function of the compensation scheme used.

The magnitude of gravity can be measured on the surface of the

Earth and occasionally under the sea, on the surface of the sea and in the air. For any known compensation scheme which converts the geoid into a cogeoid, the gravity values on the geoid can also be converted into corresponding gravity values on the cogeoid, g_c. In principle, g can be measured at each point on the Earth and reduced to the cogeoid beneath.

The size and shape of a reference ellipsoid can be defined theoretically. The value of gravity, g_{h_o}, at every point on the reference ellipsoid can be calculated using Equation (2-25).

The gravimetric survey makes use of the calculated anomaly, $g_c - g_{h_o}$, to evaluate N, δ_M and δ_p of the cogeoid relative to an ellipsoid whose mass center is at the center of the Earth and which has the assumed dimensions. Since N, δ_M and δ_p are referred to the cogeoid, not the geoid, the subscripts "c" will be used. The calculation of N_c, δ_{Mc} and δ_{pc} from the computed anomaly is based on the theorems of Stokes and Vening-Meinesz (Ref. 107, pp. 63-69) which express them, at any point, P_1, in terms of the following integrals over the entire surface of the Earth:

$$
\begin{aligned}
N_c &= \frac{R_E}{g_E} \int_0^{\pi} F(\psi)(g_c - g_{h_o})\, d\psi \\
\delta_{Mc} &= -\frac{1}{R_E} \frac{dN_c}{d\psi} \sin A \qquad (3\text{-}16) \\
\delta_{pc} &= -\frac{1}{R_E} \frac{dN_c}{d\psi} \cos A
\end{aligned}
$$

where:

$$F(\Psi) = \frac{\sin\Psi}{2}\left[1 + \csc\frac{\Psi}{2} - 6\sin\frac{\Psi}{2} - 5\cos\Psi - 3\cos\Psi \ln_e\left(\sin\frac{\Psi}{2} + \sin^2\frac{\Psi}{2}\right)\right]$$

R_E = any radius of the earth.

g_E = any value of gravity on the reference ellipsoid.

The integration is taken over a sphere whose radius is approximately that of the Earth, instead of over the ellipsoid, to sufficient accuracy, considering the sparse gravity data which is available. ψ can be interpreted geometrically as the geocentric angle from P_1, at which N and δ_V are to be measured, to the point at which g is measured.

It is assumed that the angle between the geoid and cogeoid is small so the deflection of the vertical of the geoid and cogeoid relative to the ellipsoid are equal. Heiskanen (Ref. 107, p. 73) estimates that these deflections of the vertical differ by no more than 0.1 second of arc. The height between the geoid and the cogeoid can be calculated for any compensation scheme so N can be found from N_C.

Clearly, a lack of information about g in an extensive area degrades the accuracy of N and δ_V. For example, values of g_c do not exist over most of the world's ocean areas. Errors in g_c in distant parts of the world do not affect N, δ_M and δ_P too severely because the function, $F(\psi)$, attenuates with increasing ψ. However, the areas over which g_c is unknown are so large that the weighted effect on N, δ_M and δ_P is large.

Heiskanen and his associates at the Ohio State University Mapping and Charting Laboratory have continued Tanni's work to establish a gravimetric geoid. Heiskanen has divided the globe into $1^\circ \times 1^\circ$

spherical quadrilaterals and estimated the average magnitude of gravity within each quadrilateral. In the case of unsurveyed areas, such as the Pacific Ocean, he has assumed a value zero for $g_c - g_{h_o}$ (Ref. 107, p. 271). By numerical integration of Equations (3-16) N, δ_M and δ_P are found everywhere.

The error casued by omission of data is difficult to assess. In the vicinity of P_1, gravity must be known very well to get accurate results but the effect of distant areas is not as clear (Ref. 114). For example, Heiskanen estimates that if $g_c - g_{h_o}$ is assumed to be zero for all points $\psi > 20^\circ$, the error in N is only 13 meters (Refs. 107, pp. 271ff. and 114) and if the area of radius $\psi > 25^\circ$ around the antipode of P_1 is omitted, the error is five meters (Ref. 107, p. 271 ff.). If $g_c - g_{h_o}$ is assumed to be zero for $\psi > 3^\circ$, the error in the deflection of the vertical is only four seconds of arc and if $g_c - g_{h_o} = 0$ for $\psi > 20^\circ$, the error is only two seconds of arc (Ibid.).

Figure 3-10.

Typical Heights of Columbus Geoid

above Reference Ellipsoid

(from Ref. 113)

Region	Height of Geoid above reference ellipsoid
Spain	+40 meters
East Indian Islands	+15
Wyoming	+20
Puerto Rico	-40
India	-25
Pacific Ocean	- 5

The gravimetric geoid calculated from the $1^{\circ} \times 1^{\circ}$ quadrilaterals is called the Columbus Geoid (Refs. 105 and 107, p. 289 ff.). Two meter contours are given in the United States and Europe and ten meter contours elsewhere, all with respect to a reference ellipsoid of flattening 1/297.00. Figure 3-10 shows typical heights of the geoid above the ellipsoid. An additive elevation constant corresponds to the value of g_{eq} used in the theoretical gravity formula. The Columbus geoid, though admittedly crude, shows no triaxiality.

The ideal astrogeodetic survey would use gravimetric data to decide on N_0 and δ_{V_0} at the origin and thereby provide "gravimetric control stations" to control N, δ_M and δ_P in the same manner that Laplace stations control azimuth. This has not yet been done except on an experimental scale (Ref. 107, p. 269 and 98) because of the lack of adequate gravity data over the entire Earth. Gravimetric values of δ_P are especially valuable since they reduce the necessary accuracy in measuring astronomic longitude in the astrogeodetic survey. Rice (Ref. 107, p. 268) found that the accuracy of gravimetric deflections of the vertical, in areas covered heavily with gravity measurements, can equal or surpass that of astrogeodetic deflections.

In order to obtain more gravity coverage over the Earth, the U. S. Air Force has been conducting experiments to measure gravity over large areas from an airplane (Refs. 131 and 148 and Sections 2.F.3 and 5.F.3.). In future years, as more gravity data accumulates, this method may become more valuable. The U. S. C. G. S. plans to cover the United States with ground gravity stations at six mile intervals

(Ref. 101, p. 19). Also, gravimeters are being exchanged between nations to insure identical calibration throughout the Western world. Section 3. K. discusses world-wide geodetic ties in more detail.

3. K. WORLD-WIDE GEODESY.

3. K. 1. INTERGRID TIES.

Most of the advanced nations of the world have established their own geodetic programs. Each nation (occasionally, each region, as in the case of the United States, Alaska, Canada and Mexico) has established triangulation or trilateration nets and occasionally traverse lines to cover its land area. The nets of each nation are surveyed and adjusted independently. Each nation chooses dimensions for a reference ellipsoid, chooses an origin and then orients its ellipsoid independently of the others.

By international agreement at the 1924 annual meeting of the International Geodetic Association in Madrid, most of the countries of the world adopted the same ellipsoid dimensions; those of the Hayford ellipsoid of 1909, renamed the International ellipsoid. The assumed dimensions are those shown in Figure 3-6, although Hayford's original specification contained an inconsistency between a, b and f caused by an arithmetic error. Those nations such as the United States which had begun geodetic programs early, had accumulated such a large body of data on their own national ellipsoids that a change to the International

was prohibitive.

The navigator, travelling across the world, must be independent of local reference ellipsoids and would like to operate on a world-wide ellipsoid. The need for accurate world-wide satellite tracking and navigation, the need to guide ballistic missiles and other unmanned vehicles and the invention of electronic distance measuring devices have brought about a renaissance in geodesy, with emphasis on world-wide intergrid comparisons. Failing the establishment of a world-wide grid, the geodesist or navigator would like to know the relative displacements between the national reference ellipsoids. These could be specified by giving the x, y and z rectangular coordinates of the center of one ellipsoid in the coordinates of another or by giving the geodetic latitude, longitude and height in one grid of a point in another. Some national datums are shown in Figure 3-11.

If different ellipsoids are used by countries which are located on the same land mass, they can be readily tied together by triangulation across the national boundaries. In the past, nationalistic impulses and a lack of motivation have mitigated against such cooperation. Heiskanen estimates that the coordinates of an unspecified European point or points, possibly Potsdam, East Germany, differ by 95 meters in the Danish and Swedish systems, 250 meters in the Danish and German systems and 191 meters in the English and French systems (Ref. 107, p. 233).

The misorientations of the ellipsoids can be quite pronounced. For

Figure 3-11

NATIONAL GEODETIC DATUMS

Dimensions of Reference Ellipsoids

are Shown in Figure 3-6

Nation or Region	Name of Datum	Reference Ellipsoid	Origin
United States of America, Canada, Mexico	North American Datum of 1927	Clarke, 1866	Meade's Ranch, Kansas
Germany	-	Bessel	Potsdam, East Germany
Europe	-	International	Same
U.S.S.R.	-	Krasovsky, 1942	Pulkovo Observatory
India	-	Everest	Kalianpur
Japan	Tokyo Datum	Bessel	Tokyo
Manchuria	Manchurian Principal System	Bessel	Shinkyo

Data from References 87; 98; 107, pg. 234; 149.

example, Japan's reference ellipsoid is a Bessel ellipsoid and India's is an Everest ellipsoid but both are poor fits, even within their own countries, because they are badly oriented (Refs. 87, p. 130; 98, p. 78 and 152, p. 30). The origin of the Japanese system, Tokyo, happens to be on a sharp geoidal slope where δ_V was arbitrarily chosen to be zero, thus making the Tokyo datum a poor fit to the geoid in much of Japan. The Manchurian Principal System (also a Bessel ellipsoid but differently oriented) appears to be a better fit.

A comparison between ellipsoids separated by a body of water is impossible by the classical astrogeodetic techniques. Heiskanen, in 1959, estimated that distances between points in the Eurasian and North American land masses might be in error by as much as five miles (Ref. 102) though other estimates are as low as 100 meters (Ref. 152, p. 31). The most probable separations are on the order of 500 to 1000 feet (Refs. 87, p. 337 and 146, p. 12). Several techniques have evolved to connect geodetic nets separated by bodies of water. These divide into two broad categories; those which simultaneously triangulate an object from two grids and those which observe a moving object successively in each grid, its trajectory being inferred between observations.

A rocket, flare or artificial satellite can be equipped with a flashing strobe light and launched into orbit. At least two observers, at known locations in each of the grids to be connected, view the object and triangulate it simultaneously. Each observer can compute the position of the strobe light in his own grid. Thus, the coordinates of one point, the flare or strobe light, are found simultaneously in two grids.

The observation of a flashing light instead of a steady flare reduces the need for accurate time information since, if the flash is fast enough, the observers need only be certain that they are all observing the same flash. More important, this method makes it unnecessary to know the object's trajectory.

The most serious objection to the simultaneous triangulation of a flashing light is that at large distances, it appears near the horizon and the refraction error will, for example, exceed five minutes of arc in the vertical plane, at a five degree elevation angle (Ref. 4, p. 430). Simmons (Ref. 152, p. 6) believes that although most of the vertical refraction is predictable, there is still an uncertainty of five to ten seconds of arc. He also states that horizontal angles can be measured to one second of arc but in view of atmospheric turbulence, this appears optimistic. Furthermore, additional errors are introduced by the poor strength of figure of the vertical triangles. In spite of this, the observation of flares has been widely used to connect islands to nearby mainlands.

Artificial satellites are an extremely useful geodetic tool. If the nets to be connected are close together, the satellite can be triangulated simultaneously from several stations in each net as described above.

If the orbit of the satellite can be calculated at any instant (Appendix F), then the satellite can be observed against a star background by observers in one grid as it passes overhead near the zenith and again by observers in another grid, perhaps fifteen to thirty minutes later. The time of each observation must be measured carefully, both grids

being on the same time scale. If the orbit is known, the observers can find the coordinates of each observation point in the other grid. A serious limitation to such a method is the effect of short-period perturbations of the satellite about the mean, plane elliptic orbit. Because the path of the satellite is calculated from relatively few observation stations, many observations are required to identify short-period trends. If unpredictable perturbations are large, the satellite will not follow the predicted orbit between the observation stations and the triangulation would be in error. Reference 146, pages 30 ff. gives the position error of a 1000 mile high satellite as 300 feet. It is probably safe to say that the usual position error is three times as large. The triangulation error will be roughly as large as the error in satellite position.

Section 2. F. 5 discusses the use of artificial satellites for computing the form of the gravitational potential of the Earth.

The Transit satellite (Refs. 29 and 43) is placed in orbit and its position calculated as a function of time. With this orbital information, and with a measurement of the Doppler shift of a signal from the satellite during an overhead pass, ground observers can calculate their position on a reference ellipsoid of any assumed size and shape, centered at the mass center of the Earth. Since the first such satellite has just been launched (April, 1960), it appears to be too early to assess the accuracy of Transit, even if the satellite orbit could be predicted precisely.

A third method of effecting intercontinental ties is to triangulate

an aircraft simultaneously from two geodetic nets. Hiran (high-precision Shoran) is often used for this purpose (Refs. 35 and 50). A Hiran receiver-transmitter in the aircraft simultaneously measures the distance of the aircraft from four transponders, two in each grid on the ground, as a function of time. The result is a series of coordinates of the same point, the aircraft, in both nets. By continued application of such a trilateration, a Hiran tie has been extended from Canada to Scotland by the U. S. Air Force (Refs. 116, p. 1 and 146, p. 11). Section 3. F. 2. gives the best over-all accuracy of a Hiran trilateration as one in 2×10^5 which at least equals that of a conventional trilateration.

Another triangulation technique which has been used for long-range intergrid ties is to observe the times at which the Moon occults a particular star, from points in two different grids. (Ref. 108). The method is limited by uncertainties in the rugged surface of the Moon since observers in different grids on the Earth observe the occultation behind different points on the Moon. The best published accuracy claims an eleven meter error for a 400 kilometer tie (Ref. 113, p. 99), an error of one in 40, 000. The method of lunar occultations was used to locate the South Pacific island of Palau (Ref. 137, pp. 17-18) and is being extended to other islands in the Marianas and Carolines (Ibid. and Ref. 108).

A similar triangulation method observes solar eclipses from stations in different geodetic grids (Ref. 113).

3. K. 2. WORLD-WIDE REFERENCE ELLIPSOIDS.

The various national ellipsoids have different sizes, shapes and center positions. If Laplace control is exact, they all have nominally parallel axes of symmetry. Whitten (Ref. 152, p. 31) estimates that all their axes of symmetry are within three seconds of arc of each other. Section 3. G. showed the difficulty of placing the center of a reference ellipsoid at the mass center of the Earth. The separation between the ellipsoid's center and the mass center of the Earth is estimated by Rice to be 100 meters (Ibid.) by Bomford to be 300 meters (Ref. 87, p. 337) and by Williams to be about 500 feet (Ref. 146). In order to estimate the separation between the centers of two ellipsoids, a geodetic tie must connect them. Consequently, even if the triangulation within a net were perfect, the navigator must accept an error as large as 1000 feet or more if he travels from grid to grid, unless all grids are converted to a world-wide datum.

The U. S. Army Map Service combined astrogeodetic and gravimetric data to select a world-wide ellipsoid. The result is the Hough ellipsoid (Refs. 91 and 98) whose dimensions are shown in Figure 3-6. The computations were based on the following published astrogeodetic arcs:

1. Surveys of the U. S., Canada, Alaska and Mexico on the North American Datum of 1927.

2. three long north-south arcs and several shorter north-south and east-west arcs in the Western Hemisphere. One long arc

extends the length of North and South America. One of the short arcs extends east-west from Colombia to Trinidad.

3. a survey "ring" around the Caribbean. This was triangulated over land and trilaterated using Hiran over the island chains (see also Section 3.F.2. and Ref. 116, p. 7).

4. national geodetic surveys of Europe.

5. the North African triangulation grid and the thirtieth meridian traverse north from South Africa. These surveys are tied to Europe from North Africa to Crete to Greece and from North Africa through the Levant to Greece, thus forming a closed Eastern Mediterranean "ring."

6. the Soviet grid, which overlaps the European grid at Pulkovo on the west and the Manchurian grid on the east.

7. the Manchurian Principal Grid, to which the Korean and Japanese surveys were reduced.

The technique used by Mrs. Fischer, of the Army Map Service, was first to select more than 100 points in Eurasia at the corners of $5^{o} \times 5^{o}$ squares and place all of them on a common ellipsoid. Then, she optimized the change-of-ellipsoid formula to find the parameters a, f, N_0, δ_{M_0} and δ_{P_0} (the latter three at the origin) which would minimize the mean square N over the entire net. This resulted in an optimum astrogeodetic Eastern Hemisphere ellipsoid.

131 similar points in the Western Hemisphere were analysed to find the optimum ellipsoid there. An ellipsoid with the dimensions of the Hough ellipsoid was found to yield a sufficiently small $\overline{N^2}$, though

not the unconstrained minimum. Lacking published intercontinental ties, Mrs. Fischer finally assumed that the world-wide ellipsoid has the dimensions of the Hough ellipsoid. Using gravimetric data, she was able to coarsely locate both hemispheres with respect to each other. Intergrid ties and improved geodetic data over hitherto unmapped regions will improve the selection of a world-wide optimum reference ellipsoid.

Using the Hough ellipsoid in its optimum Western Hemisphere orientation, it is found that at Meade's Ranch, δ_M and δ_P are about one second of arc and N_0 is about ten meters (Ref. 98, p. 75). Thus, Meade's Ranch is a good origin, being on a gentle, geoidal slope.

3.K.3. SUMMARY.

The geodesist can find the relative location of two fixed points on a well-surveyed land mass to within twenty meters, an ample accuracy for any navigation application. Relative locations between islands and continents can probably be specified to 300 meters because of uncertainties in the relative orientation of the respective reference ellipsoids.

The navigator does not ask that the world be mapped onto the optimum ellipsoid; any ellipsoid is satisfactory if it is universally used. For navigation applications, all points on the Earth should be mapped onto an ellipsoid whose dimensions are mutually agreed upon, though not necessarily optimum. Its orientation should be fixed with respect to

the Earth. Gravimetric and satellite measurements should be used to ascertain the proper deflection of the vertical and geoidal height needed at each national origin to retain the agreed-upon-orientation for the world-wide ellipsoid.

Finally, the vector angular velocity of the Earth and the vector gravity must be known in the geographic coordinates defined by the ellipsoid (Sections 2.F. and 4.G.). The location of the center of the world-wide ellipsoid relative to the mass center of the Earth does not affect the position accuracy between points on the surface of the Earth. However, it does affect the mechanization of the inertial navigation equations. Because the center of the ellipsoid will rotate around the spin axis of the Earth, a centripetal force field would be created which must be included in the navigation equations. For example, if a 10^{-6} gee threshold is assumed for the accelerometers, the center of the world-wide ellipsoid may be no more than 2000 meters from the mass center of the Earth.

Chapter Four

THEORY OF COORDINATE TRANSFORMATIONS

4. A. THE METRIC TENSOR.

The role of coordinate transformations in navigation is greatly illuminated by the use of tensor calculus, the general theory of coordinate transformations. This chapter discusses those aspects of three-dimensional tensor calculus which are applicable to navigation. Complete treatments of the subject are found in References 225 and 237.

Suppose y_1, y_2 and y_3 are orthogonal Cartesian coordinates which are transformed to some arbitrary curvilinear coordinates z^1, z^2 and z^3 according to the transformation:

$$y_i = y_i\,(z^j) \tag{4-1}$$

where the only restriction on the transformation is that it be single-valued, continuous and differentiable. z^i are the contravariant components of the position vector $\bar{z}$ as discussed in Section 4. C. The

upper index is not an exponent. Since the y coordinate frame is Cartesian, there is no distinction between the covariant coordinate, y_i and the contravariant coordinate, y^i (see Section 4.B.).

The Jacobian matrix of this transformation has the elements a_{ij} where:

$$a_{ij} = \frac{\partial y_i}{\partial z^j} \tag{4-2}$$

Some interesting properties of this matrix are discussed in Section 4.B.

The differential distance between neighboring points at any time is ds:

$$(ds)^2 = (dy_1)^2 + (dy_2)^2 + (dy_3)^2$$

$$= \left(\frac{\partial y_1}{\partial z^j} \partial z^j\right)^2 + \left(\frac{\partial y_2}{\partial z^j} \partial z^j\right)^2 + \left(\frac{\partial y_3}{\partial z^j} \partial z^j\right)^2$$

or more briefly:

$$(ds)^2 = \frac{\partial y_i}{\partial z^j} \frac{\partial y_i}{\partial z^k} \partial z^j \partial z^k = g_{jk} \partial z^j \partial z^k \tag{4-3}$$

where summation is understood on a repeated index. The matrix elements g_{jk} are the covariant elements of the metric tensor $\overline{\overline{g}}$. This tensor describes the nature of the transformed space at each of its points.

Clearly, the individual terms:

$$\frac{\partial y_i}{\partial z^j} \frac{\partial y_i}{\partial z^k} \partial z^j \partial z^k \qquad \text{(no sum)}$$

and:

$$\frac{\partial y_i}{\partial z^k} \frac{\partial y_i}{\partial z^j} \partial z^k \partial z^j \qquad \text{(no sum)}$$

are identical so $g_{jk} = g_{kj}$ and the matrix of the covariant elements of the tensor is symmetric.

The contravariant elements of the metric tensor, $\overline{\overline{g}}$, are g^{ij} where the matrix product of the covariant and contravariant elements :

$$g_{ij}\ g^{jk} = \delta_i^{\ k}$$
$$[g_{ij}]\,[g^{jk}] = [I] \qquad (4\text{-}4)$$

as shown on page 171. Since $[g_{ij}]$ is symmetric, its inverse, $[g^{ij}]$, is also symmetric. The notation of Equation (4-4) is that of matrix algebra (Ref. 223, Chap. 1). The metric tensor should be regarded as having intrinsic significance for any particular coordinate transformation. Convenience dictates whether covariant and contravariant components are used.

In any coordinate frame, g_{ij} or g^{ij} has nine elements of which six are independent since the matrices are symmetric. The character of the new coordinates can be inferred from either matrix:

1. If all six independent elements are general functions of position, the new coordinates are non-orthogonal and curvilinear.

2. If all elements are constant, the coordinate axes are straight lines but do not necessarily intersect orthogonally. For example, Appendix G discusses such an oblique coordinate frame in detail.

3. If the diagonal elements are functions of position but the off-diagonal elements are zero, the coordinates are curvilinear and orthogonal. Examples are the ellipsoidal and geographic coordinates discussed in Appendix D. When the g_{ij} matrix is diagonal, the non-zero elements are often designated h_i^2 and the matrix written:

$$[g_{ij}] = \begin{bmatrix} h_1^2 & 0 & 0 \\ 0 & h_2^2 & 0 \\ 0 & 0 & h_3^2 \end{bmatrix}$$

$$[g^{ij}] = \begin{bmatrix} \frac{1}{h_1^2} & 0 & 0 \\ 0 & \frac{1}{h_2^2} & 0 \\ 0 & 0 & \frac{1}{h_3^2} \end{bmatrix} \qquad (4\text{-}5)$$

4. If the off-diagonal elements are zero and the diagonal elements are unity, the new coordinates are rectangular Cartesian.

5. If the off-diagonal elements are zero and the diagonal elements are constant but different, the coordinates are rectangular with different scales along the three axes.

Figure 4-1 summarizes the results of this section.

4.B. COVARIANT AND CONTRAVARIANT ELEMENTS OF TENSORS.

Formally, the 3^M symbols:

$$T_{ijk\cdots} \qquad \text{(M indices)}$$

where the indices take on the independent values 1, 2, 3, ..., are the covariant elements of a tensor if, under a transformation of coordinates, Equation (4-1), the elements transform according to the rule:

$${}^{z}T_{ijk\cdots} = {}^{y}T_{pqr\cdots} \frac{\partial y_p}{\partial z^i} \frac{\partial y_q}{\partial z^j} \frac{\partial y_r}{\partial z^k} \cdots \qquad (4\text{-}6)$$

The superprefix y or z indicates the coordinate frame in which the elements of $\overline{\overline{T}}$ are expressed. They are the contravariant elements of a tensor if they transform according to:

$${}^{z}T^{ijk\cdots} = {}^{y}T^{pqr\cdots} \frac{\partial z^i}{\partial y_p} \frac{\partial z^j}{\partial y_q} \frac{\partial z^k}{\partial y_r} \cdots \qquad (4\text{-}7)$$

Mixed contravariant-covariant elements can be defined analagously. Since y is Cartesian, no distinction is made between y_i and y^i.

$\overline{\overline{T}}$ has significance by itself as a tensor though its elements differ in different coordinate frames and in covariant or contravariant form. A tensor of order two, $\overline{\overline{T}}$, thus has nine contravariant or covariant elements which can be written as square 3 × 3 matrices. The elements of higher order tensors cannot be so represented in a two dimensional array. A first order tensor is called a vector and its elements are often called components. First and second order tensors transform as follows:

$$
\begin{aligned}
{}^{z}T_i &= a_{ji}\,{}^{y}T_j \\
{}^{z}T^i &= a^{-1}_{ij}\,{}^{y}T_j \\
{}^{z}T_{ij} &= a_{ki}\,a_{mj}\,{}^{y}T_{km} \\
{}^{z}T^{ij} &= a^{-1}_{ik}\,a^{-1}_{jm}\,{}^{y}T_{km}
\end{aligned}
\qquad (4\text{-}8)
$$

Any vector, $\overline{V}$, which may represent position, angular velocity or acceleration has covariant and contravariant components in any coordinate system. In Cartesian coordinates, these components are equal and can be found by either of two methods:

1. The covariant components are the dot products (orthogonal projections) of $\overline{V}$ onto the unit vectors $\hat{y}_i$.

$$
{}^{y}V_i = \overline{V} \cdot \hat{y}_i
$$

The superprefix, y, indicates that the i th component is taken in the y frame. It is used only where ambiguity might arise as to which frame the vector is resolved into. The circumflex accent indicates a unit vector.

2. The contravariant components are obtained by resolving $\overline{V}$ along the Cartesian y_i coordinate axes so that $\overline{V}$ is the parallogram sum of the component vectors.

$$
\overline{V} = {}^{y}V^i\,\hat{y}_i
$$

In curvilinear coordinates, this definition of covariant and contravariant components must be modified slightly as discussed in 4. C.

When the y_i are transformed into the z_j by Equation 1, the

components ${}^{y}V_i$ of all vectors along y are transformed into ${}^{z}V_i$ and ${}^{z}V^i$ along z. The covariant and contravariant components of $\overline{V}$ in the new frame will not be equal if the new frame is not Cartesian. The formal rules for computing the covariant and contravariant components in z from the Cartesian components are:

$$\text{Covariant} \qquad {}^{z}V_i = \frac{\partial y_j}{\partial z^i} {}^{y}V_j$$

$$\text{Contravariant} \qquad {}^{z}V^i = \frac{\partial z^i}{\partial y_j} {}^{y}V_j \tag{4-9}$$

Before discussing the physical significance of the covariant and contravariant components, consider the properties of the transformation, Equation (4-1):

$$dy_i = \frac{\partial y_i}{\partial z^j} dz^j = a_{ij} dz^j \tag{4-10}$$

The inverse is:

$$dz^i = \frac{\partial z^i}{\partial y_j} dy_j$$

The matrix:

$$\left[\frac{\partial z^i}{\partial y_j}\right]$$

is the inverse of $[a_{ij}]$ since their matrix product is the unity matrix.

Consider an arbitrary vector, $\overline{V}$, whose covariant z components are ${}^{z}V_i$. Then:

$${}^{z}V_i = \frac{\partial y_j}{\partial z^i} {}^{y}V_j$$

$$= a_{ji} \, {}^{y}V_j = a_{ij}^{T} \, {}^{y}V_j$$

$$[{}^{z}V_i] = [a^T] \, [{}^{y}V_j] \tag{4-11}$$

where $[a^T]$ is the matrix whose elements are those of $[a]$. inter-

Figure 4-1

COVARIANT AND CONTRAVARIANT PROPERTIES

OF VECTORS AND TENSORS

y_i is Cartesian

z^i is arbitrary

		Covariant Form	Contravariant Form
1	Differential Distance	$(ds)^2 = g_{ij}\, dz^i\, dz^j$	$(ds)^2 = g^{ij}\, dz_i\, dz_j$
2	Jacobian Matrix	$a_{ij} = \frac{\partial y_i}{\partial z^j}$	$a^{ij} = a^{-1}_{ij} = \frac{\partial z^i}{\partial y_j}$
3	Metric Tensor	$g_{ij} = \frac{\partial y_m}{\partial z^i}\frac{\partial y_m}{\partial z^j}$	$g^{ij} = g^{-1}_{ij} = \frac{\partial z^i}{\partial y_m}\frac{\partial z^j}{\partial y_m}$
		$[g_{ij}] = [a^T][a]$	$[g^{ij}] = [g^{-1}_{ij}] = [a^{-1}][a^T]^{-1}$
4	Relations between Covariant and Contravariant Elements of Metric Tensor	$[g_{ij}][g^{ij}] = [I]$ $g_{ij}\, g^{jk} = \delta_i^{\,k}$	

5	Metric Tensor in Orthogonal Coordinates.	$[g_{ij}] = \begin{bmatrix} h_1^2 & 0 & 0 \\ 0 & h_2^2 & 0 \\ 0 & 0 & h_3^2 \end{bmatrix}$	$[g^{ij}] = \begin{bmatrix} \frac{1}{h_1^2} & 0 & 0 \\ 0 & \frac{1}{h_2^2} & 0 \\ 0 & 0 & \frac{1}{h_3^2} \end{bmatrix}$
6	Relations between Differential Distances	$dz_i = \frac{\partial y_j}{\partial z^i} dy_j$ $dy_i = \frac{\partial z^j}{\partial y_i} dz_j$	$dz^i = \frac{\partial z^i}{\partial y_j} dy_j$ $dy_i = \frac{\partial y_i}{\partial z^j} dz^j$
7	Coordinate Transformations		
	a. Vector	${}^{z}V_i = \frac{\partial y_j}{\partial z^i} {}^{y}V_j = a_{ji} {}^{y}V_j$	${}^{y}V^i = \frac{\partial z^i}{\partial y_j} {}^{y}V^j = a^{-1}_{ij} {}^{y}V^j$
	b. Second Order Tensor	${}^{z}T_{ij} = \frac{\partial y_m}{\partial z^i} \frac{\partial y_N}{\partial z^j} {}^{y}T_{MN}$ $= a_{mi} a_{Nj} {}^{y}T_{mN}$	${}^{z}T^{ij} = \frac{\partial z^i}{\partial y_m} \frac{\partial z^j}{\partial y_N} {}^{y}T^{mN}$ $= a^{-1}_{im} a^{-1}_{jN} {}^{y}T^{MN}$
8	Physical Component of a Vector along the Unit Vector, $\hat{p}$	$p^i V_i$	$p_i V^i$
9	Relation between Covariant and Contravariant Components of $\overline{V}$	${}^{z}V_i = g_{ij} {}^{z}V^j$	${}^{z}V^i = g^{ij} {}^{z}V_j$
10	Relation between Covariant, Contravariant and Physical $({}^{p}V_i)$ Components in Orthogonal Coordinates	${}^{z}V_i = h_i {}^{p}V_i$ (no sum)	${}^{z}V^i = {}^{p}V_i / h_i$ (no sum)

changed about the principal diagonal, $a^{T}_{ij} = a_{ji}$. The contravariant transformation in matrix form is:

$$
\begin{aligned}
{}^{z}V^{i} &= \frac{\partial z^{i}}{\partial y_{j}} \; {}^{y}V_{j} \\
&= a^{ij} \, {}^{y}V_{j} = a^{-1}_{ij} \, {}^{y}V_{j} \\
[{}^{z}V^{i}] &= [a^{-1}] \; [{}^{y}V_{j}]
\end{aligned}
\tag{4-12}
$$

Hence, the covariant and contravariant components are equal if and only if:

$$a^{-1}_{ij} = a^{T}_{ij}$$

This is the condition for an orthogonal transformation which is a rigid rotation from the y Cartesian frame to the z Cartesian frame. Thus, the covariant and contravariant components are equal only in Cartesian frames.

If the transformation, Equation (4-1), is a rotation:

$$a_{im} a_{jm} = \delta_{ij}$$

The matrix [a]then has only a single real eigenvalue, unity, and the only real eigenvector is the axis of rotation.

For any [a], the covariant elements of the metric tensor are expressible in terms of a_{ij} :

$$
\begin{aligned}
g_{ij} &= \frac{\partial y_{m}}{\partial z^{i}} \; \frac{\partial y_{m}}{\partial z^{j}} \\
&= a_{mi} \; a_{mj} = a^{T}_{im} \; a_{mj} \\
[g_{ij}] &= [a^{T}] \; [a]
\end{aligned}
\tag{4-13}
$$

Equation (4-13) can be used to relate the covariant and contra-

variant components of $\overline{V}$. Starting with:

$$[{}^{z}V_i] = [a^T]\,[{}^{y}V_j]$$

$$[{}^{z}V^i] = [a^{-1}]\,[{}^{y}V_j]$$

multiply the second by [a] :

$$[a]\,[{}^{z}V^i] = [a]\,[a^{-1}]\,[{}^{y}V_j] = [{}^{y}V_j]$$

and substitute into the first:

$$[{}^{z}V_i] = [a^T]\,[a]\,[{}^{z}V^j] = [g_{ij}]\,[{}^{z}V^j] \qquad (4\text{-}14)$$

Hence, the matrix of the covariant elements of the metric tensor transforms the contravariant components of $\overline{V}$ into the covariant components.

The matrix of the contravariant elements of the metric tensor is the inverse of the covariant matrix:

$$[g^{ij}] = [g_{ij}^{-1}] = [a^{-1}]\,[a^T]^{-1}$$

so:

$$\begin{aligned}[{}^{z}V^i] &= [g_{ij}^{-1}]\,[{}^{z}V_i] \\ &= [g^{ij}]\,[{}^{z}V_i] \\ &= [a^{-1}]\,[a^T]^{-1}\,[{}^{z}V_i] \end{aligned} \qquad (4\text{-}15)$$

Consequently, the elements of $[g^{ij}]$ are:

$$g^{ij} = \frac{\partial z^i}{\partial y_m}\,\frac{\partial z^j}{\partial y_m} \qquad (4\text{-}16)$$

Thus , Equations (4-14) and (4-15) relate the covariant and contravariant elements of a vector $\overline{V}$. It is clear once more that the covariant and contravariant forms of the metric tensor are identical if and only if:

$$[g_{ij}] = [g_{ij}^{-1}]$$

$$g_{ij} = \delta_{ij} \qquad [g] = [I]$$

Using the contravariant elements of the metric tensor, the differential distance between neighboring points can be found. Starting from Equation (4-3):

$$(ds)^2 = g_{ij}\, dz^i\, dz^j \tag{4-3}$$

$$= dz_i\, dz^i = dz_i\, g^{ik}\, dz_k$$

$$= g^{ik}\, dz_i\, dz_k \tag{4-17}$$

Thus, the differential distance can be expressed in terms of covariant differentials of z or contravariant differentials of z.

It is of interest to find the covariant form of the differential transformation:

$$dz^k = \frac{\partial z^k}{\partial y_j}\, dy_j$$

as follows. From Equation (4-14):

$$dz_m = g_{mk}\, dz^k \tag{4-14}$$

$$= \frac{\partial y_j}{\partial z^m}\, \frac{\partial y_j}{\partial z^k}\, \frac{\partial z^k}{\partial y_i}\, dy_i$$

$$= \frac{\partial y_i}{\partial z^m}\, dy_i \tag{4-18}$$

The inverse is found by multiplying Equation (4-18) by $\frac{\partial z^m}{\partial y_j}$:

$$dy_j = \frac{\partial z^m}{\partial y_j}\, dz_m \tag{4-19}$$

Thus, given the transformation of Equation (4-1), the covariant or contravariant differentials of z can be expressed in terms of differentials of y. Figure 4-1 summarizes the results of this section.

4. C. COMPONENTS OF VECTORS.

Unfortunately if z^i is not measured along a straight line coordinate axis, $\frac{\partial y_i}{\partial z^j}$ and $\frac{\partial z^i}{\partial y_j}$ have dimensions so the covariant and contravariant components of a vector, $\bar{V}$, do not have the same dimensions as the Cartesian components. Thus, neither is a component in the physical sense. A rate gyro or accelerometer measures the component of $\bar{V}$ along its input axis where $\bar{V}$ is inertial angular velocity or linear acceleration in inertial space minus gravitation. The physical component of $\bar{V}$ in any direction is the dot product of $\bar{V}$ with a unit vector, $\hat{p}$, in that direction. If $\hat{p}$ has the covariant and contravariant components, p_i and p^i in the z frame, the physical component of $\bar{V}$ along $\hat{p}$ is:

$$^{p}V = p_i V^i = p^i V_i$$

where the superprefix indicates resolution of $\bar{V}$ along $\hat{p}$. Wherever possible ambiguity might arise as to whether V_i is a covariant or physical component of $\bar{V}$, the prefix, "p" will be used to identify the physical component, $^{p}V_i$. Except in this chapter, V_i is always a physical component.

As an example, consider the oblique coordinate system of Appendix G. The coordinate axes are non-orthogonal straight lines. Let the contravariant components of the two unit vectors be:

$$[p^i] = \begin{bmatrix} 1 \\ 0 \end{bmatrix} \qquad [q^i] = \begin{bmatrix} 0 \\ 1 \end{bmatrix}$$

Then Appendix G calculates the covariant and contravariant components of a vector, $\overline{V}$, from the formal rule, Equation (4-9):

$$[\ {}^{z}V_i\ ] = V\begin{bmatrix}\cos 30^\circ \\ \cos 15^\circ\end{bmatrix}$$

$$[\ {}^{z}V^i\ ] = V\begin{bmatrix}-1 \\ 2\cos 15^\circ\end{bmatrix}$$

Appendix G also calculates the orthogonal projections of $\overline{V}$ onto the coordinate axes. These are simply the dot products of $\overline{V}$ with unit vectors along these coordinate axes and are identical to the covariant components. Since there are no scale factors, the covariant components are identical to the physical components. The parallelogram sum of the contravariant components are shown to be $\overline{V}$.

In a curvilinear orthogonal frame:

$$[g_{ij}] = \begin{bmatrix} h_1^2 & 0 & 0 \\ 0 & h_2^2 & 0 \\ 0 & 0 & h_3^2 \end{bmatrix}$$

and the three unit vectors are:

$$[p^i] = \begin{bmatrix}1\\0\\0\end{bmatrix} \qquad [q^i] = \begin{bmatrix}0\\1\\0\end{bmatrix} \qquad [r^i] = \begin{bmatrix}0\\0\\1\end{bmatrix}$$

Then the covariant components of a vector, $\overline{V}$, are:

$${}^{z}V_i$$

in terms of which the contravariant components are:

$$V^i = \frac{V_i}{h_i^2} \text{ (no sum)} \qquad (4\text{-}20)$$

and the physical components are:

$$\frac{V_i}{h_i} \qquad \text{(no sum)} \tag{4-21}$$

In a general non-orthogonal system, the physical components are the covariant components multiplied by scale factors which are functions of position and direction. The contravariant components are linear combinations of the covariant components:

$$V^i = g^{ij} V_j \tag{4-15}$$

Figure 4-1 summarizes the results of this section. Section 4.G. illustrates the resolution of an angular velocity vector into covariant and contravariant components in several coordinate frames.

4.D. COVARIANT FORM OF NEWTON'S LAW.

The physical components of force, inertial angular velocity and inertial acceleration are of utmost importance in inertial navigation. Two of these are related by Newton's Law:

$$\bar{F} = m \ddot{\bar{R}}\Big]_I$$

$$\bar{f}_T = \ddot{\bar{R}}\Big]_I$$

where $\bar{f}_T$ is the total specific force acting on m. This law is true only in an inertial reference frame. For example, if the coordinates are transformed by means of a time-dependent rotation, the law is not true

unless Coriolis, centripetal and angular acceleration terms are added. Can Newton's Law be written in "covariant form" so it is true in any form? Reference 237, pages 150 to 151, shows that it can be so written in either of the following forms:

$$f_{T_r} = g_{rs}\frac{d^2z^s}{dt^2} + [s\ n,\ r]\frac{dz^s}{dt}\frac{dz^n}{dt} \tag{4-22}$$

$$f_T^r = \frac{d^2z^r}{dt^2} + \left\{ {r \atop s\ n} \right\}\frac{dz^s}{dt}\frac{dz^n}{dt} \tag{4-23}$$

These forms relate the covariant or contravariant components of force, velocity and acceleration in any coordinate frame, whatsoever. Under an arbitrary time-dependent transformation, both sides of this equation transform the same way, leaving the form of the law unchanged.

$[s\ n,\ r]$ and $\left\{ {r \atop s\ n} \right\}$ are the Christoffel symbols of the first and second kind respectively:

$$[m\ n,\ r] = \frac{1}{2}\left\{ \frac{\partial g_{rm}}{\partial z^n} + \frac{\partial g_{rn}}{\partial z^m} - \frac{\partial g_{mn}}{\partial z^r} \right\} \tag{4-24}$$

$$\left\{ {r \atop m\ n} \right\} = g^{rs}[m\ n,\ s] \tag{4-25}$$

It can be readily shown that the covariant and contravariant forms of Newton's Law are identical. Multiply Equation (4-23) by g_{sr} :

$$g_{sr}f_T^r = g_{sr}\frac{d^2z^r}{dt^2} + g_{sr}\,g^{rp}[m\ n, p]\frac{dz^m}{dt}\frac{dz^n}{dt}$$

$$f_{T_s} = g_{sr}\frac{d^2z^r}{dt^2} + [m\ n,\ s]\frac{dz^m}{dt}\frac{dz^n}{dt}$$

which is exactly the form of Equation (4-22). Since f_{T_i} and f_T^i

are first order tensors, the quantities on the right side of Equations (4-22) and (4-23) must also be first order covariant and contravariant tensors respectively. They are designated:

$$f_{T_r} = \frac{\delta}{\delta t}\left(\frac{dz_r}{dt}\right)$$
$$f_T^r = \frac{\delta}{\delta t}\left(\frac{dz^r}{dt}\right) \qquad (4\text{-}26)$$

where the symbol, $\frac{\delta}{\delta t}$, is the absolute derivative operator, defined by Equations (4-22) and (4-23) (Ref. 237, pgs. 49-50). These are concise expressions of Newton's Law in covariant form.

By direct differentiation of Equation (4-24) with $g_{ij} = \frac{\partial y_m}{\partial z^i}\frac{\partial y_m}{\partial z^j}$ the Christoffel symbols can be expressed as:

$$[m\ n,\ r] = \frac{\partial y_k}{\partial z^r}\frac{\partial^2 y_k}{\partial z^m \partial z^n}$$
$$\left\{ {m \atop n}\ {p \atop } \right\} = g^{ps}[m\ n,\ s] = \frac{\partial z^p}{\partial y_k}\frac{\partial^2 y_k}{\partial z^m \partial z^n} \qquad (4\text{-}27)$$

Morse and Feshbach (Ref. 230, pg. 47) further simplify the Christoffel symbols of the second kind for the special case of an orthogonal coordinate frame:

$$\left\{ {i \atop i}\ {i \atop } \right\} = \frac{1}{h_i}\frac{\partial h_i}{\partial z^i} \qquad \text{(no sum)}$$
$$\left\{ {i \atop i}\ {j \atop } \right\} = \left\{ {j \atop i}\ {i \atop } \right\} = \frac{1}{h_i}\frac{\partial h_i}{\partial z^j} \qquad \text{(no sum)} \qquad (4\text{-}28)$$
$$\left\{ {j \atop j}\ {i \atop } \right\} = -\frac{1}{h_i^2}\frac{\partial h_j}{\partial z^i} \qquad \text{(no sum)}$$
$$\left\{ {j \atop k}\ {i \atop } \right\} = 0 \qquad i \neq j \neq k$$

The Christoffel symbols of the first kind can be calculated from Equations (4-25) and (4-28) for the case of orthogonal coordinates:

$$g_{pr} \left\{ m \; n \right\}^{r} = g_{pr} g^{rs} [\, m \; n, \; s] = [\, m \; n, \; p] \tag{4-29}$$

Thus:

$$\begin{aligned} [\, i \; i, \; i] &= h_i \frac{\partial h_i}{\partial z^i} \quad \text{(no sum)} \\ [\, i \; j, \; i] &= [\, j \; i, \; i] = h_i \frac{\partial h_i}{\partial z^j} \quad \text{(no sum)} \\ [\, j \; j, \; i] &= - h_j \frac{\partial h_i}{\partial z^j} \quad \text{(no sum)} \\ [\, i \; j, \; k] &= 0 \qquad i \neq j \neq k \end{aligned} \tag{4-30}$$

Reference 237, pages 44 to 45 and 151, shows that the covariant forms of Newton's Law, Equations (4-22) and (4-23) can be transformed to the form:

$$f_{T_r} = \frac{d}{dt} \frac{\partial T}{\partial \dot{z}^r} - \frac{\partial T}{\partial z^r} \tag{4-31}$$

where:

$$T = \frac{1}{2} g_{ij} \frac{dz^i}{dt} \frac{dz^j}{dt}$$

and has the physical significance of kinetic energy. These are the familiar Lagrange equations of motion. f_{T_r}, usually called the components of the generalized force, are in reality the covariant components of force which do work of amount:

$$dW = f_{T_i} \, dz^i = f_T{}^i \, dz_i$$

Hence the Lagrange equations are not merely energy relations in the dynamic system; they are force equations in covariant form.

When so expressed, the covariant equations of motion of a particle are valid in any coordinate frame whatever; no privileged position is attached to an inertial frame except that the equations are simplest in that frame. The desire to do the same for angular motions with respect to the fixed stars prompts the discussion of Sections 1.D. and 1.E.

The elegance of the covariant form of Newton's Law should not be minimized though its practical use is rare. It is used in Section 4.E. to transform Newton's Law into arbitrary rotating curvilinear coordinates in order to express the output of an accelerometer.

4.E. ACCELEROMETER OUTPUT IN AN ARBITRARY, UNIFORMLY ROTATING COORDINATE FRAME.

4.E.1. INTRODUCTION.

Consider a vehicle navigating near the surface of a uniformly rotating planet. Suppose a navigation coordinate frame, whose origin is at the mass center of the planet, locates the vehicle in three dimensions relative to the planet. Since the coordinates are in general curvilinear and non-orthogonal, the unit vectors have unique but different directions at each point in space.

An observer aboard the vehicle wishes to make measurements in

this coordinate frame by aligning a "stable platform" with the unit vectors, independent of the angular motion of the vehicle (Section 5.B.). The control system which decouples the stable platform from angular motions of the vehicle and causes it to align with the coordinate axes is assumed to be fast and accurate enough so its errors are negligible.

A vector accelerometer is mounted on the stable platform. "Vector accelerometer" is a generic term for an instrument which measures the three physical components along its "input axes" of the inertial acceleration minus gravitation, Section 5.B. Each instrument has three outputs, each one proportional to one of the physical components being measured, in the ideal case. If the input axes are rigidly fastened together, certain additional restrictions must be imposed on the navigation coordinate frame since in general, the angles between the unit vectors would be functions of position.

This section derives the accelerometer output in terms of the angular velocity of the planet and the metric properties of the navigation coordinate frame. It is assumed that the accelerometer input axes are aligned with the unit vectors of the navigation coordinate frame. To navigate with the accelerometer input axes oriented otherwise requires additional coordinate transformations, though it is sometimes done.

4.E.2. GENERAL DERIVATION OF ACCELEROMETER OUTPUT.

Suppose that three arbitrary curvilinear coordinates, z^1, z^2 and z^3 locate the vehicle (more exactly, they locate the accelerometer since the vehicle itself can be a quarter of a mile long) with respect to the planet. The inertial angular velocity of the planet, $\overline{\omega}_{IP}$, is assumed to be constant in direction and magnitude. No assumptions are made about the z^i in order to permit the use of coordinates which are not symmetric about the axis of rotation of the planet. Examples of such unsymmetric coordinates are those based on a triaxial reference ellipsoid or on a false-pole coordinate frame (whose pole is on the equator, to permit operation near the geographic poles with unambiguous position coordinates).

Let x_i be planetocentric, inertially non-rotating Cartesian coordinates oriented so x_3 lies along the geographic polar axis and x_1 and x_2 lie in the equatorial plane. Let y_i be planetocentric Cartesian coordinates which rotate with the planet and are oriented so y_3 is parallel to x_3 whereas y_1 and y_2 lie in the equatorial plane. At some instant of time, $t = 0$, x_1 and y_1 coincide. Section 1.J. shows that the x_i coordinate frame actually has an inertial angular velocity of 10^{-6} deg./hr. and that y_i rotates relative to x_i not only about the polar axis but also with a component of angular velocity, 5×10^{-5} deg./hr., perpendicular

to the polar axis. These small effects are neglected in this section on the assumption that the inertial instruments are incapable of detecting them,

The x_i and y_i coordinates are related by the equations:

$$x_i = a_{ij}\, y_j$$

$$[a] = \begin{bmatrix} \cos \omega_{Ip} t & -\sin \omega_{Ip} t & 0 \\ \sin \omega_{Ip} t & \cos \omega_{Ip} t & 0 \\ 0 & 0 & 1 \end{bmatrix} \qquad (4\text{-}32)$$

The z^i are curvilinear coordinates related to the y_i by the time-independent transformation:

$$y_i = y_i (z^j)$$

To derive the kinematic acceleration of the accelerometer, $\bar{f}_T$, write Newton's Law in x_i and transform successively to y_i and then to z^i. In the Cartesian x and y frames, there is no distinction between covariant and contravariant components.

$$f_{T_i} = \ddot{x}_i = \frac{d}{dt} (a_{ij} \dot{y}_j + \dot{a}_{ij}\, y_j)$$

$$= a_{ij} \ddot{y}_j + 2 \dot{a}_{ij} \dot{y}_j + \ddot{a}_{ij}\, y_j \qquad (4\text{-}33)$$

$[\dot{a}]$ and $[\ddot{a}]$ are matrices whose elements are $\frac{d}{dt} a_{ij}$ and $\frac{d^2}{dt^2} a_{ij}$ respectively. The equation is transformed into y by multiplying Equation (4-33) by a^{-1}_{ki} and summing over i:

$$f_{T_k} = a^{-1}_{ki} f_{T_i} = a^{-1}_{ki} a_{ij} \ddot{y}_j + 2 a^{-1}_{ki} \dot{a}_{ij} \dot{y}_j + a^{-1}_{ki} \ddot{a}_{ij} y_j$$

$$ {}^{y}f_{T_k} = \ddot{y}_k + 2\, a^{-1}_{ki}\, \dot{a}_{ij}\, \dot{y}_j + a^{-1}_{ki}\, \ddot{a}_{ij}\, y_j \qquad (4\text{-}34) $$

Since the transformation from y to z is independent of time, it follows that:

$$ \begin{aligned} \dot{y}_K &= \frac{\partial y_K}{\partial z^M}\, \dot{z}^M \\ \ddot{y}_K &= \frac{\partial y_K}{\partial z^M}\, \ddot{z}^M + \frac{\partial^2 y_K}{\partial z^M \partial z^N}\, \dot{z}^M\, \dot{z}^N \end{aligned} \qquad (4\text{-}35) $$

Transform Equation (4-34) into covariant force components in the z frame and substitute from Equation (4-35):

$$ \begin{aligned} {}^{z}f_{T_r} &= \frac{\partial y_K}{\partial z^r}\, {}^{y}f_{T_K} \\ &= \frac{\partial y_K}{\partial z^r}\frac{\partial y_K}{\partial z^M}\ddot{z}^M + \frac{\partial y_K}{\partial z^r}\frac{\partial^2 y_K}{\partial z^M \partial z^N}\, \dot{z}^M\, \dot{z}^N + 2\frac{\partial y_K}{\partial z^r}\, a^{-1}_{ki}\, \dot{a}_{ij}\, \frac{\partial y_j}{\partial z^M}\, \dot{z}^M + \\ &\quad + \frac{\partial y_K}{\partial z^r}\, a^{-1}_{ki}\, \ddot{a}_{ij}\, y_j\, (z^M) \end{aligned} \qquad (4\text{-}36) $$

Using Equations (4-13) and (4-27), this has the form:

$$ {}^{z}f_{T_r} = \frac{\delta}{\delta t}\left(\frac{dz^r}{dt}\right) + 2\frac{\partial y_K}{\partial z^r}\frac{\partial y_j}{\partial z^M}\, a^{-1}_{Ki}\, \dot{a}_{ij}\, \dot{z}^M + \frac{\partial y_K}{\partial z^r}\, a^{-1}_{ki}\, \ddot{a}_{ij}\, y_j\, (z^M) \qquad (4\text{-}37) $$

where the absolute derivative, defined in Equation (4-26), is taken within the rotating frame and arises from motion within that frame whereas the other two terms arise from rotation of the frame and from coupling between motion within the frame and rotation of the frame.

Equation (4-37) is easily verified for the case of non-rotating coordinates for which $[\dot{a}] = [\ddot{a}] = 0$. Then:

$$ {}^{z}f_{T_r} = \frac{\delta}{\delta t}\left(\frac{dz^r}{dt}\right) $$

which is Newton's Law in covariant form, Equation (4-26).

In an arbitrary curvilinear z frame, the unit vectors change direction from point to point in such a manner that the angles between them change. As a result, the input axes of a rigid accelerometer could not lie along these unit vectors at all points in space. Thus the navigation coordinate frame must be constrained to require that the angles between the unit vectors be independent of position. A triad, composed of the three unit vectors, must move through space as a rigidly connected framework, for engineering convenience (see Section 5.D.1.).

The simplest rigid configuration is that in which the unit vectors are everywhere orthogonal. Then from Equations (4-30) and (4-37), the three covariant force components in z are:

$$
\begin{aligned}
{}^{z}f_{T_1} &= h_1^2 \ddot{z}^1 + h_1 \frac{\partial h_1}{\partial z^1} (\dot{z}^1)^2 - h_2 \frac{\partial h_2}{\partial z^2} (\dot{z}^2)^2 - h_3 \frac{\partial h_3}{\partial z^3} (\dot{z}^3)^2 + 2h_1 \dot{z}^1 \\
&\left(\frac{\partial h_1}{\partial z^2} \dot{z}^2 + \frac{\partial h_1}{\partial z^3} \dot{z}^3 \right) + 2\omega_{ip} \dot{z}^m \left(\frac{\partial y_2}{\partial z^1} \frac{\partial y_1}{\partial z^m} - \frac{\partial y_1}{\partial z^1} \frac{\partial y_2}{\partial z^m} \right) - \\
&- \omega_{ip}^2 \left(y_1 \frac{\partial y_1}{\partial z^1} + y_2 \frac{\partial y_2}{\partial z^1} \right) \qquad (4\text{-}38)
\end{aligned}
$$

$$
\begin{aligned}
{}^{z}f_{T_2} &= h_2^2 \ddot{z}^2 + h_2 \frac{\partial h_2}{\partial z^2} (\dot{z}^2)^2 - h_1 \frac{\partial h_1}{\partial z^2} (\dot{z}^1)^2 - h_3 \frac{\partial h_3}{\partial z^2} (\dot{z}^3)^2 + 2h_2 \dot{z}^2 \left(\frac{\partial h_2}{\partial z^1} \dot{z}^1 + \right. \\
&\left. + \frac{\partial h_2}{\partial z^3} \dot{z}^3 \right) + 2\omega_{ip} \dot{z}^m \left(\frac{\partial y_2}{\partial z^2} \frac{\partial y_1}{\partial z^m} - \frac{\partial y_1}{\partial z^2} \frac{\partial y_2}{\partial z^m} \right) - \omega_{ip}^2 \left(y_1 \frac{\partial y_1}{\partial z^2} + y_2 \frac{\partial y_2}{\partial z^2} \right)
\end{aligned}
$$

$$
\begin{aligned}
{}^{z}f_{T_3} &= h_3^2 \ddot{z}^3 + h_3 \frac{\partial h_3}{\partial z^3} (\dot{z}^3)^2 - h_1 \frac{\partial h_1}{\partial z^3} (\dot{z}^1)^2 - h_2 \frac{\partial h_2}{\partial z^3} (\dot{z}^2)^2 + 2h_3 \dot{z}^3 \left(\frac{\partial h_3}{\partial z^1} \dot{z}^1 + \right. \\
&\left. + \frac{\partial h_3}{\partial z^2} \dot{z}^2 \right) + 2\omega_{ip} \dot{z}^m \left(\frac{\partial y_2}{\partial z^3} \frac{\partial y_1}{\partial z^m} - \frac{\partial y_1}{\partial z^3} \frac{\partial y_2}{\partial z^m} \right) - \omega_{ip}^2 \left(y_1 \frac{\partial y_1}{\partial z^3} + y_2 \frac{\partial y_2}{\partial z^3} \right)
\end{aligned}
$$

The physical components of specific force are $1/h_i$ times the covariant components. The accelerometer measures $\overline{f}_a = \overline{f}_T - \overline{G}$ (Figure 5-1):

$$
\begin{aligned}
h_1 {}^{\sharp}f_{a_1} &= {}^{\sharp}f_{T_1} - h_1 {}^{\sharp}G_1 \\
h_2 {}^{\sharp}f_{a_2} &= {}^{\sharp}f_{T_2} - h_2 {}^{\sharp}G_2 \\
h_3 {}^{\sharp}f_{a_3} &= {}^{\sharp}f_{T_3} - h_3 {}^{\sharp}G_3
\end{aligned}
\qquad (4\text{-}39)
$$

The electrical outputs of an accelerometer are related to the components of $\overline{f}_a$ along its input axes by means of the performance function of the accelerometer.

4.F. ACCELEROMETER OUTPUT IN SYMMETRIC, ORTHOGONAL CURVILINEAR COORDINATES.

4.F.1. SYMMETRIC COORDINATES.

An important class of orthogonal coordinate frames are symmetric about the geographic polar axis of the planet. When using such frames, it is convenient to define the geographic meridian plane as any plane containing the geographic polar axis and to select the geographic longitude, λ_g, as a coordinate. λ_g is the angle between the meridian plane containing the vehicle and the reference meridian plane (on the Earth, the geographic meridian plane of Greenwich), measured positively eastward.

The other two coordinates locate the vehicle in the meridian plane.

For example, Figure (5-6) shows three coordinate frames which are symmetric about the geographic polar axis. In each case, $\hat{z}^1$ is oriented eastward, normal to the meridian plane containing the vehicle. $\hat{z}^2$ is horizontal and north and $\hat{z}^3$ is vertically up. The direction of the vertical is defined differently in each coordinate frame.

a. Spherical Coordinates. $\hat{z}^1$ lies along the radius vector from the mass center of the Earth.

b. Geographic Coordinates. $\hat{z}^1$ lies along the projected normal to the reference ellipsoid.

c. Ellipsoidal Coordinates. $\hat{z}^1$ is normal to an ellipsoid which is confocal to the reference ellipsoid and which passes through the vehicle.

Appendix D discusses the geometry of these coordinate frames in detail.

The transformation from y_i to z^j in symmetric coordinates is of the form:

$$\begin{aligned} y_1 &= s_1(z^2, z^3)\cos\lambda_g \\ y_2 &= s_1(z^2, z^3)\sin\lambda_g \\ y_3 &= s_2(z^2, z^3) \end{aligned} \tag{4-40}$$

Because the coordinates are orthogonal, the metric tensor is diagonal and the non-zero terms are:

$$g_{11} = h_1^2 = \frac{\partial y_i}{\partial \lambda}\frac{\partial y_i}{\partial \lambda} = S_1^2$$

$$g_{22} = h_2^2 = \frac{\partial y_i}{\partial z^2}\frac{\partial y_i}{\partial z^2} = \left(\frac{\partial S_1}{\partial z^2}\right)^2 + \left(\frac{\partial S_2}{\partial z^2}\right)^2$$

$$g_{33} = h_3^2 = \frac{\partial y_i}{\partial z^3}\frac{\partial y_i}{\partial z^3} = \left(\frac{\partial S_1}{\partial z^3}\right)^2 + \left(\frac{\partial S_2}{\partial z^3}\right)^2 \qquad (4\text{-}41)$$

Equations (4-38) then become:

$$^{z}f_{T_\lambda} = h_1^2\ddot{\lambda} + 2(\omega_{1P} + \dot{\lambda})h_1\left(\frac{\partial h_1}{\partial z^2}\dot{z}^2 + \frac{\partial h_1}{\partial z^3}\dot{z}^3\right)$$

$$= \frac{d}{dt}\left[h_1^2(\omega_{1P} + \dot{\lambda})^2\right]$$

$$^{z}f_{T_2} = h_2^2\ddot{z}^2 + h_2\dot{z}^2\left(\frac{\partial h_2}{\partial z^2}\dot{z}^2 + 2\frac{\partial h_2}{\partial z^3}\dot{z}^3\right) - h_1\frac{\partial h_1}{\partial z^2}(\omega_{1P} + \dot{\lambda})^2 - h_3\frac{\partial h_3}{\partial z^2}(\dot{z}^3)^2$$

$$^{z}f_{T_3} = h_3^2\ddot{z}^3 + h_3\dot{z}^3\left(\frac{\partial h_3}{\partial z^3}\dot{z}^3 + 2\frac{\partial h_3}{\partial z^2}\dot{z}^2\right) - h_1\frac{\partial h_1}{\partial z^3}(\omega_{1P} + \dot{\lambda})^2 - h_2\frac{\partial h_2}{\partial z^3}(\dot{z}^2)^2$$

(4-42)

In symmetric orthogonal coordinate frames, Equations (4-42) can be checked by a more direct method, that of Lagrange.

The kinetic energy can be written in the generalized coordinates u^i where:

$$u^1 = \omega_{1P}t + \lambda$$

$$u^2 = z^2$$

$$u^3 = z^3$$

in which case:

$$T = \frac{1}{2}\, g_{ij}\, u^i\, u^j$$

$$= \left[h_1^2(\omega_{1P} + \dot{\lambda})^2 + h_2^2(\dot{z}^2)^2 + h_3^2(\dot{z}^3)^2\right]$$

The h_i are as in Equations (4-41) since they are independent of λ.

Then the covariant components of force, found by substituting into Equation (4-32), are identical to Equations (4-42), obtained by specializing the general Equations (4-38). The physical components are $1/h_i$ times the covariant components. The accelerometer measures the physical components of $\bar{f}_a = \bar{f}_T - \bar{G}$ which are related to the covariant components by Equations (4-39).

Note the particularly simple form of the longitude equation. In terms of the physical components of force in the longitude direction, ${}^{P}f_{a_\lambda} = \frac{{}^{z}f_i}{h_i}$:

$$\omega_{IP} + \dot{\lambda} = \frac{1}{h_1^2}\int h_1 (f_{a_1} + G)\,dt \qquad (4\text{-}42)$$

Thus, longitude could be obtained very simply in any symmetric orthogonal system by means of a weighted integral of the output of an ideal accelerometer.

The calculation of the other two components of $\bar{f}_a$, which the accelerometer measures, can be simplified if z^3 measures altitude in some way (z^3 can be r, h_g or ζ of Appendix D, for example). In such a case, $\dot{z}^3 \approx 0$ for a vehicle such as a ship or transport aircraft whose paths are sensibly horizontal. Then:

$$\begin{aligned} h_2 f_{a_2} &= f_{T_2} - h_2 G_2 \\ &= h_2^2 \ddot{z}^2 - h_1 \frac{\partial h_1}{\partial z^2}(\omega_{IP} + \dot{\lambda})^2 + h_2 \frac{\partial h_2}{\partial z^2}(\dot{z}^2)^2 - h_2 G_2 \end{aligned} \qquad (4\text{-}43)$$

$$\begin{aligned} h_3 f_{a_3} &= f_{T_3} - h_3 G_3 \\ &= h_3^2 \ddot{z}^3 - h_1 \frac{\partial h_1}{\partial z^3}(\omega_{IP} + \dot{\lambda})^2 - h_2 \frac{\partial h_2}{\partial z^3}(\dot{z}^2)^2 - h_3 G_3 \end{aligned}$$

The last equation could not be used for navigation but might be used to infer the value of gravity or gravitation from measurements made by the vertical accelerometer. Clearly though $\dot{z}^3$ may be negligible, $\ddot{z}^3$ would not necessarily be small compared to $h_3 G_3$.

4. F. 2. ACCELEROMETER OUTPUT IN SPHERICAL COORDINATES.

The covariant elements of the metric tensor are shown in Equation (D-4). Thus longitude can be calculated from Equation (4-42):

$$\dot{\lambda} = -\omega_{IP} + \frac{1}{r^2 \cos^2 L_c} \int r \cos L_c \left(f_{a_1} + G_1\right) dt \qquad (4\text{-}44)$$

In the mechanization of this equation, the calculated value of G_1 must be zero unless information is available about the prime deflection of the vertical. Improper knowledge of G_1 will produce an error in the integral and hence in $\dot{\lambda}$.

The latitude and vertical mechanizations, and the differential form of the longitude mechanization, are found from Equations (4-43) and (4-44):

$$\begin{aligned}
{}^z f_{a_1} &= r \ddot{\lambda} \cos L_c + 2\left(\omega_{IP} + \dot{\lambda}\right)\left(\dot{r} \cos L_c - r \dot{L}_c \sin L_c\right) - {}^c G_1 \\
{}^z f_{a_2} &= r \ddot{L}_c + r\left(\omega_{IP} + \dot{\lambda}\right)^2 \frac{\sin 2L_c}{2} + 2 \dot{r} \dot{L}_c - {}^c G_2 \\
{}^z f_{a_3} &= \ddot{r} - r\left(\omega_{IP} + \dot{\lambda}\right)^2 \cos^2 L_c - r \dot{L}_c^2 - {}^c G_3
\end{aligned} \qquad (4\text{-}45)$$

Section 5.E.2. shows the spherical equations in terms of $\bar{g}$, instead of $\bar{G}$. In this mechanization, $\bar{r}$ is the distance from the center of the Earth to the vehicle which is a function of latitude, even if the vehicle flies at constant altitude on an ellipsoidal Earth, Section 5.E.4.D.

4.F.3. ACCELEROMETER OUTPUT IN GEOGRAPHIC COORDINATES.

The covariant elements of the metric tensor are shown in Equation (D-12). Thus the integral mechanization of the longitude channel is:

$$\dot{\lambda} = -\omega_{IP} + \frac{1}{(\rho_P + h_g)^2 \cos^2 L_g} \int (\rho_P + h_g)(f_{a_1} + G_1) \cos L_g \, dt \qquad (4\text{-}46)$$

The latitude and vertical mechanizations and the differential form of the longitude mechanization are:

$$\begin{aligned}
{}^{z}f_{a_1} &= (\rho_P + h_g)\ddot{\lambda}\cos L_g + 2(\omega_{IP} + \dot{\lambda})\left[\dot{h}_g \cos L_g - (\rho_m + h_g)\dot{L}_g \sin L_g\right] - {}^{g}G_1 \\
{}^{z}f_{a_2} &= (\rho_m + h_g)\ddot{L}_g + (\rho_P + h_g)(\omega_{IP} + \dot{\lambda})^2 \frac{\sin 2L_g}{2} + \frac{3}{2}\frac{\rho_m e^2 \sin 2L_g}{1 - e^2 \sin^2 L_g} + 2\dot{h}_g \dot{L}_g - {}^{g}G_2 \\
{}^{z}f_{a_3} &= \ddot{h}_g - (\rho_P + h_g)(\omega_{IP} + \dot{\lambda})^2 \cos^2 L_g - (\rho_m + h_g)\dot{L}_g^2 - {}^{g}G_3
\end{aligned} \qquad (4\text{-}47)$$

ρ_P and ρ_M are the prime and meridian radii of curvature of the

reference ellipsoid. h_g is height above the reference ellipsoid, not above the geoid or the terrain. Section 5. F. discusses suitable approximations to the calculation of h_g for various applications. Section 5. F. 3. discusses the use of the last equation for the measurement of gravity.

Section 5. F. 1. shows the geographic equations in terms of $\bar{g}$ instead of $\bar{G}$.

4. F. 4. ACCELEROMETER OUTPUT IN ELLIPSOIDAL COORDINATES.

The covariant elements of the metric tensor are given in Equation (D-16). Thus, the integral form of the longitude mechanization is:

$$\dot{\lambda} = -\omega_{ip} + \frac{1}{c\cosh^2\xi\cos^2\eta}\int(f_{a_1} + G_1)\cosh\xi\cos\eta\,dt \qquad (4\text{-}48)$$

The latitude and vertical mechanizations and the differential form of the longitude mechanization are:

$$f_{a_1} = c\cosh\xi\cos\eta\,\dot{\lambda}' + 2c(\omega_{ip}+\dot{\lambda})(\dot{\xi}\sinh\xi\cos\eta - \dot{\eta}\cosh\xi\sin\eta) - \overset{\varepsilon}{G}_1 \qquad (4\text{-}49)$$

$$f_{a_2} = h_2\ddot{\eta} + \frac{c\dot{\xi}\dot{\eta}\sinh 2\xi}{(\cosh^2\xi - \cos^2\eta)^{1/2}} + \frac{c\sin 2\eta}{2(\cosh^2\xi - \cos^2\eta)^{1/2}}\left[(\omega_{ip}+\dot{\lambda})^2\cosh^2\xi + \dot{\eta}^2 - \dot{\xi}^2\right] - \overset{\varepsilon}{G}_2$$

$$f_{a_3} = h_3 \ddot{\zeta} + \frac{c^2 \sin 2\eta}{h_3} \dot{\zeta}\dot{\eta} + \frac{c \sinh 2\zeta}{2(\cosh^2\zeta - \cos^2\eta)^{1/2}} \left[\dot{\zeta}^2 - \dot{\eta}^2 - \right.$$

$$\left. -(\omega_{IP} + \dot{\lambda})^2 \cos^2\eta \right] - {}^{E}G_3 \qquad (4\text{-}49)$$

4.G. GYROSCOPE DRIVE SIGNALS IN ARBITRARY ROTATING COORDINATES.

4.G.1. GENERAL DRIVE SIGNALS.

Sections 4.E. and 4.F. discuss the outputs of a vector accelerometer, mounted on a stable platform, if that platform is caused to follow an arbitrary navigation coordinate frame. This section considers the kinematics of driving the platform to follow that frame.

Some device is needed on the stable platform to provide information about the angular velocity of the platform in inertial space, $\overline{\omega}_{IA}$. Such an inertial sensor ("inersor") might be a star-tracker, gyroscope or other instrument sensitive to angular motions in inertial space. The terms "gyroscope" or "inersor" are hereafter used as generic terms to denote an instrument which measures the component along its input

axis of its angular velocity in inertial space, Figure 5-1. Three such instruments or their equivalent, mounted on the stable platform, with their input axes non-coplanar will fully specify the angular velocity of the stable platform in inertial space. A control system is readily designed to cause the stable platform to align with the unit vectors of the navigation coordinate frame, independent of angular motions of the vehicle provided that the gyros are supplied with the correct components of the desired angular velocity of the platform in inertial space. The physical mechanization of such a control system is discussed in Section 5.B. In this chapter, perfect alignment is assumed.

If arbitrary coordinates, z^i, are used, which rotate with the planet, a general scheme for computing the physical components of $\bar{\omega}_{IA}$ along the z^i axes must be partly geometric. The angular velocity of the platform in inertial space can usually be resolved geometrically into the Cartesian y_i coordinates. Since y is a Cartesian frame, the covariant, contravariant and physical components of $\bar{\omega}_{IA}$ are all identical and are designated ${}^{y}\omega_i$.

The covariant components along the z^i can be found from the geometrically resolved components along y:

$$ {}^{z}\omega_i = \frac{\partial y_j}{\partial z^i} {}^{y}\omega_j \qquad (4\text{-}50) $$

and the physical components along z^i are:

$$ {}^{b}\omega_i = \frac{{}^{z}\omega_i}{h_i} \qquad \text{(no sum)} \tag{4-51} $$

These are the required gyro drive signals in arbitrary rotating coordinates.

The polar migration, astronomic precession and nutation are neglected but could be included in the navigation equations by allowing the y_1 and y_2 components of $\overline{\omega}_{IE}$ to be non-zero. For example, migration of the pole can be included as follows. Let s be the angle between the instantaneous pole and the geographic pole in a meridian γ west of Greenwich (Figure A-3). Then:

$$ {}^{y}\omega_{IE_1} = \omega_{IE} S \cos\gamma $$
$$ {}^{y}\omega_{IE_2} = \omega_{IE} S \sin\gamma $$
$$ {}^{y}\omega_{IE_3} = \omega_{IE} $$

where ω_{IE_3} might include some major components of the spin rate fluctuation. Omission of the polar migration compensation merely causes the inersors to exhibit an apparent drift rate which fluctuates with periods of 439 days, one year, etc. More important, when sufficiently accurate inersors are developed, they could be used to measure the polar migration.

For the case of orthogonal symmetric coordinates, as discussed in Section 4. F., the physical components of $\overline{\omega}_{IA}$ along z^i can be expressed

more simply. The geographic, spherical or ellipsoidal longitude, λ, locates the meridian plane containing the vehicle in the y_i frame. Within the meridian plane, let $\hat{z}^3$ make an angle, L, with the y_1 -y_2 plane where the following physical interpretations can be ascribed to L:

a. spherical coordinates, $L = L_c$

b. geographic coordinates, $L = L_g$

c. ellipsoidal coordinates, $L = L_E$

The components of $\bar{\omega}_{IA}$ in the y_i frame are:

$$ {}^{y}\bar{\omega}_{IA} = \begin{bmatrix} \dot{L}\sin\lambda \\ -\dot{L}\cos\lambda \\ (\omega_{IP}+\dot{\lambda}) \end{bmatrix} \tag{4-52} $$

and the transformation from the y_i frame to the symmetric z^j frame is given in Equations (4-40). Thus:

$$ \begin{aligned} {}^{z}\omega_i &= \frac{\partial y_j}{\partial z^i}\,{}^{y}\omega_j \\ {}^{z}\omega_1 &= -h_1\dot{L} \\ {}^{z}\omega_2 &= (\omega_{IP}+\dot{\lambda})\frac{\partial S_2}{\partial z^2} \\ {}^{z}\omega_3 &= (\omega_{IP}+\dot{\lambda})\frac{\partial S_2}{\partial z^3} \end{aligned} \tag{4-53} $$

The physical components of $\bar{\omega}_{IA}$ along the z^i are $\frac{{}^{z}\omega_i}{h_i}$ (no sum):

$$ \begin{aligned} {}^{p}\omega_1 &= -\dot{L} \\ {}^{p}\omega_2 &= \frac{1}{h_2}(\omega_{IP}+\dot{\lambda})\frac{\partial S_2}{\partial z^2} \end{aligned} \tag{4-54} $$

$$^{p}\omega_3 = (\omega_{IP} + \dot{\lambda})\frac{\partial \zeta_2}{\partial z^3} \tag{4-54}$$

These are the signals which must drive the stable platform in inertial space if it is to follow the navigation coordinate frame. Equations (4-54) are specialized for three symmetric coordinate frames of interest in the next three subsections.

4.G.2. GYRO DRIVE SIGNALS IN SPHERICAL COORDINATES.

In spherical coordinates, Equation (D-3) can be substituted into (4-54) to find the gyro drive signals:

$$\begin{aligned} ^{c}\omega_1 &= -\dot{L}_c \\ ^{c}\omega_2 &= (\omega_{IP}+\dot{\lambda})\cos L_c \\ ^{c}\omega_3 &= (\omega_{IP}+\dot{\lambda})\sin L_c \end{aligned} \tag{4-55}$$

4.G.3. GYRO DRIVE SIGNALS IN GEOGRAPHIC COORDINATES.

The gyro drive signals in geographic coordinates are found by substituting Equations (D-9) into (4-54):

$$^{g}\omega_1 = -\dot{L}_g \tag{4-56}$$

$$^{g}\omega_2 = \frac{\omega_{ip}+\dot{\lambda}}{h_2}\left[(R_{Bc}+h_g)\cos L_g + \frac{dR_{Bc}}{dL_g}\sin L_g\right] = (\omega_{ip}+\dot{\lambda})\cos L_g \qquad (4\text{-}56)$$

$$^{g}\omega_3 = (\omega_{ip}+\dot{\lambda})\sin L_g$$

Equations (4-55) and (4-56) are identical to those predicted geometrically and hence confirm the theory of Section 4.G. In more complicated coordinates, these might not be as readily predicted geometrically.

4.G.4. GYRO DRIVE SIGNALS IN ELLIPSOIDAL COORDINATES.

In ellipsoidal coordinates, the gyro drive signals can be found by substituting Equations (C-14) into (4-54). The ellipsoidal latitude, L_E, can be expressed in terms of ξ and η using Figure (C-3):

$$\tan L_E = \coth \xi \tan \eta$$

$$\dot{L}_E = \frac{\dot{\eta}\sinh 2\xi - \dot{\xi}\sin 2\eta}{2(\cosh^2\xi - \cos^2\eta)} \qquad (4\text{-}57)$$

Thus the gyro drive signals are:

$$^{E}\omega_1 = -\dot{L}_E = \frac{\dot{\xi}\sin 2\eta - \dot{\eta}\sinh 2\xi}{2(\cosh^2\xi - \cos^2\eta)} \qquad (4\text{-}58)$$

$$^{E}\omega_2 = \frac{(\omega_{1P} + \dot{\lambda}) \sinh \xi \cos \eta}{(\cosh^2 \xi - \cos^2 \eta)^{1/2}}$$

(4-58)

$$^{E}\omega_3 = \frac{(\omega_{1P} + \dot{\lambda}) \cosh \xi \sin \eta}{(\cosh^2 \xi - \cos^2 \eta)^{1/2}}$$

These are predictable geometrically, with some difficulty. For large ξ the ellipsoidal drive signals approach the spherical drive signals, as expected. Near the surface of the planet, $L_E \longrightarrow L_g$ and Equations (4-58) approach Equations (4-56).

Chapter Five

APPLIED INERTIAL NAVIGATION

5.A. THE PROBLEM.

Consider a vehicle navigating near the surface of a uniformly rotating planet, say the Earth. The vehicle may be located with respect to the Earth by giving its three coordinates in a navigation coordinate frame which is fixed relative to the Earth. The coordinates of all points on the Earth can be specified in this navigation coordinate frame.

The operator of the vehicle may prefer his position to be specified either in terms of the navigation coordinates, such as latitude, longitude and height or distance and direction to his destination. The former would probably be desired on a slow-moving ship; the latter on an aircraft. If the instantaneous navigation coordinates of the vehicle and of the destination are known, the distance and direction to the destination can be calculated.

The navigation coordinates of the vehicle can be measured in many ways. The most direct method is to locate

the vehicle with respect to ground stations whose coordinates are known. This can be done visually or electronically but is subject to the limitations that communication is often unavailable, unreliable or inaccurate and that radiation must be emitted or received.

The navigation coordinates can also be measured by sighting celestial bodies and solving the resulting celestial triangles. If the navigator knows the time of observation and knows the coordinates of the stars from an ephemeris, he can calculate his astronomic latitude and longitude. A coordinate transformation then yields the navigation coordinates, subject to the geodetic limitations discussed in Chapter Three. This method is limited by the necessity of obtaining clear skies for a star-sight, by the unknown deflection of the vertical, by the need for a stable platform from which to measure and by the length of time usually needed to make a measurement.

Inertial navigation is a means of measuring the navigation coordinates by measuring the forces acting on test masses carried aboard the vehicle and solving the equations of dynamics, with the proper initial conditions, to find the navigation coordinates of these test masses, and hence of the vehicle, as functions of time. Near a planet, pure inertial navigation is impossible in all three dimensions as shown in Section 5.E.3. In two dimensions, no external

information is required but the system is sensitive to instrument errors, being essentially an open-loop or dead-reckoning device. Inertial navigation may be supplemented by external velocity, position or orientation information to form a hybrid system, as discussed in Section 5.C.

5.B. THE INSTRUMENTATION OF AN INERTIAL NAVIGATOR.

The force sensors are basic to an inertial navigation system. The archetypal force sensor is a single-axis accelerometer, Figure 5-1. This device can be pictured as a case on which a fixed direction is designated the "input Axis." The instrument generally has some inertial acceleration, $\bar{f}_T$, in a gravitational field, $\bar{G}$. The ideal, single-axis accelerometer measures the component along its input axis of $\bar{f}_T - \bar{G}$. The actual output of an ideal single-axis accelerometer, f_{a_i} , is: $f_{a_i} = S_a(\bar{F}_T - \bar{G})_i$ where S_a is a non-dynamic sensitivity.

The output of a "velocimeter" or "integrating accelerometer" is the time integral of f_{a_i} . Accelerometers may contain, for example, a restrained sliding mass or pendulum, an unbalanced single-degree-of-freedom gyroscope or an unbalanced, eddy-current-restrained rotor. "Exotic" accelerometers based on solid-state properties of certain materials

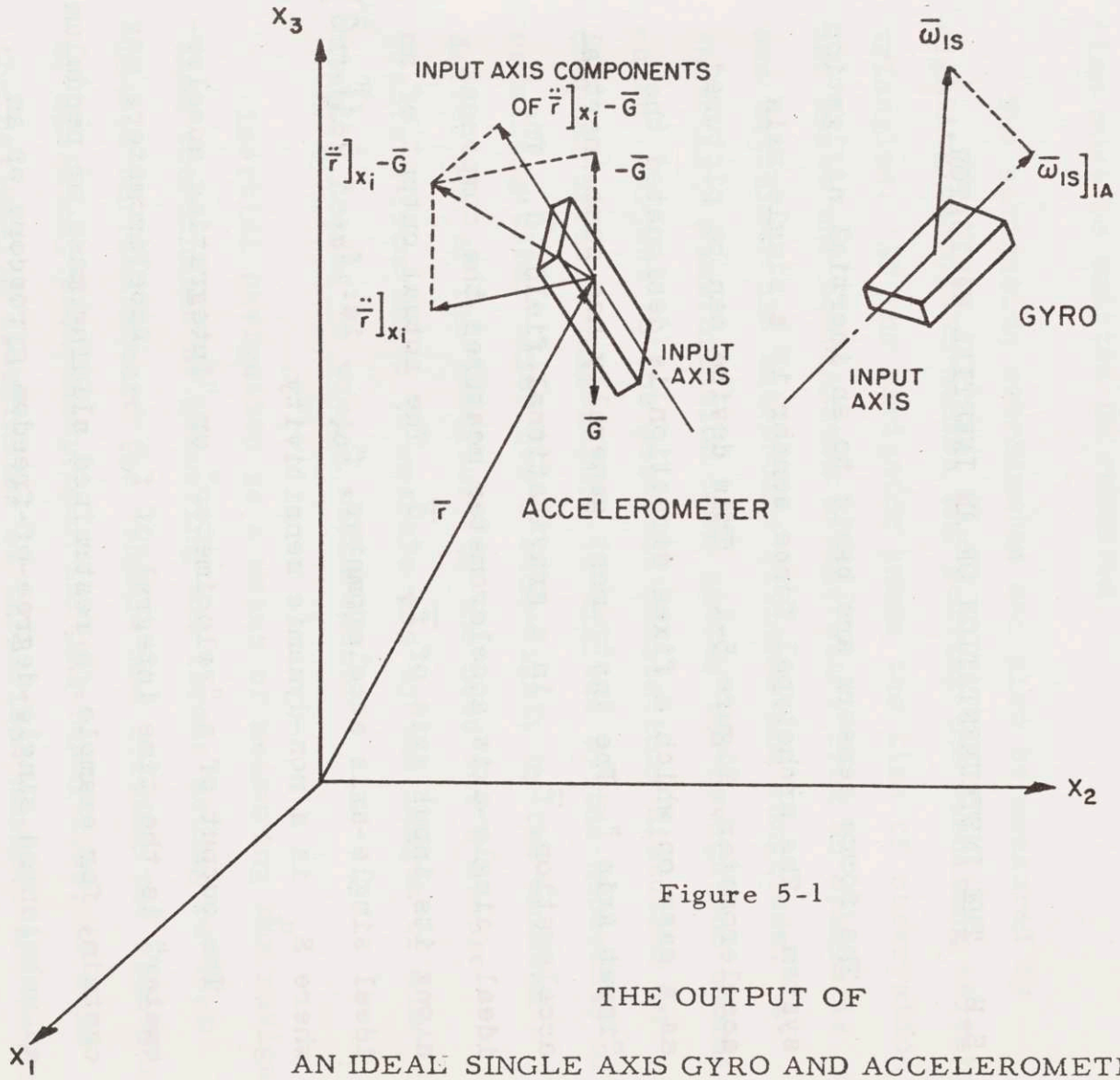

Figure 5-1

THE OUTPUT OF

AN IDEAL SINGLE AXIS GYRO AND ACCELEROMETER

are presently under study. Actual accelerometers are subject to linearity, resolution, threshold and saturation errors and to cross-coupling of acceleration and angular motion from the other axes into the input axis.

A "vector accelerometer" measures more than one component of $\overline{f}_T - \overline{G}$. It may consist of a rigid array of single-axis accelerometers whose input axes are non-coplanar. Its output is a vector, $\overline{f}_a$ each of whose components is proportional to a component of $\overline{f}_T - \overline{G}$ along one of the input axes. The single-axis accelerometers are commonly assembled so their input axes are nominally orthogonal, thus measuring the components of $\overline{f}_T - \overline{G}$ in a nominally orthogonal coordinate frame. A vector accelerometer can be mounted on an "accelerometer platform."

In order to interpret $\overline{f}_a$ in terms of position in the navigation coordinate frame, the angular velocity of the accelerometer platform in the coordinate frame must be known. If the accelerometer's angular motion is aimless and unmeasured, its output is useless. Sensing the angular motion of the accelerometer platform is the function of the angular inertial sensors.

The fundamental sensor of angular motion in inertial space is designated an "inersor." The most commonly used inersor, the gyroscope, is built in single-degree-of-freedom and two-degree-of-freedom forms.

The single-axis inersor can be pictured as a case on which a fixed direction is designated the "input axis," Figure 5-1. If an ideal single-axis inersor has an angular velocity, $\overline{\omega}_{IS}$ in inertial space, its electrical output measures the component of $\overline{\omega}_{IS}$ along its input axis. An integrating inersor measures the time integral of $\overline{\omega}_{IS}]_{I.A.}$ In general, the output of an integrating inersor has no direct physical interpretation but is used only for engineering convenience. If the input axis has a fixed inertial direction, the time integral of the component of inertial angular velocity along its input axis has the physical interpretation of angle of rotation about the input axis.

A "vector inersor" is a rigid array of three single-axis inersors whose input axes are non-coplanar. Each single-axis instrument measures the component of $\overline{\omega}_{IS}$ along its input axis so as a whole, the vector inersor measures $\overline{\omega}_{IS}$ In practice, the input axes are usually made nominally orthogonal.

The output of an ideal vector integrating inersor is a vector, each of whose components is the time integral of the component of $\overline{\omega}_{IS}$ along the input axis of one of the single-axis instruments. This vector has no physical significance except if the inersor always maintains nearly

the same nominal inertial orientation. In that case, the output measures its vector angle of departure from the nominal orientation.

A two-degree-of-freedom inersor consists of a source of angular momentum, gimballed or otherwise supported with respect to a case. Pickoffs on the device measure two orientation parameters of the case relative to the source of momentum. Thus the device measures orientation with respect to some previously defined line in inertial space.

In order to measure the three independent angular velocities of the accelerometer platform, two two-degree-of-freedom inersors or one two-degree and one single-degree of freedom inersor or three single-degree-of-freedom inersors are needed. For precision applications, the inersors are used as nulling instruments.

The only inersors which have thus far attained engineering application are single-degree and two-degree-of-freedom gyroscopes. The output of an actual gyroscope is not merely proportional to the component of $\overline{\omega}_{IS}$ along its input axis but may also include instrument noise errors, acceleration-dependent errors and terms proportional to other components of $\overline{\omega}_{IS}$ and their derivatives. Fluid and air supported single-degree-of-freedom gyroscopes have been in general use for nearly ten years. Now, gas spin

bearing and cryogenic two-degree-of-freedom gyroscopes are being developed and exotic sensors, using nuclear and solid-state properties of materials, are being studied.

Inersors are used to measure the angular velocity of the accelerometer platform in inertial space. Two general methods are in common use.

In one method, the vector accelerometer and the requisite number of inersors are rigidly mounted relative to each other as a "stable platform" or "space integrator." The platform is isolated from angular motions of the vehicle which carries it by means of three or four servo-driven gimbals. The inersors are so connected that the stable platform will maintain a fixed orientation in inertial space, independent of angular motions of the vehicle, unless commanded to change its orientation in response to an external signal to the inersors (Ref. 16). The system mechanization which results when the stable platform carries both inersors and accelerometers has been called an "analytic mechanization" by Wrigley et al. (Ref. 82).

In another method of mechanization, the inersors and accelerometer platform are physically separate. The inersors are allowed to remain non-rotating in inertial space or are rotated in some prescribed manner. Then,

the angle between the accelerometer platform and the inersors is measured. This mechanization, which Wrigley et al. called "geometric," not only measures the angular velocity of the accelerometer platform relative to the inersors but has the added advantage of measuring the angle between them directly. It leads to a geometric analog of the inertial navigation problem in which the gimbals serve many of the functions which the computer performs in the analytic mechanization. The entire assembly of accelerometers and inersors must be isolated from angular motions of the vehicle by means of three or four servo-driven gimbals.

The design of the gimbals, servos and electronics for a stable platform in order to achieve adequate isolation from angular motions of the vehicle is itself a highly developed art (Refs. 8, 16, 42 and 73). The stable platform will normally engage in small coupled oscillations whose amplitude is several seconds of arc, about the nominal commanded orientation, exclusive of gyro drift.

The trend in future stable platforms appears to be to mount much of the electronic equipment on the platform. Eventually, the use of isolation gimbals may give way to body-mounted accelerometer platforms. If the accuracy of inersors increases at its present rate (for example, Ref. 36 states that 10^{-4} deg./hr. cryogenic gyros are

Figure 5-2

THE NAVIGATION PROCESS

Five Classes of Parameters are Needed for Inertial Navigation in the Vicinity of a Planet

Parameters	How Obtained?
The transformation equations $y_i = y_i(z^j)$	These define the navigation coordinate frame, at the designer's discretion.
$\bar{G}$ or $\bar{g}$	Must be computed as a function of the z^i. $\bar{G}$ or $\bar{g}$ can either be calculated from a mathematical model, read out from a previously stored memory or both.
The inertial angular velocity of the accelerometer platform, $\bar{\omega}_{IA}$	Measured with gyros or other inersors.
Initial conditions: 3 of position } of vehicle 3 of velocity } 3 of orientation } of platform 3 of angular velocity }	Geodetic information. Ground-based or en-route gyrocompassing. Requires external velocity sensor such as Doppler. Celstial monitor on platform. Electronic position aids such as Loran or Transit. Transfer from an auxiliary platform.
Inertial spin rate of the planet and time.	On the Earth, the spin rate measures time within 10^{-7} Earth rate.

under development), the polar migration and astronomic precession will have to be inserted into the navigation equations in a few more years, as shown in Section 4.G.1.

5.C. THE NAVIGATION PROCESS.

5.C.1. INTRODUCTION.

The navigator, whether human or automatic, must obtain three, or sometimes two coordinates of the vehicle in a navigation coordinate frame which is fixed with respect to the planet. The inertial navigator seeks to determine these coordinates by measuring the forces on test masses aboard the vehicle and solving the equations of motion for the positions of these masses. The accelerometers, which contain these test masses, are mounted on a platform which is given some prescribed angular velocity in inertial space.

Figure 5-2 outlines the five classes of parameters which are always needed to determine the navigation coordinates no matter what coordinate frame is used. These are discussed one at a time in the following five subsections.

5.C.2. THE NAVIGATION COORDINATES AND NAVIGATION EQUATIONS.

The navigation equations express the kinematic relations between the navigation coordinates, z^i, the physical components of the inertial angular velocity of the inersors, $\overline{\omega}_{is}$, and the accelerometer outputs, $\overline{f}_a$. To define these coordinates, the intermediary coordinate frames x_i and y_i must be defined as in Sections 4.E.1. and 5.D.1.

The mass center of a planet is a suitable origin for an operational inertial coordinate frame, within limits discussed in Sections 1.J. and 4.E.1. Such a frame is the planet-centered, "inertially-non-rotating" Cartesian coordinate frame, x_i, whose x_3 axis lies along the geographic polar axis of the planet. This coordinate frame has an inertial angular velocity determined by the astronomic precession and polar migration of the planet. In the case of the Earth, x_i is inertial for angular velocity measurements greater than 10^{-6} deg./hr. and for acceleration measurements insensitive to 10^{-7} gee.

The planet-centered, planet-fixed Cartesian frame, y_i, is fundamental for defining positions on a planet. Its origin coincides with that of x_i at the mass center of the planet and its y_3 axis coincides with x_3. The y_i coordinate frame actually rotates relative to x_i about an axis which very nearly coincides with $\hat{x}_3$-$\hat{y}_3$. The period of rotation

about the common x_3 - y_3 axis is constant to one part in 10^7 and equals 86,164.10 mean solar (Ephemeris) seconds. The component of relative angular velocity perpendicular to $\hat{x}_3$-$\hat{y}_3$ is about 5×10^{-5} deg./hr.

The navigation coordinates, z^j, are contravariant coordinates (coordinates in the usual sense) which are related to the y_i by means of the time-independent transformation, $y_i = y_i(z^j)$. Covariant coordinates do not generally exist since the equations, $dz_i = g_{ij}\, dz^j$, are not integrable.

The physical components of a vector, such as $\overline{\omega}_{IS}$ or $\overline{f}_a$, are neither its covariant nor contravariant components but are related to them according to Equation (4-21). Where the symbol, V_i, is used without further specification, it hereafter refers to a physical component of the vector, $\overline{V}$, and not to a covariant component. In Cartesian coordinates, there is no distinction between covariant and contravariant components.

The first task of the navigation system designer is to select the navigation coordinate frame and the accelerometer tracking frame (Section 5.D.). Then he must derive the navigation equations which compute the navigation coordinates and inersor drive signals in terms of the accelerometer outputs and certain other parameters (Figure 5-2). Finally, the equations must be simplified for convenient computation with a digital computer. Except in certain particular mechanizations, the

accelerometer platform aligns with the unit vectors of the navigation coordinate frame.

Equations (4-37) relate the arbitrary non-orthogonal curvilinear coordinates, z^i, to the kinematic output of the accelerometers, for the case in which the input axes of the accelerometers align with the unit vectors of the navigation coordinate frame. These navigation equations always involve partial derivatives, $\frac{\partial y_i}{\partial z^j}$. Many of these derivatives combine to form elements of the metric tensor but except in the case of a symmetric, orthogonal system (Equations 4-38), some partial derivatives are always required in addition to the elements of the metric tensor.

Some basic limitations on the navigation equations are shown in Figures 5-14 and 5-15.

5.C.3. THE INERTIAL ANGULAR VELOCITY OF THE ACCELEROMETER PLATFORM.

The inertial angular velocity of the accelerometer platform is needed in order to interpret the accelerometer outputs in terms of position. In the analytic mechanization, $\bar{\omega}_{IA}$ is known from the gyro drive signals; in the geometric mechanization, from the gimbal angle drives. The actual platform angular velocity differs from the commanded $\bar{\omega}_{IA}$

because of errors in the computed drive signals and gyro drift (Sections 5.E.4.B. and 5.E.4.C.)

5.C.4. GRAVITY AND GRAVITATION.

The components of gravity or gravitation along the input axes of the accelerometers are required everywhere in the region of navigation. At each point, the component of $\overline{G}$ along the accelerometer input axis must be added to the output of that accelerometer, $\overline{f}_a$, to obtain the indicated components of kinematic inertial acceleration, f_{T_i}. If $\overline{G}$ is imperfectly calculated at any point, the corrected accelerometer output will not be $\overline{f}_T$ but will be in error by the error in calculating $\overline{G}$. Chapter Two discusses the prediction of $\overline{G}$ and $\overline{g}$ in the space surrounding a planet. Though the results are applicable to any planet, detailed data is available only for the Earth.

At any point near the Earth, the gravity field is by definition perpendicular to the local geop. Thus at a geop, the component of $\overline{g}$ along the geop is zero. But if the geoid is approximated by an ellipsoid of rotation the component of $\overline{g}$ along the ellipsoid is not zero unless the geoid is parallel to the ellipsoid there.

For navigation purposes, resolution of $\overline{G}$ or $\overline{g}$ below 10^{-5} gee is

seldom necessary but even to this fineness, the $\overline{g}$ or $\overline{G}$ field around the Earth is exceedingly complicated. At any point near the Earth, neither $\overline{G}$ nor $\overline{g}$ generally lies along the geographic, spherical or ellipsoidal vertical; there is a "horizontal" component of $\overline{G}$ or $\overline{g}$. This horizontal component is treated as the sum of a systematic horizontal component, g'_L or G'_L plus a deflection of the vertical, δ_{vG_L} or δ_{vg_L} where L may be L_c, L_g or L_E. The mathematical model of the systematic horizontal portion of $\overline{g}$ or $\overline{G}$ is selected to match as nearly as possible the actual horizontal component yet be simple enough for on-board computation. Section 2.F.5. discusses mathematical models which use one or two terms of the spherical harmonic expansion of the gravitational potential of the Earth. Any fine-structure difference between the actual and model components of $\overline{G}$ and $\overline{g}$ causes a deflection of the vertical. Equations (2-30), (2-40), (2-42), (2-49) and (2-50) show suggested models for the horizontal components of gravity and gravitation within navigational distances of the Earth whereas Figures 2-10 and 2-12 show sample deflections of the vertical with respect to these models. It is essential to note that the amount of the deflection depends as much on the selection of a reference ellipsoid as on the existence of mass anomalies within the Earth.

In local-level mechanizations, the navigation equations contain only the horizontal components of $\overline{g}$ and $\overline{G}$. If inertial navigation is to achieve

an RMS position error of "several hundred feet by 1963-1965" (Ref. 76), the horizontal components of $\overline{g}$ or $\overline{G}$ in the navigation coordinate frame cannot be omitted from the navigation equations.

On the surface of the Earth, the projected normal to the reference ellipsoid is implicitly used as a reference direction for measuring the deflection of the vertical. Deflections of the vertical at sea and at altitudes above the Earth have not been measured directly. In the former case, deflections of the vertical over the oceans probably do not materially differ from those over land because of the mountainous nature of the ocean floor; in the latter case, it is likely that deflections of the vertical increase slightly with altitude before decreasing to zero at large distances from the Earth.

The navigation equations contain ${}^{z}G_{1}$ and ${}^{z}G_{2}$ or ${}^{z}g_{1}$ and ${}^{z}g_{2}$, the horizontal components of $\overline{G}$ or $\overline{g}$ in the navigation coordinate frame. These must be mechanized to solve the equations correctly. A knowledge of horizontal gravity or gravitation is essential if the accelerometer platform is to properly align with the navigation coordinate frame at all times.

If the horizontal component of gravity is not inserted en route, the platform will tend to align with $\overline{g}$ instead of with the navigation coordinate frame, the difference increasing as the vehicle speed decreases. This causes a position error since not only do the navigation equations omit

the proper horizontal components of $\overline{g}$ but the metric of the actual space which the platform follows is so complicated that the navigation equations are in fact incorrect.

The effect of an anomalous horizontal component of gravity is usually analysed by assuming that the platform does align exactly with the navigation coordinate frame and that the horizontal components of gravity are forcing functions in the navigation equations.

In the majority of missions, the horizontal components of gravity tend to average out to zero during long voyages but the random fluctuations of g_1 and g_2 cause fluctuations in the position error. To first order, an error in horizontal gravity has the same effect as an accelerometer error, Section 5.E.4.A. For any desired course and speed, the power spectral density of horizontal gravity, $\Phi_{gg}(s)$, can be estimated and the power spectral density of position error, $\Phi_{xx}(s)$, found as in Equation (5-15). The mean square position error is:

$$MS(x) = \oint \Phi_{xx}(s)\, ds$$

Wilmoth (Ref. 79) attempts a simplified form of this calculation. RMS position errors in typical regions of the Earth, caused by the omission of random horizontal components of gravity from the mechanization, appear to be on the order of several hundred feet.

The next subsection discusses some effects of deflection of the vertical on system alignment.

5.C.5. ALIGNMENT.

5.C.5.A. INTRODUCTION.

Twelve initial conditions must be inserted during the initial alignment and again en route, whenever it is desirable to realign the system. Realignment may be necessary to update the initial conditions because of cumulative errors, because of a loss of reference due to power failure or because of the necessity of repairing the system en route.

The twelve initial conditions are the initial position and velocity of the vehicle and the initial orientation and angular velocity of the accelerometer platform. If inersor errors are neglected, only nine of these are independent because of the constraint imposed by the feeding-back of inersor drive signals from the computer. The precise definition of positions and orientations on the Earth are problems in geodesy (Chapter Three); their measurement is an instrumentation problem.

In order to perform the alignment, external measurements of z^i and

Figure 5-3

ASTRONOMIC AZIMUTH ERROR IN THE

PRESENCE OF A DEFLECTION OF THE VERTICAL

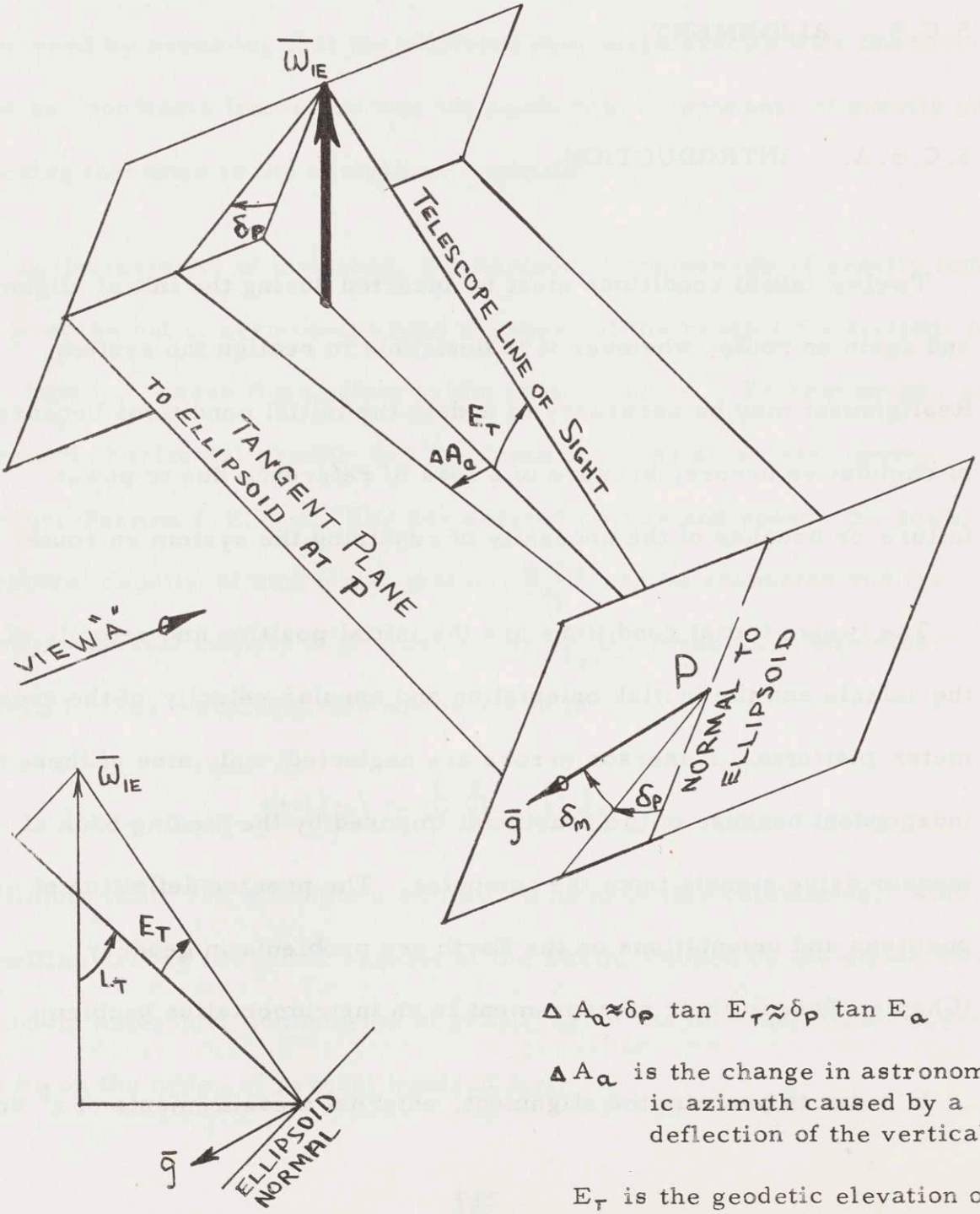

$\Delta A_a \approx \delta_p \tan E_T \approx \delta_p \tan E_a$

ΔA_a is the change in astronomic azimuth caused by a deflection of the vertical

E_T is the geodetic elevation of the telescope

$\dot{z}^i$ and of platform orientation relative to the $\hat{z}^i$ must be made. These are difficult processes at best since no physical vectors correspond to the unit vectors of the navigation coordinate frame.

Such independent measurements of position or velocity of the vehicle or of orientation of the accelerometer platform can have the effect of damping the navigation system. If the system is realigned at discrete time intervals en route, it is damped discontinuously because system errors are suddenly reduced at discrete times. If sufficiently accurate external information is available continuously, damping of the system is continuous. System damping is discussed in detail by Wrigley (Ref. 82), Duncan (Ref. 19), Fried (Ref. 24) and Stevens (Ref. 71).

5.C.5.B. ANGULAR ALIGNMENT.

The platform must be oriented relative to the unit vectors of the navigation coordinate frame about the level and azimuth axes. When the vehicle is stationary on the Earth, level axis alignment is normally accomplished by quick-torquing the platform until the horizontal accelerometer outputs are nulled. Azimuth alignment in a stationary vehicle is accomplished optically (if the area has been previously surveyed) or by gyrocompassing. In the gyrocompass mode, the azimuth gyro is

Figure 5-4

GYROCOMPASSING IN THE PRESENCE OF

A DEFLECTION OF THE VERTICAL

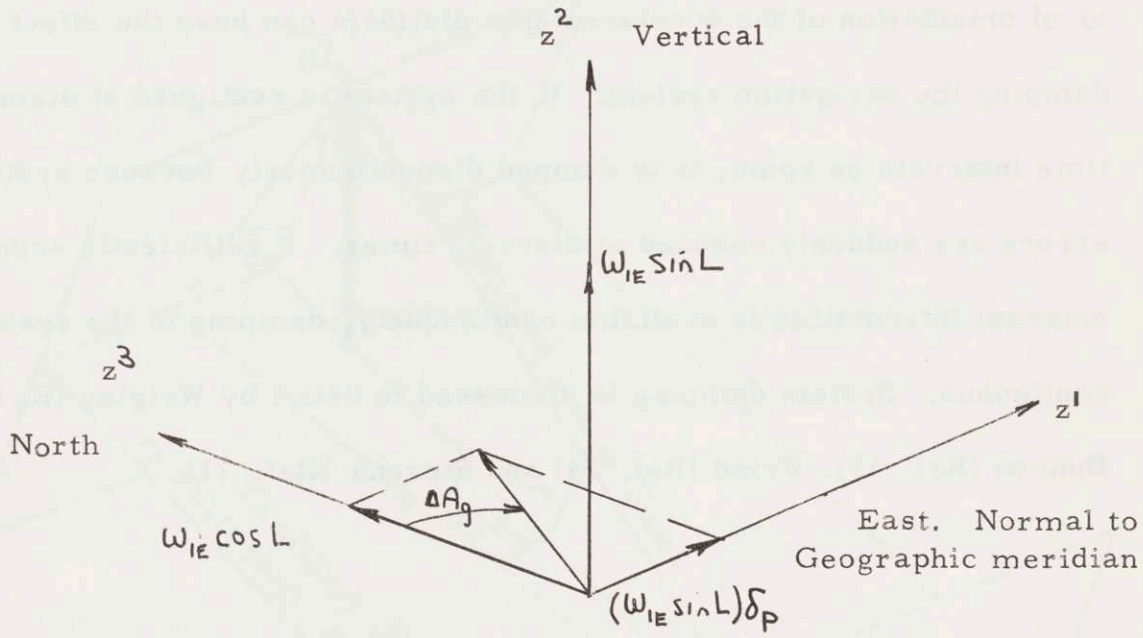

$L = L_c$, L_g or L_E .

z^2 and z^3 are in the plane of the geographic meridian.

An astronomically level gyrocompass, on a stationary vehicle, tracks the astronomically horizontal component of Earth rate, with a geographic azimuth error = $\delta_p \tan L$.

torqued until the inertial rate indicated by the east gyro is zero. The input axis of the east gyro then points east within geodetic limitations.

If the deflection of the vertical is not zero at the point of departure and if the platform is levelled along $\overline{g}$ there, its initial orientation with respect to the navigation coordinate frame is incorrect. Since deflections of the vertical of ten or more seconds of arc are common, the accelerometer platform will be misaligned by this amount in the level axes.

Though it is not immediately obvious, an error in azimuth results if the platform is aligned in a region of non-zero prime deflection of the vertical. The presence of a prime deflection of the vertical means that $\overline{g}$ and the geographic polar axis are skew lines and cannot be coplanar. Consequently, an astronomic north sight at an elevation, E, is projected along the astronomic vertical onto the reference ellipsoid with the geodetic azimuth:

$$A_1 = \delta_p \tan E \qquad (5-1)$$

instead of at an azimuth, $A_1 = 0$, Figure 5-3. Similarly, from Figure 5-4, the astronomic horizontal component of vertical Earth rate does not point toward geodetic north. This is because a component of vertical Earth rate, $\omega_{ie} \delta_p \sin L$, is projected along the astronomic east-west direction. Hence a stationary, astronomically-level gyrocompass points north with a geodetic azimuth A_2:

$$A_z = \delta_p \tan L \qquad (5\text{-}2)$$

In surveyed areas, these azimuth errors can be calculated and corrected by compensating the east accelerometer with the local east horizontal component of $\bar{g}$. However if the platform is aligned in an unsurveyed area, its geodetic azimuth can be in error by twenty seconds of arc or more. Such azimuth errors would presumably result wherever en route alignment is attempted.

If the platform is initially aligned in a surveyed area, the misalignment could be removed by inserting the horizontal component of gravity into the mechanization. For example, in a north-seeking, locally-level system, g_1 is added to the output of the east accelerometer and g_2 to the north accelerometer. With these level axis compensations, the platform would be properly aligned with the unit vectors of the navigation coordinate frame so azimuth measurements would be geodetically correct.

En route alignment may procede in essentially the same manner except that en route gyrocompassing requires an independent knowledge of vehicle velocity in order to identify the horizontal component of Earth rate.

A major obstacle to en route alignment is the absence of measurements of the deflection of the vertical at altitudes and in unsurveyed areas. These deflections of the vertical at sea and at altitude are not

less than those on the surface of the Earth and hence cause position and azimuth errors comparable to those resulting from alignment in unsurveyed areas of the Earth's surface. A lower limit on the accuracy attainable without access to deflections of the vertical might be one third to one half mile.

5.C.5.C. INSERTION OF VEHICLE VELOCITY.

External measurements of vehicle velocity, which are more accurate than the accumulated inertial velocity, can be inserted into the navigation system as shown in Figure 5-5. The indicated velocity, $\dot{z}_I^i$, is based on combined inertial and external measurements. The externally-derived and indicated velocity signals are compared and the difference used to correct the velocity integrator, through a filter. Hence if the two velocity measurements differ persistently, the difference tends to drive the indicated velocity to match the externally-derived velocity.

The externally-measured velocity must be resolved into the navigation coordinate frame. Very commonly, the stable platform gimbals perform this resolution. In Figure 5-5, the heading angle resolver indicates this resolution (in azimuth) and the h_i are scale factors to convert the externally-measured velocity components to rates of change of navigation

Figure 5-5

INSERTION OF EXTERNALLY-MEASURED VELOCITY INTO AN INERTIAL NAVIGATOR.

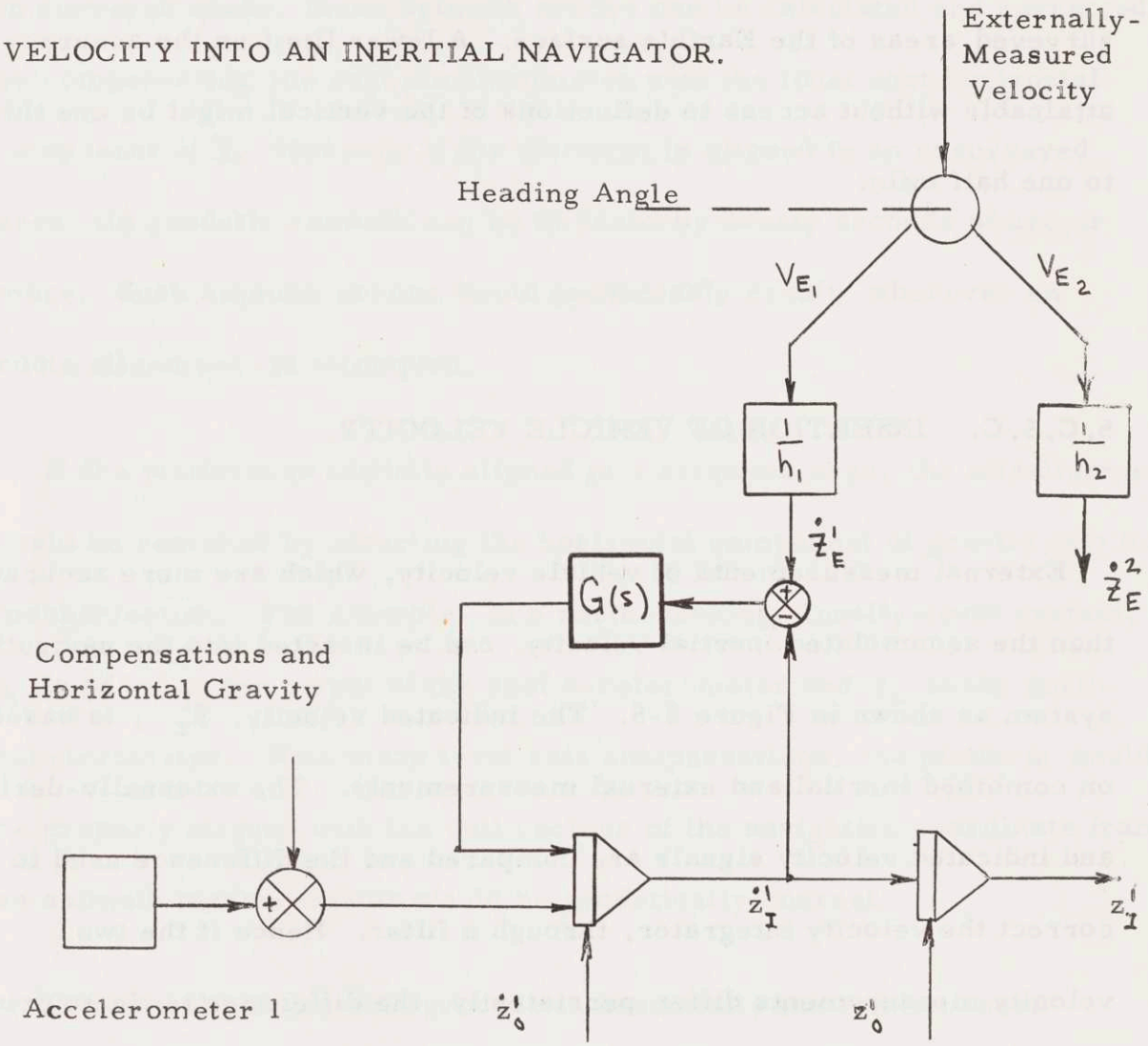

$\dot{z}_I$ is indicated

$\dot{z}_E$ is externally-measured

coordinates. Alternatively, the system could be mechanized to yield the indicated physical components of velocity, $h_i \dot{z}^i$ (no sum), which could be directly compared to the external velocities.

The non-inertial and indicated velocities are both apt to differ statistically from the true velocity. The difference is probably a non-stationary stochastic process reflecting noise in the gyros, accelerometers and external sensors. Thus the system design of a hybrid navigator reduces to the selection of an optimum filter, G(s), which will minimize some function of the indicated velocity error. If the velocity difference can be considered stationary (for any particular operating regime) and thus characterized by its autocorrelation function, the powerful Wiener-Lee procedure (Ref. 232) could be used to select an optimum filter to minimize the mean square velocity error. The optimum filter may adapt to different operating regimes.

The earliest external velocity aid was derived from air-speed (or water-speed) measurements and was often called "air-mass damping." Because of the unknown velocity distribution of the wind, large constant and stochastic errors resulted thus causing large position errors. The best filter would still produce a large mean square position error.

Today airborne velocity measurements are frequently made with Doppler radar (Refs. 19, 24 and 25 for example). The usual Doppler

radar radiates a pattern of narrow beams from the aircraft. The antennas are either stabilized with respect to the navigation coordinates or held at a constant attitude relative to the airframe. By observing the Doppler frequency shifts between pairs of these beams and resolving through the stable platform, the components of the aircraft's velocity relative to the surface are obtained, resolved into indicated navigation coordinate axes. The frequency shifts between various pairs of beams are compared in order to reduce the frequency stability requirements of the transmitter. In the crudest systems, the antennas are levelled with a pendulum and the velocity resolved in azimuth through a magnetic compass.

Over sloping ground, the Doppler rad ar does not measure velocity relative to the ellipsoid. The fractional error is of the order $\frac{\theta^2}{2}$ where θ is the ground slope. Hence over a 4% ground slope, the velocity error is 0.08% or 1.5 knots at Mach Three. Thus ground slope variations can significantly spread the frequency spectrum of the reflected beams.

When ocean currents cause the water to move en masse relative to to the Earth or when sea spray disturbs the water surface, a measurement of velocity relative to the sea surface does not give ground speed over the ellipsoid. The constant error caused by systematic ocean currents or spray can only be corrected if the water's velocity relative to the Earth is known. This is seldom possible,even approximately.

Non-systematic errors caused by waves, spray, terrain slope and finite beam width cause the returned frequency spectrum to be widened, thus making the measurement of exact ground speed less precise. The selection of an optimum coupling filter, G(s), depends on the power spectral density of the Doppler velocity signal. Hence over different types of terrain or sea states, different filters could be used, the filter characteristics being adjusted automatically or by the navigator. A near minimum mean square error is thus possible over a wide variety of terrain.

A very stable frequency source such as an atomic clock can be carried aboard a vehicle and compared in frequency to a similar unit on the ground. The Doppler shift between them would measure the rate of change of the line of sight distance to the ground station. Three such frequency measurements, in non-coplanar directions, would give three independent components of the aircraft velocity in a non-orthogonal coordinate system. The aircraft velocity vector could then be readily reconstructed.

5.C.5.D. INSERTION OF VEHICLE POSITION.

External measurements of vehicle position are required for initial alignment and may be used en route to damp system errors.

In order to define position on the Earth, the discussion of Chapter Three regarding the establishment of reference ellipsoids is reviewed. On a well-surveyed, continuous land-mass, an ellipsoid can be selected to optimally represent the geoid. The projection of any point of the land-mass onto the ellipsoid can be located within fifty meters. The definition of an optimum ellipsoid to represent the geoid over oceans or unsurveyed land is necessarily crude. Furthermore the selection of a single ellipsoid to represent the geoid over land masses separated by water is complicated by the difficulty of making accurate intergrid ties over water. Thus although observers on different land-masses may use ellipsoids of identical dimensions, the centers of these ellipsoids may lie as much as one third of a mile apart. An unknown separation between reference ellipsoids on different continents introduces distance and direction errors between points on these continents. Also since the origin of an operational inertial frame must be at the mass center of the Earth, the center of an offset ellipsoid will accelerate in a circle in the inertial frame, creating a general centripetal force field over the entire Earth. The geodetic coordinates of the points of departure and destination must be known on

the same world-wide reference ellipsoid.

Electronic position aids such as Tacan, Shoran or Loran (Refs. 4, Chap. 12; 30, 35, 50, 59 74) yield two coordinates of the vehicle's position and can be used to periodically reset the position integrators. Such position aids cannot correct velocity, levelling or azimuth errors. Such electronic aids locate the vehicle with respect to fixed ground stations which have been previously surveyed relative to local geodetic grids. If the relation between the local grid and a world-wide reference is known, the vehicle can be located in a world-wide reference frame.

A star-tracker carried aboard the vehicle can potentially provide position and orientation information (Refs. 20 and 31). If the vehicle operates at a sufficiently high altitude that cloud cover is improbable and that the ratio of star signal to background optical noise is adequate, then a telescope aboard the vehicle can accurately locate stars relative to the inertial platform.

Three non-coplanar star sights, either taken simultaneously with three telescopes or successively with one, permit the position of the vehicle and orientation of the platform to be found simultaneously. The local deflection of the vertical must be known for high precision. With three star sights and a known deflection of the vertical, the accelerometer platform can be realigned relative to the navigation coordinate frame in

all three axes and the two position integrators can be reset to updated values. If the position of the vehicle is known from other external information (perhaps Shoran or Transit satellite), then only three orientation parameters are unknown. These can be found from two star sights. The addition of a Doppler radar would permit updating of the velocities and hence the reinsertion of nine of the twelve initial conditions.

The Transit satellite program suggests the possibility of periodic position checks, perhaps every three hours, anywhere on the Earth within a few more years (Refs. 29 and 43). By recording the Doppler shift versus time of a transmitted signal from the satellite and knowing the satellite's orbit, the most probable position of the observer can be inferred, on an ellipsoid whose center is at the mass center of the Earth. It is expected that a small receiver-transmitter-computer will be available to perform this task. Since the satellite moves too rapidly for an optical sighting, it cannot be used to update the platform orientation.

5.C.6. TIME AND THE ANGULAR VELOCITY OF THE PLANET.

The angular velocity of the planet is needed to permit coordinate transformations from inertial space to the planet. With sensitive enough inersors, the polar migration and astronomic precession must be included

in the transformation from inertial to planet coordinates(Section 4.G.1.). Time is needed as the explicit variable of integration in the computer. On the Earth, to an accuracy of one part in 10^7 , time is measured by ω_{IE} while Earth rate is constant and equal to the inertial spin rate, not the sidereal rate, Section 1.J.

Figure 5-14 shows some limitations on the measurement of time.

5.D. THE SELECTION OF A COORDINATE FRAME.

5.D.1. INTRODUCTION.

As has already been noted, the navigation system designer's first task is to select a navigation coordinate frame, z^j , and derive the transformation equations from y_i to z^j . As discussed in Section 4.E., the navigation coordinate frame selected will of necessity be orthgonal.

The selection of an orthogonal system for which $g_{ij} = 0$ when $i \neq j$ simplifies the navigation equations (4-37) to the form (4-38). Furthermore, an accelerometer platform is most readily constructed with its accelerometers rigidly mounted relative to each other. Thus, it could not align with the unit vectors of a curvilinear, non-orthogonal coordinate frame unless the accelerometers were rotated relative to each other on the platform; a complexity gaining nothing in return. If fixed mounted, non-orthogonal accelerometers are used, the navigation coordinate axes are non-orthogonal straight lines. Such an oblique system has no advantages over a Cartesian frame and has the disadvantage of non-zero, off-diagonal metric elements and thus more complicated navigation equations.

Hence, except to analyze the effect of unintentional non-orthogonality of components, all navigation equations must be written in orthogonal, though perhaps curvilinear, coordinate frames.

Though systems are sometimes mechanized in the x_i or y_i coordinate frames, it is often more convenient to select a coordinate frame which is related to the surface of the Earth.

The Earth rotates about an instantaneous spin axis which itself migrates relative to the mantle, roughly in a conical

spiral whose maximum half-angle is one half second of arc and whose predominate periods are 365 and 439 days (see Appendix A). A geographic polar axis is selected, fixed in the Earth, at approximately the mean position of the migrating spin axis.

The "figure of the Earth" is commonly defined in terms of the equipotentials of gravity near its surface (the geops), Figure 2-9. One of these equipotentials of $\bar{g}$, which approximately coincides with mean sea level, is identified as the geoid. Section 2.D. shows that the shape of the geoid varies only about three inches with motions of the heavenly bodies and is approximately described as an ellipsoid of rotation about the geographic polar axis. The geoid is always within 100 meters of a well-chosen elliposid of rotation. Any meridian section of the ellipsoid is an ellipsoid of eccentricity, $\epsilon = 0.082$ (Figure 3-7). Geodesists usually specify the ellipticity or flattening, $f = \frac{a-b}{a}$. Though some measurements show that triaxial ellipsoids of ellipsoids of slightly different dimensions may match the geoid more exactly (Sections 2.F.9. and Figures 2-13 and 3-6), the navigator is not so much interested in the best shape of the geoid as in insuring that observers everywhere on the Earth use the same ellipsoid for mapping purposes. The International ellipsoid of 1924 (Figures 2-13 and 3-6) is used throughout this thesis.

Height above the ellipsoid is definable in a number of ways. Each of the next three sections discusses a coordinate frame resulting from a different definition of height, Figure 5-6.

5.D.2. GEOGRAPHIC COORDINATES.

The simplest method of defining height for vehicles within 35 nautical miles of the surface of the Earth, is to measure geodetic height, h_g , along that projected normal to the ellipsoid which passes through the point in question. A line along this projected normal is geographically vertical.

Section 3.B. introduces the terms, "geodetic longitude and latitude," λ_T and L_T , when referring to calculated longitude and latitude on some local reference ellipsoid of unknown center position. Geographic longitude, λ_g , latitude, L_g , and height, h_g , refer to these same coordinates on a world-wide reference ellipsoid whose origin is sufficiently close to the mass center of the Earth. These are a generalization of the geographic coordinates, λ_g and L_g , defined by Wrigley et al. (Ref. 82, pg. 19). The covariant elements of the metric tensor for the geographic coordinate frame are shown in Equation (D-12).

The geographic coordinate frame has the virtue that the surface defined by $h_g = 0$ coincides with the reference ellipsoid.

The suggested mathematical model for the systematic horizontal components of gravity is, from Equation (2-40):

$$g_1' = 0$$

$$g_2' = -5.44\left(\frac{h_g}{a}\right)\sin 2L_g \qquad \text{cm./sec.}^2 \qquad (2\text{-}40)$$

This model gives the systematic horizontal component of gravity to an accuracy of 10^{-5} gee. The actual horizontal component of gravity may commonly differ as much as 5×10^{-5} gee from this model. In regions where such large differences occur, it may be desirable to compute the actual horizontal component of gravity from gravimetric data and store it in the vehicle's navigation computer.

Section 5.F. mechanizes three typical navigation systems in geographic coordinates. Figure 5-6 summarizes relevant properties of this coordinate frame.

5.D.3. SPHERICAL COORDINATES.

For vehicles at large distances from a planet, say the Earth, the spherical coordinate frame is simplest for

Figure 5-6

COMPARISON BETWEEN

SPHERICAL, GEOGRAPHIC AND ELLIPSOIDAL COORDINATES

	Spherical	Geographic	Ellipsoidal
Illustration	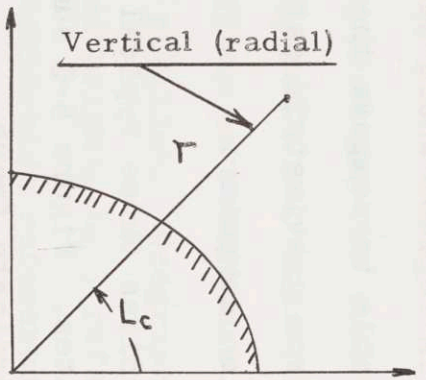	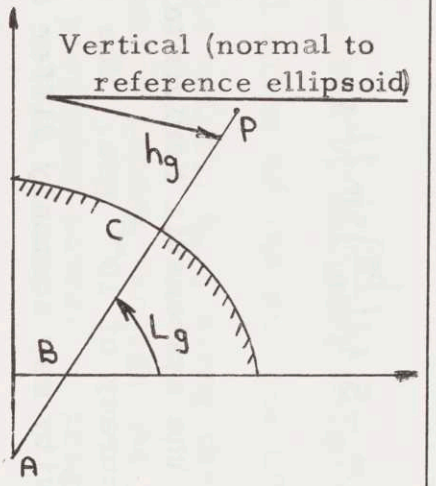	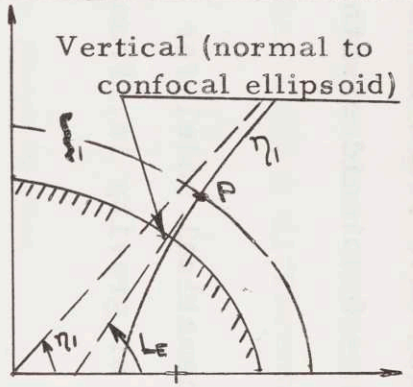
Transformation Equations	$y_1 = r \cos L_c \cos\lambda$ $y_2 = r \cos L_c \sin\lambda$ $y_3 = r \sin L_c$	$y_1 = (\rho_p + h_g) \cos L_g \cos\lambda$ $y_2 = (\rho_p + h_g) \cos L_g \sin\lambda$ $y_3 = [h_g + \rho_m(1-\epsilon^2 \sin^2 L_g)] \sin L_g$	$y_1 = c \cosh\xi \cos\eta \cos\lambda$ $y_2 = c \cosh\xi \cos\eta \sin\lambda$ $y_3 = c \sinh\xi \cos\eta$

Covariant Elements of Metric Tensor	$\begin{bmatrix} r^2\cos^2 L_c & 0 & 0 \\ 0 & r^2 & 0 \\ 0 & 0 & 1 \end{bmatrix}$	$\begin{bmatrix} (\rho_p+h_g)^2\cos^2 L_g & 0 & 0 \\ 0 & (\rho_m+h_g)^2 & 0 \\ 0 & 0 & 1 \end{bmatrix}$	$c^2\begin{bmatrix} \cosh^2\xi\cos^2\eta & 0 & 0 \\ 0 & \cosh^2\xi-\cos^2\eta & 0 \\ 0 & 0 & \cosh^2\xi-\cos^2\eta \end{bmatrix}$
Systematic Horizontal Component of Gravitation. cm./sec.^{2} $\pm 5\times10^{-6}$ gee	$G'_{L_c} = -1.591\left(\frac{a}{r}\right)^4 \sin 2L_c$ $g'_{L_c} = G'_{L_c} - \frac{\omega_{IE}^2 r}{2}\sin 2L_c$ $g'_{L_c}\big]_{h=0} = -3.299\sin 2L_c$ cm./sec.^{2}	$G'_{L_g} = 1.71\sin 2L_g\left(1-3.72\frac{h_g}{a}\right)$ cm./sec.^{2} $h_g<40$ mi. $g'_{L_g} = -5.44\frac{h_g}{a}\sin 2L_g$ cm./sec.^{2} $h_g<40$ mi.	$G'_\eta = \frac{37650\sin 2\eta}{\sinh^4\xi}$ cm./sec.^{2} $g'_\eta = G'_\eta - \frac{\omega_{IE}^2 C\cosh^2\xi\sin 2\eta}{2(\cosh^2\xi-\cos^2\eta)^{1/2}}$
Gyro Drives East	$-\dot{L}_c$	$-\dot{L}_g$	$\frac{-\dot\eta\sinh 2\xi + \dot\xi\sin 2\eta}{2(\cosh^2\xi-\cos^2\eta)}$
North	$(\omega_{IE}+\dot\lambda)\cos L_c$	$(\omega_{IE}+\dot\lambda)\cos L_g$	$(\omega_{IE}+\dot\lambda)\frac{\sinh\xi\cos\eta}{(\cosh^2\xi-\cos^2\eta)^{1/2}}$
Azimuth	$(\omega_{IE}+\dot\lambda)\sin L_c$	$(\omega_{IE}+\dot\lambda)\sin L_g$	$(\omega_{IE}+\dot\lambda)\frac{\cosh\xi\sin\eta}{(\cosh^2\xi-\cos^2\eta)^{1/2}}$

navigation since the exact shape of the planet is no longer of interest. A vertical line in this frame has a direction along the radius vector to the mass center of the Earth (or to the center of the reference ellipsoid). The geocentric coordinates, λ_c , L_c and r, are merely the spherical coordinates of the point in question in the Earth-fixed, Cartesian coordinate frame, y_i . Equation (D-4) gives the covariant elements of the metric tensor of this coordinate frame.

At orbital distances, where non-gravitational forces are negligible, the horizontal inertial positions may be calculated by integrating the computed gravitational field. Unless drag forces or gravitational gradients can be detected, accelerometers aboard the vehicle measure nothing. Since an error in the computation of gravity causes an unbounded position error, it is especially important that $\overline{G}$ be calculated accurately enough so no appreciable systematic error exists.

The systematic horizontal components of $\overline{G}$ and $\overline{g}$ are:

$$G_1' = 0$$
$$G_2' = -1.591\left(\frac{a}{r}\right)^4 \sin 2L_c \quad \text{cm./sec.}^2 \tag{2-30}$$

$$g'_{1(h=0)} = 0$$
$$g'_{2(h=0)} = -3.30 \sin 2L_c \quad \text{cm./sec.}^2 \tag{2-33}$$

The accuracy of calculation is limited by anomalies.

Section 5.E. uses spherical coordinates to mechanize an inertial navigation system for a ship. Figure 5-6 summarizes the navigational properties of this frame.

5.D.4. CONFOCAL ELLIPSOIDAL COORDINATES.

If the ellipsoidal shape of the Earth is important while navigating over an altitude range of several thousand miles, a coordinate frame is suggested consisting of ellipsoids of rotation which are confocal to the reference ellipsoid. The resulting confocal ellipsoidal coordinates are discussed in Appendix C and D.5. A vertical line in ellipsoidal coordinates is parallel to the normal to that ellipsoid which passes through the point in question. The covariant elements of the metric tensor of this coordinate frame are shown in Equation (D-16).

These coordinates are convenient since the reference ellipsoid is the surface defined when the elliptic variable, ξ , takes on some value, ξ_o . Furthermore, when $\xi \longrightarrow \infty$ at large distances, these coordinates become spherical.

Equation (2-49) shows that the systematic horizontal component of gravitation is:

$$G_1' = 0$$

$$G_2' = 37650 \frac{\sin 2\eta}{\sinh^4 \xi} \quad \text{cm./sec.}^2 \qquad (2\text{-}49)$$

within 2 x 10^{-5} gee.

Because of the complexity of the ellipsoidal coordinates, they are suggested only in applications such as launching a twenty-four hour satellite where navigation is necessary over a wide altitude range while still referring precisely to points on an ellipsoidal Earth. Figure 5-6 summarizes important navigational properties of this frame.

5.D.5. LOCAL-LEVEL COORDINATE FRAMES.

The accelerometer platform is most often required to align with the unit vectors of a local-level coordinate frame. This procedure has the advantages:

A. the orientation of the accelerometers relative to $\overline{g}$ varies only slightly. Thus, the accelerometers can be better designed. This applies equally well to the inersors if they are mounted on the accelerometer platform.

B. a vertical accelerometer is unnecessary; the two horizontal channels are stable.

C. the attitude of the vehicle is readily derived from the isolation gimbal angles.

The direction of the vertical is either geographic, ellipsoidal or spherical, as discussed in the preceding three sections. The platform's azimuth orientation may be:

A. north-pole seeking as in Sections 5.E. and 5.F.

B. false-pole seeking, when navigating near the Earth's poles. A false pole is selected, perhaps on the equator at the Greenwich meridian, and the platform is driven in azimuth so the input axis of one accelerometer always points toward it in the same manner that the north accelerometer points toward the north pole in the conventional north-seeking system. The false-pole mechanization is simplest in spherical coordinates, with ellipticity corrections for the radius and horizontal gravity. A simplified false-pole coordinate frame is discussed in Reference 45.

C. great-circle seeking, in which case the azimuth gyro is driven to align the input axis of one accelerometer with the direction along a desired great-circle course.

D. free-azimuth, in which case the vertical component of $\overline{\omega}_{IA}$ is zero; the azimuth gyro is not torqued. This azimuth mechanization retains the attitude advantages of the local-level systems and yet does not sacrifice accuracy because of errors in the azimuth gyro torquer.

In order to remain locally level, the gyros on the platform must be driven with the components along their input axes of the desired inertial angular velocity. These gyro drive signals are derived from rates of change of the navigation coordinates as in Section 4.G. This procedure

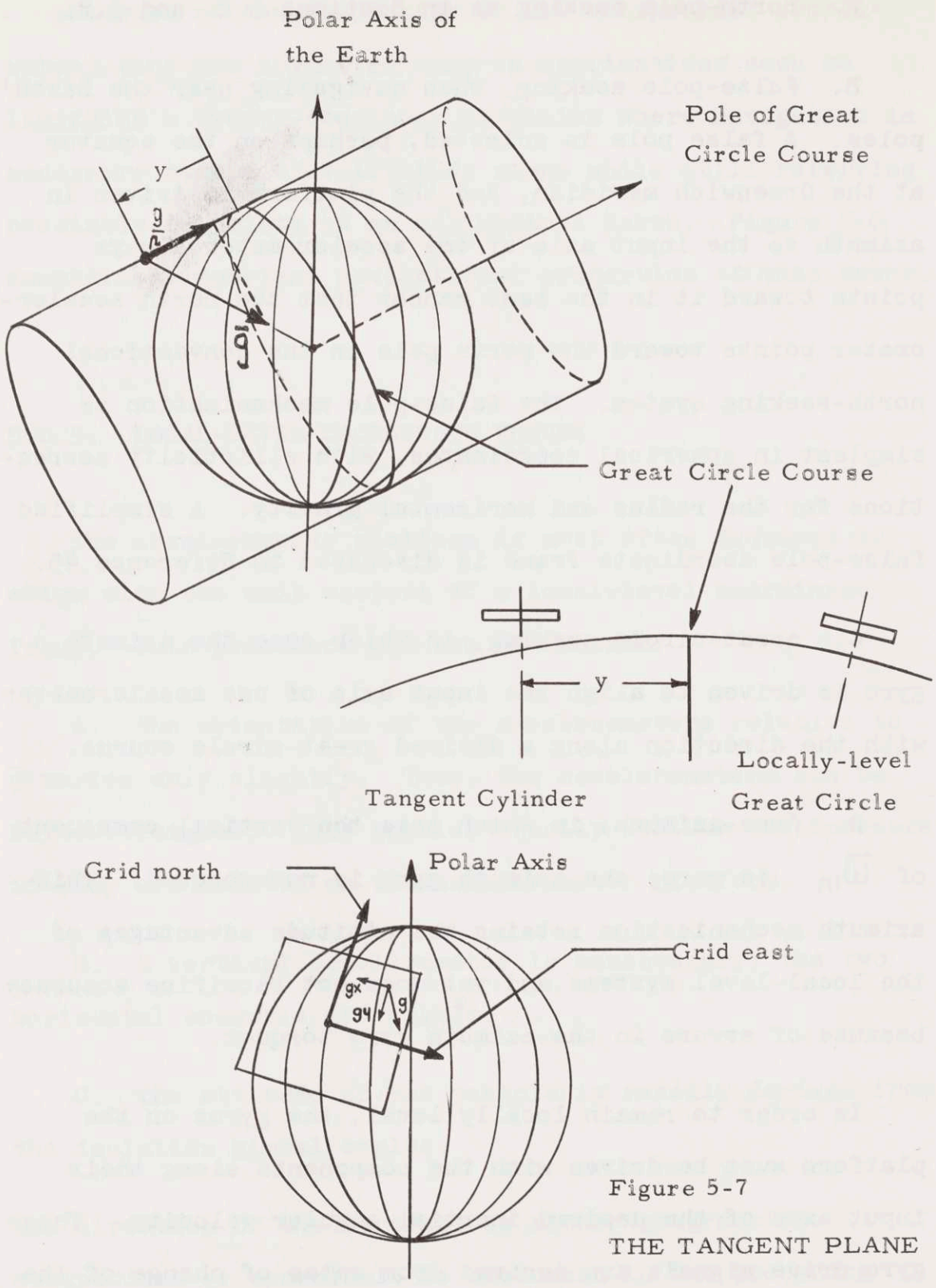

Figure 5-7

THE TANGENT PLANE AND TANGENT CYLINDER MECHANIZATIONS.

is known as Schuler tuning since to first order, it results in 84 minute oscillations in the two level channels, as shown in Section 5.E.3. No actual tuning occurs; the oscillations merely result from the mechanization of the navigation equations.

Azimuth errors must increase unbounded with time since gyro drift and torquer errors are not self-correcting. Thus though the level platform provides a heading reference, the reference deteriorates with time unless externally corrected.

5.D.6. NON-LEVEL SYSTEMS.

A. inertially-non-rotating coordinate frame in which the inersors hold the accelerometer platform nominally non-rotating in inertial space. Then the accelerometers measure $\ddot{x}_i - {}^{*}G_i$, which lend themselves readily to computation of the x_i. Since all the ${}^{*}G_i$ components contain a vertical component of gravitation, this mechanization is generally unstable. The mechanization is useful for short times of operation in which case the y_i or z^i can be calculated by means of a coordinate transformation. However, all three components of $\overline{G}$ must be calculated in the Earth-centered, Cartesian frame. On the contrary, only the horizontal components of $\overline{g}$ are needed in a local-level mechanization. These are usually regarded as zero.

B. cylinder, tangent to the Earth. The locally-level great-circle mechanization discussed in 5.D.5.C. places the input axis of the range accelerometer parallel to the plane of the great circle at all times. When deviating off the great-circle, that platform remains level, rotating around the range accelerometer's input axis. In the tangent cylinder mechanization, the input axis of the range accelerometer also remains parallel to the plane of the great-circle at all times but when the vehicle departs from the great-circle plane, the platform remains perpendicular to that plane instead of remaining locally level. Figure 5-7 shows this distinction clearly. The cross-track channel is biased by the amount of horizontal gravity perpendicular to the great circle. For small departures, y, from the great-circle, the cross-track horizontal component of gravity is roughly $-g\frac{y}{r_E}$.

C. plane, tangent to the Earth. For operation near a fixed base, the tangent cylinder can be unrolled into a tangent plane. When the vehicle departs from its base, its platform remains parallel to the level plane at the base. Any desired azimuth orientation can be used with the tangent plane mechanization. If the azimuth drive is simply $\omega_{IE}\sin L_{BASE}$ and does not change as the vehicle moves away from its base, the coordinate outputs can be expressed in a simple x-y rectangular grid which coincides

with the vehicle operator's maps. Gravity can be approximately computed as:

$$g_x = -g\frac{x}{r_E} \qquad g_y = -g\frac{y}{r_E}$$

D. inertial great-circle. This mechanization is suitable for orbital vehicles which fly on a nominal great-circle course in inertial space. A platform on board such a vehicle could be torqued to follow either an inertial cylinder, passing through the orbit or inertial, spherical coordinates. These are analagous to the use of a tangent cylinder or local-level, great-circle mechanization on the Earth.

E. body-mounted accelerometer platform which is rigidly mounted on the vehicle and participates in its comparatively violent angular motions. Inersors on the vehicle measure its orientation or angular velocity relative to the navigation coordinates so the accelerometer outputs can be transformed into these coordinates and integrated. Component limitations presently mitigate against the use of body-mounted systems for inertial grade applications, though they are widely used for autopilots. Reference Three discusses some of the pertinent problems.

F. map grid coordinates. Geodetic maps are often plotted in local x-y rectangular grids which distort the spheroid onto a plane. The extent of the maps is small

enough so the distortion is acceptably small (Section 3.H.). Since navigators often use such grids, it may sometimes be desirable for an inertial navigator to read-out in grid coordinates. The grid coordinates can either be calculated directly from the accelerometer outputs using suitable navigation equations which are mechanized in grid coordinates or they can be calculated from geodetic latitude and longitude by means of a coordinate transformation.

5.D.7. APPLICATIONS.

The selection of a coordinate frame will depend on the application. Some examples are discussed in this section.

A. A ship, operating in moderate latitudes, should navigate in a geographic coordinate frame so the computed coordinates will be immediately familiar to the crew. Section 5.F. mechanizes such a system and shows that since the height of the ship above the reference ellipsoid probably does not exceed 300 feet, it is always negligible in the navigation equations.

B. A submarine, cruising in polar waters, would probably navigate in false-pole latitude and longitude coordinates. As a practical consideration, a conventional second mode of operation is necessary for lower latitudes.

C. An aircraft, which flies nominal great-circle missions, might navigate in tangent cylinder or local-level, great-circle coordinates.

D. The guidance system for a satellite-launching booster might be mechanized in the Earth-centered inertial coordinate frame, x_i , because the satellite orbit is defined in inertial space. In this case, the Earth is of interest only to furnish initial conditions and as the source of a gravitational field. For ease in initial alignment, the platform would be maintained locally-level prior to launching.

E. A short-range helicopter could probably use a tangent plane, grid coordinate system. The navigation system would then be relatively simple and would read-out in coordinates which correspond to the pilot's map.

5.D.8. COMPUTER OPTIMIZATION.

For each application, the system designer must select navigation and tracking coordinates and derive simplified navigation equations. This has been largely an art during the twelve year history of inertial navigation.

Clearly, certain coordinate frames require considerably less calculation than others, for any given application.

It is interesting to speculate whether the general navigation equations, Equations (4-38), could be used to optimize a navigation system with respect to minimum size or weight, subject to certain operating constraints such as desired accuracy and vehicle motion.

The optimization of the computer is simplified by recognizing that digital computers are in nearly universal use today. The number of computations to be performed per unit time is a direct criterion of the size and reliability of a digital computer.

Thus, the optimization problem may be phrased, "What choice of transformation equations:

$$y_i = y_i(z^j)$$

will result in a minimum number of computations per unit time, subject to certain constraints on the vehicle's motion and the desired accuracy?"

The solution of this variational problem is far from obvious. This writer suggests that future studies investigate the possibility of using Equations (4-38) to select optimum navigation coordinate frames (implicitly restricted to the case where the accelerometers align with the unit vectors of the navigation coordinate frame). It should not be surprising, however, if the selection of coordinate frames continues to be a matter of engineering judgment for a long time to come.

5.E. NAVIGATION ERRORS IN SPHERICAL COORDINATES.

5.E.1. INTRODUCTION.

In this section, spherical coordinates are used to illustrate the mechanization of an inertial navigation system. An ellipsoidal, rotating Earth and a realistic gravity field are assumed. However the vehicle is assumed to operate solely on the surface of the reference ellipsoid at a speed of less than twenty knots. The desired accuracy is one mile.

Let x_i be the Earth-centered, "inertially-non-rotating" coordinate frame discussed in Sections 4.E.2. and 5.C.2. whose x_3 axis lies along the geographic polar axis. In this frame, the reference ellipsoid rotates at a constant speed, ω_{IE}, about the x_3 axis to an accuracy of 5×10^{-5} deg./hr., limited by migration of the pole.

Let the spherical coordinates λ, L_c and r locate the vehicle in the planet-fixed Cartesian y_i frame where λ and L_c are the spherical longitude and latitude and r is the radius.

The accelerometer platform, on which the gyros are mounted, is always driven to be nominally perpendicular to the radius vector. Any azimuth mechanization could be used, for each of which the azimuth

gyro drive signals would be different. For this example, the platform is north-seeking in azimuth. Thus the platform nominally aligns with the spherical unit vectors, $\hat{\lambda}, \hat{L}_c$ and $\hat{r}$.

5.E.2. THE NAVIGATION EQUATIONS.

The navigation equations in spherical coordinates are given in Equations (4-44) and (4-45). Equation (4-44), for the longitude channel, is the integral form of the first of the differential equations, (4-45), as can be verified by direct differentiation.

An alternative derivation uses Coriolis Law to derive the components of acceleration in spherical coordinates in terms of the components in rectangular coordinates. If $\overline{\omega}_{IA}$ is the inertial angular velocity of the accelerometer platform:

$$\overline{\omega}_{IA} = -\dot{L}_c \hat{\lambda} + (\omega_{IE} + \dot{\lambda})(\hat{L}_c \cos L_c + \hat{n} \sin L_c)$$

Then:

$$\ddot{\overline{r}}\Big]_{X_i} = \ddot{r}\,\hat{r} + \overline{\omega}_{IA} \times (\overline{\omega}_{IA} \times \overline{r}) + 2\overline{\omega}_{IA} \times \dot{\overline{r}}\Big]_{Z^i} + \mathring{\overline{\omega}}_{IA}\Big]_{Z^i} \times \overline{r}$$

and:

$$\overline{f}_a = \ddot{\overline{r}}\Big]_{X_i} - \overline{G}$$

When expanded, these result in Equations (4-45). Equations (4-45) can be written in terms of gravity, $\bar{g}$, not gravitation, $\bar{G}$, by using the relation:

$$\bar{g} = \bar{G} - \bar{\omega}_{IE} \times (\bar{\omega}_{IE} \times \bar{r})$$

$$\begin{aligned} g_1 &= G_1 \\ g_2 &= G_2 - \omega_{IE}^2 \, r \sin L_c \cos L_c \\ g_3 &= G_3 + \omega_{IE}^2 \, r \cos^2 L_c \end{aligned} \tag{5-3}$$

Substituting into Equations (4-45):

$$\begin{aligned} f_{a_1} &= r\ddot{\lambda}\cos L_c - 2r\dot{L}_c(\omega_{IE}+\dot{\lambda}) \sin L_c + 2\dot{r}\,(\omega_{IE}+\dot{\lambda}) \cos L_c - {}^c g_1 \\ f_{a_2} &= r\,\ddot{L}_c + r\,\dot{\lambda}\,(2\omega_{IE}+\dot{\lambda}) \sin L_c \cos L_c + 2\dot{r}\dot{L}_c - {}^c g_2 \\ f_{a_3} &= \ddot{r} - r\,\dot{L}_c^2 - r\dot{\lambda}(2\omega_{IE}+\dot{\lambda}) \cos^2 L_c - {}^c g_3 \end{aligned} \tag{5-4}$$

These are the equations which relate λ and L_c to the f_{a_i}. Since the vehicle always operates on the reference ellipsoid, r is a known function of L_c, Equations (C-6) and (C-7). The platform drive signals, which are the components of $\bar{\omega}_{IA}$ along the navigation coordinate axes, are given in Equations (4-55).

If the geoid were an ellipsoid of rotation enclosing a homogenous fluid mass, $\bar{g}$ would be normal to it at its surface so the horizontal component of $\bar{g}$ along the ellipsoid would vanish. But Section 2. F. 8. shows that a gravity field based on such a model is not sufficiently

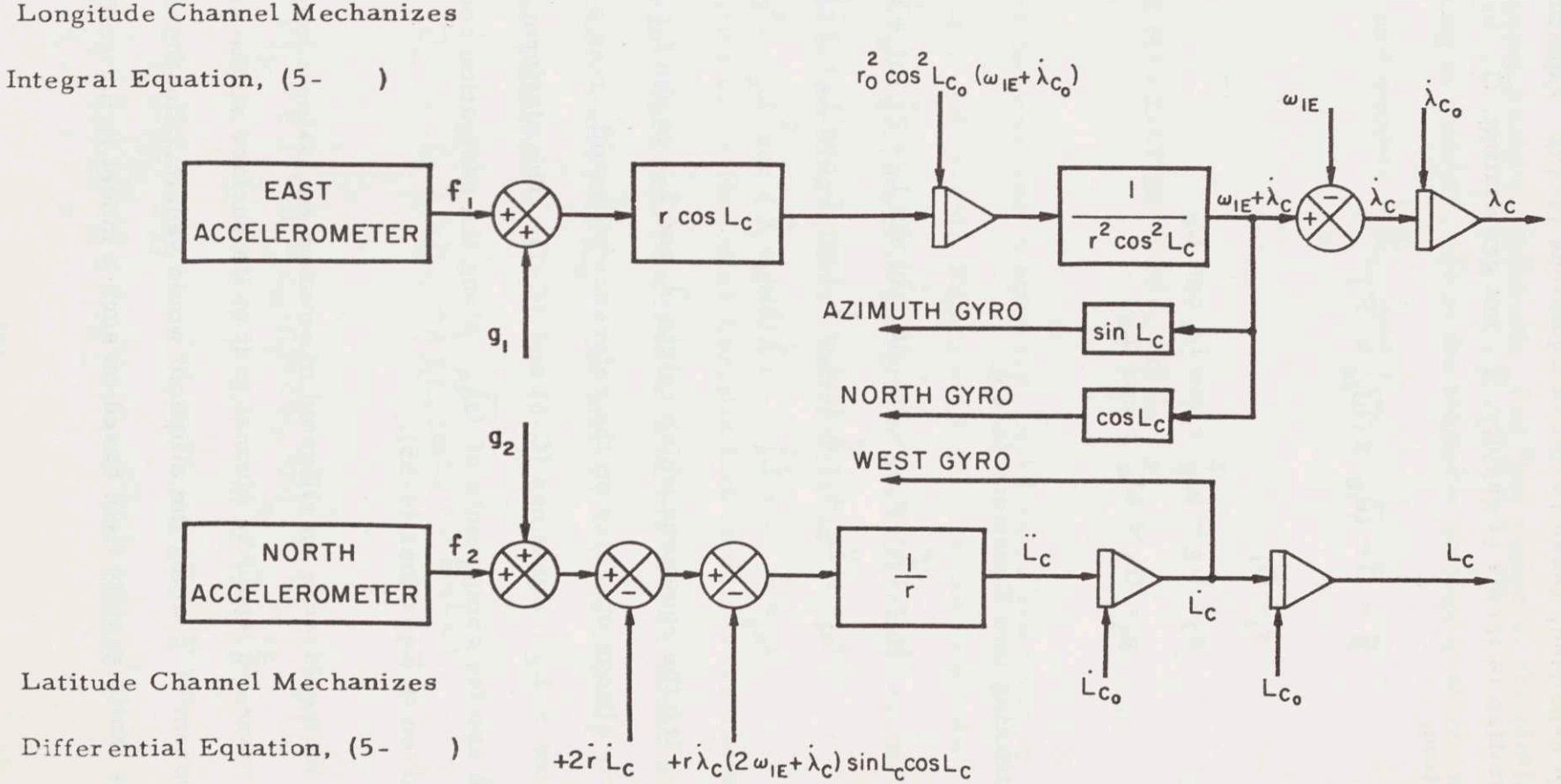

Figure 5-8

EXACT MECHANIZATION OF SPHERICAL EQUATIONS

accurate. The simplest valid model for the systematic portion of the Earth's gravitational field postulates an inhomogeneous Earth (whose density is a function of $\{\ \}$) enclosed by an ellipsoid of rotation. For such a model, Equation (2-33) gives the systematic horizontal components of $\bar{g}$ on the surface of the ellipsoid as:

$$g'_1\big]_{h=0} = 0$$

$$g'_2\big]_{h=0} = -f\frac{\gamma m_E}{a^2}\sin 2L_c$$

in spherical coordinates, to an accuracy of 2×10^{-5} gee. For the Earth, $\frac{\gamma m_E}{a^2} = 979.1$ cm./sec.^{2} and the flattening, f, is 1/297 for the International ellipsoid. In fact, the geoid undulates slightly, producing a deflection of the vertical which does not exceed ten seconds of arc in most places. g_3, the vertical component of gravity, has a negative magnitude and is a weak function of position on the ellipsoid. Hereafter, let $g_3 = -g$ in the level equations.

Figure 5-8 shows the mechanization of the two horizontal channels. The vertical channel is unstable, as shown in Section 5.E.3. The longitude channel illustrates the integral mechanization which Sections 5.F.1. and 5.F.4. show is less practical than the differential mechanization for slow-moving vehicles. If geographic coordinates are desired, they can be calculated either from the geocentric coordinates using the transformation:

$$L_g = L_c + f\sin 2L_c$$

or directly, using the geographic mechanization of Section 5.F.

5.E.3. ERROR PROPAGATION.

Suppose the accelerometer platform is misaligned relative to the $\hat{z}^i$ unit vectors by a small vector angle $\bar{\phi}$:

$$\bar{\phi} = \phi_1 \hat{\lambda} + \phi_2 \hat{L}_c + \phi_3 \hat{r} \qquad (5\text{-}5)$$

ϕ_1 is the misalignment about the east axis, ϕ_2 about north and ϕ_3 in azimuth. In the misaligned coordinate frame, the accelerometers measure $\bar{f}'_a$, which is related to $\bar{f}_a$ according to the transformation:

$$\begin{bmatrix} f'_{a_1} \\ f'_{a_2} \\ f'_{a_3} \end{bmatrix} = \begin{bmatrix} 1 & \phi_3 & -\phi_2 \\ -\phi_3 & 1 & \phi_1 \\ \phi_2 & -\phi_1 & 1 \end{bmatrix} \begin{bmatrix} f_{a_1} \\ f_{a_2} \\ f_{a_3} \end{bmatrix} + \begin{bmatrix} A_1 \\ A_2 \\ A_3 \end{bmatrix} \qquad (5\text{-}6)$$

where A_i are the instrumentation and accelerometer errors.

The compensations shown in Equations (5-4) are computed without knowing the amount of the misalignment. Thus, computed gravity, $\bar{g}'$, is added to the accelerometer outputs. Since the compensations are small, it does not matter to first order whether they involve the actual coordinates, λ , L_c and r , or the computed coordinates, λ' , L'_c and r'. The computed coordinates are related to the actual accelerometer outputs according to Equations (5-4), written entirely in primed (computed) quantities. Substituting Equations (5-6) into (5-4) with

primed variables and neglecting small quantities to first order:

$$\begin{aligned} r' \ddot{\lambda}' \cos L_c &= r \ddot{\lambda} \cos L_c - g\phi_2 + A_1 + g_1' - g_1 \\ r' \ddot{L}_c' &= r \ddot{L}_c + g\phi_1 + A_2 + g_2' - g_2 \\ \ddot{r}' &= \ddot{r} + A_3 + g - g' \end{aligned} \tag{5-7}$$

If $\dot{\sigma}_2$ and $\dot{\sigma}_1$ are the gyro drift rates about the latitude and longitude axes, the level axis errors are:

$$\begin{aligned} \dot{\lambda}' \cos L_c' + \dot{\sigma}_2 &= \dot{\lambda} \cos L_c + \dot{\phi}_2 \\ \dot{L}_c' - \dot{\sigma}_1 &= \dot{L}_c - \dot{\phi}_1 \end{aligned} \tag{5-8}$$

and substituting into Equations (5-7) with $r' \cos L_c' \approx r \cos L_c$:

$$\begin{aligned} \ddot{\phi}_1 + \frac{g}{r_E} \phi_1 &= \ddot{\sigma}_1 - \frac{A_2}{r_E} \\ \ddot{\phi}_2 + \frac{g}{r_E} \phi_2 &= \ddot{\sigma}_2 + \frac{A_1}{r_E} \end{aligned} \tag{5-9}$$

where $\omega_s^2 = \frac{g}{r_E}$ is the square of the Schuler frequency.

These are the first order error equations in terms of the misalignment angles. Equations (5-8) are the error equations in position. To first order, the two level axes exhibit undamped oscillations with Schuler period ω_s = 84.4 minutes, on the surface of the Earth. A more detailed analysis which suppresses the accelerometer outputs and closes a feedback loop through the compensations shows the presence of a long-period oscillation (Ref. 18). On a stationary vehicle, the period is the Foucault period, $2\pi / \omega_{IE} \sin L_c$.

INSTRUMENT ERROR	POSITION ERROR Δx	VERTICALITY ERROR ϕ
CONSTANT ACCELEROMETER BIAS, A_0	$\Delta x = \frac{A_0}{\omega_s^2}(1-\cos\omega_s t)$	$\phi = \frac{A_0}{g}(1-\cos\omega_s t)$
ACCELEROMETER BIAS DRIFT: $A = at$	$\Delta x = \frac{a}{\omega_s^2}(t-\frac{\sin\omega_s t}{\omega_s})$	$\phi = \frac{a}{g}(t-\frac{\sin\omega_s t}{\omega_s})$
CONSTANT GYRO DRIFT RATE: (LEVEL AXES): $\dot{\sigma}_0$	$\Delta x = r\dot{\sigma}_0(t-\frac{\sin\omega_s t}{\omega_s})$	$\phi = \frac{\dot{\sigma}_0}{\omega_s}\sin\omega_s t$ $\dot{\phi}_0 = \dot{\sigma}_0$
INITIAL LEVEL MISALIGNMENT, ϕ_0	$\Delta x = r\phi_0(1-\cos\omega_s t)$	$\phi = \phi_0\cos\omega_s t$
STOCHASTIC ERRORS IN THE GYROS AND ACCELEROMETERS DISCUSSED IN THE TEXT		

Figure 5-9

SYSTEM ERRORS FOR SOME SIMPLE INSTRUMENT ERRORS

Using Laplace transforms, the level axis errors are:

$$(s^2+\omega_s^2)\phi(s) = s\dot{\sigma}(s) - \frac{A(s)}{\Pi_E} \tag{5-10}$$

$$\Delta x(s) = \frac{g\phi(s)}{s^2} + \frac{A(s)}{s^2\Pi_E} = \frac{g\dot{\sigma}(s)}{s(s^2+\omega_s^2)} - \frac{A(s)}{s^2+\omega_s^2}$$

where $a\Delta L = a(L'_c - L_c)$ is typical of the position error, Δx. s is the Laplace transform operator. The last equation also represents the first order error propagation in the longitude channel with $\Delta x = \Pi' \cos L'_c - r \cos L_c$. Higher order error analyes usually require a digital computer simulation.

The first order system errors for particular instrument errors are shown in Figure 5-9. Stochastic errors are discussed in Sections 5.E.4.A. and 5.E.4.B.

The correct azimuth drive rate should be $(\omega_{IE} + \dot{\lambda})\sin L_c$. Because of gyro and computer errors, the input axis of the north accelerometer drifts off the geodetic meridian at a rate $\dot{\phi}_3$:

$$\dot{\phi}_3 = \dot{\sigma}_3 + \delta(\omega_{IE} + \dot{\lambda})\sin L_c \tag{5-11}$$

$$= \dot{\sigma}_3 + \omega_{IE}\cos L_c\,\delta L_c + (\delta\omega_{IE})\sin L_c + \delta(\dot{\lambda}\cos L_c)\tan L_c$$

to first order where the last term is $\approx \tan L_c \delta\phi_z$, using the terminology of Equation (5-9). Substituting the first order latitude and longitude

errors from Equation (5-10) into (5-11):

$$s\phi_3(s) = \dot{\sigma}_3(s) + \frac{s\dot{\sigma}_1(s) - \frac{A_2(s)}{R_E}}{s^2+\omega_s^2}\omega_{IE}\cos L_c + \frac{s^2\sigma_2(s) + sA_1(s)}{s^2+\omega_s^2}\frac{1}{R_E}\tan L_c \qquad (5\text{-}12)$$

Hence errors in all three gyros and in both level accelerometers cause azimuth errors to first order, in accordance with Equation (5-12). In the steady-state:

$$\phi_3 = \sigma_3 + \frac{\omega_{IE}\dot{\sigma}_1}{\omega_s^2}\cos L_c - \frac{\omega_{IE}A_2 t\cos L_c}{g} + \frac{A_2\tan L_c}{g} \qquad (5\text{-}13)$$

In this application, the fact that the vehicle is constrained to the ellipsoid allows r to be computed as a function of L_c. However, in other applications, the vehicle is free to move vertically and the mechanization becomes more complicated, as in Section 5. F.

The third of Equations (5-7) describes the error propagation in the vertical channel. Since:

$$g - g' = \frac{\gamma m_E}{r^2} - \frac{\gamma m_E}{r'^2} \simeq \frac{2\gamma m_E}{r^3}\Delta r$$

it follows that:

$$\Delta\ddot{r} - \frac{2\gamma m_E}{r^3}\Delta r = A_3 \qquad (5\text{-}14)$$

where $\Delta r = r' - r$. The vertical errors increase exponentially to first order. Altitude cannot be measured inertially for long periods of time

but the vertical channel might be used to provide short-term filtering for a non-inertial altitude measuring device.

5.E.4. NUMERICAL EXAMPLE.

A vehicle, assumed to be a ship, operates on the reference ellipsoid at velocities less than twenty knots. The desired position accuracy is one mile. The gyro drift rate is 0.005 deg./hr. (Refs. 36 and 41) and has known statistical properties discussed on page 263. The accelerometer threshold is 5×10^{-5} gee and drifts at 10^{-5} gee/hr. The statistical properties of the accelerometer are discussed on page 261.

The navigation system is designed in detail below. It bears no intentional resemblance to any other navigation system, operation or contemplated.

5.E.4.A. ACCELEROMETER ERRORS.

A constant threshold of 5×10^{-5} gee causes a position error of:

$$\Delta x = \frac{A_0}{\omega_s^2}\left(1 - \cos\omega_s t\right)$$

$$= 0.173\ \left(1 - \cos\omega_s t\right) \quad \text{naut. mi.}$$

and a verticality error of:

$$\phi = \frac{A_o}{g}(1 - \cos \omega_s t)$$

$$= 10\ (1 - \cos \omega_s t) \qquad \text{sec. of arc.}$$

A bias drift of 10^{-5} gee/hr. causes a position error of:

$$\Delta\chi = 0.035\ (t - 0.224 \sin\omega_s t) \qquad \text{naut. mi.}$$

and a verticality error of:

$$\phi = 2.0\ (t - 0.224 \sin\omega_s t) \qquad \text{sec. of arc}$$

The necessarily small accelerations of the ship minimize the effect of non-linearity errors in the accelerometer on position and verticality.

Much of the accelerometer error is statistical. If the mean square accelerometer error is MS(A), with a bandwidth $\omega_N = 2\pi/\tau_N$, the power spectral density of A can be represented as:

$$\Phi_{AA}(s) = \frac{MS(A)}{\pi} \frac{\tau_N}{1 - \tau_N^2 s^2}$$

and the power spectral density of verticality error, $\Phi_{\phi\phi}(s)$, computed according to:

$$\Phi_{\phi\phi}(s) = \frac{1}{\Omega_E} \frac{\Phi_{AA}(s)}{(s^2 + 2\zeta\omega_s s + \omega_s^2)(s^2 - 2\zeta\omega_s s + \omega_s^2)} \qquad (5\text{-}15)$$

where damping has been added to the Schuler oscillation to produce a convergent mean square verticality error. The mean square verticality

error, MS(ϕ), can be numerically calculated from page 372 of Reference 232:

$$MS(\phi) = \int \Phi_{\phi\phi}(s)\,ds = \frac{\tau_N MS(A)}{2\zeta\Omega_E\omega_s^3} \frac{1+2\zeta\omega_s\tau_N}{1+2\zeta\omega_s\tau_N+\omega_s^2\tau_N^2} \qquad (5\text{-}16)$$

Assume that the noise bandwidth, ω_N, is ten radians per minute so $\omega_s\tau_N = 2\pi\frac{\omega_s}{\omega_N}$ is much less than unity. Then:

$$MS(\phi) = \frac{\pi}{\zeta}\,\frac{\omega_s}{\omega_N}\,\frac{MS(A)}{g^2}$$

Thus if $\zeta = 0.1$ and the RMS acceleration error is 2×10^{-5} gee:

$$RMS(\phi) = 2.0 \text{ sec. of arc}$$

The corresponding mean square position error is less than a thirtieth of a mile. Hence the accelerometer causes relatively small system errors.

The RMS position error caused by the omission of the horizontal component of gravity from the mechanization is evaluated analagously, to first order, as shown in Section 5.C.5.

5.E.4.B. GYRO ERRORS IN THE LEVEL AXES.

The effective gyro drift rate is composed of the RMS sum of the 0.005 deg./hr. drift caused by uncertainty torques and the apparent drift caused by torquer non-linearity. The latter is negligible about the east axis because of the slow torquing rate there, but is appreciable in the north channel. For example, a torquer error of five parts in 10^4 causes the near-Earth-rate north gyro drive to be in error by $5 \times 10^{-4} (\omega)_{IE}$ = 0.0075 deg./hr. Thus the net drift rates are 0.005 deg./hr. about the east axis and 0.0125 deg./hr. about the north axis. Strictly, the error probabilities in the two channels are different but for simplicity, assume an average drift rate of 0.008 deg./hr. in both channels.

A constant gyro drift rate of 0.008 deg./hr. causes position and verticality errors:

$$\Delta x = 0.48 \left(t - 0.224 \sin \omega_s t \right) \quad \text{naut. mi.}$$

$$\phi = 6.4 \sin \omega_s t \quad \text{sec. of arc}$$

If the ship must realign its platform periodically with a star-tracker, errors of about fifteen seconds of arc are assumed to result at each alignment. The errors resulting from initial level axis misalignment are:

$$\Delta x = 0.26 \left(1 - \cos \omega_s t \right) \quad \text{naut. mi.}$$

$$\phi = 15 \left(1 - \cos \omega_s t \right) \quad \text{sec. of arc}$$

The output of a well-constructed gyro consists almost entirely of noise since predictable errors have largely been eliminated. For statistical studies, the transfer function of the system can be simplified to:

$$\Delta x(s) = \frac{r_E \dot{\sigma}(s)}{s}$$

$$\phi(s) = \frac{s^2 \Delta x(s)}{g} = \frac{s\dot{\sigma}(s)}{\omega_s^2}$$

Then the mean square error after a long time of operation is:

$$MS(\Delta x) = r_E^2 \, t \int \phi_{\dot{\sigma}\dot{\sigma}}(\mu) \, d\mu$$

If the autocorrelation function for the gyro noise is assumed to be exponential with a correlation time, τ_c, of one minute:

$$\phi_{\dot{\sigma}\dot{\sigma}}(t) = MS(\dot{\sigma}) e^{\frac{-|t|}{\tau_c}}$$

Thus, if the RMS drift rate is 0.005 deg./hr.:

$$MS(\Delta x) = 2 r_E^2 \, t \, MS(\dot{\sigma}) \tau_c$$

$$RMS(\Delta x) = 0.05 \sqrt{t} \quad \text{naut. mi.} \qquad (5\text{-}17)$$

The RMS verticality error is correspondingly small. If the gyro is unbalanced or anisoelastic, it will drift in the presence of vibration or acceleration. Such erors are neglected in the relatively hospitable environment of a ship.

5.E.4.C. GYRO ERRORS IN THE AZIMUTH AXIS.

The azimuth angular error, ϕ_3, is composed of the initial misalignment, ϕ_{30}, the net azimuth drift rate = 0.008 deg./hr. (as on page 262) and the effects of coupling from the level axes, shown in Equation (5-13). The magnitudes of the terms in Equation (5-13) are:

$$\frac{\omega_{IE}\dot{\sigma}_1}{\omega_s^2}\cos L_c \approx 0.25 \text{ sec. of arc}$$

$$\frac{\omega_{IE}A_2}{g}\cos L_c \approx 8\times10^{-4} \text{ deg./hr.}$$

$$\frac{A_z \tan L_c}{g} < 20 \text{ sec. of arc}$$

Thus, ϕ_3 has the form:

$$\phi_3 = \phi_0 + 0.008t \qquad \text{degrees}$$

where ϕ_0 is the RMS sum of the initial misalignment, ϕ_{30} = 15 seconds of arc, and the 20 seconds of arc constant error resulting from level axis coupling.

If the vehicle moves at constant velocity, V_0, virtually no position error results, to first order, from a small azimuth drift, ϕ_3, since the computer continues to integrate the correct velocity components. However, to be conservative, it is assumed that the output of the velocity integrators are always correct. Thus, a cross-track error

of approximately:

$$\Delta x = \int V_0 \phi_3 \, dt$$

results. Substituting ϕ_3 :

$$\Delta x = 0.0014 t + 0.0014 t^2 \quad \text{naut. mi.}$$

The position error resulting from azimuth misalignment is small, to first order.

5.E.4.D. COMPUTER ERRORS.

Errors in the computation of the horizontal component of gravity produce the same system errors as do accelerometer errors. In longitude, the systematic horizontal component of $\bar{g}$ is zero. In latitude the systematic horizontal component of $\bar{g}$ is computed from Equation (2-33). Its maximum magnitude is 3×10^{-3} gee which must be calculated to an accuracy of 1%. Hence terms of order ϵ^4 are indeed negligible. Because of an unmapped deflection of the vertical at sea, an anomalous horizontal component of gravity as large as 5×10^{-5} gee may be encountered unknowingly. The resulting position and verticality error in the steady-state would be:

$$\Delta x = 0.173 \ (1 - \cos \omega_s t) \quad \text{naut. mi.}$$

$$= 10 \ (1 - \cos \omega_s t) \quad \text{sec. of arc}$$

If the statistical properties of the horizontal component of $\bar{g}$ were known, their dynamic effect on the system could be estimated. To an overall accuracy of one mile, the small horizontal components of $\bar{g}$ can barely be ignored.

The compensation terms in the navigation equations can be simplified as follows. They must be calculated to an accuracy of about 2×10^{-5} gee to preserve a system accuracy of one mile.

a. In the longitude channel, the term, $2r\dot{L}_c (\omega_{IE}+\dot{\lambda}) \sin L_c$ need only be calculated to 10%. To that accuracy, the term can be mechanized as $2a\dot{L}_c \omega_{IE} \sin L_c$. If the latitude range of operation is sufficiently small, $\sin L_c$ can be taken constant or linearized.

b. In the latitude channel, the term, $r \dot{\lambda} (2\omega_{IE}+\dot{\lambda}) \sin L_c \cos L_c$ can be represented as $a\dot{\lambda}\omega_{IE} \sin 2L_c$ which could be further simplified if the latitude range were sufficiently small.

c. In the latitude channel, the term $2 \dot{r} \dot{L}_c$ appears. Equation (C-6) gives the radius of the ellipsoid as a function of latitude. Thus:

$$\dot{r} = - \frac{a\epsilon^2}{2} \sin 2L_c \dot{L}_c + \ldots\ldots$$

and $2 \dot{r} \dot{L}_c \approx 1.1 \times 10^{-8}$ gee, which is negligible. This term need not be mechanized.

d. The longitude channel contains the term $2\dot{r}(\omega_{IE}+\dot{\lambda})\cos L_c$ whose maximum magnitude is approximately 5×10^{-7} gee. This term need not be mechanized.

e. In order to compute λ and L_c, it is necessary to divide the compensated accelerometer outputs by r cos L and r, respectively. Errors in the divisor always affect the position error since the compensation signals must be divided, even when the accelerometer output is zero.

The maximum magnitude of the compensations is about 5×10^{-4} gee which, if divided to an accuracy of 1%, results in a maximum position error of 0.08 nautical mile. If the ship accelerates to 20 knots in a short time compared to the Schuler period, and the divisor is calculated to 1%, the position error responds as if to an impulse of 20×10^{-2} knot in A(s). The resulting position error is:

$$x = 0.045 \sin\omega_s t \quad \text{naut. mi.}$$

Thus, from either viewpoint, r may be approximated as a constant.

An interesting simplification results in the longitude channel if it is recognized that the differential equation:

$$f_{a_1} = a\ddot{\lambda}\cos L_c - 2a\dot{L}_c(\omega_{IE}+\dot{\lambda})\sin L_c$$

is identical to the integral equation:

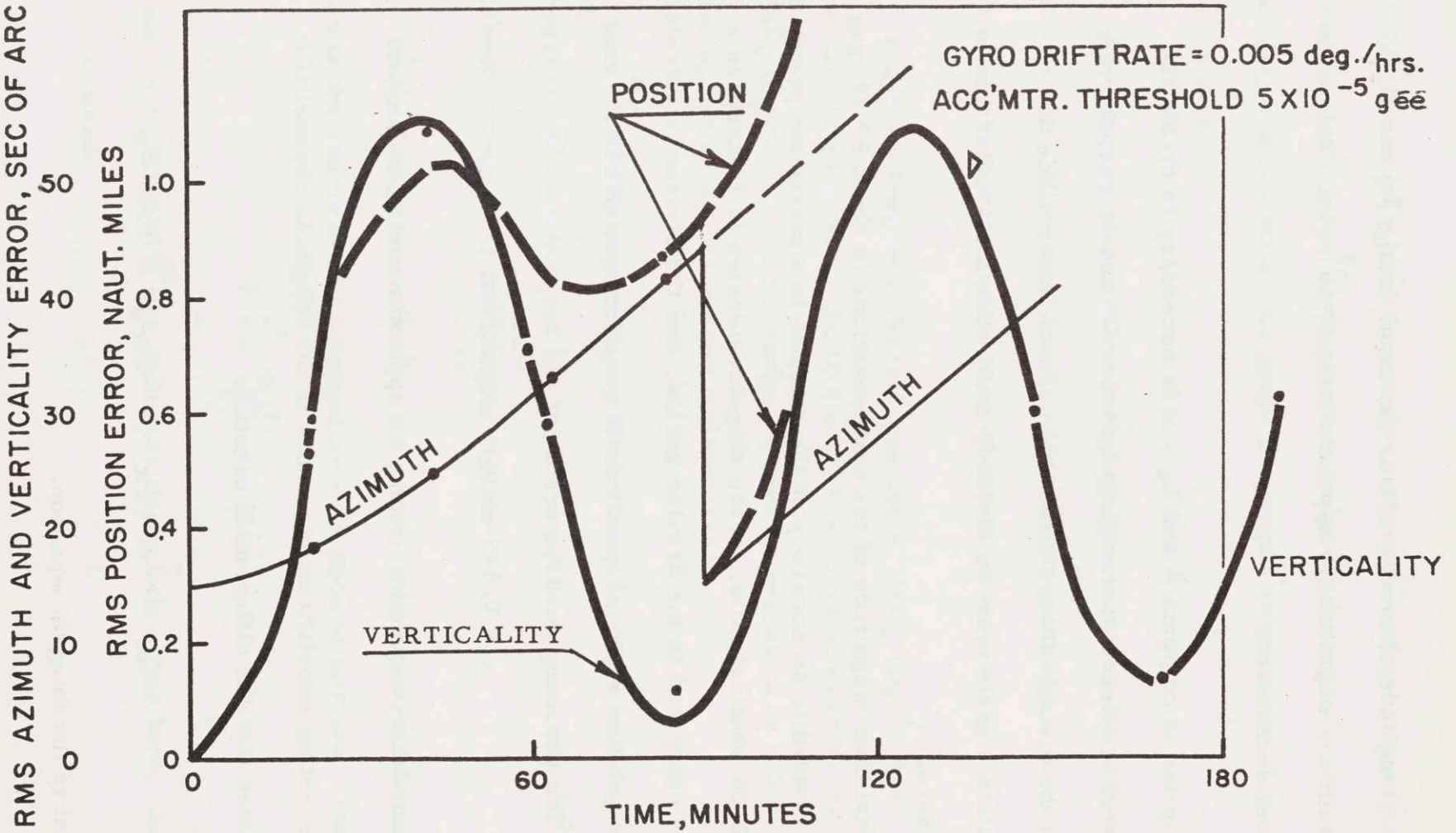

Figure 5-10 RMS ERROR PROPAGATION IN HYPOTHETICAL INERTIAL NAVIGATION SYSTEM

$$\dot{\lambda} = -\omega_{IE} + \frac{1}{r\cos^2 L_c}\int (f_{a_1} + g_1)\cos L_c \, dt$$

with constant r. As explained in Section 5. F. 1., the integral mechanization is not suitable for low-speed vehicles, where $\dot{\lambda} << \omega_{IE}$. For improved calibration, a may be replaced by the mean radius of curvature of the ellipsoid in the region of operation.

The RMS system error for a large number of missions is computed from the RMS sum of the individual errors. The total error at any time is assumed to be the RMS sum of the per-channel errors. Figure 5-10 shows the RMS position, velocity and azimuth errors for this hypothetical example. Clearly the system must be realigned approximately every hour and a half.

5. F. NAVIGATION ERRORS IN GEOGRAPHIC COORDINATES.

5. F. 1. THE NAVIGATION EQUATIONS.

The previous section mechanizes an inertial navigator in spherical coordinates in which a systematic horizontal component of $\bar{g}$ appears in the latitude channel. A mathematical model of $\bar{g}$ is used to compute

this horizontal component of gravity which, in turn, compensates the latitude channel and forces the platform to align with the radius vector to the center of the reference ellipsoid, within geodetic limitations.

Equations (4-46) and (4-47) show the accelerometer outputs when the accelerometer platform aligns with the unit vectors of the geographic coordinate frame. Equation (4-46) gives the integral form of the longitude mechanization:

$$\dot{\lambda}_g = -\omega_{IP} + \frac{1}{(\rho_p+h_g)^2\cos^2 L_g}\int (f_{a_1}+g_1)(\rho_p+h_g)\cos L_g \, dt \qquad (4\text{-}46)$$

For low-speed vehicles, the differential equation is probably more suitable than the integral equation since the latter computes $\omega_{IP}+\dot{\lambda}$ directly and then subtracts ω_{IP} to calculate the small $\dot{\lambda}$. Thus, a small fractional error in ω_{IP} would result in a large fractional error in calculating $\dot{\lambda}$. The integral mechanization requires an accurate multiplication and division; the differential equation requires an accurate division and several relatively inexact calculations of compensations. For high-speed vehicles, the integral equation is ideally suited to digital computation.

Near the Earth, it is preferable to mechanize in terms of $\overline{g}$, not $\overline{G}$ since the geographic horizontal component of $\overline{g}$ on the ellipsoid is nominally zero:

$$\bar{g} = \bar{G} - \bar{\omega}_{IE} \times (\bar{\omega}_{IE} \times \bar{r})$$

$$\begin{aligned} g_1 &= G_1 \\ g_2 &= G_2 - (\rho_P + h_g)\omega_{IE}^2 \sin L_g \cos L_g \\ g_3 &= G_3 + (\rho_P + h_g)\omega_{IE}^2 \cos^2 L_g \end{aligned} \tag{5-18}$$

Substituting into Equations (4-47):

$$f_{a_1} = (\rho_P + h_g)\ddot{\lambda}\cos L_g + 2\dot{h}_g(\omega_{IE} + \dot{\lambda})\cos L_g - 2(\omega_{IE} + \dot{\lambda})(\rho_m + h_g)\dot{L}_g \sin L_g - g_1$$

$$f_{a_2} = (\rho_m + h_g)\ddot{L}_g + (\rho_P + h_g)\dot{\lambda}(2\omega_{IE} + \dot{\lambda})\frac{\sin 2L_g}{2} + 2\dot{L}_g\dot{h}_g + \frac{3}{2}\frac{\epsilon^2 \sin 2L_g}{1 - \epsilon^2 \sin^2 L_g}\dot{L}_g^2 - g_2 \tag{5-19}$$

$$f_{a_3} = \ddot{h}_g - (\rho_P + h_g)\dot{\lambda}(2\omega_{IE} + \dot{\lambda})\cos^2 L_g - (\rho_m + h_g)\dot{L}_g^2 - g_3$$

The gyro drive signals are given by Equations (4-56).

Thus the complete equations can be mechanized in the manner of Section 5.E. The computed compensations and the horizontal components of gravity are added to the accelerometer outputs, the results divided by $(\rho_M + h_g)$ in latitude or $(\rho_P + h_g)\cos L_g$ in longitude and twice integrated. L_g, λ and their derivatives are fed back to compute the compensations, the gyro drive signals and gravity. The longitude channel can be

Figure 5-11

GEOGRAPHIC MECHANIZATION

Table One

Operating Range	Application		
	Ship	Mach One Fighter	Mach Three Transport
Altitude range above the Ellipsoid, feet	300	50,000	200,000
Maximum velocity, knots	20	600	1800
Maximum vertical velocity, feet/second	4.0 oscillating	400	100
Maximum latitude rate, $\dot{L}_g \approx \frac{V}{a}$. Units of Earth rate.	$0.022\omega_{IE}$	$0.67\omega_{IE}$	$2.0\omega_{IE}$
Maximum longitude rate, $\dot{\lambda}_g \approx \frac{V}{a\cos L} \approx 2\frac{V}{a}$ Units of Earth-rate.	$0.044\omega_{IE}$	$1.3\omega_{IE}$	$4.0\omega_{IE}$
Maximum $\lvert\omega_{IE} + \dot{\lambda}_g\rvert$ Units of Earth-rate	$1.04\omega_{IE}$	$2.3\omega_{IE}$	$5.0\omega_{IE}$
Maximum $\lvert 2\omega_{IE} + \dot{\lambda}_g\rvert$ Units of Earth-rate	$2.0\omega_{IE}$	$3.3\omega_{IE}$	$6.0\omega_{IE}$

mechanized using either the differential or integral form of the navigation equations. The vertical equation is unstable as before so the height above the reference ellipsoid must be found by non-inertial means.

5.F.2. SIMPLIFICATION OF THE MECHANIZATION.

In this section, typical navigation systems are mechanized in geographic coordinates for three different applications. One is a surface ship traveling at twenty knots. Another is a Mach One fighter aircraft whose altitude limit is 50,000 feet. The third is a supersonic Mach Three transport limited to 200,000 feet of altitude. For each system, the mechanization equations are suitably simplified and shown in Figures 5-12 and 5-13.

The operating parameters of the vehicles are summarized in Figure 5-11. For simplicity, the latitude range is supposed to be $\pm 60°$ so $|\cos L_g| > \frac{1}{2}$. The desired position accuracy is on the order of a mile.

The gyro drift rates and velocity computation accuracies are assumed to be 10^{-4} Earth-rate = 0.0015 deg./hr. (Refs. 36 and 41). The maximum permissible error in computing the compensations is 2×10^{-5} gee. The first order position errors caused by simple accelerometer and gyro errors are very nearly the same as those shown in Figure 5-9.

Figure 5-12

GEOGRAPHIC MECHANIZATION, LATITUDE CHANNEL

Table Two

Compensations	Application		
	Ship	Mach One	Mach Three
1. $(\rho_p + h_g)\,\dot{\lambda}_g(2\omega_{IE} + \dot{\lambda}_g)\,\frac{\sin 2L_g}{2}$			
a. Maximum value travelling east.	$0.04\omega_{IE}^2 a$	$2.14\omega_{IE}^2 a$	$12\omega_{IE}^2 a$
gee	1.5×10^{-4}	7.4×10^{-3}	4.1×10^{-2}
b. Fractional error for 2×10^{-5} gee	13%	1/370	1/2050
c. Mechanization of $(2\omega_{IE} + \dot{\lambda}_g)$ $(\rho_p + h_g)$	$2\omega_{IE}$ a_m	$(2\omega_{IE} + \dot{\lambda}_g)$ a_m	$h_g + a(1+f\sin^2 L_g)$
2. $\frac{3}{2}\frac{\rho_m}{}\frac{\epsilon^2 \sin 2L_g}{1-\epsilon^2\sin^2 L_g}\dot{L}_g^2$			
a. Maximum value $\approx 3af\dot{L}_g^2$ gee	1.7×10^{-8}	1.5×10^{-5}	1.4×10^{-4}
b. Fractional error for 2×10^{-5} gee	Omit	Omit	14.5 %
c. Mechanization	Omit	Omit	$\frac{a_m}{100}\dot{L}_g^2 \sin 2L_g$
3. $2\dot{L}_g\dot{h}_g$ added impulsively at take-off causes a max. position error: feet	0.8	300	11,000
Thus, the fractional error for 0.1 mile accuracy is:	Omit	Omit	5 %
4. The divisor, $\rho_m + h_g$			
a. Accuracy $\approx \frac{10^{-n}\omega_{IE}}{\dot{L}_{MAX}}$	5×10^{-3} (n = 4)	1.5×10^{-3} (n = 3)	2×10^{-4} (n = 3.5)
b. Mechanization	a_m	$h_g + a[1 + (\frac{3}{2}\sin^2 L_g - 1)\epsilon^2]$	

5. F. 2. A. THE LATITUDE CHANNEL.

The three compensation terms in the second of Equations (5-19) are simplified in Figure 5-12, for each of the three applications. ρ_P and ρ_M are constant to an accuracy of 0.3% and may be taken equal to a_m where a_m may be "tuned" for optimum performance. a_m may equal the semi-major axis of the reference ellipsoid or the mean radius of curvature at the latitude of operation. If the latitude range of operation is sufficiently limited, sin L_g and cos L_g can often be linearized or chosen as constants without serious system errors.

The term $\frac{3}{2}\rho_m \frac{\epsilon^2 \sin 2L_g}{1-\epsilon^2 \sin^2 L_g} \dot{L}_g^2$ is always so small that it need only be included for the Mach Three vehicle and even then, to an accuracy of only 15%. Hence switching logic in the computer could be used to program this term coarsely, in increments, as a function of heading angle and speed. The $2\dot{L}_g\dot{h}_g$ term might be similarly simplified or its integral could be calculated only during climb or descent maneuvers when it would be switched in as a function of barometric altitude only. This is especially feasible for the Mach One aircraft since it operates in a limited latitude range from any one base.

The necessary accuracy in computing the divisor, $\rho_M + h_g$, for the Mach One and Mach Three aircraft requires a digital computer.

Figure 5-13

GEOGRAPHIC MECHANIZATION, LONGITUDE CHANNEL

Table Three

Compensations	Application		
	Ship	Mach One	Mach Three
DIFFERENTIAL MECHANIZATION			
1. $2(\omega_{IE}+\dot{\lambda}_g)(\rho_m+h_g)\dot{L}_g \sin L_g$			
a. Maximum value on 30° heading. gee.	$0.04\omega_{IE}^2 a$ 1.4×10^{-4}	$2.0\omega_{IE}^2 a$ 8×10^{-3}	$12\omega_{IE}^2 a$ 4.1×10^{-2}
b. Fractional error for 2×10^{-5} gee accuracy	15%	1/390	1/2100
c. Mechanization of: $(\omega_{IE}+\dot{\lambda}_g)$ (ρ_m+h_g)	ω_{IE} a_m	$(\omega_{IE}+\dot{\lambda}_g)$ a_m $h_g + a[1+(\frac{3}{2}\sin^2 L_g - 1)\epsilon^2]$	$(\omega_{IE}+\dot{\lambda}_g)$
2. $2(\omega_{IE}+\dot{\lambda}_g)\dot{h}_g \cos L_g$ added impulsively causes a position error: feet	12	2400	14,000
Thus, the fractional error for 0.1 mile accuracy is:	Omit	25%	4.3 %
3. $(\rho_p + h_g)\cos L_g$, the divisor.			
a. Accuracy $\approx \frac{10^{-N}\omega_{IE}}{\dot{\lambda}_{max}}$	1/440 (n=4)	1/1330 (n=3)	10^{-4} (n=3.5)
b. Mechanization	$a[1 + f\sin^2 L_g]\cos L_g$	$[h_g + a(1+f\sin^2 L_g)]\cos L_g$	
INTEGRAL MECHANIZATION			
Accuracy of multiplier, $(\rho_p+h_g)\cos L_g$, and divisor, $(\rho_p+h_g)^2\cos^2 L_g$. $\approx \frac{10^{-N}\omega_{IE}}{\omega_{IE}+\dot{\lambda}_{max}}$	1/10,000 (n = 4)	1/23,000 (n = 3)	6×10^{-5} (n = 3.5)
Mechanization	not suitable	order ϵ^2, h_g	order ϵ^2, h_g^2

5.F.2.B. THE LONGITUDE CHANNEL.

The mechanization of the longitude differential equation is similar to the mechanization of the latitude equation. The same approximations are permissible and necessary to reduce the calculations to reasonable form. Figure 5-13 shows the detailed simplification of the mechanization.

The mechanization of the integral equation is conceptually simpler than that of the differential equation, especially in the case of the Mach Three aircraft. Instead of computing three complicated compensations to moderate accuracy and one divisor to high accuracy, only one divisor and one multiplier must be found to high accuracy. The major disadvantage of the integral formulation appears to result in the slow-speed vehicle when the direct calculation of $\omega_{IE}+\dot{\lambda}$, which is only slightly different than ω_{IE}, will result in a very inaccurate calculation of $\dot{\lambda}$ at slow speeds.

The integral computation, with digital computers, appears extremely attractive for the Mach Three transport. Notice that the initial condition on the velocity integrator is not merely $\dot{\lambda}_0$ but is $(\rho_{p_0}+h_{g_0})^2(\omega_{IE}+\dot{\lambda}_0)\cos^2 L_{g_0}$ T_h is requires the addition of a small, initial condition computer.

5.F.3. THE DYNAMIC MEASUREMENT OF GRAVITY.

If the vertical channel were used to measure altitude inertially, the system errors would increase unbounded. It can however be used to measure $|\bar{g}|$. Accurate measurements of $|\bar{g}|$ have been made on a very small fraction of the Earth's surface. Virtually no measurements have been made in the air or in unexplored regions and relatively few have been made at sea. Accurate gravimetric measurements should be in error by no more than 1/2 milligal (5×10^{-7} gee) but measurements as inaccurate as ten milligals (10^{-5} gee) are useful in gravimetric geodesy.

The output of a vertical accelerometer could be compensated according to the third of Equations (5-19) to compute g_3, the vertical component of gravity. The major difficulty in computing g_3 from that equation arises from the large vertical acceleration, $\ddot{h}_g$, of the vehicle. A sufficiently accurate measurement of $\ddot{h}_g$ is presently impossible so g must probably be obtained by averaging over a sampling interval, τ_L :

$$g_{3(AV.)} = \frac{1}{\tau_L} \int_0^{\tau_L} g_3(t)\, dt$$

$g_{3(AV.)}$ is calculated by integrating each term of Equation (5-19) separately. An integrating accelerometer measures $\int_0^{\tau_L} f_{a_3}\, dt$ directly. Geodesists rely upon pendulums and mass-spring devices which must be observed for many minutes to obtain one reading. Such

devices are essentially averaging accelerometers which measure

$$\frac{1}{\tau_L}\int_0^{\tau_L} f_{a_3}(t)\,dt$$

Thompson and Lacoste (Ref. 148) and Nettleton et al. (Ref. 131) are presently attempting airborne measurements of average gravity over thirty to sixty mile intervals, with relatively crude compensations.

The maximum accuracy in computing the compensations can be estimated as follows, using Figure 5-11. The two compensation terms are calculated to 5×10^{-6} gee.

The maximum value of $(\rho_P + h_g)(2\omega_{IE} + \dot{\lambda})\,\dot{\lambda}\,\cos^2 L_g$ on a Mach One aircraft is approximately 1.5×10^{-2} gee which must be calculated to 0.03%. This requires that altitude above the reference ellipsoid be known to 5000 feet and that ρ_P be calculated to order ϵ^2.

The maximum value of $(\rho_M + h_g)\,\dot{L}_g^2$ is approximately 1.5×10^{-3} gee which must be calculated to 0.3 %. Thus the term $(\rho_M + h_g) \approx a_m$ where a_m is some mean radius of curvature of the Earth in the vicinity of operation.

On a ship, the required accuracy of $(\rho_P + h_g)(2\omega_{IE}+\dot{\lambda})\,\dot{\lambda}\,\cos^2 L_g$ is 0.2% and the $(\rho_m + h_g)\,\dot{L}_g^2$ term can be omitted entirely.

Averaging does not significantly relax these accuracy requirements. Even if the accelerometer platform is misaligned as much as one minute of arc from the geographic vertical, the error in $|\bar{g}|$ is only five parts

in 10^{8}, which is totally negligible. Thus platform oscillations will not disturb the measurements.

5.F.4. SUMMARY.

The approximate equations which the navigation computer must solve are shown below. The necessary accuracy of computation of each term is shown:

A. SHIP.

$$f_{a_1} + g_1 = a\ddot{\lambda}(1+f\sin^2 L_g)\cos L_g - 2a\omega_{IE}\dot{L}_g \sin L_g$$
(0.25%, 15%)

$$f_{a_2} + g_2 = a\ddot{L}_g + a\dot{\lambda}\omega_{IE}\sin L_g$$
(13%)

(5-20)

B. MACH ONE AIRCRAFT.

$$f_{a_1} + g_1 = \left[h_g + a(1+f\sin^2 L_g)\right]\ddot{\lambda}\cos L_g + 2(\omega_{IE}+\dot{\lambda})(\dot{h}_g\cos L_g - a\dot{L}_g\sin L_g)$$
(0.075%, 25%, 0.26%)

$$f_{a_2} + g_2 = \left\{h_g + a\left[1+f(3\sin^2 L_g - 2)\right]\right\}\ddot{L}_g - a(2\omega_{IE}+\dot{\lambda})\dot{\lambda}\frac{\sin 2L_g}{2}$$
(0.15%, 0.27%)

(5-21)

or alternatively in longitude:

$$\dot{\lambda}_g = -\omega_{IE} + \frac{1-2f\sin^2 L_g - 2\frac{h_g}{a}}{a^2\cos^2 L_g}\int (f_{a_1}+g_1)\left[h_g + a(1+f\sin^2 L_g)\right]\cos L_g\, dt$$
(0.0044%)

C. MACH THREE AIRCRAFT.

$$f_{a_1} + g_1 = \underset{0.01\%}{\left[h_g + a(1+f\sin^2 L_g)\right]}\ddot{\lambda}\cos L_g + \underset{4.3\%}{2(\omega_{IE}+\dot{\lambda})\dot{h}_g}\cos L_g -$$

$$- 2(\omega_{IE}+\dot{\lambda})\dot{L}_g \sin L_g \underset{0.048\%}{\left\{h_g + a\left[1+f(3\sin^2 L_g - 2)\right]\right\}} \tag{5-22}$$

$$f_{a_2} + g_2 = \underset{0.02\%}{\left\{h_g + a\left[1+f(3\sin^2 L_g - 2)\right]\right\}}\ddot{L}_g + \underset{0.05\%}{(2\omega_{IE}+\dot{\lambda})\dot{\lambda}}\frac{\sin 2L_g}{2} \times$$

$$\times \left[h_g + a(1+f\sin^2 L_g)\right] + \underset{15\%}{\frac{a}{100}}\dot{L}_g^2 \sin 2L_g + \underset{5\%}{2\dot{L}_g \dot{h}_g}$$

or alternatively, Equation (4-47) can be mechanized in longitude with:

$$\rho_p + h_g = h_g + a(1+f\sin^2 L_g)$$

$$(\rho_p + h_g)^2 = h_g^2 + 2ah_g(1+f\sin^2 L_g) + a^2(1+2f\sin^2 L_g)$$

To an accuracy of 5×10^{-5} gee, below 200,000 feet, g_2 consists of a systematic portion (Equation 2-40) and an anomalous portion which should be stored in an on-board digital computer in regions where it exceeds 5×10^{-5} gee. At altitudes below 35 nautical miles, even the

systematic portion of horizontal gravity can barely be neglected. The systematic portion of g_l is zero but the anomalous portion of g_l should be programmed as a function of position in regions where it exceeds 5×10^{-5} gee.

The details of the first-order error propagation are identical to those of the spherical mechanization, Section 5.E.3. Uncoupled, undamped Schuler oscillations and a Foucault oscillation appear in all three channels.

Except in the case of the ship, the distinction between the prime and meridian radii of curvature must be maintained in at least some of the compensation terms and altitude must be included in the computations. The most accurate altitude measurements are required in the integral mechanization of the longitude equation for the Mach Three aircraft. Here since the $\rho_P + h_g$ terms must be mechanized to one part in 50,000 at maximum altitude, h_g must be measured to an accuracy of 600 feet. A serious limitation results because suitable altitude sensors may not be available. Since h_g is altitude above the ellipsoid, not above the terrain, a radar altimeter may measure it incorrectly. A barometric altimeter, which correctly measures potential height, will not function at extreme altitudes and velocities.

The integral mechanization of the longitude channel avoids the explicit calculation of Coriolis terms, as noted in Section 5.F.2.B., but instead

requires two accurate multiplications or divisions. If suitable sensors are available, a digital computer can readily achieve this accuracy.

The altitude rate terms can probably be simplified by computing their integrals in terms of altitude and adding the integrated compensation to the output of the velocity integrator.

All questionable simplifications should be investigated by simulation with a digital computer before being incorporated into the proposed system.

The horizontal component of gravity has been omitted from the mechanization. An error in computing g_1 or g_2 of 5×10^{-5} gee produces a position error whose maximum amplitude is 0.34 nautical mile. Thus for high accuracy, it is mandatory that large systematic horizontal components of gravity be inserted into the navigation equations. The deflection of the vertical in a geographic coordinate frame can be referred to the projected normal to the reference ellipsoid.

The navigator must recognize that in most areas of the world, the deflection of the vertical is unknown relative to any ellipsoid whatsoever. The deflection of the vertical at altitude can be obtained only by calculation from gravimetric data.

5.G. NAVIGATION ON OTHER PLANETS.

It cannot be long before the technological problems of reaching the Moon and planets will have been solved and vehicles will be navigating on their surfaces. This thesis has been written in such a manner that it is applicable to navigation on other heavenly bodies.

Having placed unmanned, and then manned vehicles on a planet, it is not sufficient to allow them merely to rest at their landing points; they must explore the surface. Such exploratory vehicles would roam the planet's surface establishing bases, taking samples and performing such experiments as the measurement of gravity and the study of magnetic fields and seismic disturbances. It would be unfortunate if the vehicle were unable to find its base, thus granting its possible occupants the privilege of being the first permanent human inhabitants of the planet.

The heavenly bodies most likely to be explored within the next thirty years are, in order, the Moon, Mars, Venus and the larger moons of Jupiter and Saturn. All these bodies are referred to as "planets" for simplicity.

Planetary navigation can be accomplished in many ways:

1. Visual observation of landmarks will serve to orient the human occupant or remote television viewer. This navigation technique is

decidedly limited in view of the unfamiliar terrain, possible clouds and dust storms and the probable necessity of navigating beneath the surface of a liquid on Venus.

2. Electronic beacons or transponders can be located on the surface in the same manner as Tacan, Loran and Shoran are used on the Earth. During the first phases of exploration, only homing beacons will probably be used. Later, Shoran- or Loran- type networks may be established.

Though electronic devices would probably constitute the primary navigation aids, few vehicles would be entrusted to exclusive dependence on one means alone because of the possibility of equipment failure. Furthermore, electronic beacons are subject to propagation disturbances, such have been identified on Jupiter, and to solar interference with transmission, which might be serious on Venus.

3. Taking their cue from Theseus, the very earliest vehicles may navigate simply by laying out a cable and following it back to their base.

4. Celestial observations can be used in the same manner as on the Earth, wherever and whenever visibility permits. Stars, the Sun and other planets would be observed but with new right ascension and declination coordinates to correspond to the planet's pole.

It is not feasible to control the exploring vehicle by direct observation from the Earth.

5. Magnetic azimuth measurements may be possible after the magnetic fields have been mapped. Early explorers certainly cannot rely upon them.

6. Natural and artificial satellites will undoubtedly serve the same useful purpose on other planets that Transit will on the Earth. A Transit satellite would be most useful on Venus where optical astronomic measurements may be impossible. Though Venus has no large natural moons which might perturb the Transit orbit significantly, the Sun's gradient at Venus is twice the Moon's gradient at the Earth.

7. Inertial and inertial-hybrid systems will undoubtedly be carried aboard any vehicle that ventures more than fifty miles from a base, to supplement information from electronic and celestial observations.

The navigation process on other planets is complicated by:

1. an initially unknown magnetic and gravity field on the planet.

2. an uncertain rotation rate and polar position of some of the planets. This is true chiefly of Venus and the moons of the major planets. On the major planets themselves, the angular velocity of the fluid surface appears to be a function of latitude and altitude.

3. cloud cover (Venus), dust storms (Mars), radio noise (Jupiter) and liquid surface (Venus, the major planets).

4. large eccentricity of a reference ellipsoid which closely approximates the geoid. This eccentricity is small except for Mars and the major planets. On these bodies, the flattening exceeds that of the Earth ($f \approx 1/300$) so the geographic mechanization equations become extremely complicated for high-speed vehicles.

5. large rotation rates of the major planets. This complicates the mechanization since compensation terms are large. The low rotation rate of Venus and the Moon may prevent gyrocompassing, even on stationary vehicles.

On the Moon where visibility is ideal (unless the dust cover is so thick that vehicles move about in perpetual clouds of stirred-up dust), a celestial-inertial system will provide supplementary navigation information to the network of electronic beacons.

On Mars, dust storms may rule out celestial measurements for periods of many hours. Therefore a celestial-Doppler-inertial navigation system may be needed to bound the position errors during periods of poor visibility.

On Venus, a Doppler-inertial system is needed, supplemented by an orbiting Transit satellite to insert initial position and possibly azimuth. The navigation equations on Venus are somewhat simpler than on the Earth because of a smaller flattening and probably lower

Figure 5-14

LIMITATIONS ON THE USE OF INERSORS

FOR TERRESTRIAL INERTIAL NAVIGATION

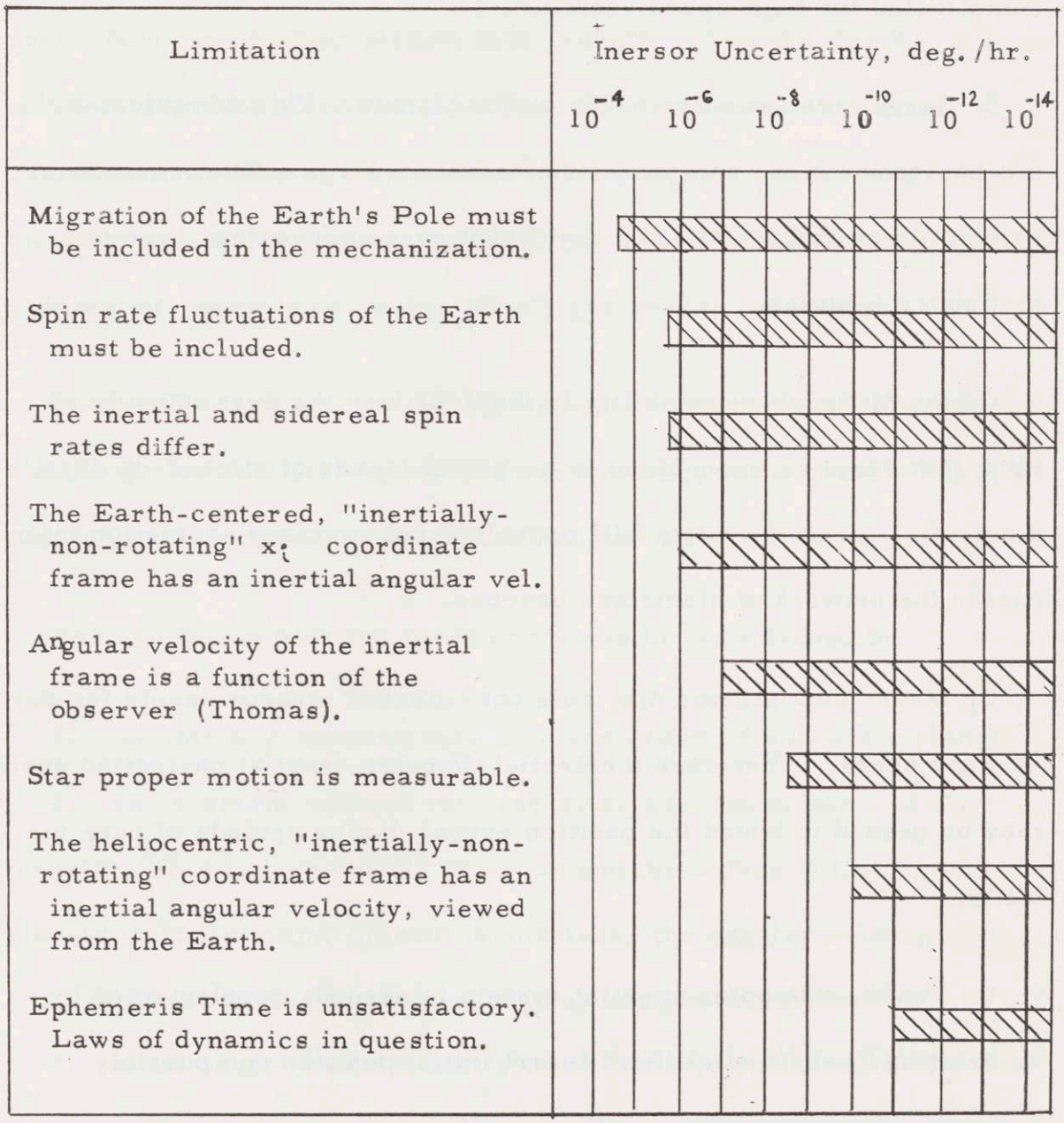

Figure 5-15

LIMITATIONS ON THE MEASUREMENT OF POSITION AND ACCELERATION FOR TERRESTRIAL INERTIAL NAVIGATION

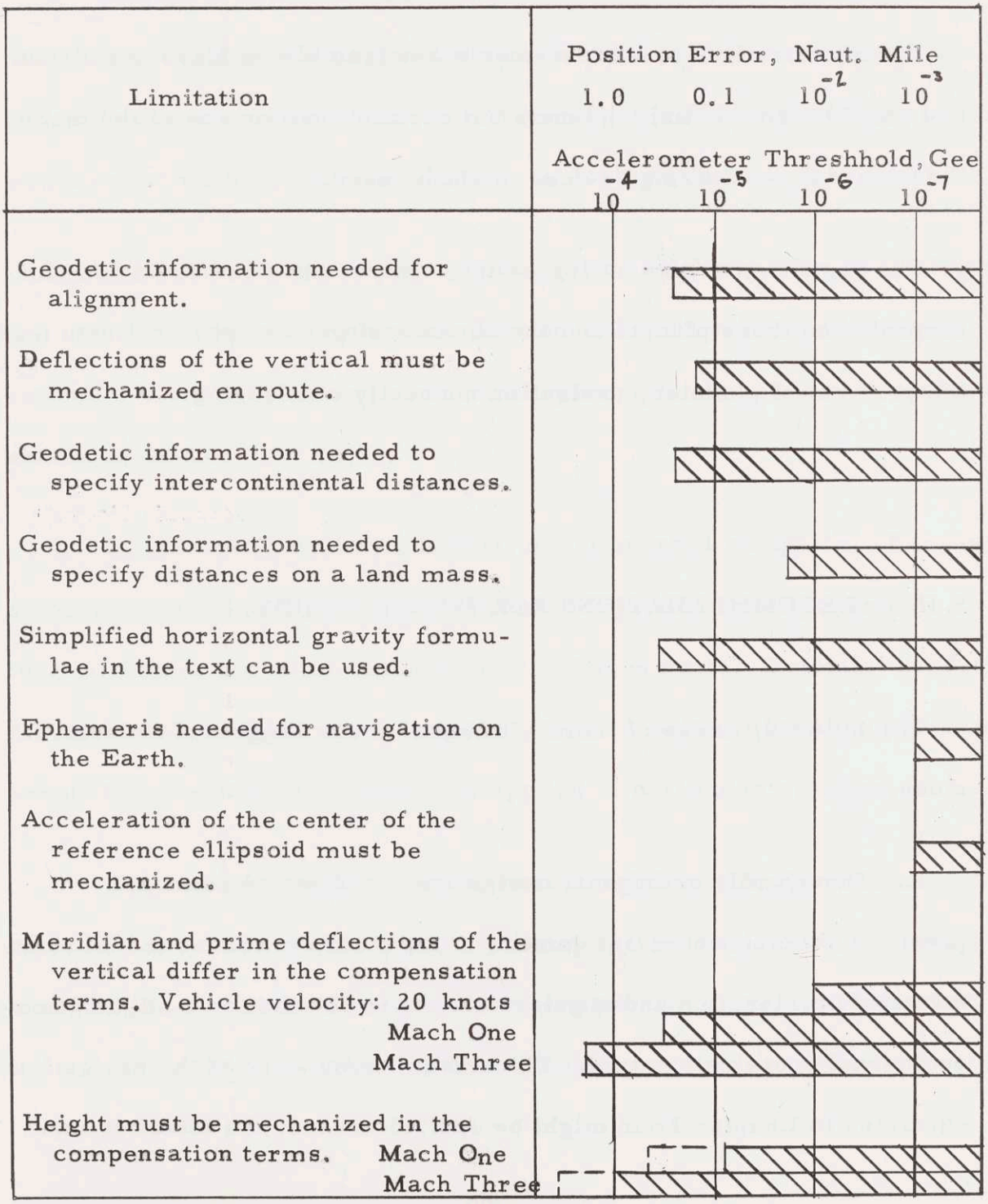

rotation rate. However the slow rotation rate makes the determination of azimuth initial conditions difficult - a problem common to all forms of navigation. The inertial navigator provides a stable platform for use on the possibly-liquid Venusian surface.

Barometric altitude measurements are feasible on Mars and Venus and possibly on the major planets but certainly not on any of the moons, though radar or ionizing devices might be used.

The hostile environment (pressure, temperature and radiation, for example) on these planets and the absence of precise physical data make the problem of planetary navigation unusually challenging.

5.H. RECOMMENDATIONS FOR FUTURE STUDY.

The following areas of inertial navigation are suggested for future study.

1. Though only orthogonal navigation coordinate frames are practical, component misalignment on the platform causes the measurements of acceleration and angular velocity to be made in a slightly non-orthogonal coordinate frame. The tensor formulation of the navigation equations in Chapter Four might be applied to study the effect of such

non-orthogonality on system errors. Mr. John Hovorka suggests that this approach could be extended to the study of flexure, "cocking," and misalignment within the instruments themselves.

2. Section 5.D.8. introduced the possibility of selecting an optimum navigation coordinate frame for any particular application. Though the author believes it unlikely, further study might lead to a procedure which would select such an optimum system, at least in certain special cases.

3. The problems connected with navigation on the surface of the Moon and other planets were outlined in Section 5.G. Though practical applications are still years away, low-level university studies of this problem should begin now.

4. Initial conditions are essential for an inertial navigator. Because of component limitations, the system errors degrade to such an extent, on long missions, that it is desirable to realign en route. Potential schemes for en route alignment and transfer of initial conditions between platforms should be investigated in detail and applied to particular systems.

5. The conventional first-order error analysis of Section 5.E.3. and 5.F. is usually used to rougly predict system performance, before studying the mechanization on a digital computer. Two questions arise:

How close do actual flight test results come to the error analysis predictions?

What general criteria should be used to judge the performance of inertial navigation systems?

Such a study would probably be hampered by the necessity of obtaining test data from manufacturers of navigation systems.

6. The design of a geodetic gyroscope, perhaps to detect the polar migration or spin rate fluctuations, may soon be practical. It could be made in any size, allowed to operate under the most rigidly controlled laboratory conditions and observed frequently to reduce statistical uncertainties.

7. The necessity of measuring the magnitude of gravity from a moving vehicle is already established. Though Section 5. F. 3. shows that instantaneous measurements are difficult because of the unmeasurable vertical acceleration of the vehicle, average gravity measurements are clearly practical, perhaps with an accelerometer-type instrument instead of a pendulum. This investigation should be pursued on an experimental basis.

8. With increasing interest in astronautics, a descriptive and critical bachelor's or master's thesis on the precise measurement of time is essential. Such a study would emphasize astronautical and navigational applications of time measurement. This writer believes that the United States Naval Observatory would provide information and guidance to such a study.

Appendix A

CHANGES IN THE VECTOR SPIN RATE OF THE EARTH

A.1. INTRODUCTION.

The spin axis of the Earth does not remain fixed relative to the Earth but describes a bounded, spiral-like motion of small amplitude about the "geographic pole." In addition, the magnitude of the spin rate varies slightly. This appendix discusses the magnitude and predictability of such changes. Their effect on navigation is discussed in Chapter Five.

A.2. THE DIRECTION OF THE SPIN AXIS RELATIVE TO THE EARTH.

Observatories throughout the world have been repeatedly and accurately measuring their astronomic latitudes for more than 75 years. In 1891 S.C. Chandler compared many such measurements made by several observatories over a period of years and concluded that the angle between

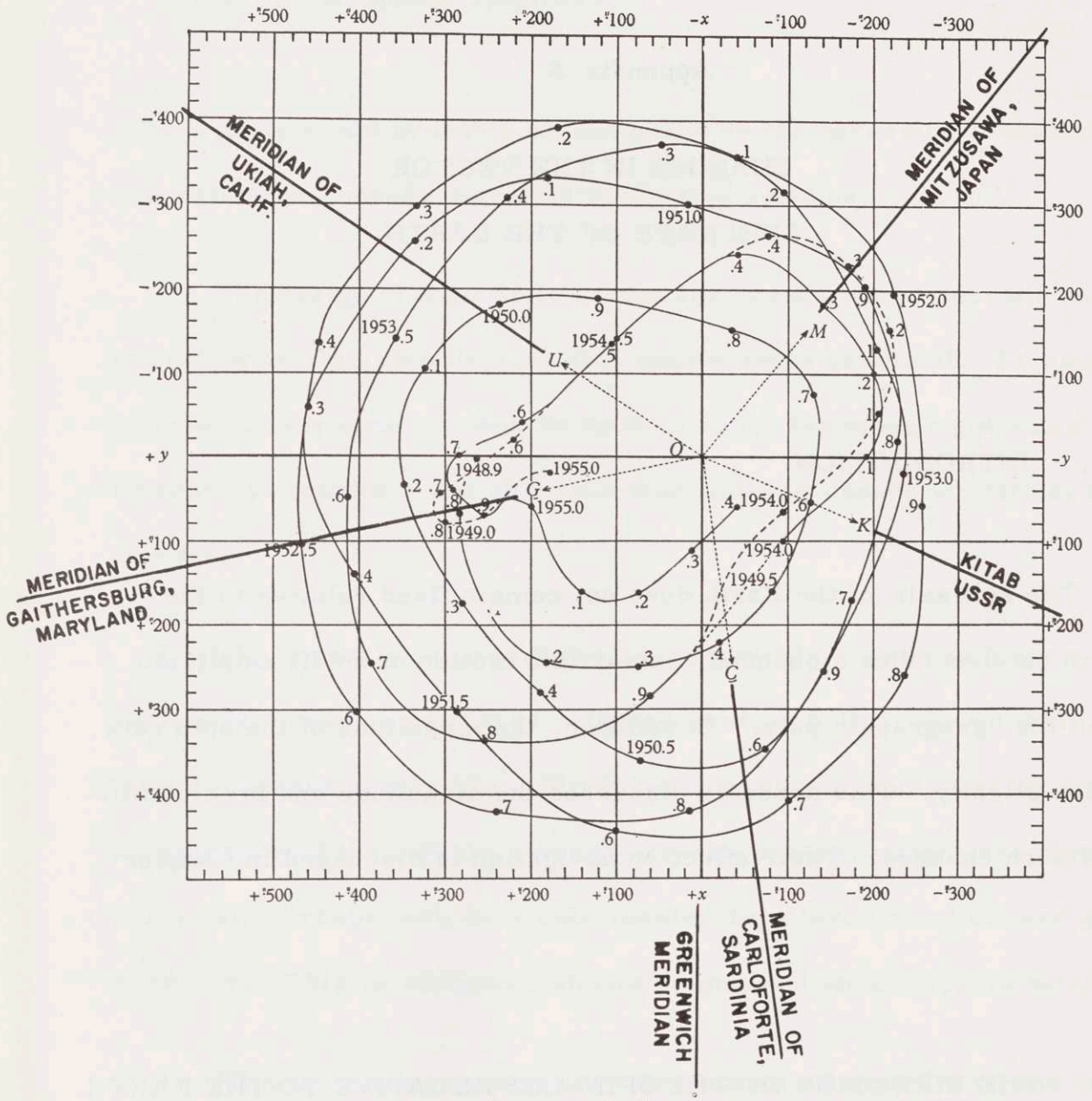

Figure A-1

POSITION OF THE EARTH'S POLE FROM 1949 TO 1955

Plan View Looking Down at North Pole

(from Reference 195, pg. 278)

the instantaneous spin axis and the local vertical at any point varies slightly with time (Ref. 121, pg. 212). Since measurements at different observatories correlated so well, the only reasonable explanation was that the spin axis migrates relative to the comparatively rigid mantle of the Earth.

Since the turn of the century, a considerable body of theory and observation has accumulated concerning the polar migration. Figure A-1 shows the position of the instantaneous north pole as a function of time from 1949 to 1955. The motion of the polar axis appears bounded, at least for short geologic times.

The mean position with respect to the mantle during the decade 1900 to 1910 is designated the "geographic polar axis" (Ref. 195, pg. 278). The question of whether large excursions of the pole, measured in thousands of miles, are possible in geologic time is not considered here since for many decades, the departure of the instantaneous polar axis from the geographic polar axis is not likely to increase drastically. Figure A-1 shows the departure of the instantaneous pole from the geographic pole, at the origin. The x axis measures the angular displacement of the pole along the astronomic meridian of Greenwich, toward Greenwich. The y axis measures the angular displacement of the instantaneous pole along the 90° W. astronomic meridian.

The migration of the pole relative to the Earth should not be confused with its precession and nutation in inertial space. Physically, the instantaneous spin axis precesses and nutates in inertial space while the geographic polar axis "wobbles" around it.

A network of six International Latitude Observatories was established in 1900 along the 39° 8' N. parallel of latitude at the locations shown in Figure A-2 (Ref. 200, pg. 117).

Figure A-2

INTERNATIONAL LATITUDE OBSERVATORIES

(Ref. 156, pgs. 434-448)

Site	L°	λ°
Carloforte, Sardinia	39°8'	-8°19'
Gaithersburg, Maryland	39°8'	77°12'
Jakarta, Indonesia	-6°16'	-106°53'
Kitab, Uzbek SSR (Soviet Union)	39°8'	-66°53'
Mizusawa, Japan	39°8'	-141°8'
Ukiah, California	39°8'	123°13'

Cincinnati, Ohio apparently was among the original six but seems to have been replaced by Jakarta. Each observatory measures its latitude every night that weather permits and forwards the results to the International Latitude Service of the International Astronomical Union (presently at L'Osservatorio Astronomico di Torino in Turin, Italy) which collates these data and publishes x and y coordinates of the polar axis. Inspection of these data indicate that the pole position can usually be predicted within ±0.2 second of arc, one year in advance.

The simplest mathematical model for studying the migration of the pole represents the Earth as a torque-free rigid body. The slow precession and nutation of the geographic polar axis in inertial space is caused largely by solar and lunar torques which act on the Earth. The most rapid appreciable period, caused by the inertial precession of the Moon's orbit, results in a nutation of 18.6 year period and nine seconds of arc amplitude. Thus, for intervals on the order of a year, the Earth is torque-free, as a crude approximation. Making the additional assumption that the Earth rotates rigidly and hence without damping, it executes a Poinsot motion (Refs. 219, pgs. 159-163 and 238, pgs. 418-429) in which the vector angular momentum, $\overline{H}$, is constant while the spin rate vector, $\overline{\omega}_{IE}$, and the axis of figure (which are not coincident, in this mathematical model) rotate about the angular momentum vector. If α, the angle between the spin axis and the axis of figure, is small, the

rate at which $\bar{\omega}_{IE}$ rotates about $\bar{H}$, as viewed by an Earth-bound observer, is (Ref. 238, pg. 428):

$$\omega_n = \frac{I_s - I_T}{I_s} \omega_{IE}$$

where:

I_s is the polar moment of inertia of the Earth

I_T is the transverse moment of inertia of the Earth

Astronomic measurements of the inertial precession rate and calculations of the solar torque infer that for the Earth (Ref. 87, pg. 337):

$$\frac{I_s - I_T}{I_s} = 0.0032724 \pm (7 \times 10^{-7})$$

so:

$$\omega_n = 0.0032724\, \omega_{IE} = \frac{\omega_{IE}}{305}$$

$$\tau_n = 305 \text{ days}$$

Thus on the assumption that the Earth rotates rigidly and without applied torques, a natural period of 305 days, called the Euler period, is expected. However, the observed natural period is 439 days. This discrepancy between the observed and predicted natural periods is caused by the inapplicability of the rigid, torque-free model. Clearly, unless the Earth has considerable rigidity, α must be zero because the Earth will adjust its axis of symmetry to follow a slowly changing spin axis. The axis of symmetry should adjust to the spin axis in approximately the time taken for elastic waves to traverse the Earth; about one hour. Inglis (Ref. 179) discusses elastic Earth models in detail.

Thus the actual angular motion of the Earth in space consists of an

inertial precession of the instantaneous spin axis while the Earth itself wobbles with respect to that axis.

The observed variation in latitude is analysed on a statistical basis as a response to numerous random impulses of torque (Ref. 213). Harmonic analysis has identified periods of (Ref. 121, pg. 220):

439 ± 5.8 mean solar days
one year
six months
irregular

The first is the Chandler period and is believed to be the "305 day" natural period as modified by elasticity. It is excited by those same changes in moment of inertia which excite the other harmonics and is damped by viscous and electromagnetic coupling between the mantle and the core (Ref. 179), by the viscous drag of the oceans and the atmosphere and by dissipation within the mantle (Ref. 88). Estimates of the damping ratio vary from 0.013 (Ref. 121, pg. 220) to 0.06 (Ref. 213). These have been calculated from the "relaxation times" (time for the envelope of the step response to decay to 1/e of its original value) shown in these references.

The annual and semi-annual periods are forced responses excited by ocean currents, atmospheric winds, snowfall and vegetation growth. Moving currents of mass such as ocean currents and winds have angular momentum which slightly changes the direction of the total angular

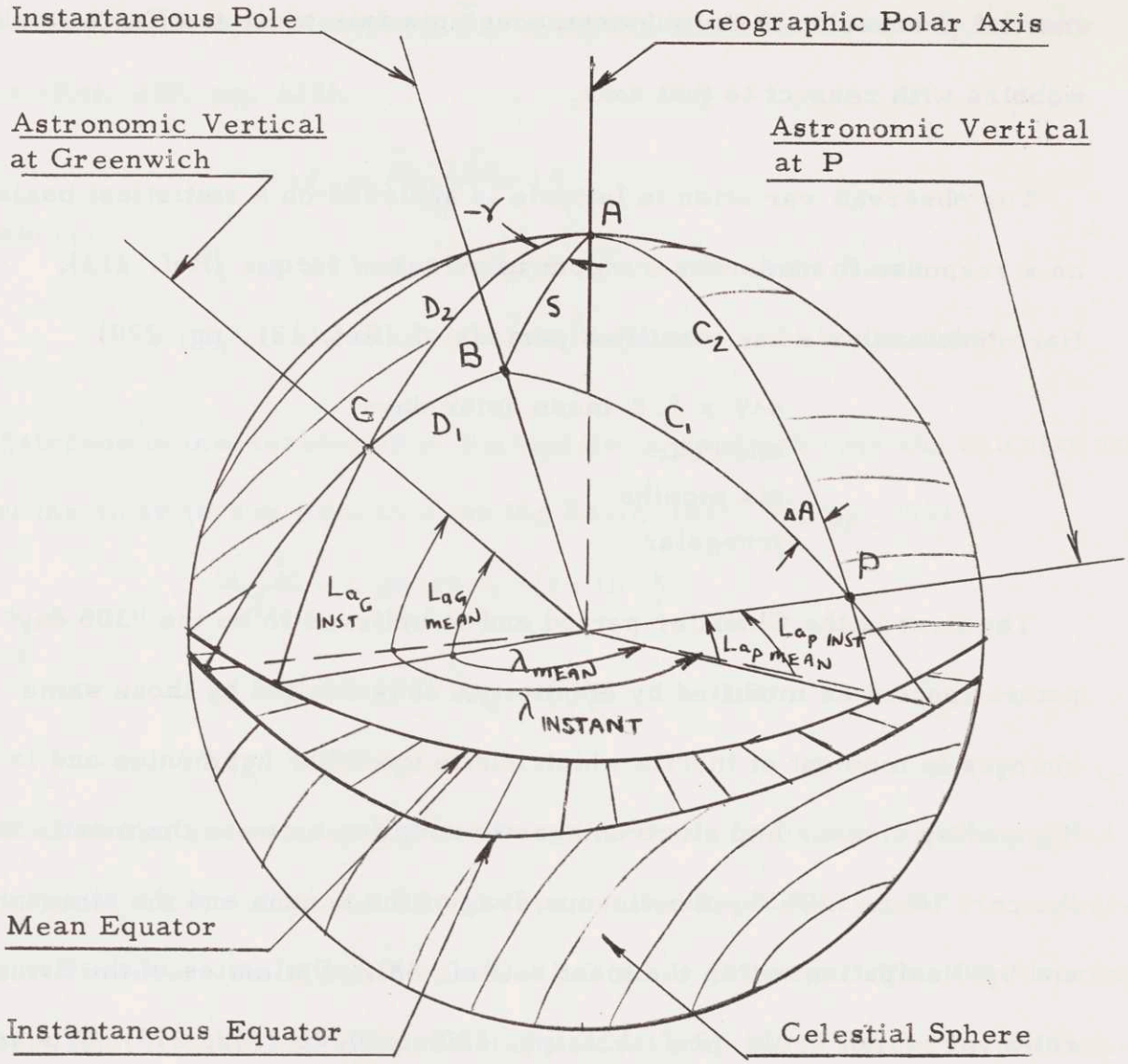

$\widehat{AP} = C_2$
$\widehat{BP} = C_1$
$\widehat{AG} = D_2$
$\widehat{BG} = D_1$

$\lambda_1 = \lambda_{P(MEAN)} = \measuredangle GAP$

$\lambda_2 = \lambda_{P(INST)} = \measuredangle GBP$

Figure A-3

GEOMETRY OF THE POLAR MIGRATION

(Exaggerated)

momentum of the Earth. Snowfall and vegetation growth cause changes in the elements of the Earth's inertia tensor which act as disturbing torques on the Earth. For example, as small an effect as the seasonal growth of vegetation is estimated to cause a polar migration of 0.004 second of arc (Ref. 121, pg. 226). The irregular fluctuations in the position of the pole are apparently due to mountain-building and seismic activity within the Earth, which alter the elements of the Earth's inertia tensor.

Advanced latitude predictions can account for the Chandler variation and for much of the annual and semi-annual variations but must necessarily remain ignorant of the bulk of the irregular fluctuations.

Figure A-3 shows a projection onto the celestial sphere of the ast ronomic verticals at Greenwich and at some point, P, and of the geographic and instantaneous polar axes. D_1 and D_2 are the instantaneous and mean astronomic colatitudes of Greenwich. C_1 and C_2 are the instantaneous and mean astronomic colatitudes of P. ΔA is the change in the astronomic azimuth of north, as viewed from P, caused by migration of the pole.

A migration of the pole to a point (x, y) in Figure A-1, causes readily determined changes in the astronomic latitude, longitude and azimuth. The x and y coordinates of the instantaneous pole can be

written in polar coordinates, s and γ :

$$s^2 = x^2 + y^2$$

$$\tan \gamma = \frac{y}{x}$$

Then using spherical trigonometry in Figure A-3:

$$\cos C_1 = \cos s \cos C_2 + \sin C_2 \sin s \cos (\lambda_1 + \gamma)$$

If s is a small angle:

$$\cos C_1 - \cos C_2 \approx (C_2 - C_1) \sin C_2 = s \sin C_2 \cos (\lambda_1 + \gamma)$$

Thus:

1. instantaneous-mean astronomic latitude = $(90° - C_1) - (90° - C_2)$

$$= C_2 - C_1 = s \cos (\lambda_1 + \gamma) = x \cos \lambda_1 - y \sin \lambda_1$$

2. instantaneous - mean astronomic azimuth = ΔA

$$\frac{\sin \Delta A}{\sin s} = \frac{\sin (\lambda_1 + \gamma)}{\sin C_1}$$

$$\Delta A \approx s \sec L_{aP} \sin (\lambda_1 + \gamma)$$

$$= \sec L_{aP} (x \sin \lambda_1 + y \cos \lambda_1)$$

3. instantaneous - mean astronomic longitude = $\lambda_2 - \lambda_1$

Since the areas of the triangles ABP and ABG are small, the sum of the angles of each triangle is nearly 180°. Thus:

$$\lambda_2 - \lambda_1 = s \sec L_{aP} \sin (\lambda_1 + \gamma) - s \sec L_{aG} \sin \gamma$$

$$= (x \sin \lambda_1 + y \cos \lambda_1) \sec L_{aP} - y \sec L_{aG}$$

where L_{aP} and L_{aG} are the astronomic latitudes of P and Greenwich, respectively.

A.3. CHANGES IN THE MAGNITUDE OF THE SPIN RATE.

Comparisons between the Earth's spin rate and the clocks of the 1940's showed a consistent tendency for the clocks to vary in rate relative to the spin rate of the Earth. In the 1950's, astronomic observations of the Sun, Moon, Mars and Venus showed that all these heavenly bodies appeared to accelerate and decelerate in unison, compared to their predicted positions as established by the rotation of the Earth, thus leading to the inescapable conclusion that the repetitive events established by the rotation of the Earth are not uniform compared to the repetitive events established by the motions of the planets or by the radiation from an atom. Since intervals established by the latter events depend only on the gravitational and atomic constants being independent of epoch, it is more reasonable (invoking Occam's Razor) to define uniform time on the basis of the planetary motions rather than the spin of the Earth. Ephemeris Time was introduced to avoid ambiguity between such slightly different time scales.

Figure A-4 shows the phase error between a clock pacing the Earth's spin rate and an ephemeris clock. The estimates are based on recent and ancient records of astronomic phenomena using the year 1750 as a reference.

Figure A-4

VARIATION OF THE SPIN RATE OF THE EARTH

COMPARED TO EPHEMERIS TIME

after Clemence (Ref. 164)

Year	Earth rate clock minus Ephemeris Clock
2000 B.C.	-2.6 hours
1750 A.D.	0
1850	-2 seconds
1900	3.9 sec.
1940	24.5 sec.

About twenty year's observations of the Earth's spin rate against Ephemeris Time have shown that at least three harmonics exist in the fluctuation of Earth rate (Ref. 188).

a. A secular decrease in the spin rate causes the days to lengthen about 0.0016 second per century. This is caused largely by the viscous drag of the ocean tides which the Sun and Moon sweep across the Earth each day. In deep water, the tides produce little relative motion between water and the sea bottom but in shallow seas, considerable energy dissipation can occur, Figure A-5. Jeffreys (Ref. 121, pg. 244)

Figure A-5

DAMPING OF THE EARTH'S SPIN RATE

CAUSED BY TIDAL FRICTION

After Jeffreys (Ref. 121, pg. 224)

Sea	Percent of total observed Damping
Western Hemisphere	
Bay of Fundy	1.4 %
Fox Strait	5.1
Europe	
Irish Sea	2.2
North Sea	2.5
English Channel	4.0
Asia	
Yellow Sea	4.0
Bering Sea	54.0
Malacca Strait	4.0
Total of Above Eight Seas	80 %

estimates that the energy dissipation in the eight shallow seas tabulated in Figure A-5 is 80% of the dissipation needed to account for the observed secular slowing of the Earth.

Since the spin rate of the Earth itself measures mean solar time, large phase errors can accumulate between mean solar and Ephemeris Time because of a mere 0.0016 second/century acceleration in the length of the day. If τ_s is the length of the day in ephemeris seconds and t_c is time, in tropical centuries measured from some convenient reference:

$$\tau_s = 86,400 + 0.0016\, t_c \quad \text{seconds}$$

Then after t_c centuries the error, t_E = mean solar minus ephemeris time, is:

$$t_E = 29.2\, t_c^2 \quad \text{seconds}$$

After one century, a phase error of 29.2 seconds accumulates and after 4000 years, a phase error of thirteen hours accumulates which is much greater than the 2.6 hour error noted in the eclipse records. Both Jeffreys (Ref. 121, Chap. 8) and Russell, Dugan and Stewart (Ref. 200, pg. 289) mention that the amount of tidal damping in the past is uncertain. An accumulated phase error should not be confused with a secular change in the spin rate.

b. Annual and semi-annual fluctuations of ± 0.06 second phase

error, caused by the same yearly changes in the elements of the inertia tensor of the Earth as cause the variation in direction of the spin rate, have been identified (Ref. 206, pg. 100). These are largely predictable in the form:

$$\text{Ephemeris Time} - \text{Universal Time} = a \sin\omega_{IE}t + b \cos\omega_{IE}t + c \sin 2\omega_{IE}t + d \cos 2\omega_{IE}t$$

where a, b, c and d have been measured to an accuracy of one millisecond. Presently (1959), the coefficients are (Ref. 189, pg. 107):

a = + 22 millisec. c = - 7 millisec.

b = - 17 millisec. d = + 6 millisec.

c. Irregular fluctuations in the length of the day appear at a maximum instantaneous rate of 1.4 seconds/year with a phase error of as much as thirty seconds in recent years (Ref. 260, pg. 290). More typical fluctuations in the length of the day occur at a rate of 1/2 millisecond per year. Until last year, the irregular component of the spin rate fluctuation was thought to remain constant for long periods of time and then suddenly change at random intervals of about twenty to forty years. The widespread use of atomic clocks has suggested that the changes occur smoothly and continuously (Ref. 189, pg. 110). In addition, harmonics of one millisecond amplitude and periods of one-half day, one-half month and one month, caused by lunar tides within the Earth's mantle, have been detected (Ref. 188, pg. 228).

A.4. SUMMARY.

The Earth's spin axis can be rotated as much as 1/2 second of arc from the mean position, the geographic pole. However if necessary, advance predictions can usually be made of the position of the pole to an accuracy of about 0.2 second, one year in advance. The migration of the pole causes calculable changes in the astronomic latitude, longitude and azimuth of any point on the Earth of as much as one second of arc in moderate latitudes.

If the rotation of the Earth is used as a measure of time interval, an error of one part in 10^7 during a year's time must be accepted in the clock, compared to Ephemeris Time.

Information on the variation in spin rate and the migration of the poles of the other navigable planets does not exist to this writer's knowledge.

Appendix B

SPHERICAL HARMONICS

A family of functions $u_0(x)$, $u_1(x)$, ... $u_n(x)$ is said to be orthonormal with respect to the weighting function, $r(x)$, in the interval $a < x < b$ if:

$$\int_a^b r(x)\ u_n(x)\ u_m(x)\ dx = \delta_{nm} \quad \begin{matrix} =0 & n \neq m \\ =1 & n = m \end{matrix} \qquad \text{(B-1)}$$

If such a family is complete, then in the range $a < x < b$, any function, $f(x)$, satisfying very general conditions (Ref. 222, pg. 231) can be expressed as a linear combination of the $u_n(x)$:

$$f(x) = \sum_{n=0}^{\infty} a_n\ u_n(x) \qquad \text{(B-2)}$$

One means of insuring that a family of $u_n(x)$ is complete is to take the $u_n(x)$ as the solutions of an appropriate Sturm-Liouville problem (Ref. 223, pgs. 95 ff.). This appendix treats the complete set of u_n generated by the equation:

$$\frac{1}{\cos L_c}\frac{d}{dL_c}\left(\cos L_c \frac{dy}{dL_c}\right) + n(n+1)y = 0 \quad \left[-\frac{\pi}{2} < L_c < \frac{\pi}{2}\right] \qquad \text{(B-3)}$$

which are called Legendre functions of the first kind of degree n, $P_n(\sin L_c)$. The first few P_n are (Ref. 222, pg. 174):

$$P_0 = 1$$

$$P_1 = \sin L$$

$$P_2 = \frac{3\sin^2 L_c - 1}{2}$$

$$P_3 = \frac{5\sin^3 L_c - 3\sin L_c}{2}$$

$$P = \frac{35\sin^4 L_c - 30\sin^2 L_c + 3}{8} \qquad \text{(B-4)}$$

The reason for selecting this particular set of u_n is now investigated.

In the space outside a mass, m, the gravitational potential is described by the equation:

$$\nabla^2 V = 0$$

where ∇^2 is the Laplacian operator whose form is dictated by the coordinate frame in which the problem is to be solved. Thus in the spherical coordinates of Figure 2-1, if V is not a function of λ, the Laplacian is (Ref. 222, pg. 329):

$$\frac{\partial}{\partial r}\left(r^2 \frac{\partial V}{\partial r}\right) + \frac{1}{\cos L_c} \frac{\partial}{\partial L_c}\left(\cos L_c \frac{\partial V}{\partial L_c}\right) = 0 \qquad \text{(B-5)}$$

Assume a solution in the form:

$$V(r, L_c) = V_1(r)\ V_2(L_c)$$

whereupon Equation (B-5) separates into two equations:

$$r^2 \frac{d^2 V_1}{dr^2} + 2r \frac{dV_1}{dr} - n(n+1) V_1 = 0$$

$$\frac{1}{\cos L_c} \frac{\partial}{\partial L_c}\left(\cos L_c \frac{\partial V_2}{\partial L_c}\right) + n(n+1) V_2 = 0 \qquad \text{(B-6)}$$

The first is Euler's equidimensional equation (Ibid., pg. 14) for which:

$$V_1(r) = C_1' r^n + C_2' r^{-(n+1)} \qquad \text{(B-7)}$$

On physical grounds, when $r \to \infty$, V_1 should go to zero. Thus, C_1' must be zero.

The second of Equations (B-6) is the Legendre equation, Equation (B-3) which has the solution:

$$V_2 (L_c) = d_1 P_n(\sin L_c) + d_2 Q_n(\sin L_c) \qquad \text{(B-8)}$$

where $Q_n(\sin L_c)$ is the Legendre function of the second kind of degree n which is not finite on the z axis. Hence, in order that V_2 remain bounded everywhere outside the mass, $d_2 = 0$ and n must be a positive integer (Ibid., pg. 175).

Hence one possible solution of Laplace's equation is:

$$V(r, L_c) = V_1(r)\, V_2(L_c) = C_2' r^{-(n+1)} d_1 P_n(\sin L_c)$$

and since $\nabla^2 V = 0$ is linear, a linear combination of solutions is also a solution:

$$V(r, L_c) = \sum_{n=0}^{\infty} a_n r^{-(n+1)} P_n(\sin L_c) \qquad \text{(B-9)}$$

This expansion can represent any single-valued function of two variables with a finite number of finite discontinuities. In particular, it can describe the gravitational potential around a planet if the field (or function) is symmetric about the z axis. The a_n are then usually normalized to the size of the planet (of mass, m_p) so that:

$$a_n = \gamma m a^n J_n$$

$$V(r, L_c) = \frac{\gamma m_p}{r} \sum_{n=0}^{\infty} J_n \left(\frac{a}{r}\right)^n P_n(\sin L_c) \qquad \text{(B-10)}$$

where γ is the Newtonian gravitational constant. a is usually the semi-major axis of the reference ellipsoid describing the geoid of the planet but is sometimes its mean radius.

The symmetry properties of V about the equator, $L_c = 0$, are now investigated. Since sin L_c is an odd function:

$$P_n (L_c) = P_n(-L_c) \qquad n \text{ even}$$

$$P_n (L_c) = - P_n(- L_c) \qquad n \text{ odd}$$

The even harmonics are symmetric about the equator while the odd harmonics are antisymmetric. Thus, if the planet potential is symmetric about the equator, it can be described only by even harmonics and conversely, if it contains only even harmonics, it is symmetric about $L_c = 0$.

If the restriction that the potential be symmetric about the z axis (that is, be independent of λ) is removed, the problem of representing the potential becomes three dimensional. At each point (r, L_c, λ) in space, V is uniquely defined as a function of r, L_c and λ. Bomford (Ref. 87, pgs. 423 ff.) introduces the tesseral harmonics of order m and degree n, P_{nm}, to describe such a field:

$$P_{nm}(L_c) = \cos^m L_c \frac{d^m}{dx^m} P_n(x)$$

corresponding to Hildebrand's associated Legendre function of the first kind of degree n and order m (Ref. 222, pg. 178). The tesseral harmonics of order zero, P_{no}, are the Legendre functions. In terms of the tesseral harmonics:

$$V(\lambda, L_c, r) = \sum_{n=0}^{\infty} \sum_{m=0}^{\infty} \left(\frac{a}{r}\right)^{n+1} \left(b_{mn} \cos m\lambda + C_{mn} \sin m\lambda\right) P_{nm}(L_c) \qquad (B-11)$$

The coefficients, b_{mn} and c_{mn}, can be adjusted to match any suitable V in three dimensions. This solution of Laplace's equation in tesseral harmonics is suited to spherical boundaries where r is constant. For ellipsoidal boundary conditions, $\nabla^2 V = 0$ can be solved in terms of Lamé functions (Ref. 231, pgs. 1306 ff.).

Appendix C

CONFOCAL ELLIPSOIDAL COORDINATES

Ellipsoidal coordinates are of interest in this thesis because the geoids of the Earth and of other planets are conveniently approximated as oblate ellipsoids of rotation.

C.1. THE PLANE ELLIPSE.

The ellipse is a closed plane geometric figure defined in the Cartesian coordinates (u, v) by the equation:

$$\frac{u^2}{a_E^2} + \frac{v^2}{b_E^2} = 1 \qquad (C-1)$$

a_E and b_E are the semi-major and semi-minor axes, respectively.

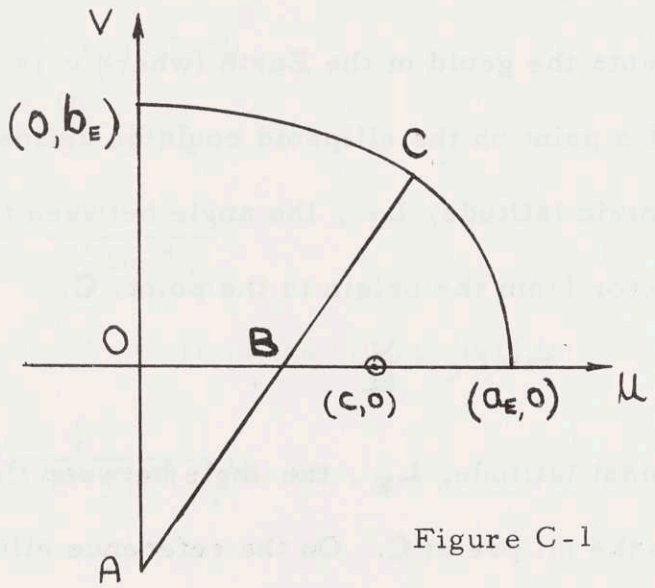

Figure C-1

THE ELLIPSE

The foci of the ellipse are at $u = \pm c$, $v = 0$ where c is the focal distance of the ellipse. Several geometric definitions of the ellipse exist and many elegant properties can be derived (Ref. 221, pgs. 192-197).

Some geometric properties of interest are:

a. focal distance, $c^2 = a_E^2 + b_E^2$

b. semi-latus rectum, $p = b_E^2 / a_E$ (C-2)

c. eccentricity, $\epsilon = c/a_E < 1$

d. flattening, $f = \frac{a_E - b_E}{a_E} = 1 - (1 - \epsilon^2)^{1/2}$

These quantities can all be expressed in terms of ϵ :

$$\epsilon = f(2-f)$$

$$b_E = a_E (1 - \epsilon^2)^{1/2} \qquad \text{(C-3)}$$

$$p = a_E (1 - \epsilon^2)$$

If the plane ellipse were a meridian section of an ellipsoid of rotation which represents the geoid of the Earth (where v is the polar axis), the latitude of a point on the ellipsoid could be defined as:

a. geocentric latitude, L_C , the angle between the u axis and the radius vector from the origin to the point, C.

$$\tan L_C = \frac{v}{u}$$

b. ellipsoidal latitude, L_E , the angle between the u axis and the normal to the ellipse at C. On the reference ellipsoid, $L_E = L_g$, the geographic latitude.

$$\tan L_E = -\frac{1}{dv/d\mu} = \frac{1}{1-\epsilon^2}\,\frac{v}{\mu} \qquad (C-4)$$

The angle between the radius vector and the normal to the ellipse at C is $L_E - L_C$ where:

$$\tan (L_E - L_C) = \left(\frac{1}{b_E^2} - \frac{1}{a_E^2}\right)\mu v \qquad (C-5)$$

Some important dimensions of the ellipse are:

a. The radius vector, $r = \overline{OC}$:

$$r^2 = \mu^2 + v^2 = \frac{b_E^2}{1 - \epsilon^2 \cos^2 L_C} \qquad (C-6)$$

which can be expanded using the binomial theorem:

$$r^2 = a_E^2 [\, 1 - \epsilon^2 \sin^2 L_C - \epsilon^4 \sin^2 L_C \cos^2 L_C \ldots] \qquad (C-7)$$

$$r = a_E [\, 1 - \frac{\epsilon^2}{2} \sin^2 L_C - \frac{\epsilon^4}{8} \sin^2 L_C \,(4 - 3 \sin^2 L_C) \ldots .]$$

b. The lengths $\overline{AC}$ and $\overline{BC}$, measured along the normal to the ellipse, can be found from Figure C-1:

$$\frac{\mu}{\overline{AC}} = \cos L_E \qquad \frac{v}{\overline{BC}} = \sin L_E$$

Using equations (C-1) and (C-4):

$$R_{AC}^2 = \frac{a_E^2}{1 - \epsilon^2 \sin^2 L_E} \qquad (C-8)$$

$$R_{BC}^2 = \frac{p^2}{1 - \epsilon^2 \sin^2 L_E}$$

c. The radius of curvature of the ellipse at C is:

$$\rho_M = \frac{p}{(1 - \epsilon^2 \sin^2 L_E)^{3/2}} \qquad (C-9)$$

C.2. THE PLANE HYPERBOLA.

The hyperbola is an open, plane, geometric figure defined in the Cartesian coordinates (u, v) by the equation:

$$\frac{u^2}{a_H^2} - \frac{v^2}{b_H^2} = 1 \qquad (C\text{-}10)$$

The vertices are at $u = \pm a_H$, $v = 0$ and the foci at $u = \pm c$, $v = 0$. The semi-conjugate axis, b_H, is defined analagously to the ellipse but has no direct physical interpretation:

$$c^2 = a_H^2 + b_H^2$$

As in the case of the ellipse, several geometric definitions of the hyperbola are possible and many elegant properties can be derived (Ref. 231, pgs. 213-220 and 192-197).

The eccentricity of the hyperbola is defined as for the ellipse:

$$\epsilon = \frac{c}{a_H} > 1$$

The asymptotes make an angle, η, with the u axis where η can be found from Equation (C-10) as $u \to \infty$:

$$\frac{u^2}{a_H^2} \to \frac{v^2}{b_H^2}$$

$$\tan \eta \longrightarrow \frac{v}{u} = \pm \frac{b_H}{a_H}$$

C.3. PLANE CONFOCAL ELLIPTIC COORDINATES.

Consider the (u, v) plane in which a pair of fixed foci, $u = \pm c$, $v = 0$, are established. A family of ellipses is constructed each of which has these foci but whose sizes and eccentricities are different, Figure C-2.

Similarly, a family of hyperbolae can be constructed using the same two foci. If a_ε and b_ε are the semi-major and semi-minor axes of the ellipses and a_H and b_H of the hyperbolae, then the families defined by Equations (C-1) and (C-10) are orthogonal everywhere except at the foci, as shown on page 325 . Except in this appendix, the symbols a and b, without subscripts, refer to the ellipse.

If the ellipses and hyperbolae are numbered with the symbols ξ and η respectively, each point in the (u, v) plane can be described by the numbers ξ and η. Consequently the generalized coordinates are as suitable for identifying points in the plane as are the Cartesian coordinates, u and v.

To define the relation between ξ, η and u, v consider the complex transformation from:

$$\bar{z} = u + i v$$

to:

$$\bar{w} = \xi + i\eta$$

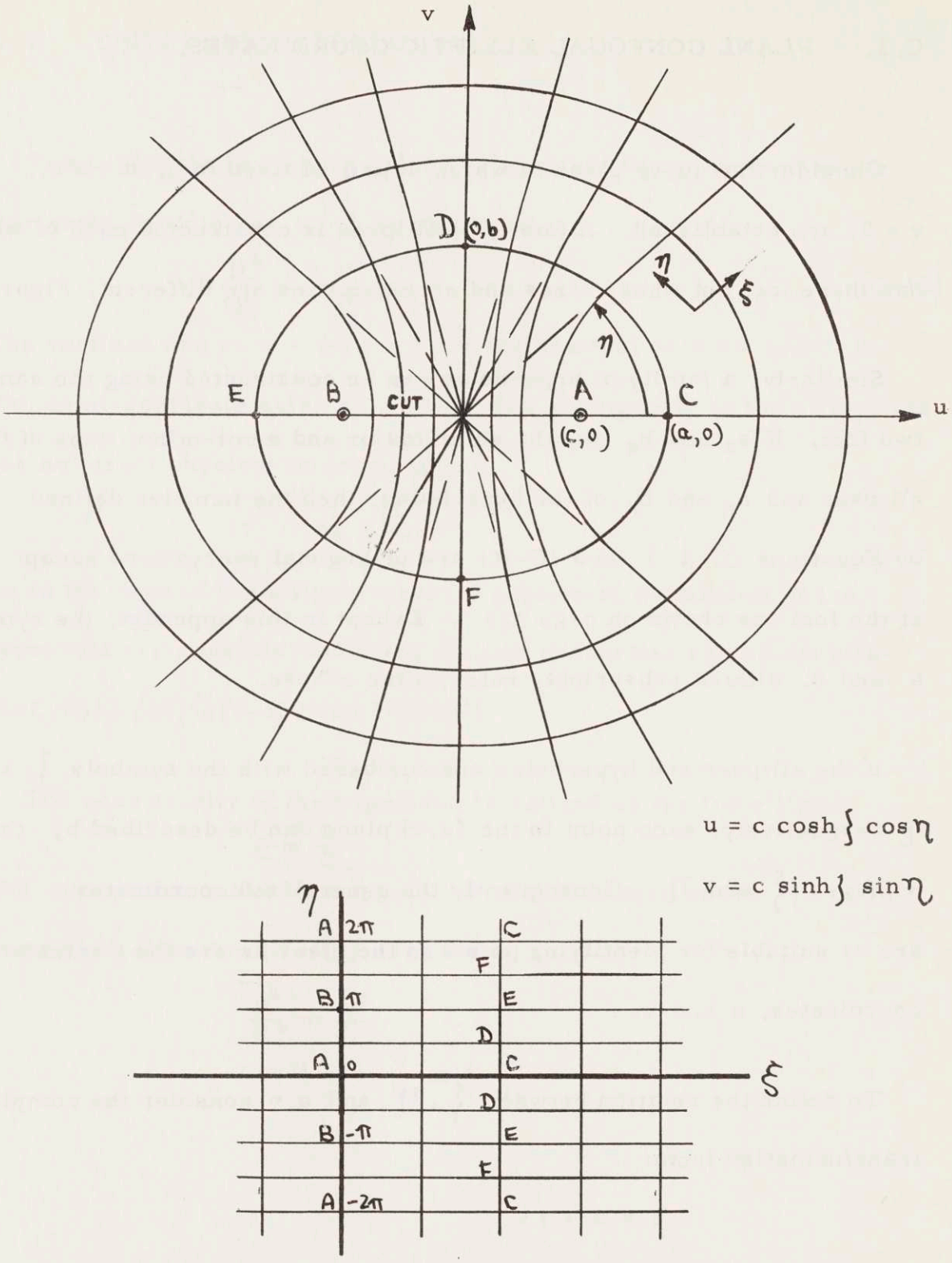

Figure C-2. CONFOCAL ELLIPTIC COORDINATES.

in the form:

$$\bar{z} = c \cosh \bar{w} \qquad (C\text{-}11)$$

$$= c \cosh (\xi + i\eta)$$

then:

$$u + i v = c (\cosh \xi \cosh i\eta + \sinh \xi \sinh i\eta)$$

$$= c (\cosh \xi \cos \eta + i \sinh \xi \sin \eta)$$

so:

$$\boxed{\begin{aligned} u &= c \cosh \xi \cos\eta \\ v &= c \sinh \xi \sin\eta \end{aligned}} \qquad (C\text{-}12)$$

and:

$$\frac{u^2}{c^2\cosh^2\xi} + \frac{v^2}{c^2\sinh^2\xi} = \cos^2\eta + \sin^2\eta = 1$$

$$\frac{u^2}{c^2\cos^2\eta} - \frac{v^2}{c^2\sin^2\eta} = \cosh^2\xi - \sinh^2\xi = 1$$

Thus curves of constant ξ are ellipses for which $a_E = c \cosh\xi$ and $b_E = c \sinh\xi$ whereas curves of constant η are hyperbolae for which $a_H = c \cos\eta$ and $b_H = c \sin\eta$. The transformation, Equation (C-11) superimposes an orthogonal net of confocal ellipses and hyperbolae on the (u, v) plane, Figure C-2.

The uniqueness of the transformation must be carefully investigated:

a. $\xi = 0$, $\eta = 0$ corresponds to the two foci, $u = \pm c$, $v = 0$.

b. $\xi = 0$, $\eta = \frac{2N+1}{2}\pi$ corresponds to the origin of the $\bar{z}$ plane, $u = v = 0$.

Each strip in the $\bar{w}$ plane of width $2N\pi < \eta < (2N+1)\pi$ maps into the entire $\bar{z}$ plane, for successive integral values of N.

Figure C-3

LATITUDE IN ELLIPTIC COORDINATES

	L_C	L_E
sin L	$\dfrac{\sinh \xi \sin \eta}{(\cosh^2 \xi - \sin^2 \eta)^{1/2}}$	$\dfrac{\cosh \xi \sin \eta}{(\cosh^2 \xi - \cos^2 \eta)^{1/2}}$
cos L	$\dfrac{\cosh \xi \cos \eta}{(\cosh^2 \xi - \sin^2 \eta)^{1/2}}$	$\dfrac{\sinh \xi \cos \eta}{(\cosh^2 \xi - \cos^2 \eta)^{1/2}}$
tan L	$\tanh \xi \tan \eta$	$\coth \xi \tan \eta$

c. The quadrant, $u > 0$, $v > 0$, corresponds to the region $\xi > 0$, $0 < \eta < \frac{\pi}{2}$.

Thus the transformation is not a one-to-one correspondence between points in the $\bar{z}$ and $\bar{w}$ planes. An examination of the derivative:

$$\frac{d\bar{z}}{d\bar{w}} = c \sinh \bar{w}$$

shows that singular points occur when:

a. $\frac{d\bar{z}}{d\bar{w}} = 0$ whereupon $\cosh \xi \sin \eta = 0$ and $\sinh \xi \cos \eta = 0$ which occurs only at $\xi = 0$, $\eta = N\pi$ corresponding to the points $u = \pm c$, $v = 0$. These are branch points (Ref. 233, pg. 28).

b. $\frac{d\bar{z}}{d\bar{w}} = \infty$ which occurs only for $\xi = \infty$. The point at infinity is an isolated essential singularity (Ibid., pg. 99).

The transformation can be made unique by cutting the (u, v) plane between the branch points as in Figure C-2. The cut prevents paths of integration from circling either branch point. Such a cut is practical in these applications since the interiors of the innermost ellipsoids are of no interest, being inside the planets. In the region outside any ellipsoid, $\xi = \xi_0 > 0$, the (u, v) plane is analytic and single-valued. The limits on ξ and η then are:

$$\xi > 0$$

$$0 \leq \eta < 2\pi$$

and η is specified differently in each of the four quadrants.

The properties of the ellipse and hyperbola derived in this appendix can be transformed into elliptic coordinates:

a. $a_E = c \cosh \xi \qquad b_E = c \sinh \xi$

b. $a_H = c \cos \eta \qquad b_H = c \sin \eta$

c. for the ellipse:

$$\epsilon = \frac{c}{a_E} = \operatorname{sech} \xi$$

$$f = 1 - (1 - \epsilon^2)^{1/2} = 1 - \tanh \xi$$

$$p = \frac{b_E^2}{a_E} = c \sinh \xi \tanh \xi = a \tanh^2 \xi \qquad \text{(C-13)}$$

d. $1 - \epsilon^2 \cos^2 L_C = 1 - \frac{1}{\cosh^2 \xi} \frac{\cosh^2 \xi \cos^2 \eta}{\cosh^2 \xi - \sin^2 \eta} = \frac{\sinh^2 \xi}{\cosh^2 \xi - \sin^2 \eta}$

e. $1 - \epsilon^2 \sin^2 L_E = 1 - \frac{1}{\cosh^2 \xi} \frac{\cosh^2 \xi \sin^2 \eta}{\cosh^2 \xi - \cos^2 \eta} = \frac{\sinh^2 \xi}{\cosh^2 \xi - \cos^2 \eta}$

f. $\tan (L_E - L_C) = \frac{\sin 2\eta}{\sinh 2\xi}$

g. $r^2 = c^2 (\cosh^2 \xi - \sin^2 \eta) = c^2 (\sinh^2 \xi + \cos^2 \eta)$

h. $R_{AC}^2 = \frac{a^2 (\cosh^2 \xi - \cos^2 \eta)}{\sinh^2 \xi}$

j. $R_{BC}^2 = \frac{a^2 (\cosh^2 \xi - \cos^2 \eta)}{\cosh^2 \xi} \tanh^2 \xi$

k. $\rho_M = \frac{a (\cosh^2 \xi - \cos^2 \eta)^{3/2}}{\cosh^2 \xi \sinh \xi}$

l. The tangent of the asymptote angle of the hyperbola $= \pm \frac{b_H}{a_H}$ $= \pm \tan \eta$. Hence the definition of η on page 318 is identical to the generalized coordinate, η.

The simplicity of these expressions in elliptic coordinates, as compared to rectangular coordinates, is apparent.

To establish the orthogonality of the families of intersecting ellipses and hyperbolae, consider the slope of the ellipse of Equation (C-1):

$$\frac{dv}{d\mu} = -\tanh^2 \xi \coth \xi \cot \eta$$

and of the hyperbola of Equation (C-10):

$$\frac{dv}{d\mu} = +\coth \xi \tan \eta$$

The product of the slopes is -1 except at $\xi = 0$, $\eta = N\pi$. Hence, except at these points, the curves are orthogonal. The exceptions are the foci, the two finite singular points of the transformation.

The coordinates ξ and η can be interpreted physically. The coordinate, ξ, measures the eccentricity of the ellipse through the point in question ($\epsilon = \operatorname{sech} \xi$). The coordinate, η, is the asymptote angle of the hyperbola through the point.

C.4. CONFOCAL ELLIPSOIDAL COORDINATES.

If the confocal elliptic coordinates of Appendix C-3 are rotated in a right-handed sense about the v axis through an angle, λ, measured from some reference direction, then any point in space can be located by the three coordinates λ, η and ξ. λ locates the direction of the (u, v) plane while ξ and η locate the point within the plane.

More exactly, consider the transformation from the Cartesian y_1, y_2, y_3 coordinates in the form:

$$\begin{aligned} y_1 &= c \cosh\xi \cos\eta \cos\lambda \\ y_2 &= c \cosh\xi \cos\eta \sin\lambda \\ y_3 &= c \sinh\xi \sin\eta \end{aligned} \qquad \text{(C-14)}$$

Here, y_3 corresponds to v of the previous section and $y_1^2 + y_2^2$ corresponds to u^2.

As shown in Figure C-4:

a. the surface of constant λ is a plane through the y_3 axis. On the Earth, if λ is measured from the geographic meridian of Greenwich, it corresponds to east longitude.

b. the surface of constant η is a hyperboloid of revolution of one sheet whose minimum cross-section radius is $a_H = c \cos\eta$.

c. the surface of constant ξ is an oblate ellipsoid of rotation whose polar axis is $b_E = c \cosh\xi$ and whose equatorial semi-diameter is $a_E = c \sinh\xi$.

All the ellipsoids and hyperboloids have the focal circle z=0, $y_1^2 + y_2^2 = c^2$. The geometric properties of any plane section containing the y_3 axis are those of the plane elliptic coordinates. The addition of a third dimension introduces the following additional properties:

a. volume of the ellipsoid of rotation $= \frac{4}{3}\pi a_E^2 b_E = \frac{2}{3}\pi c^3 \cosh\xi \sinh 2\xi$

b. radius of curvature in the meridian plane is that for the plane ellipse, Equations (C-9) and (C-13k).

c. radius of curvature in the east-west direction is the "prime radius of curvature" which is the length AC in Figure C-1 (Ref. 87, pg. 394):

$$\rho_P = \frac{a_E}{(1-\epsilon^2 \sin^2 L_E)^{1/2}} = R_{AC} \qquad (C\text{-}15)$$

d. the radius of curvature in a direction at an azimuth, A, is found from the principal axis transformation:

$$\frac{1}{\rho_A} = \frac{\cos^2 A}{\rho_M} + \frac{\sin^2 A}{\rho_P} \qquad (C\text{-}16)$$

e. Since ρ_M and ρ_P are the principal radii of curvature, the total or Gaussian curvature is:

$$K = \frac{1}{\rho_M \rho_P} = \frac{(1-\epsilon^2 \sin^2 L_E)^2}{a_E p}$$

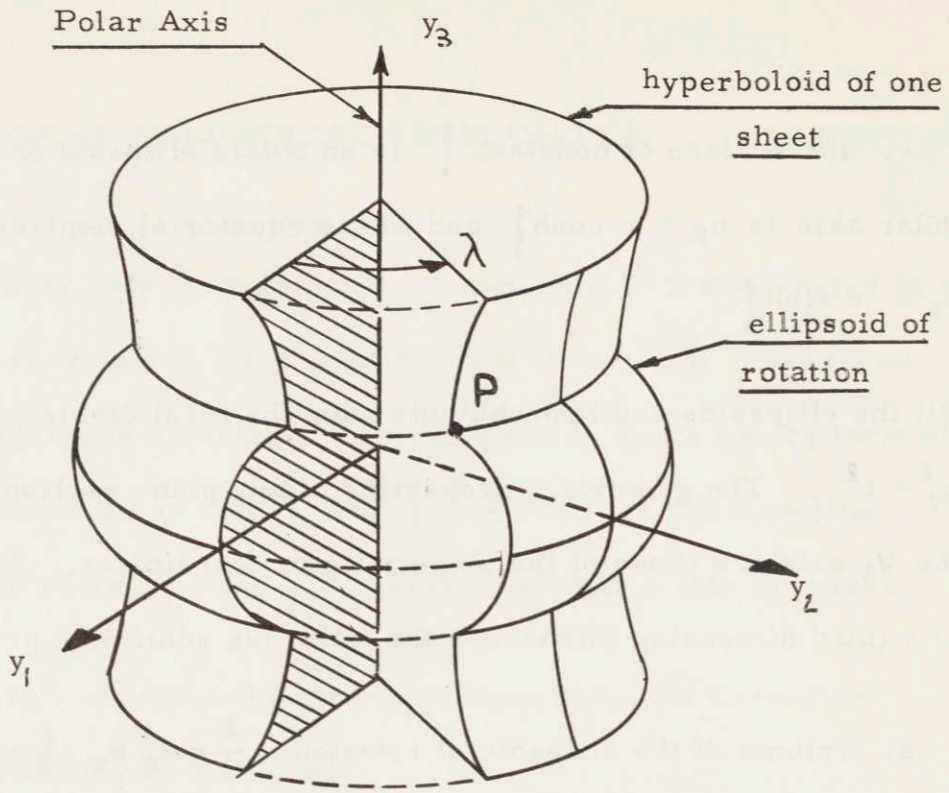

Figure C-4

OBLATE, CONFOCAL ELLIPSOIDAL COORDINATES.

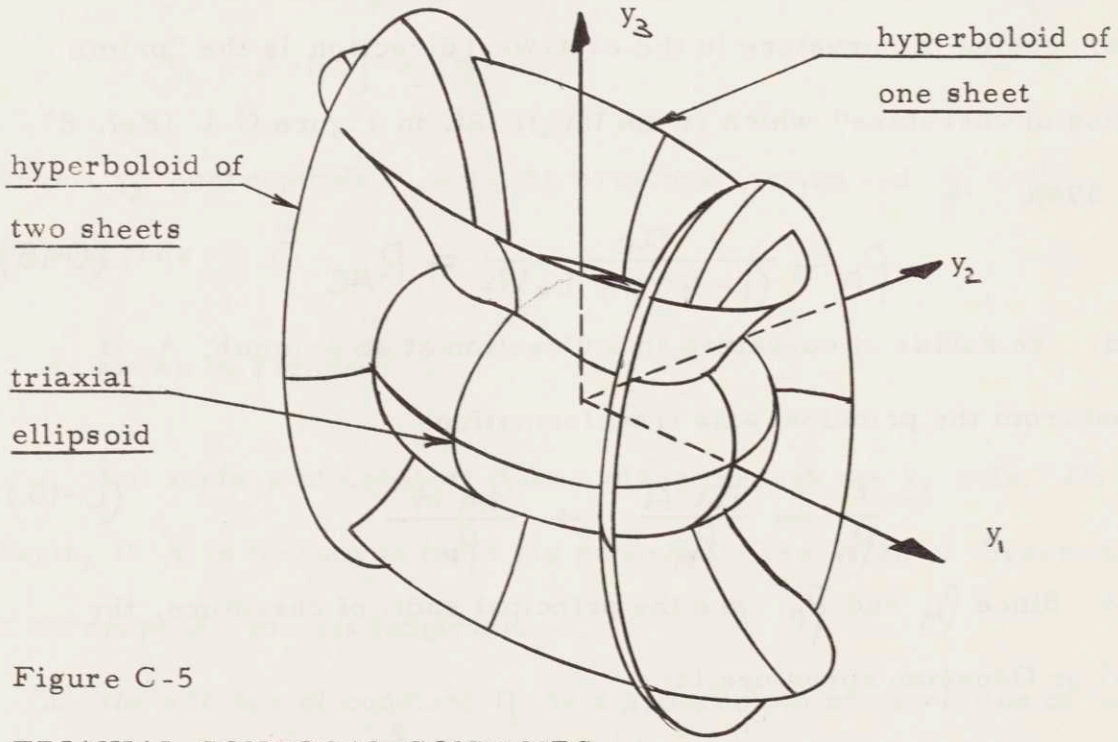

Figure C-5

TRIAXIAL CONFOCAL CONICOIDS

(after Hilbert, Ref. 221, pgs. 14-25 and 183-192)

f. the spherical excess, E, of a spheroidal triangle can be expressed as follows. Let a triangle whose vertices are at P_1 , P_2 and P_3 be drawn on the surface of an oblate ellipsoid of rotation. The sides are geodesics of length L_1 , L_2 and L_3. r_M is the mean Gaussian radius of curvature of the triangle, as defined below. Then if the sides of the triangle are small enough that:

$$\left(\frac{L_i}{r_M}\right)^4 << 1$$

the spherical excess, E = sum of angles of the triangle minus 180°, is (Ref. 87, pg. 402):

$$E = \frac{A_{eq}}{r_M^2}\left(1 + \frac{m^2}{8 r_m^2}\right)$$

where:

A_{eq} is the area of a plane triangle whose sides are L_1 , L_2 and L_3

$$3m^2 = L_1^2 + L_2^2 + L_3^2$$

$$\frac{3}{r_M^2} = \frac{1}{\rho_{M_1}\rho_{P_1}} + \frac{1}{\rho_{M_2}\rho_{P_2}} + \frac{1}{\rho_{M_3}\rho_{P_3}}$$

ρ_{M_i} and ρ_{P_i} are the principal radii of curvature at the vertex i.

For applications where the ellipsoidal coordinates must be triaxial, the confocal conicoids are defined as in Figure C-5 by the orthogonal intersections of families of:

triaxial ellipsoids

hyperboloids of one sheet

hyperboloids of two sheets

all of which have the same focal curves (Ref. 221, pgs. 19 to 25). Hilbert discusses the construction of such coordinates (Ibid., pgs. 19 to 25 and 183 to 192).

Appendix D

PROPERTIES OF SPECIAL COORDINATE FRAMES

D.1. CARTESIAN COORDINATES.

Consider a Cartesian coordinate frame y_1, y_2, y_3. For definiteness, suppose this frame to be fixed in a planet with its origin at the mass center of the planet. y_3 lies along the geographic polar axis of the planet while y_1 and y_2 define the geographic equatorial plane. Let y_1 lie in the reference geographic meridian on which longitude is defined to be zero.

This is the fundamental coordinate frame for all measurements on the planet. A vehicle moving near the planet is located by means of the coordinates y_1, y_2 and y_3, and the differential distance between neighboring points is:

$$(ds)^2 = (dy_1)^2 + (dy_2)^2 + (dy_3)^2 \qquad \text{(D-1)}$$

The gradient operator and Laplacian are:

$$\nabla = \hat{y}_1 \frac{\partial}{\partial y_1} + \hat{y}_2 \frac{\partial}{\partial y_2} + \hat{y}_3 \frac{\partial}{\partial y_3}$$

$$\nabla^2 = \frac{\partial^2}{\partial y_1^2} + \frac{\partial^2}{\partial y_2^2} + \frac{\partial^2}{\partial y_3^2} \qquad \text{(D-2)}$$

where $\hat{y}_i$ is a unit vector in the y_i direction.

D.2. SPHERICAL COORDINATES.

Figure 2-1 defines the spherical coordinate frame in which a point, P, is identified by the coordinates:

$$z^1 = \lambda$$

$$z^2 = L_c$$

$$z^3 = r$$

which are related to the Cartesian coordinates according to:

$$\begin{aligned} y_1 &= r \cos L_c \cos \lambda \\ y_2 &= r \cos L_c \sin \lambda \\ y_3 &= r \sin L_c \end{aligned} \tag{D-3}$$

The unit vectors form a right-handed system in the order λ, L_c, r.

Hildebrand gives the h_i of the metric tensor on pages 328-329 of Reference 222:

$$[g_{ij}] = \begin{bmatrix} r^2 \cos^2 L_c & 0 & 0 \\ 0 & r^2 & 0 \\ 0 & 0 & 1 \end{bmatrix} \tag{D-4}$$

That reference also gives the gradient and Laplacian operators as:

$$\overline{\nabla} = \frac{\hat{\lambda}}{r \cos L_c} \frac{\partial}{\partial \lambda} + \frac{\hat{L}_c}{r} \frac{\partial}{\partial L_c} + \hat{r} \frac{\partial}{\partial r} \tag{D-5}$$

$$\nabla^2 = \frac{1}{r^2 \cos^2 L_c} \frac{\partial^2}{\partial \lambda^2} + \frac{1}{r^2 \cos L_c} \frac{\partial}{\partial L_c} \left(\cos L_c \frac{\partial}{\partial L_c} \right) + \frac{1}{r^2} \frac{\partial}{\partial r} \left(r^2 \frac{\partial}{\partial r} \right)$$

D.3. CYLINDRICAL COORDINATES.

Figure 2-1 defines a cylindrical coordinate frame in which points are located by the coordinates s, λ and z. If:

$$z^1 = s$$

$$z^2 = \lambda$$

$$z^3 = z$$

so the unit vectors form a right-handed system in that order, the transformation is:

$$\begin{aligned} y_1 &= s \cos\lambda \\ y_2 &= s \sin\lambda \\ y_3 &= z \end{aligned} \tag{D-6}$$

Hildebrand (Ref. 222) gives the h_i of the metric tensor on page 327:

$$[g_{ij}] = \begin{bmatrix} 1 & 0 & 0 \\ 0 & s^2 & 0 \\ 0 & 0 & 1 \end{bmatrix} \tag{D-7}$$

The same reference gives the gradient and Laplacian operators as:

$$\nabla = \hat{s}\frac{\partial}{\partial s} + \frac{\hat{\lambda}}{s}\frac{\partial}{\partial \lambda} + \hat{z}\frac{\partial}{\partial z} \tag{D-8}$$

$$\nabla^2 = \frac{1}{s}\frac{\partial}{\partial s}\left(s\frac{\partial}{\partial s}\right) + \frac{1}{s^2}\frac{\partial^2}{\partial \lambda^2} + \frac{\partial^2}{\partial z^2}$$

Figure D-1

GEOGRAPHIC COORDINATES

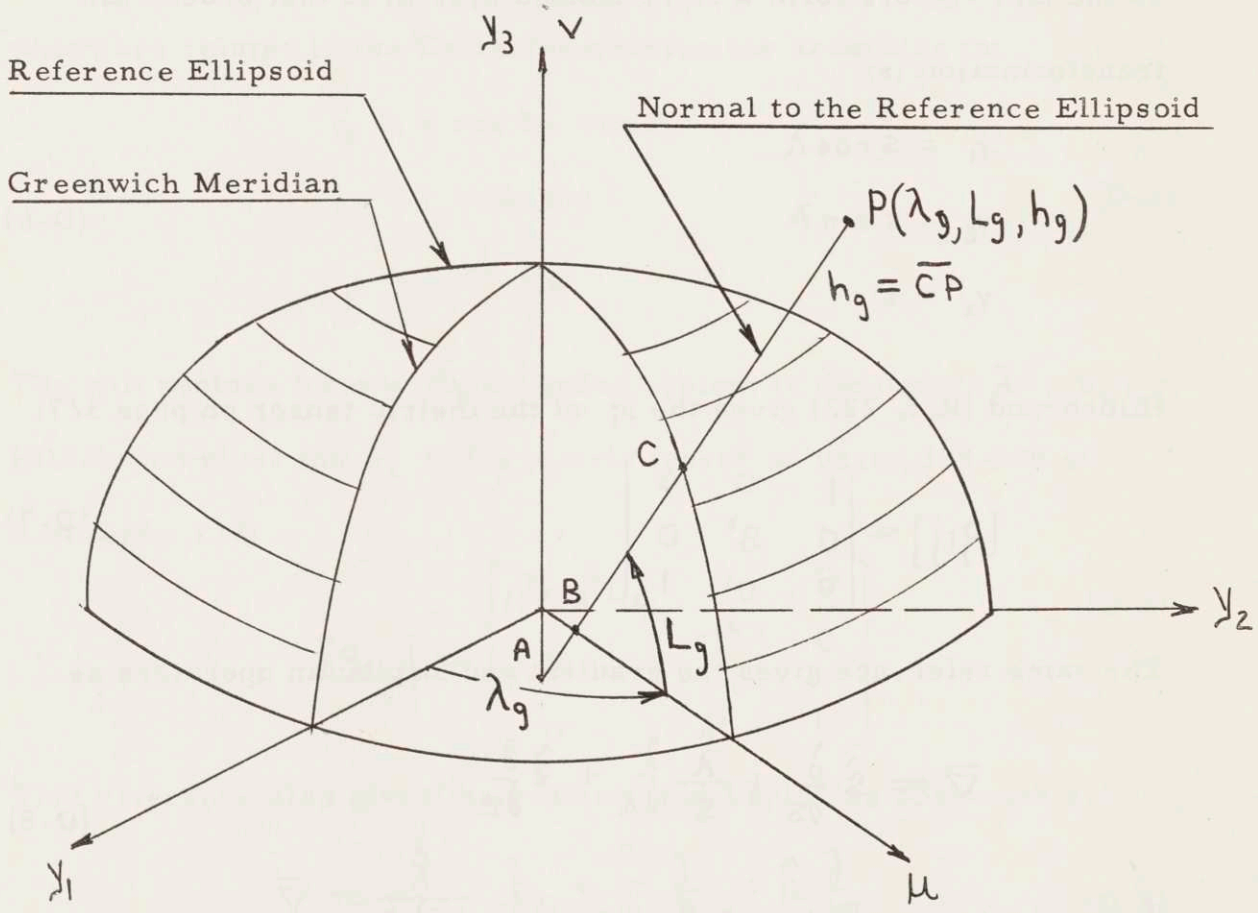

D. 4. GEOGRAPHIC COORDINATES.

These coordinates are defined to correspond exactly to the geographic definition of latitude, longitude and altitude. They are symmetric about the y_3 axis and defined in conjunction with some reference ellipsoid of rotation. Figure D-1 shows a meridian section of the reference ellipsoid of rotation whose meridian eccentricity is ϵ . The geographic coordinates are constructed by projecting downward from any point, P, along whichever normal to the reference ellipsoid passes through P. Then a family of curves could be constructed which are everywhere orthogonal to these normals. The equations of these curves are complicated but the metric properties of the space can be found without recourse to them.

Then:

$z^1 = \lambda_g$, the usual definition of east longitude.

$z^2 = L_g$, the geographic latitude. L_g is the angle between the equatorial plane of the reference ellipsoid and whichever normal to that ellipsoid passes through P.

$z^3 = h_g$, the height of P above the reference ellipsoid. The symbol, h_g , should not be confused with h_i^2 , the elements of the metric tensor in an orthogonal coordinate frame.

The unit vectors are right-handed in this order. From Figure D-1, the

transformation is:

$$
\begin{aligned}
y_1 &= (R_{AC} + h_g)\cos L_g \cos\lambda \\
y_2 &= (R_{AC} + h_g)\cos L_g \sin\lambda \\
y_3 &= (R_{BC} + h_g)\sin L_g
\end{aligned}
\qquad (D\text{-}9)
$$

where R_{AC} and R_{BC} are given in Equations (C-8). R_{AC} and R_{BC} are related to the principal radii of curvature of the reference ellipsoid:

$$
\rho_P = R_{AC} \qquad (D\text{-}10)
$$

$$
\rho_M = \frac{R_{BC}}{1-\epsilon^2\sin^2 L_g}
$$

The derivatives of R_{AC}, R_{BC} and ρ_M are:

$$
\begin{aligned}
\frac{dR_{AC}}{dL_g} &= \frac{\epsilon^2}{2(1-\epsilon^2)}\rho_M \sin 2L_g \\
\frac{dR_{BC}}{dL_g} &= \frac{\epsilon^2}{2}\rho_M \sin 2L_g \\
\frac{d\rho_M}{dL_g} &= \frac{3}{2}\epsilon^2\frac{\rho_M}{1-\epsilon^2\sin^2 L_g)}\sin 2L_g
\end{aligned}
\qquad (D\text{-}11)
$$

from which the differential distance can be evaluated by the laborious process of calculating all of the $\frac{dy_m}{dz^i}\frac{dy_m}{dz^j}$: Thus, the covariant elements of the metric tensor are:

$$
[g_{ij}] = \begin{bmatrix} (\rho_P + h_g)^2\cos^2 L_g & 0 & 0 \\ 0 & (\rho_M + h_g)^2 & 0 \\ 0 & 0 & 1 \end{bmatrix} \qquad (D\text{-}12)
$$

These can be verified using the derivation of Section 4. F. 1, Equations (4-40) and (4-41) where:

$$S_1 (z^2 , z^3) = (R_{AC} + h_g) \cos L_g$$

$$S_2 (z^2 , z^3) = (R_{BC} + h_g) \sin L_g$$

The fact that $[g_{ij}]$ is diagonal shows mathematically that the geographic coordinates are orthogonal.

The mechanizations of Section 5. F. require an expansion of the metric elements as follows:

$$(\rho_P + h_g) = h_g + a\left[1 + \frac{\epsilon^2}{2}\sin^2 L_g + \frac{3}{8}\epsilon^4 \sin^4 L_g - \cdots\right]$$

$$(\rho_M + h_g) = h_g + a\left[1 + \epsilon^2\left(\frac{3}{2}\sin^2 L_g - 1\right) + \frac{3}{2}\epsilon^4 \sin^2 L_g \left(\frac{5}{4}\sin^2 L_g - 1\right) - \cdots\right]$$

(D-13)

The transformation between spherical and geographic coordinates can be found geometrically:

$$r^2 = (R_{AC} + h_g)^2 \cos^2 L_g + (R_{BC} + h_g)^2 \sin^2 L_g$$

$$= \frac{a^2\left[1 + \epsilon^2(\epsilon^2 - 2)\sin^2 L_g\right]}{1 - \epsilon^2 \sin^2 L_g} + 2h_g a\left(1 - \epsilon^2 \sin^2 L_g\right)^{1/2} + h_g^2$$

$$r \sin L_c = (R_{BC} + h_g) \sin L_g$$

(D-14)

At large distances, the geographic coordinates become spherical:

$$h_\lambda = (R_{AC} + h_g)\cos L_g \longrightarrow r\cos L_c$$

$$h_L = (\rho_M + h_g) \longrightarrow r$$

$$h_h = 1$$

The gradient and Laplacian operators are found from the general expressions given in Reference 222, pgs. 324 and 326:

$$\overline{\nabla} = \frac{\hat{\lambda}}{(\rho_p + h_g)\cos L_g}\frac{\partial}{\partial\lambda} + \frac{\hat{L}_g}{(\rho_M + h_g)}\frac{\partial}{\partial L_g} + \hat{h}_g\frac{\partial}{\partial h_g} \qquad (D\text{-}15)$$

$$\nabla^2 = \frac{1}{(\rho_p+h_g)^2\cos^2 L_g}\frac{\partial^2}{\partial\lambda^2} + \frac{1}{(\rho_p+h_g)(\rho_M+h_g)\cos L_g}\left\{\right.$$

$$\left.\left\{\frac{\partial}{\partial L_g}\left[\frac{(\rho_p+h_g)\cos L_g}{(\rho_m+h_g)}\frac{\partial}{\partial L_g}\right] + \frac{\partial}{\partial h_g}\left[(\rho_M+h_g)(\rho_p+h_g)\cos L_g\frac{\partial}{\partial h_g}\right]\right\}\right.$$

D. 5. CONFOCAL ELLIPSOIDAL COORDINATES.

These coordinates are defined by Equations (C-14). The differential distance is:

$$(ds)^2 = \frac{\partial y_m}{\partial z^i}\frac{\partial y_m}{\partial z^j}\,dz^i\,dz^j$$

$$= c^2\cosh^2\xi\cos^2\eta(d\lambda)^2 + c^2(\cosh^2\xi - \cos^2\eta)[(d\eta)^2 + (d\xi)^2]$$

and the metric tensor is:

$$[g_{ij}] = c^2 \begin{bmatrix} \cosh^2\xi \cos^2\eta & 0 & 0 \\ 0 & (\cosh^2\xi - \cos^2\eta) & 0 \\ 0 & 0 & (\cosh^2\xi - \cos^2\eta) \end{bmatrix}$$

(D-16)

The gradient and Laplacian operators are found as on the preceding page:

$$\bar{\nabla} = \frac{\hat{\lambda}}{c \cosh\xi \cos\eta} \frac{\partial}{\partial\lambda} + \frac{1}{c(\cosh^2\xi - \cos^2\eta)^{1/2}} \left(\hat{\eta} \frac{\partial}{\partial\eta} + \hat{\xi} \frac{\partial}{\partial\xi} \right)$$

$$\nabla^2 = \frac{1}{c^2 \cosh^2\xi \cos^2\eta} \frac{\partial^2}{\partial\lambda^2} + \frac{1}{c^2(\cosh^2\xi - \cos^2\eta)} \left[\frac{1}{\cosh\xi} \frac{\partial}{\partial\xi} \left(\cosh\xi \frac{\partial}{\partial\xi} \right) + \right.$$

$$\left. + \frac{1}{\cos\eta} \frac{\partial}{\partial\eta} \left(\cos\eta \frac{\partial}{\partial\eta} \right) \right] \qquad \text{(D-17)}$$

Comparing the spherical, geographic and ellipsoidal coordinate frames, it is clear that they represent three ways of defining the vertical above a planet:

a. along the radius vector (spherical)

b. along the normal to the reference ellipsoid (geographic)

c. along the normal to the local ellipsoid which is confocal to the reference ellipsoid.

Appendix E

GRAVITATIONAL POTENTIAL OF A HOMOGENEOUS ELLIPSOID OF ROTATION

E.1. GRAVITATION IN ELLIPSOIDAL AND CYLINDRICAL COORDINATES.

Consider a planet-centered ellipsoid of rotation whose axis of symmetry is the y_3 axis. Let the y_1 and y_2 axes be fixed in the equatorial plane. If y_3 is the axis of a cylindrical coordinate frame, (s, λ, z), then Eichhorn (Ref. 95) gives the potential outside the ellipsoid as:

$$V = \pi a^2 b \gamma \rho \left\{ \frac{2}{c} \tan^{-1} \frac{c}{(b^2+\mu)^{1/2}} - \frac{s^2}{c^3} \left[\tan^{-1} \frac{c}{(b^2+\mu)^{1/2}} - \frac{c(b^2+\mu)}{a^2+\mu} \right] + \frac{2z^2}{c^3} \left[\tan^{-1} \frac{c}{(b^2+\mu)^{1/2}} - \frac{c}{(b^2+\mu)^{1/2}} \right] \right\} \qquad (E\text{-}1)$$

where:

a is the semi-major axis of the ellipsoid

b is its semi-minor axis

c is its focal distance

ρ is the density of the ellipsoid

γ is the Newtonian gravitational constant

μ is the positive solution of the equation:

$$\frac{s^2}{a^2+\mu} + \frac{z^2}{b^2+\mu} = 1$$

The potential is transformed into the ellipsoidal coordinates of Appendix C by the substitution:

$$s = c \cosh\xi \cos\eta$$

$$z = c \sinh\xi \sin\eta$$

$$a^2 + \mu = c^2 \cosh^2\xi$$

$$b^2 + \mu = c^2 \sinh^2\xi$$

whereupon after some lengthy algebra:

$$V = \frac{3}{4} \frac{\gamma m_p}{c} \left[2\theta \cos^2\eta + (2 - 3\cos^2\eta)(\theta \cosh^2\xi - \sinh\xi) \right] \qquad \text{(E-2)}$$

where:

$\tan\theta = \operatorname{csch}\xi$

m_p is the mass of the homogeneous ellipsoid $= \frac{4}{3}\pi a^2 b \rho$.

This sdution is readily checked by verifying that $\nabla^2 V = 0$. ∇^2 in ellipsoidal coordinates is given in Equation (D-17).

This expression is equivalent to that obtained independently by Professor W. Wrigley of the M.I.T. Department of Aeronautics and

Astronautics in an unpublished memorandum.

The components of gravitation in ellipsoidal coordinates are:

$$\overline{G} = \overline{\nabla}\, V$$

$$\overline{G} = \frac{1}{c(\cosh^2\xi - \cos^2\eta)^{1/2}}\left[\hat{\xi}\frac{\partial V}{\partial \xi} + \hat{\eta}\frac{\partial V}{\partial \eta}\right]$$

$$G_\lambda = 0 \qquad \text{(E-3)}$$

$$G_\eta = \frac{3}{4}\frac{\gamma m_p}{c^2}\frac{\sin 2\eta}{(\cosh^2\xi - \cos^2\eta)^{1/2}}\left[-2\theta + 3(\theta\cosh^2\xi - \sinh\xi)\right]$$

$$G_\xi = \frac{3}{4}\frac{\gamma m_p}{c^2}\frac{1}{(\cosh^2\xi - \cos^2\eta)^{1/2}}\left[-2\cos^2\eta\,\operatorname{sech}\xi + (2 - 3\cos^2\eta)(\theta\sinh 2\xi - 2\cosh\xi)\right]$$

These components are shown in Section 2. F. 8., not to represent the actual field of the Earth to navigational accuracy.

E. 2. GRAVITY IN ELLIPSOIDAL COORDINATES.

The gravity potential, U, is V + V' where V' in ellipsoidal coordinates is given by Equation (2-7). The components of gravity are $\overline{g} = \overline{\nabla}\, U$:

$$g_\lambda = 0 \qquad \text{(E-4)}$$

$$g_\eta = \frac{\sin 2\eta}{c(\cosh^2\xi - \cos^2\eta)^{1/2}}\left\{\frac{3}{4}\frac{\gamma m_p}{c}\left[-2\theta + 3(\theta\cosh^2\xi - \sinh\xi)\right] - \frac{\omega_{ip}^2 c^2}{2}\cosh^2\xi\right\}$$

$$g_\xi = \frac{1}{c(\cosh^2\xi - \cos^2\eta)^{1/2}}\left\{\frac{3}{4}\frac{\gamma m_p}{c}\left[-2\cos^2\eta\,\mathrm{sech}\,\xi + (2-3\cos^2\eta)\times\right.\right.$$

$$\left.\left.\times(\theta\sinh 2\xi - 2\cosh\xi)\right] + \frac{\omega_{ip}^2 c^2}{2}\cos^2\eta\sinh 2\xi\right\}$$

The gravity force on the surface of a fluid ellipsoid in static equilibrium must be normal to that surface. Thus on an ellipsoid of meridian eccentricity ϵ, g_η must be zero. Hence from the preceding equation:

$$\frac{\omega_{ip}^2}{4\pi\rho\gamma} = \sinh\xi_0\left[-\theta_0 + \frac{3}{2}\left(\theta_0\cosh^2\xi_0 - \sinh\xi_0\right)\right] \quad \text{(E-5)}$$

This is the condition which must be satisfied by a rotating homogeneous ellipsoid of rotation, held together by its own gravitation. It is the equation of the MacLaurin ellipsoids, Figure 2-3.

E.3. GRAVITATIONAL POTENTIAL IN SPHERICAL COORDINATES.

The potential is needed in spherical coordinates when navigating in such coordinates. Though the potential in cylindrical or ellipsoidal coordinates is expressible in closed form, the potential in spherical coordinates is not. The conversion from the closed form ellipsoidal expression to the infinite series in spherical coordinates is accomplished as follows. Outside the ellipsoid $\cosh^2\xi > 1$ and $\tan\theta$ is small.

Thus θ can be expanded in the series:

$$\theta = \tan^{-1}\{\operatorname{csch}\xi\} = \frac{1}{\sinh\xi} - \frac{1}{3\sinh^3\xi} + \frac{1}{5\sinh^5\xi} - \cdots$$

and the potential becomes:

(E-6)

$$V = \frac{3}{4}\frac{\sigma m_p}{c}\left[2\theta\cos^2\eta + (2-3\cos^2\eta)(\theta\cosh^2\xi - \sinh\xi)\right]$$

$$= \frac{3}{4}\frac{\sigma m_p}{c}\frac{4}{\sinh\xi}\left[\frac{1}{3} - \frac{1}{15}\frac{1+\cos^2\eta}{\sinh^2\xi} + \frac{1}{35}\frac{1+2\cos^2\eta}{\sinh^4\xi} - \cdots\right]$$

This series is converted to spherical coordinates term-by-term.

From Appendix C:

$$\tan\eta = \coth\xi \tan L_c$$

$$\cos^2\eta = \frac{\sinh^2\xi\cos^2 L_c}{\sinh^2\xi + \sin^2 L_c} \qquad (E\text{-}7)$$

The radius of the ellipsoid is given by Equation (C-13g). Combining:

$$\cos^4\eta - \left(1 + \frac{r^2}{c^2}\right)\cos^2\eta + \frac{r^2}{c^2}\cos^2 L_c = 0$$

which can be solved for $\cos^2\eta$:

$$\cos^2\eta = \cos^2 L_c\left[1 - \frac{c^2}{r^2}\sin^2 L_c + \left(\frac{c}{r}\right)^4(2\cos^4 L_c - 3\cos^2 L_c + 1)\right] \qquad (E\text{-}8)$$

From the equation for r, to order $\left(\frac{c}{r}\right)^4$:

$$\frac{1}{\sinh\xi} = \left(\frac{c}{r}\right)\left[1 + \frac{1}{2}\left(\frac{c}{r}\right)^2\cos^2 L_c + \left(\frac{c}{r}\right)^4\left(\frac{3}{8}\cos^4 L_c - \frac{1}{2}\sin^2 L_c\cos^2 L_c\right) - \cdots\right] \qquad (E\text{-}9)$$

$$\frac{1}{\sinh^2\{} = \left(\frac{c}{\pi}\right)^2\left[1+\left(\frac{c}{\pi}\right)^2\cos^2 L_c - \left(\frac{c}{\pi}\right)^4\cos^2 L_c\left(1-2\cos^2 L_c\right)+ \cdots\right]$$

$$\frac{1}{\sinh^4\{} = \left(\frac{c}{\pi}\right)^4$$

$$V = \frac{\gamma m_p}{\pi}\left[1-\frac{1}{5}\left(\frac{c}{a}\right)^2\left(\frac{a}{\pi}\right)^2 P_2(\sin L_c) + \frac{3}{35}\left(\frac{c}{a}\right)^4\left(\frac{a}{\pi}\right)^4 P_4(\sin L_c) + \cdots\right] \qquad (E\text{-}10)$$

where $P_n(\sin L_c)$ is the Legendre function of the first kind of order n. Equation (E-10) is the symmetrical spherical harmonic expansion of the potential. It is used in Section 2. F. 5.

Thus if a rotating planet had the shape of a homogeneous ellipsoid of rotation whose meridian eccentricity was ϵ, the theoretical coefficients of the spherical harmonic expansion of its gravitational potential would be:

$$J_2 = -\frac{1}{5}\epsilon^2$$

$$J_3 = 0$$

$$J_4 = +\frac{3}{35}\epsilon^4$$

Figure 2-11 compares these to the measured values for the Earth. They differ from the measured values because of systematic density irregularities in the Earth. An inhomogeneous ellipsoidal model of a planet is discussed in Section 2. F. 5.

Appendix F

THE ORBIT OF A POINT MASS CIRCLING A FINITE-SIZED PRIMARY

The fields of astronomy, geodesy and navigation are concerned with the orbits of the planets about the Sun and of the natural satellites about the planets. The character of the gravitational field surrounding a planet is inferred from motions of its natural and artificial satellites. Furthermore, artificial satellites can be used for geodetic triangulation and for navigation. This appendix summarizes the motion of a small satellite circling a large primary. Oblateness and rotation of the primary, atmospheric drag and relativistic effects are considered.

Consider the motion of two isolated point masses acted on only by their mutual gravitational attraction. It is well-known that if an inertially-non-rotating coordinate frame is erected at either mass particle, the other describes an unvarying, plane, elliptic orbit about the first as focus. The orbit can be predicted fully by specifying five

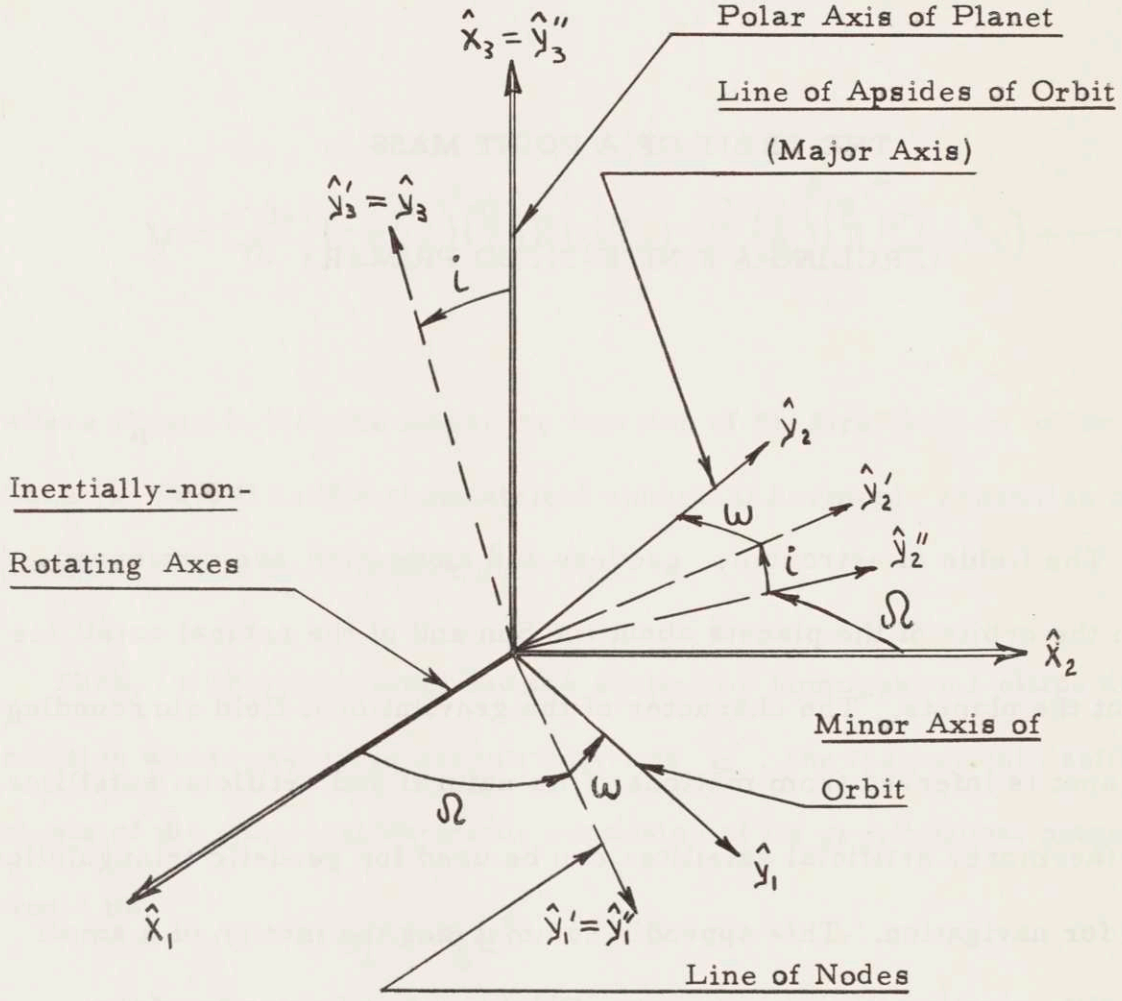

Figure F-1

ORBITAL ELEMENTS OF A SATELLITE

space parameters and two time parameters as follows.

In Figure F-1, (x_1, x_2, x_3) is an inertially-non-rotating coordinate frame whose origin is at the particle, m_2. (y_1, y_2, y_3) is a triad whose origin is also at m_2 but which is oriented so $y_1 - y_2$ lies in the plane of the elliptic orbit, $\hat{y}_1$ being the line of apsides (major axis).

The y_i coordinate frame can be oriented relative to the x_i frame by specifying three successive Euler angles in the following order. The symbols used are those conventionally used in astronomy (Ref. 200, pg. 248):

a. Let $(\hat{y}_1, \hat{y}_2, \hat{y}_3)$ initially coincide with $(\hat{x}_1, \hat{x}_2, \hat{x}_3)$ respectively.

b. Rotate the y_i frame through the angle, Ω, about the $\hat{x}_3$ axis to $(\hat{y}_1'', \hat{y}_2'', \hat{y}_3'')$.

c. Rotate the y_i'' frame through the angle, i, about the $\hat{y}_1''$ axis, the "line of nodes," to $(\hat{y}_1', \hat{y}_2', \hat{y}_3')$.

d. Rotate the y_i' frame through the angle, ω, about the $\hat{y}_3'$ axis to $(\hat{y}_1, \hat{y}_2, \hat{y}_3)$, the position of the actual orbit.

The elliptic orbit intercepts the line of nodes at two points 180° apart. That point where the satellite crosses the $\hat{x}_1 - \hat{x}_2$ plane from $-x_3$ to $+x_3$ is the "ascending node" and the other is the "descending node."

For astronomical purposes, the $\hat{x}_1$ reference is commonly an equinox. A fixed equinox is inertially-non-rotating but the mean or true equinox is not. When Ω is measured along the ecliptic from an equinox, as in heliocentric problems, it is called the "longitude of the ascending node." When Ω is measured along the celestial equator from an equinox, as in planetocentric problems, it is called the "right ascension of the ascending node." i is the "inclination" and is referred either to the ecliptic or to the celestial equator, when navigating on the Earth. ω is the "argument of perigee" or "argument of perihelion" measured from the line of nodes to the periapse side of the line of apsides. The angle $\pi = \Omega + \omega$, called the "longitude or right ascension of the periapse," is often used in astronomy though it is not an angle in the conventional sense.

Having determined the orientation of the ellipse, its size and shape are fully specified by the semi-major axis, a, or semi-latus rectum, p, and by the eccentricity, ϵ (see Appendix C).

This completes the discussion of the geometry of the orbit. Ω, ω, i, a and ϵ fully describe the ellipse. In order to predict the location of the moving satellite on the ellipse at any time, two more parameters are needed. The mass of the primary plus secondary $\times$ the Newtonian constant of gravitation, $\gamma (m_1 + m_2)$, or the satellite period, τ, is needed to set the dynamic time scale. These are

related by:

$$\tau = \frac{2\pi a^{3/2}}{\sqrt{\gamma(m_1 + m_2)}}$$

The final parameter is an intial condition, t_0, which might be the time of crossing the ascending node or of crossing the periapse. These seven parameters enable the future position of the satellite to be calculated at any time.

If the secondary remains a point mass but the primary is allowed to have finite size, three complications arise:

a. The primary's gravitational potential may not simply be $V = \frac{\gamma m_2}{r}$ but may include all tesseral harmonics (Appendix B).

b. The primary may have an atmosphere through which the satellite travels. Aerodynamic drag will then affect the orbit.

c. Rotation of the primary will cause periodic forces to act on the satellite if the gravitational field is not symmetric about the axis of rotation or if appreciable aerodynamic drag exists.

The motions of real planets and satellites are additionally perturbed by the other masses in the universe.

For the simplified case of an isolated primary-satellite system in which aerodynamic drag is negligible, it is found that the satellite in general traverses a non-planar, non-closed curve. However, if $\gamma (m_1 + m_2)$ is known and if, at any time, the satellite's position,

$\bar{r}$, and velocity, $\bar{v}$, relative to an inertially-non-rotating coordinate frame whose origin is at the mass center of the primary are known, an instantaneous or "osculating" ellipse can be derived. The satellite is regarded as tracing this osculating ellipse which is continually changing.

a. $\bar{r} \times \bar{v}$ defines the normal to the instantaneous plane of the orbit. The direction of this nprmal fixes the instantaneous Ω and i .

b. The instantaneous semi-latus rectum is:

$$p = \frac{(\bar{\pi} \cdot \bar{v})^2}{\gamma(m_1 + m_2)}$$

c. The semi-major axis is:

$$\frac{1}{a} = \frac{2}{|\bar{r}|} - \frac{\bar{v} \cdot \bar{v}}{\gamma(m_1 + m_2)}$$

d. The eccentricity is found from:

$$\epsilon^2 = 1 - \frac{p}{a}$$

e. If the angle from the periapse to $\bar{r}$ is θ:

$$\frac{\epsilon \sin \theta}{1 + \epsilon \cos \theta} = \tan \cos^{-1} \frac{\bar{\pi} \cdot \bar{v}}{|\bar{r}||\bar{v}|}$$

If the gravitational potential around the primary is symmetrical about the x_3 axis, then a , ϵ and i show periodic oscillations with constant mean values when taken over a full period whereas Ω and ω each show a periodic oscillation superimposed on a secular trend Ref. 132). If the potential does not depart appreciably from that of a

point mass, the amplitude of these oscillations is small and a mean osculating orbit is defined which is described by the mean values of $a, \epsilon, \Omega, \omega$ and i and which partakes only in the secular trend of Ω and ω. The mean osculating orbit is described by a_0, ϵ_0, i_0, Ω_0 and ω_0 where the last two have constant rates of change. Hence, the nominal satellite motion is a precessing ellipse in a precessing plane because ω_0 and Ω_0 change. Superimposed on the precession of the ellipse is a slight motion in and out of the plane because ω, Ω and i oscillate and a slight change in the size and shape of the ellipse as a and ϵ oscillate. As long as these oscillations about the mean values are small the orbit can be defined by the seven ellipse parameters: a_0, i_0, Ω_0, ω_0, ϵ_0, τ and t_0 where ω_0 and Ω_0 change slowly with time.

The motion of a satellite about a rotating primary whose potential contains all tesseral harmonics has not yet been solved. Fortunately the present accuracy of measurement usually permits the assumption of a potential distribution which is symmetric about the x_3 axis. Such a distribution has been expressed in many ways by many authors (see Refs. 93, pg. 230; 121, pg. 136; 132. pg.12 134, pg. 902 and 143, pg. 310) but in this thesis will be written as in Equation (2-19). In that case, the secular precession is described by the equations:

$$\frac{d\Omega_0}{dt} = \sum_{n=2}^{\infty} a_n J_n$$

$$\frac{d\omega_0}{dt} = \sum_{n=2}^{\infty} b_n J_n$$

where the a_n and b_n depend on the orbit radius, inclination, shape, etc. Each of the a_n and b_n are zero for odd n and for n=0. Odd n terms cause oscillations but not secular changes in these orbital elements (Ref. 188, pg. 903). The even terms cause ω_o and Ω_o to change secularly and also cause perturbations in the values of all the elements. Combining the results of Singer (Ref. 143), Cook (Ref. 93), and O'Keefe (Ref. 134), the a_n and b_n are expressed in terms of the satellite's angular velocity, ω_a, between successive crossings of the ascending node:

$$\frac{d\Omega_o}{dt} = \frac{3}{2}\omega_a\left(\frac{a}{p}\right)^2\cos i\left[J_2 + \frac{3}{2}J_2^2\left(\frac{a}{p}\right)^2\left(\frac{19}{12}\sin^2 i - 1\right) - \frac{105}{112}J_4\left(\frac{a}{p}\right)^2\left(7\sin^2 i - 4\right)\right]$$

$$\frac{d\omega_o}{dt} = -3\omega_a\left(\frac{a}{p}\right)^2 J_2\left(1 - \frac{5}{4}\sin^2 i\right)$$

O'Keefe (Ref. 134, pg. 903) states that there is much controversy over the form of the higher order terms in these equations. Notice that because J_2 is negative, $\frac{d\Omega_o}{dt}$ is negative and the line of nodes regresses in a direction opposite to the direction of travel of the satellite. $\frac{d\omega_o}{dt}$ has a positive sign for $\sin^2 i < \frac{4}{5}$ so the line of apsides may advance or regress.

Artificial satellites may approach close enough to the primary so that the drag force is an appreciable fraction of the local weight but not so large that drag dominates. In such a case, the orbit is nearly that discussed above, with additional drag perturbations. The drag force acts

in a direction opposite to the velocity of the satellite relative to the atmosphere. The calculation of the drag perturbation is difficult since the angular velocity and density distribution of the outer atmosphere are uncertain. Furthermore, the satellite tumbles in its orbit causing the drag force to vary with attitude.

The significant alterations in the orbit caused by drag are, from Nielsen (Ref. 132), that the semi-major axis, a, the eccentricity, e, and the period, T, decrease secularly with superimposed oscillations at the satellite orbital frequency. The apsides rotate so rapidly that they mask the advance of the perigee caused by oblateness. Because of rotation of the atmosphere, Ω and i acquire slight secular rates.

Cook (Ref. 93, pg. 232) estimates that for artificial satellites of the Earth, the perturbations caused by other masses in the universe have an effect less than 10^{-4} that of the oblateness.

For completeness, the well-known advance of the apsides caused by relativistic effects derives from an addition to the gravitational potential of:

$$V = \frac{\gamma(m_1+m_2)}{r}\left(\frac{V_{horizontal}}{c}\right)^2\left(\frac{a}{r}\right)^2$$

This has almost the same effect as an addition to J_2 but it produces a minute advance of the apsides and no change in Ω. For close satellites where such an effect might accumulate to an observable value, atmospheric drag masks it. It is observable at least in the orbits of Mars

and Mercury and with less certainty in the orbits of Venus and the Earth (Ref. 162, pg. 6).

In addition, the rotation of the primary "drags" inertial space along (Thirring Effect) at a slight angular velocity thus causing an apparent additional precession of the periapse (Ref. 176). This effect is not observable in any planet or satellite of the solar system.

Appendix G

EXAMPLE OF AN OBLIQUE COORDINATE FRAME

Consider the two-dimensional oblique coordinate frame shown in Figure G-1. The coordinate axes are non-orthogonal straight lines.

Since V^i, the contravariant components, sum up to $\overline{V}$ by the parallelogram rule, the transformation equations from y_i to z^j are obtained simply by resolving the z^j components into the Cartesian axes, y_i :

$$\begin{aligned} y_1 &= z^1 \cos 30° + z^2 \cos 45° \\ y_2 &= z^1 \sin 30° + z^2 \sin 45° \end{aligned} \tag{G-1}$$

Then the Jacobian matrix is:

$$[a] = \left[\frac{\partial y_i}{\partial z^j}\right] = \begin{bmatrix} \cos 30° & \cos 45° \\ \sin 30° & \sin 45° \end{bmatrix}$$

$$[a^T] = \begin{bmatrix} \cos 30° & \sin 30° \\ \cos 45° & \sin 45° \end{bmatrix} \tag{G-2}$$

$$[a^{-1}] = \frac{1}{\sin 15°} \begin{bmatrix} \sin 45° & -\cos 45° \\ -\sin 30° & \cos 30° \end{bmatrix}$$

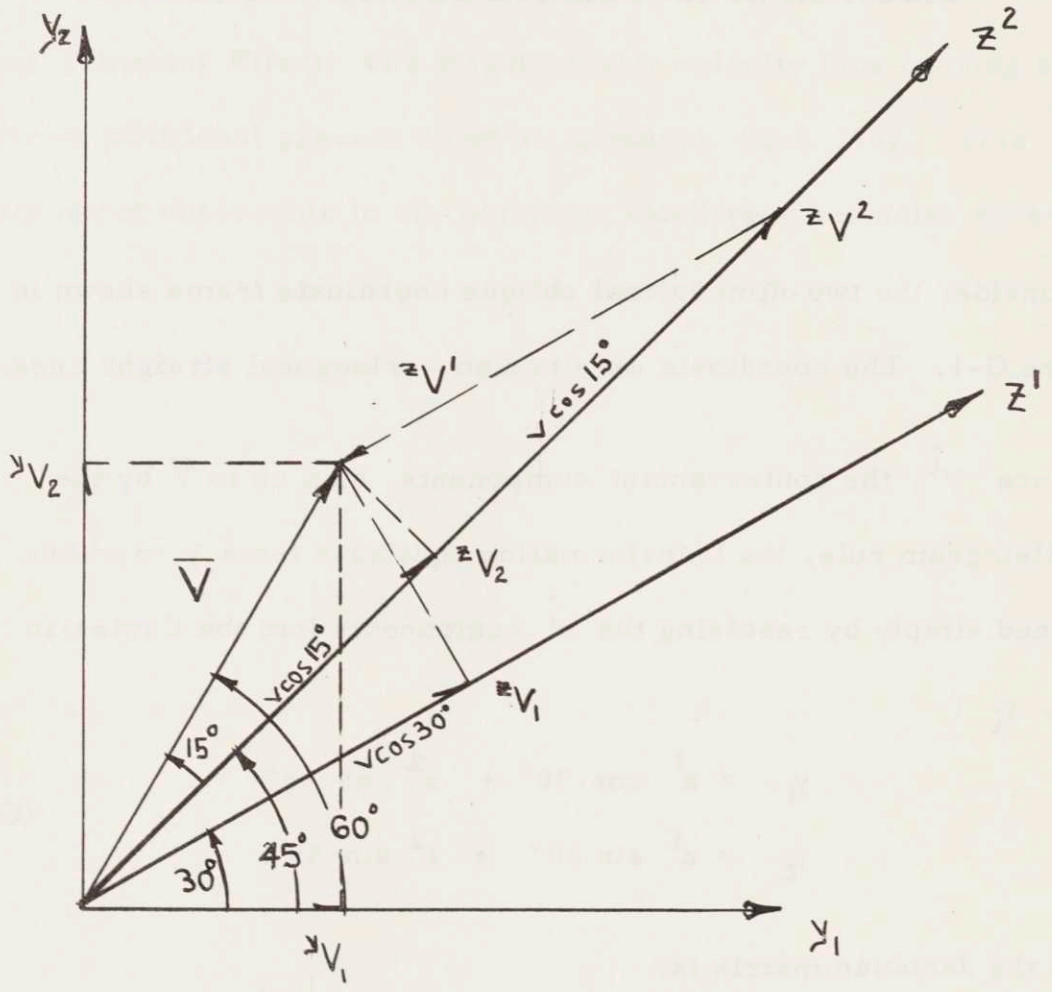

Figure G-1

AN EXAMPLE OF AN OBLIQUE COORDINATE FRAME

z^1 and z^2 are non-orthogonal coordinate axes

${}^zV^i$ and ${}^zV_i$ are contravariant and covariant components of $\overline{V}$

The covariant and contravariant elements of the metric tensor are:

$$[g_{ij}] = [a^T][a] = \begin{bmatrix} 1 & \cos 15^\circ \\ \cos 15^\circ & 1 \end{bmatrix} \qquad \text{(G-3)}$$

$$[g^{ij}] = [g_{ij}^{-1}] = \frac{1}{\sin^2 15} \begin{bmatrix} 1 & -\cos 15^\circ \\ -\cos 15^\circ & 1 \end{bmatrix} \qquad \text{(G-4)}$$

Since these matrices are not diagonal, the coordinates are formally shown to be non-orthogonal.

In Figure G-1, the vector, $\overline{V}$, has the Cartesian components:

$$[{}^y V_i] = V \begin{bmatrix} \cos 60^\circ \\ \sin 60^\circ \end{bmatrix} \qquad \text{(G-5)}$$

These can be transformed into covariant and contravariant components in the z frame:

$${}^z V_i = \frac{\partial y_j}{\partial z^i} {}^y V_j = a^T_{ij} {}^y V_j$$

$$[{}^z V_i] = [a^T][{}^y V_j] = V \begin{bmatrix} \cos 30^\circ \\ \cos 15^\circ \end{bmatrix} \qquad \text{(G-6)}$$

$${}^z V^i = \frac{\partial z^i}{\partial y_j} {}^y V_j = a^{-1}_{ij} {}^y V_j$$

$$[{}^z V^i] = [a^{-1}][{}^y V_j] = V \begin{bmatrix} -1 \\ 2\cos 15^\circ \end{bmatrix} \qquad \text{(G-7)}$$

The relations connecting the covariant and contravariant components

of $\overline{V}$:

$$V_i = g_{ij} V^j \tag{4-14}$$

$$V^i = g^{ij} V_j \tag{4-15}$$

can be verified as follows:

$$[V_i] = [g_{ij}][V^j] = \begin{bmatrix} 1 & \cos 15^\circ \\ \cos 15^\circ & 1 \end{bmatrix} V \begin{bmatrix} -1 \\ 2\cos 15^\circ \end{bmatrix} = V \begin{bmatrix} \cos 30^\circ \\ \cos 15^\circ \end{bmatrix} \tag{G-8}$$

$$[V^i] = [g^{ij}][V_j] = \frac{1}{\sin^2 15^\circ} \begin{bmatrix} 1 & -\cos 15^\circ \\ -\cos 15^\circ & 1 \end{bmatrix} V \begin{bmatrix} \cos 30^\circ \\ \cos 15^\circ \end{bmatrix} = V \begin{bmatrix} -1 \\ 2\cos 15^\circ \end{bmatrix}$$

The covariant and contravariant components of $\overline{V}$ can also be found by geometric resolution of $\overline{V}$ as in Figure G-1. Because the scale factors are unity, the covariant components are the orthogonal projections of $\overline{V}$ onto the z^1 and z^2 axes. The contravariant components are the lengths of the sides of a parallelogram parallel to the coordinate axes:

$$[V_i] = V \begin{bmatrix} \cos 30^\circ \\ \cos 15^\circ \end{bmatrix}$$

$$[V^i] = V \begin{bmatrix} -1 \\ 2\cos 15^\circ \end{bmatrix}$$

These are identical to the components obtained by the formal method of Equations (G-6) and (G-7).

The physical components are the orthogonal projections of $\overline{V}$ onto the z^1 and z^2 axes since the scale factors are unity. Hence the physical components are identical to the covariant components in this case.

BIOGRAPHICAL NOTE

Myron Kayton was born in New York City on April 26, 1934. He attended New York's public primary schools and graduated from the Bronx High School of Science in June, 1951. He was awarded the degrees of Bachelor of Mechanical Engineering from The Cooper Union in June, 1955 and Master of Science from Harvard University in June, 1956.

Mr. Kayton held the position of Assistant Systems Engineer with the Research and Advanced Development Division of the Avco Corporation from June, 1956 to September, 1957 and during the summer of 1958. He was employed during the summers of 1959 at Litton Industries and 1955 at Ford Instrument Company. He has been associated with the M.I.T. Instrumentation Laboratory since 1957.

In 1957, Mr. Kayton entered M.I.T. where he served as a teaching assistant for the fall term 1958-1959. He was a National Science Foundation Fellow at M.I.T. and Harvard. He also held a Sperry Gyroscope Company fellowship at M.I.T. and a New York State University Scholarship at The Cooper Union. Mr. Kayton is the author of "Drift of an Attitude Control Gyro Platform During Sustained Acceleration,"

published in the Ramo-Wooldridge Second Ballistic Missiles Symposium (June, 1957) and coauthor (with Wrigley, Hovorka, et al.) of INERTIAL GUIDANCE-TERRESTRIAL AND INTERPLANETARY, published by M.I.T. as notes for a 1960 Special Summer Course.

Mr. Kayton is a former chapter President of Tau Beta Pi, Vice-President of Pi Tau Sigma and a member of Sigma Xi, Sigma Gamma Tau, A.S.M.E. and A.R.S. He is married and has twin daughters.

BIBLIOGRAPHY

References in the Text Correspond

to Numbered Items in this Bibliography

A. NAVIGATION

1. Anderson, J.E. "Analysis of Errors in Inertial Navigation Systems." Minneapolis-Honeywell Regulator Co. Unpublished note, no date. 11 pgs.

2. Berger, F.B. "Application of Doppler Techniques to Space Navigation," NAVIGATION. 6: 460-464 (Autumn, 1959).

3. Blazek, H. "The Performance of Inertial Components on an Unstabilized Base." A.R.S. Paper 775-59 (April, 1959). 14 pgs.

4. Bowditch, N. AMERICAN PRACTICAL NAVIGATOR. U.S. Navy Hydrographic Office Pub. No. 9. Washington: U.S. Government Printing Office, 1958. 1524 pgs.

5. Broxmeyer, C. FOUCAULT PENDULUM EFFECT IN A SCHULER TUNED SYSTEM. M.I.T. Instrumentation Laboratory Report E-654 (July, 1957). 26 pgs.

6. Campbell, M.E. and J.M. Slater. "A Precision Gyrocompass for Use on Fixed Bases," NAVIGATION. 6: 347-353 (Summer, 1959).

7. Cannon, R.H. "Kinematic Drift of Single-Axis Gyroscopes." A.S.M.E. Paper 57-A-72 (December, 1957). 4 pgs.

8. Cannon, R.H. and D.P. Chandler. "Stable Platforms for High Performance Aircraft." I.A.S. Preprint 738 (June, 1957). 22 pgs.

9. Clemence, G.M. "Interplanetary Navigation," PROCEEDINGS OF THE I.R.E. 48: 497-499 (Apr., 1960).

10. Colin, R.I. and S.H. Dodington. PRINCIPLES AND FEATURES OF TACAN. Clifton, N.J.: Federal Telephone and Radio Co., 1956. 30 pgs.

11. Davidson, M. (editor). THE GYROSCOPE AND ITS APPLICATIONS. London: Hutchinson's Scientific and Technical Publications, 1946. 256 pgs.

12. Davis, B.W. "Factors Contributing to Errors in Inertial Navigation Systems," Indianapolis, Ind.: G.M. Corp., Allison Div. Report EDR 1383. April, 1959. 39 pgs.

13. Deimel, R.F. MECHANICS OF THE GYROSCOPE. New York: The MacMillan Co., 1929. 192 pgs.

14. Dillon, R.S. "Vibration Effects on the Design of a Stellar-Inertial Guidance System." Hawthorne, Calif.: Northrop Corp., Nortronics Div., Feb., 1959. 22 pgs.

15. Draper, C.S. "The Inertial Gyro- an Example of Basic and Applied Research," AMERICAN SCIENTIST. 48: 9-19 (March, 1960).

16. Draper, C.S., W. Wrigley and L.R. Grohe. "The Floating Integrating Gyro and its Application to Geometrical Stabilization Problems on Moving Bases." I.A.S. Publication FF-13, 1955. 111 pgs.

17. Dubner, H. "Long Range Detection by Star Occultation," ADVANCES IN ASTRONAUTICAL SCIENCES, Vol. 4. New York: Plenum Press, Inc., Nov., 1958. pgs. 226-247.

18. Duncan, D.B. "Inertial Guidance and Space Navigation," NAVIGATION. 6: 30-33 (Spring, 1958).

19. Duncan, D.B. "Combined Doppler Radar and Inertial Navigation Systems," NAVIGATION. 6:321-327 (Spring, 1959).

20. Eaton, E.P. "Star Trackers," NAVIGATION. 6: 24-29 (Spring, 1958).

21. Eggers, A.L., "The Possibility of a Safe Landing," Chapter 13 in SPACE TECHNOLOGY edited by H.S. Siefert. New York: John Wiley and Sons, Inc., 1959. 53 pgs.

22. Ehricke, K.A. SPACE FLIGHT, ENVIRONMENT AND CELESTIAL MECHANICS. Vol. 1. Princeton, N.J.: D. Van Nostrand Co., Inc., 1960. 513 pgs.

23. Finkel, M. "High-Speed Inertial Platform Stabilization and Control." Hawthorne, Calif.: Northrop Corp., Nortronics Div., 1960. 29 pgs.

24. Fried, W.R. "Performance Analysis of Doppler Navigating Systems, NAVIGATION. 6: 284-292 (Spring, 1959).

25. General Precision Laboratory. MANUAL FOR RADAN 500 DOPPLER NAVIGATING SYSTEM. No date. 16 pgs.

27. Golay, M.J.E. "Velocity of Light and Measurement of Interplanetary Distances," SCIENCE. 131: 31-32 (Jan. 1, 1960).

28. Goodman, L.E. and A.R. Robinson. "Effect of Finite Rotations on Gyroscopic Sensing Devices," A.S.M.E. Paper No. 57-A-30. Dec., 1957. 4 pgs.

29. Guier, W.H. and G.C. Weiffenbach. "A Satellite Doppler Navigating System." Proceedings of the I.R.E. 48: 507-516 (April, 1960).

30. Henry, W.O. "Some Developments in Loran," JOURNAL OF GEOPHYSICAL RESEARCH. 65: 506-513 (Feb., 1960).

31. Horsfall, R.B. "Stellar-Inertial Navigation," Transactions of the I.R.E., Professional Group on Aeronautical and Navigational Electronics. ANE-5: 106-114 (June, 1958).

32. Hutchinson, R.C. GEOMETRICAL AND ASTRONOMICAL ASPECTS OF EMPLOYING A STAR TRACKER TO CORRECT THE ATTITUDE OF A STABLE PLATFORM. M.I.T. Instrumentation Laboratory Report R-255. September, 1959. 111 pgs.

33. Iverson, J.R. "Advanced Doppler Navigation for the U.S. Army," AERO/SPACE ENGINEERING. 17: 81-85 (May, 1958).

34. Jensen, L.K., B.H. Evans and R.B. Clark. "Evaluation of Precision Gyros for Space Boost Guidance Applications." A.R.S. Paper 1175-60 (May, 1960). 11 pgs.

35. Jordan, P.W. "Hiran Instrumental Developments," JOURNAL OF GEOPHYSICAL RESEARCH. 65: 462-466 (Feb., 1960).

36. Klass, P.J. "Cryogenic Gyro Cuts Random Drift Rate," AVIATION WEEK. 72: 72-74 (Feb. 1, 1960).

37. Knight, F. A GUIDE TO OCEAN NAVIGATION. New York: St. Martin's Press, Inc., 1959. 177 pgs.

38. Larmore, L. "Celestial Observations for Space Navigation," AERO/SPACE ENGINEERING. 18: 37-42 (Jan., 1959).

39. Leshnover, S. "Prediction of Anisoelastic and Vibropendulous Effects on Inertial Navigation Systems Performance in Linear Random Vibration Environments," I.A.S. Proceedings of the National Specialists Meeting on Guidance of Aerospace Vehicles. May, 1960. pgs. 220-250.

40. Litton Industries. "Descriptive Literature. Litton LN-3 Inertial Navigation System for the F-104-5 Aircraft. Jan., 1959. 16 pgs.

41. McMurray, L.R. "Alignment of an Inertial Autonavigator." A.R.S. Technical Paper (unnumbered) given at the Semi-Annual Meeting in Los Angeles, May, 1960. 20 pgs.

42. Mitsutomi, T. "Characteristics and Stabilization of an Inertial Platform," Transactions of the I.R.E. ANE-5: 95-105 (June, 1958).

43. Moody, A.B. "Navigation Using Signals from High-Altitude Satellites," Proceedings of the I.R.E. 48: 500-506 (April, 1960).

44. Myers, G.H. and T.H. Thompson. "Guidance Constraints on the Tiros I Orbit." A.R.S. Paper 1113-60, May, 1960. 13 pgs.

45. Nash, W.B. "Consideration of Various Terrestrial Coordinate Systems," NAVIGATION. 3: 123-128 June, 1952).

46. Newton, G.C. "Inertial Guidance Limitations Imposed by Fluctuation Phenomena in Gyroscopes," Proceedings of the I.R.E. 48:520-527 (April, 1960).

47. Newton, R.R. "Applications of Doppler Measurements to Problems in Relativity, Space Probe Tracking and Geodesy." ibid. pg. 754-758.

48. O'Donnell, C.F. "Inertial Navigation," JOURNAL OF THE FRANKLIN INSTITUTE. 266: 257-277 (Oct., 1958) and 266: 373-402 (Nov., 1958).

49. Ortman, F.W. and H.M. Green. "Isoelasticity in Gyro Rotor Bearings," A.S.M.E. Paper No.57-F-34. Sept., 1957. 29 pgs.

50. Owen, S.D. "Evaluation of Hiran Networks," JOURNAL OF GEOPHYSICAL RESEARCH. 65: 467-471 (Feb., 1960).

51. Pfeiffer, C.G. "Rudimentary Launch Guidance Methods for Deep Space Missions." A.R.S. Paper No. 1172-60 (May, 1960). 19 pgs.

52. Rawlings, A.L. THE THEORY OF THE GYROSCOPIC COMPASS AND ITS DEVIATIONS. New York: The MacMillan Co., 1944. Second Edition. 182 pgs.

53. Richardson, K.I.T. THE GYROSCOPE APPLIED. London: Hutchinson's Scientific and Technical Publications, 1954. 384 pgs.

54. Rickey, F. "An Inertial Navigator's View of Old and New Gyroscopes," NAVIGATION. 6: 465-469 (Autumn, 1959).

55. Roberson, R.E. "Gravitational Torque on a Satellite Vehicle," JOURNAL OF THE FRANKLIN INSTITUTE. 265: 13-22 (Jan., 1958).

56. Roberson, R.E. "Torques on a Satellite Vehicle from Internal Moving Parts." A.S.M.E. Paper No. 57-A-39 (Dec., 1957). 5 pgs.

57. Russel, W.T. "Inertial Guidance for Rocket-Propelled Missiles," JET PROPULSION. 28: 17-24 (Jan., 1958).

58. St. Lawrence, W.P. "Submarine Navigation," NAVIGATION. 6: 343-346 (Summer, 1959).

59. Sandretto, P.C. ELECTRONIC AVIGATION ENGINEERING. New York: International Telephone and Telegraph Corp., 1958. 771 pgs.

60. Scarborough, J.B. THE GYROSCOPE; THEORY AND APPLICATIONS. New York: Interscience Publishers, 1958. 257 pgs.

61. Schock, L.L. "Navigation of a Guided Missile Ship," NAVIGATION. 5: 299-302 (Summer, 1957).

62. Shoemaker, G.B. "An Extension of the Geographic Coordinate System as Applied to Automatic Ground Position Computation," NAVIGATION. 6: 370-373 (Summer, 1959).

63. Slater, J.M. "Better Inertial Instruments," CONTROL ENGINEERING. 7: 88-92 (Feb., 1960).

64. Slater, J.M. "Gyroscopes for Inertial Navigators." A.S.M.E. Paper No. 57-SA-39 (June, 1957). 7 pgs.

65. Slater, J.M. "Choice of Coordinate Systems in Inertial Navigation," NAVIGATION. 5: 58-62. (June, 1956).

66. Slater, J.M. "The Measurement and Integration of Acceleration in Inertial Navigation." A.S.M.E. Paper No. 56-A-160 (Nov., 1956). 11 pgs.

67. Slater, J.M. and D.E. Wilcox. "How Precise are Inertial Components?" CONTROL ENGINEERING. 5: 86-90 (July, 1958).

68. Spence, W.N. "On the Adequacy of ICBM Guidance Capability for a Mars Launch." A.R.S. Paper No. 1174-60 (May, 1960). 20 pgs.

69. Stearns, E.V. "Interplanetary Applications of Automatic Navigation," ADVANCES IN ASTRONAUTICAL SCIENCES, Vol. 2. New York: Plenum Press, Inc., 1958. Paper Number 40. 12 pgs.

70. Stevens, F. "Trends in Inertial Navigation." Hawthorne, Calif.: Northrop Corp., Nortronics Div., 1959. 10 pgs.

71. Stevens, F. "Aids to Inertial Navigation," NAVIGATION. 6: 166-175 (Autumn, 1958).

72. Stewart, R.M. "Some Effects of Vibration and Rotation on the Drift of Gyroscopic Instruments," A.R.S. JOURNAL. 29: 22-28 (Jan., 1959).

73. Stockard, J.L. "Dynamics of a Space Integrator." M.I.T. Sc.D. thesis, unpublished.

74. Tacan, Various Descriptive Articles. ELECTRICAL COMMUNICATION. 34: (Sept., 1957). 275 pgs.

75. Tillotson, J.H. "Effect of Azimuth Gimbal Orthogonality Errors." Unpublished note, Litton Industries. April, 1959. 6 pgs.

76. "U.S., Soviets Race to Develop Air-Launched Ballistic Missile," AVIATION WEEK. 72: 26-28 (Feb. 22, 1960).

77. Vaccaro, R.J. and D.D. Martin. "Investigation of Steady-State Anisoelastic Torques in Gimbal Systems under Vibration." A.S.M.E. Paper No. 58-A-250 (1958). 21 pgs.

78. Weiss, E. KINEMATIC AND GEOMETRIC RELATIONS ASSOCIATED WITH MOTION OVER THE EARTH. M.I.T. Instrumentation Laboratory Report R68. March, 1954.

79. Wilmoth, E.D. AN INVESTIGATION OF METHODS FOR DETERMINING GRAVITY ANOMALIES FROM AN AIRCRAFT. M. I. T. Sc.D. Thesis. Department of Aeronautics and Astronautics. May, 1959.

80. Wilson, R.E. and J.B. Lewis. "Cross-Coupling in Inertial Navigation Systems." AERO/SPACE ENGINEERING. 17: 60-65 (May, 1958).

81. Wrigley, W. SCHULER TUNING CHARACTERISTICS IN NAVIGATIONAL INSTRUMENTS. M.I.T. Instrumentation Laboratory Report 6398-S-14. April, 1951. 23 pgs.

82. Wrigley, W., R.B. Woodbury and J. Hovorka. "Inertial Guidance." I.A.S. Paper No. FF-16 (1957). 69 pgs.

83. Wrigley, W., J. Hovorka, M. Kayton, et al. INERTIAL GUIDANCE, TERRESTRIAL AND INTERPLANETARY. Cambridge, Mass.: M. I. T. (Summer, 1960). 3 volumes.

B. GEODESY

84. Anthony, M.L. "Planar Motions about an Oblate Planet," A.R.S. Paper No. 1231-60 (May, 1960). 22 Pgs.

85. Bascomb, W. "The Mohole," SCIENTIFIC AMERICAN. 200: 41-49 (April, 1959).

86. Blitzer, L. "Earth Oblateness in Terms of Satellite Orbit Periods," SCIENCE. 129: 329 (Feb. 6, 1959).

87. Bomford, G. GEODESY. London:Oxford at the Clarendon Press, 1952. 452 pgs.

88. Bondi, H. and T. Gold. "On the Damping of the Free Nutation of the Earth," MONTHLY NOTICES OF THE ROYAL ASTRONOMICAL SOCIETY. 115: 41-46 (1955).

89. Bouchard, H. and F.H. Moffitt. SURVEYING. Scranton, Pa.: International Textbook Co., 1959. Fourth ed. 664 pgs.

90. Brenner, J.L., R. Fulton and N. Sherman. "Symmetry of the Earth's Figure," A.R.S. JOURNAL. 30: 278-279 (March 1960).

91. Chovitz, B. and I. Fischer. " A New Determination of the Figure of the Earth from Arcs," TRANSACTIONS OF THE AMERICAN GEOPHYSICAL UNION. 37: 534-545 (Oct., 1956).

92. Cook, A.H. "Recent Developments in the Absolute Measurement of Gravity," BULLETIN GEODESIQUE. 44: 34-59 (June, 1957).

93. Cook, A.H. "Reports on the Progress of Geophysics Developments in Dynamical Geodesy," THE GEOPHYSICAL JOURNAL OF THE ROYAL ASTRONOMICAL SOCIETY. 2: 222-240 (Sept., 1959).

94. Cook, A.H. "The External Gravity Field of a Rotating Spheroid," ibid. pg. 199-214.

95. Eichhorn, H. "Bemerkung zum Potential eines homogenen Rotationsellipsoids," ASTRONOMISCHE NACHRICHTEN. 283: 249-250 (1957).

96. Ewart, D.G. "On the Motion of a Particle about an Oblate Spheroid," JOURNAL OF THE BRITISH INTERPLANETARY SOCIETY. 17: 162-168 (Nov.-Dec., 1959).

97. Fairbridge, R.W. "The Changing Level of the Sea," SCIENTIFIC AMERICAN. 202: 70-79 (May 1960).

98. Fischer, I. "A Tentative World Datum from Geoidal Heights Based on the Hough Ellipsoid and the Columbus Geoid," JOURNAL OF GEOPHYSICAL RESEARCH 64: 73-84 (Jan., 1959).

99. Fischer, I. "An Astrogeodetic World Datum from Geoidal Heights Based on the Flattening, f=1/298.3." JOURNAL OF GEOPHYSICAL RESEARCH. 65:2067-2076. (July, 1960).

100. Gardner, M. "The Games and Puzzles of Lewis Carroll," SCIENTIFIC AMERICAN. 202: 172(March, 1960). Quoted from Chas. L. Dodgson's SYLVIE AND BRUNO.

101. Gossett, F.R. MANUAL OF GEODETIC ASTRONOMY. U.S. Coast and Geodetic Survey Special Pub. 247. Washington: U.S. Government Printing Office, 1950. 344 pgs.

102. Heiskanen, W.A. "Geodesy," ENCYCLOPEDIA BRITANNICA. 10: 126-135 (1959).

103. Heiskanen, W.A. "Geodetic Base Lines," JOURNAL OF GEOPHYSCIAL RESEARCH. 65: 454-456 (Feb., 1960).

104. Heiskanen, W.A. "The Earth's Gravity," SCIENTIFIC AMERICAN. 193: 164-174 (Sept., 1955).

105. Heiskanen, W.A. "The Columbus Geoid," TRANSACTIONS OF THE AMERICAN GEOPHYSICAL UNION. 38: 841-848. (Dec., 1957).

106. Heiskanen, W.A. "The Size and Shape of the Earth," SCIENCE. 125: 558-563 (Mar.22, 1957).

107. Heiskanen, W.A. and F.A. Vening-Meinesz. THE EARTH AND ITS GRAVITY FIELD. New York: McGraw-Hill Book Co., 1958. 470 pgs.

108. Henriksen, S.W., S.H. Genatt, M.Q. Marchant and C.D. Batchlor. "Surveying by Occultation," TRANSACTIONS OF THE AMERICAN GEOPHYSICAL UNION. 38: 651-656 (Oct., 1957).

109. Hinks, A.R. MAP PROJECTIONS. London: Cambridge at the University Press, 1912. 126 pgs.

110. Hirvonen, R.A. "Gravity Anomalies and Deflections of the Vertical Above Sea Level," Mapping and Charting Research Laboratory. Ohio State University Research Foundation. May, 1952. 13 pgs. No number.

111. Hirvonen, R.A. "Computation of Traingulation on the Ellipsoid by the Aid of Closed Formulas," BULLETIN GEODESIQUE. March 1, 1957, pg. 3-15. No volume number.

112. Hirvonen, R.A. "The Gravity Field of Disturbing Masses in the Earth's Crust," Mapping and Charting Research Laboratory, Ohio State University Research Foundation, Technical Paper No. 170 (Dec., 1952). 23 pgs.

113. Hirvonen, R.A. "The Size and Shape of the Earth," in H.E. Landsberg and J. Van Meighem, ADVANCES IN GEOPHYSICS, VOLUME 5. New York: Academic Press, Inc., 1958. pgs. 93-117.

114. Hirvonen, R.A. "On the Precision of the Gravimetric Determination of the Geoid," TRANSACTIONS OF THE AMERICAN GEOPHYSICAL UNION. 37: 1-8 (Feb., 1960).

115. Honkasalo, T. "Measurements of Standard Base Lines with the Vaisala Light-Interference Comparator," JOURNAL OF GEOPHYSICAL RESEARCH. 65: 457-460 (Feb., 1960).

116. Hoskinson, A.J. GEODETIC OPERATIONS IN THE UNITED STATES AND IN OTHER AREAS THROUGH INTERNATIONAL COOPERATION. 1939-1953. U.S. Coast and Geodetic Survey Special Pub. 320. Washington: U.S. Government Printing Office, 1954. 37 pgs.

117. Hoskinson, A.J. and J.A. Duerksen. MANUAL OF GEODETIC ASTRONOMY. U.S. Coast and Geodetic Survey Special Pub. 237. Washington: U.S. Government Printing Office, 1947. 206 pgs.

118. Jardetzsky, W.S. THEORIES OF FIGURES OF CELESTIAL BODIES. New York: Interscience Publishers, Inc., 1958. 185 pgs.

119. Jeffreys, H. "The Figure of Rotating Planets," MONTHLY NOTICES OF THE ROYAL ASTRONOMICAL SOCIETY. 113" 97-105 (1953).

120. Jeffreys, H. "Second Order Terms in the Figure of Saturn," M.N.R.A.S. 114: 413-436 (1954).

121. Jeffreys, H. THE EARTH, ITS ORIGIN AND PHYSICAL CONSTITUTION. London: Cambridge at the University Press, 1959. Fourth Ed. 420 pgs.

122. Jones, H.S. "Dimensions and Rotation," in G.P. Kuiper, THE SOLAR SYSTEM, VOLUME II, THE EARTH AS A PLANET. University of Chicago Press, 1954. pgs. 1-41.

123. Kaula, W.M. "Accuracy of Gravimetrically Computed Deflections of the Vertical," TRANSACTIONS OF THE AMERICAN GEOPHYSICAL UNION. 38: 297-305 (June, 1957).

124. Kaula, W.M. "Statistical and Harmonic Analysis of Gravity," Technical Report 24. Washington: Army Map Service, March, 1959. 141 pgs.

125. Kelsey, J. and R.C.A. Edge. "Trials of the Tellurometer.....," BULLETIN GEODESIQUE. Sept., 1958 pgs. 1-7. No volume number.

126. Kirmser, P.G. and I. Wakabayashi. "Triangulation- A Precise Method for Satellite Tracking," JOURNAL OF THE FRANKLIN INSTITUTE. 268: 337-351(Nov., 1959).

127. Lambert, W.D. "Geodesy," ENCYCLOPEDIA BRITANNICA. 10: 126P-134 (1959).

128. Message, P.F. "The Second Order Theory of the Figure of Jupiter," MONTHLY NOTICES OF THE ROYAL ASTRONOMICAL SOCIETY. 115: 550-557 (1955).

129. Molodensky, M.S. "New Methods for Studying the Figure of the Earth," BULLETIN GEODESIQUE. Dec., 1958. pgs. 17-21. No volume number.

130. Murray, B.C. "The Artificial Satellite- A New Geodetic Tool." A.R.S. Paper No. 1221-60 (May, 1960). 12 pgs.

131. Nettleton, L.L., L.J.B. Lacoste and J.C. Harrison. "Tests of an Airborne Gravity Meter," GEOPHYSICS. 25: 181-202 (Feb., 1960).

132. Nielsen, J.N., F.K. Goodwin and W.A. Mersman. THREE DIMENSIONAL ORBITS OF EARTH SATELLITES INCLUDING EFFECTS OF EARTH OBLATENESS AND ATMOSPHERIC ROTATION. NASA Memo. 12-4-58A. Washington: U.S. Government Printing Office, Dec., 1958. 85 pgs.

133. O'Keefe, J.A. "Determination of the Earth's Gravitational Field," SCIENCE. 131: 607-608 (Feb. 26, 1960).

134. O'Keefe, J.A. "I.G.Y.Results on the Shape of the Earth," A.R.S. JOURNAL. 29: 902-904 (Dec., 1959).

135. O'Keefe, J.A., A. Eckels and R.K. Squires. "Vanguard Measurements Give Pear-Shaped Component of Earth's Figure," SCIENCE. 129: 565-566 (Feb. 27, 1959).

136. Parkhurst, D.L. GEODETIC LEVELING INSTRUMENTS. U.S. Coast and Geodetic Survey Special Pub. 334. Washington: U.S. Government Printing Office, 1955. 19 pgs.

137. Pierce, C. GEODETIC OPERATIONS IN THE UNITED STATES AND IN OTHER AREAS THROUGH INTERNATIONAL COOPERATION, 1954-1956. U.S. Coast and Geodetic Survey Special Pub. 60-1. Washington: U.S. Government Printing Office, 1957. 24 pgs.

138. Poincaré, H. FIGURES D'EQUILIBRE D'UNE MASSE FLUIDE. Paris: C. Naud, 1902. 210 pgs.

139. Poling, A.C. TELLUROMETER MANUAL. U.S.C.G.S. Pub. 62-1. Washington: U.S. Government Printing Office, 1959. 66 pgs.

140. Rainsford, H.S. SURVEY ADJUSTMENTS AND LEAST SQUARES. New York: Frederick Unger Pub. Co., 1958. 326 pgs.

141. Rappleye, H.S. MANUAL OF GEODETIC LEVELLING. U.S.C.G.S. Special Pub. 239. Washington: U.S. Government Printing Office, 1948. 94 pgs.

142. Rappleye, H.S. MANUAL OF LEVELLING COMPUTATION AND ADJUSTMENT. U.S.C.G.S. Special Pub. 240. Washington: U.S. Government Printing Office, 1948. 178 pgs.

143. Singer, S.F. "Geophysical Research with Artificial Earth Satellites," in H.E. Landsberg, ADVANCES IN GEOPHYSICS, VOLUME 3. New York: Academic Press, Inc., 1956. pgs. 301-367.

144. Stommel, H. "The Anatomy of the Atlantic," SCIENTIFIC AMERICAN. 192: 30-35 (Jan., 1955).

145. Svenska AB Gasaccumulator Co. Descriptive Literature Concerning the Geodimeter. Stockholm, Sweden. 1958. 16 pgs.

146. Systems Laboratories Corp. THE GEODETIC USE OF ARTIFICIAL EARTH SATELLITES. FINAL REPORT-PART I. Sherman Oaks, Calif., Aug., 1959. 119 pgs.

147. Thomas, P.D. CONFORMAL PROJECTIONS IN GEODESY AND CARTOGRAPHY. U.S. Coast and Geodetic Survey Special Pub. 251. Washington: U.S. Government Printing Office, 1952. 142 pgs.

148. Thompson, L.G.D. and L.J.B. Lacoste. "Aerial Gravity Measurements," JOURNAL OF GEOPHYSICAL RESEARCH. 65: 305-322 (Jan., 1960).

149. U.S. Coast and Geodetic Survey. HORIZONTAL CONTROL DATA. Special Pub. 227. Washington: U.S. Government Printing Office, 1957. 22 pgs.

150. Upton, E., A. Bailie and P. Musen. "Lunar and Solar Perturbations on Satellite Orbits," SCIENCE. 130: 1710-1711 (Dec. 18, 1959).

151. Whitmore, G.D., M.W. Thompson and J.L. Speert. "Modern Instruments for Surveying and Mapping," SCIENCE. 130: 1059-1066 (Oct.23, 1959).

152. Whitten, C.A. and K.H. Drummond (editors). CONTEMPORARY GEODESY. Publication 708. Washington: American Geophysical Union of National Academy of Sciences-National Research Council, 1959. 88 pgs.

153. Wilson, R.N. "A Gravitational Force Function for the Earth Representing all Deviations from a Spherical Geoid," JOURNAL OF THE FRANKLIN INSTITUTE. 268: 378-387 (Nov., 1959).

154. Woolard, G.P. "The Earth's Gravitational Field and its Exploitation," in H.E. Landsberg, ADVANCES IN GEOPHYSICS, VOLUME 1. New York: Academic Press, Inc., 1952. pgs. 281-311.

155. Allais, M.F.C. "Should the Laws of Gravity be Reconsidered?," AERO/SPACE ENGINEERING. 18: 46-52 (Sept., 1959) and 18: 51-55(Oct.,1959).

156. AMERICAN EPHEMERIS AND NAUTICAL ALMANAC FOR THE YEAR 1960. Washington: U.S. Government Printing Office, 1958. 533 pgs.

157. Andrade, E.N.D. "Isaac Newton," in J.R. Newman, THE WORLD OF MATHEMATICS, VOLUME 1. New York: Simon and Schuster, Inc., 1956. pgs. 255-276.

158. Baker, R.H. ASTRONOMY. Princeton, N.J.: D. Van Nostrand Co., Inc., 1959. Seventh Ed. 547 pgs.

159. Blatt, J.M. "Time Reversal," SCIENTIFIC AMERICAN. 195: 107-114 (August, 1956).

160. Brown, E.W. TABLES OF THE MOTION OF THE MOON. New Haven: Yale University Press, 1919.

161. Cedarholm, J.P. and C.H. Townes. "A New Experimental Test of Special Relativity," NATURE. 184: 1350-1351 (Oct. 31, 1959).

162. Clemence, G.M. "Astronomical Time," REVIEWS OF MODERN PHYSICS. 29: 2-8 (Jan., 1957).

163. Clemence, G.M. "Dynamics of the Solar System," in E.U. Condon and H. Odishaw, HANDBOOK OF PHYSICS. New York: McGraw-Hill Book Co., 1958. pgs. 2-55 to 2-59.

164. Clemence, G.M. "Standards of Time and Frequency," SCIENCE. 123: 567-573 (April 6, 1956).

165. Dicke, R.H. "Gravitation-An Enigma," AMERICAN SCIENTIST. 47: 25-40 (March, 1959).

166. Dicke, R.H. "New Research on Old Gravitation," SCIENCE. 129: 621-624 (March 6, 1959).

167. Eddington, A.S. THE MATHEMATICAL THEORY OF RELATIVITY. Cambridge University Press, 1952. 270 pgs.

168. Eddington, A.S. "Centaurus," ENCYCLPEDIA BRITANNICA. 5: 126 (1959).

169. Ehricke, K.A. "Interplanetary Operations," in H.S. Siefert, SPACE TECHNOLOGY. New York: John Wiley and Sons, Inc., 1959. 54 pgs.

170. Essen, L. "Report on the Precision of Atomic Time Standards," THE ASTRONOMICAL JOURNAL. 64: 120-123 (April, 1959).

171. Fedorov, E.P. "Nutation as Derived from Latitude Observations." Ibid. pgs. 81-84.

172. Fock, V. "Three Lectures on Relativity Theory," REVIEWS OF MODERN PHYSICS. 29: 325-333 (July, 1957).

173. Fock, V. THE THEORY OF SPACE, TIME AND GRAVITATION. Translated by N. Kemmer. New York: Pergamon Press, Inc., 1959. 411 pgs.

174. Freundlich, E.F. CELESTIAL MECHANICS. New York: Pergamon Press, Inc., 1958. 150 pgs.

175. Gallagher, W.J. and W.H. Hansen, "Mass of the Moon from Satellite Observations," SCIENCE. 128: 1207 (Nov. 14, 1958).

176. Ginsburg, V.L. "Artificial Satellites and the Theory of Relativity," SCIENTIFIC AMERICAN. 200: 149-160 (May, 1959).

177. Gradecak, V. "On Gravitation " in ADVANCES IN ASTRONAUTICAL SCIENCES. New York: Plenum Press, Inc., 1959. pgs. 98-113.

178. Her Majesty's Nautical Almanac Office. PLANETARY COORDINATES FOR THE YEARS 1960-1980. London, 1958.

179. Inglis, D.R. "Shifting of the Earth's Axis of Rotation," REVIEWS OF MODERN PHYSICS. 29: 9-19 (Jan., 1957).

180. Jammer, M. CONCEPTS OF SPACE. Cambridge: Harvard University Press, 1954. 196 pgs.

181. Jammer, M. CONCEPTS OF FORCE. Cambridge: Harvard University Press, 1957. 269 pgs.

182. Jeffreys, H. SCIENTIFIC INFERENCE. New York: The MacMillan Co., 1931.

183. Jeffreys, H. "Nutation and the Variation in Latitude," THE ASTRONOMICAL JOURNAL. 64: 84-86(Apr., 1959).

184. Jeffreys, H. "Dynamics of the Earth-Moon System," in G.P. Kuiper (editor), THE SOLAR SYSTEM, Volume II, THE EARTH AS A PLANET. University of Chicago Press, 1954. pgs. 42-56.

185. Kellogg, P.J. ROTATING COORDINATE SYSTEMS IN THE GENERAL THEORY OF RELATIVITY. M.I.T. B.S. Thesis, Physics Department, 1950. 11 pgs.

186. Landau, L. and E. Lifshitz. THE CLASSICAL THEORY OF FIELDS. Translated by M. Hamermesh. Reading, Mass.: Addison-Wesley Pub. Co., 1951. 354 pgs.

187. Mandelker, J. A NEW THEORY OF GRAVITATION. New York: The Philosophical Library, 1951.

188. Markowitz, W. "Time Measurement," ENCYCLOPEDIA BRITANNICA. 22: 224-229 (1959).

189. Markowitz, W. "Variations in the Rotation of the Earth," THE ASTRONOMICAL JOURNAL. 64: 106-113 (April, 1959).

190. McClain, E.F. "The 600 Foot Radio Telescope," SCIENTIFIC AMERICAN. 202: 45-51 (Jan., 1960).

191. Mehlin, T.G. ASTRONOMY. New York: John Wiley and Sons, Inc., 1959. 392 pgs.

192. Milne, E.A. KINEMATIC RELATIVITY. Oxford, at the Clarendon Press, 1948. 238 pgs.

193. Moon, P. and D.E.Spencer. "The Cosmological Principle and the Cosmological Constant," JOURNAL OF THE FRANKLIN INSTITUTE. 266: 47-58 (July, 1958).

194. Moulton, F.R. AN INTRODUCTION TO CELESTIAL MECHANICS. New York: The MacMillan Co., 1914. 437 pgs.

195. Oosterhoff, P.H. (editor). "Report of the Commission on the Variation of Latitude," TRANSACTIONS OF THE INTERNATIONAL ASTRONOMICAL UNION. 9: 270-283 (1955).

196. Parvin, R.H. "The Earth and Inertial Space," AERO/SPACE ENGINEERING.

Part I. "Motions of the Earth." 18:34-37 (April, 1959).
Part II. "The Shape of the Earth." 18: 33-37 (May, 1959).

197. Pecker, J.C. and E. Schatzman. ASTROPHYSIQUE GENERALE. Paris: Masson et Cie., 1959. 756 pgs.

198. Peek, B.M. THE PLANET JUPITER. London: Faber and Faber Co., 1958. 283 pgs.

199. Price, R., P.E. Green et al. "Radar Echoes from Venus," SCIENCE. 129: 751-753 (Mar. 20, 1959).

200. Russell, H.N., R.S. Dugan and J.Q. Stewart. ASTRONOMY, VOLUME I. THE SOLAR SYSTEM. Boston: Ginn and Co., 1945. 490 pgs.

201. Sciama, D.W. "Inertia," SCIENTIFIC AMERICAN. 196: 99-109 (Feb., 1957).

202. Sciama, D.W. "On the Origin of Inertia," MONTHLY NOTICES OF THE ROYAL ASTRONOMICAL SOCIETY. 113: 34-42 (1953).

203. Sciama, D.W. THE UNITY OF THE UNIVERSE. Garden City, New York: Doubleday and Co., Inc., 1959. 228 pgs.

204. Smart, W.M. CELESTIAL MECHANICS. London: Longmans, Green and Co., 1953. 381 pgs.

205. Smith, H.M. "Quartz Clocks of the Greenwich Time Service," MONTHLY NOTICES OF THE ROYAL ASTRONOMICAL SOCIETY. 113: 67-80 (1953).

206. Smith, H.M. and R.H. Tucker. "The Annual Fluctuation in the Rate of Rotation of the Earth," M.N.R.A.S. 113: 251-257 (1953).

207. Struve, O. "Stellar Motions," SKY AND TELESCOPE. 18: 664-672 (October, 1959).

208. Struve, O., B. Lynds and H. Pillans. ELEMENTARY ASTRONOMY. New York: Oxford Univ. Press, 1959. 396 pg.

209. Tolman, R. C. RELATIVITY THERMODYNAMICS AND COSMOLOGY. Oxford at the Clarendon Press, 1934. 501 pgs.

210. Urey, H. C. THE PLANETS, THEIR ORIGIN AND DEVELOPMENT. New Haven: Yale University Press, 1952. 245 pgs.

211. Vallarta, M. S. "Gravitation," ENCYCLOPEDIA BRITANNICA. 10: 663-667 (1959).

212. van der Waerden, B. L. "The Irregular Rotation of the Earth," THE ASTRONOMICAL JOURNAL. 64: 96-97 (Apr., 1959).

213. Walker, A. M. and A. Young. "The Analysis of the Observations of the Variation of Latitude," MONTHLY NOTICES OF THE ROYAL ASTRONOMICAL SOCIETY. 115:443-459 (1955).

214. Whipple, F. L. and G. P. Kuiper. "Planet," ENCYCLOPEDIA BRITANNICA. 17: pg. 1002 (1959).

215. Wolfe, H. C. "Gravitation," in E. U. Condon and H. Odishaw, HANDBOOK OF PHYSICS. New York: McGraw-Hill Book Co., 1958. pgs. 2-55 to 2-59.

GENERAL- MATHEMATICS AND PHYSICS

216. Byerly, W. E. AN INTRODUCTION TO THE USE OF GENERALIZED COORDINATES IN MECHANICS AND PHYSICS. Boston: Ginn and Co., 1916. 118 pgs.

217. Becker, G. F. and C. E. van Nostrand. HYPERBOLIC FUNCTIONS (Tables). Washington: The Smithsonian Institution, 1924. 321 pgs.

218. Easthope, C. E. THREE DIMENSIONAL DYNAMICS, A VECTORIAL TREATMENT. New York: Academic Press, Inc., 1958. 277 pgs.

219. Goldstein, H. CLASSICAL MECHANICS. Cambridge; Addison-Wesley Pub. Co., 1953. 399 pgs.

220. Herrick, S. and R. M. L. Baker. "Recent Advances in Astrodynamics," JET PROPULSION. 28:649-654 (Oct., 1958).

221. Hilbert, D. and S. Cohn-Vossen. GEOMETRY AND THE IMAGINATION. Translated by P. Nemenyi. New York: Chelsea Pub. Co., 1956. 357 pgs.

222. Hildebrand, F. B. ADVANCED CALCULUS FOR ENGINEERS. Englewood Cliffs, N. J.: Prentice-Hall, Inc., 1948. 594 pgs.

223. Hildebrand, F. B. METHODS OF APPLIED MATHEMATICS. Ibid., 1956. 523 pgs.

224. Hodgman, C. C., editor. HANDBOOK OF CHEMISTRY AND PHYSICS. Cleveland: Chemical Rubber Pub. Co., 1959-1960. 41 st. edition.

225. Jeffreys, H. and B. S. METHODS OF MATHEMATICAL PHYSICS. Cambridge at the University Press, 1956. 714 pgs.

226. Lamb, H. HYDRODYNAMICS. Cambridge at the University Press, 1932. 738 pgs. 6 th. edition.

227. Lyons, H. "Atomic Clocks," SCIENTIFIC AMERICAN. 196: 71-82 (Feb., 1957).

228. Mach, E. THE SCIENCE OF MECHANICS. London: Open Court Pub. Co., 1942. 635 pgs. 5 th. edition.

229. Miller, F. H. ANALYTIC GEOMETRY AND CALCULUS. New York: John Wiley and Sons, Inc., 1949. 658 pgs.

230. Milne-Thomson, L. M. THEORETICAL HYDRODYNAMICS. New York: The MacMillan Co., 1955. 632 pgs. 3 rd. edition.

231. Morse, P. M. and H. Feshbach. METHODS OF THEORETICAL PHYSICS. New York: McGraw-Hill Book Co., 1953. 1978 pgs. Two volumes.

232. Newton, G. C., L. A. Gould and J. F. Kaiser. ANALYTIC DESIGN OF LINEAR FEEDBACK CONTROLS. New York: John Wiley and Sons, Inc., 1957. 419 pgs.

233. Phillips, E. G. FUNCTIONS OF A COMPLEX VARIABLE. Edinburgh: Oliver and Boyd, 1954. 144 pgs.

234. Pierce, B.O. A SHORT TABLE OF INTEGRALS. Boston: Ginn and Co., 1929. 156 pgs. 3 rd. edition.

235. Richtmyer, F.K., E.H. Kennard and T. Lauritsen. INTRODUCTION TO MODERN PHYSICS. New York: McGraw-Hill Book Co., 1955. 666 pgs. 5 th. edition.

236. Routh, E.J. A TREATISE ON ANALYTIC STATICS. PART 2. London: MacMillan and Co., Ltd., 1930. 484 pgs. 6 th. ed.

237. Ruark, A.E. and H.C. Urey. ATOMS, MOLECULES AND QUANTA. New York: McGraw-Hill Book Co., 1930. 790 pgs.

238. Synge, J.L. and B.A. Griffith. PRINCIPLES OF MECHANICS. New York: McGraw-Hill Book Co., 1949. 530 pgs.

239. Synge, J.L. and A. Schild. TENSOR CALCULUS. Toronto: University of Toronto Press, 1956. 324 pgs.

240. Tables of the Exponential Function e^x. National Bureau of Standards, Applied Mathematics Series No. 14. Washington: U.S. Government Printing Office, June, 1951. 537 pgs.

241. Webster, A.G. THE DYNAMICS OF PARTICLES AND OF RIGID, ELASTIC AND FLUID BODIES. New York: Dover Publications, 1959. 588 pgs. 2 nd. edition.

242. Whittaker, E.T. A TREATISE ON THE ANALYTIC DYNAMICS OF PARTICLES AND RIGID BODIES. New York: Dover Publications, 456 pgs. 4 th. edition.